



LUND UNIVERSITY

Analysis and Modelling of Desalination Brines

Bashitialshaaer, Raed

2011

[Link to publication](#)

Citation for published version (APA):

Bashitialshaaer, R. (2011). *Analysis and Modelling of Desalination Brines* (1052 ed.). [Doctoral Thesis (compilation), Division of Water Resources Engineering]. Lund University.

Total number of authors:

1

General rights

Unless other specific re-use rights are stated the following general rights apply:

Copyright and moral rights for the publications made accessible in the public portal are retained by the authors and/or other copyright owners and it is a condition of accessing publications that users recognise and abide by the legal requirements associated with these rights.

- Users may download and print one copy of any publication from the public portal for the purpose of private study or research.
- You may not further distribute the material or use it for any profit-making activity or commercial gain
- You may freely distribute the URL identifying the publication in the public portal

Read more about Creative commons licenses: <https://creativecommons.org/licenses/>

Take down policy

If you believe that this document breaches copyright please contact us providing details, and we will remove access to the work immediately and investigate your claim.

LUND UNIVERSITY

PO Box 117
221 00 Lund
+46 46-222 00 00

Analysis and Modelling of Desalination Brines

Raed Bashitialshaaer



LUND
UNIVERSITY

Akademisk avhandling för avläggande av teknologie doktorsexamen vid tekniska fakulteten vid Lunds universitet kommer att offentligens försvaras vid Institutionen för Bygg- och Miljöteknologi, John Ericsson väg 1, Lund, hörsal V:B, måndagen den 21 mars 2011, kl 10.15.

Academic thesis submitted to Lund University in partial fulfilment of the requirements for the degree of Doctor of Philosophy (Ph.D. Engineering). The thesis will be publically defended at the Department of Building and Environmental Technology, John Ericsson väg 1, lecture hall V:B, Monday, March 21, 2011, at 10:15 a.m.


Fakultetsopponent/Faculty Opponent: Professor Lars Bergdahl, Water Environment Technology, Civil and Environmental Engineering, Chalmers University of Technology.

Organization LUND UNIVERSITY Water resources engineering Box 118, S-221 00 LUND Sweden	Document name Doctoral dissertation Date of issue February 2011 Coden: LUTVDG/(TVVR-1052)(2011)	
Author: Raed Bashithalshaaer		
Title and subtitle: Analysis and Modelling of desalination Brines		
Abstract Seawater desalination constitutes an important water supply to the population bordering the Arabian Gulf, the Mediterranean Sea and the Red Sea. The three regions represent about 11.8% of the world land area and the countries hosted approximately 9% of the world population in 1950 and 2008 and are also projected to do so in 2050. The results obtained for desalination capacity in the study area were 62%, 58% and 60% of the world capacity for 1996, 2008, and 2050, respectively. The increase in the recovery ratio is considered an important factor in this study. In 1996 this ratio was about 30 to 35%, and in 2008 it was 40 to 45%, although in some plants it reached up to 50%. The gulf desalination capacities were obtained as 50, 40 and 45% of total world capacity at the end of 1996, 2008 and 2050 (prognosis) respectively. All Middle Eastern countries suffer from a shortage of water along with increasing demand due to high population growth. Desalination can be a cost-effective way to produce fresh water and possibly electricity. A suggested solution for Sinai and the Gaza Strip involves the building of a joint power and desalination plant, located in Egypt close to the border with Gaza. This joint Egypt-Palestine project would increase the water supply by 500,000 m ³ /d and the power supply by 500MW. The result emerged from field work and the two experiments can also be applied to the design of this project. Water and salt mass balances for the Dead Sea were modelled by including and excluding the water from the proposed Red Sea Dead Sea Canal project, RSDSC. Precipitation, evaporation, river discharges, ground water flows, input/output from potash companies and salt production in addition to brine discharge were included in the models. The mixing time in the Dead Sea was modelled using a single-layer (well-mixed) and a two-layer (stratified) system. An efficient method for increasing the dilution rate of brine water discharged into the sea is an inclined negatively buoyant jet of a single port or multi-diffuser. Two small-scale experimental studies were conducted to investigate the behaviour of a dense jet discharged into lighter ambient water. The first lab-scale experiment concerned the benefit of the initial angle of inclined dense jets, where the slope increased for the maximum levels as a function of this angle. An angle of 60 deg. led to a better result than 30 or 45 deg. An empirical prediction was found based on five geometric quantities to be considered in the future plan. Field work measurements have been conducted in Cyprus, where the brine from a desalination plant and the Mediterranean Sea coastline have been investigated at the Eastern Mediterranean University. The result from the measured data demonstrates the need for more than one outfall (a series of outfalls) to the sea to avoid or minimize environmental impact on the coastline. The result also agreed well with simple, two dimensional mathematical models assuming Gaussian distribution. The calculated bottom slope is about 7.4%, which can explain the pollution that appears at the coast close to the discharge point. Thus small slope could be one reason. The second lab-scale experiment studied the near and intermediate fields of negatively buoyant jets. The dilution along the flow was increased by about 10% and 40% with bottom slope and bottom slope together with a 30 degree jet inclination, respectively. This method can be applied in brine discharge outlets to recipients to minimize concentration and facilitate faster and greater dilution. Over 16% bottom slope and more field work is needed for comparison with this result. It was found that an inclination of 30 degrees with 16 % bottom slope was more sustainable in designing brine discharge outfall. A Matlab code can be used to describe the lateral spreading and centerline dilution of buoyant jets and plumes in near and intermediate fields.		
Key words: Desalination, Water supply, Brine discharge, Experiment, Negatively buoyant jet, Field data analysis, Modelling.		
Classification system and/or index terms (if any)		
Supplementary bibliographic information		Language: English
ISSN and key title: 1101-9824		ISBN: 978-91-7473-058-6
Recipient notes		Number of pages Price
Security classification		

Distribution by the Division of water resources engineering, Lund University, Box 118, 221 00 Lund, Sweden

I, the undersigned, being the copyright of the abstract of the above- mentioned dissertation, hereby grant to all reference sources permission to publish and disseminate the abstract of the above-mentioned dissertation.

Signature _____



Date _____ 12/02/2011 _____

**WATER RESOURCES ENGINEERING, FACULTY OF
ENGINEERING, LUND UNIVERSITY
LUTVDG: TVVR-1052 (2011)**

Doctoral Thesis

ANALYSIS AND MODELLING OF DESALINATION BRINES

Raed Bashitialshaaer



**LUND
UNIVERSITY**

February, 2011

Analysis and Modelling of Desalination Brines

© Raed Bashitialshaaer, unless otherwise stated

Doktorsavhandling
Teknisk Vattenresurslära
Institution för Bygg- och Miljöteknologi
Lunds Tekniska Högskola, Lunds Universitet

Doctoral Thesis
Water Resources Engineering
Department of Building & Environmental Technology
Faculty of Engineering
Lund University
P.O. Box 118
Se-221 00 LUND
Sweden

<http://www.tvrl.lth.se>

Cover: Brine discharge from a desalination plant, field work analysis from Cyprus and inclined negatively buoyant jet experimental work at the Water Resources Engineering lab, Lund University.

CODEN: LUTVDG/(TVVR-1052)(2011)
ISBN: 978-91-7473-058-6
ISSN: 1101-9824
Report No.: 1052

Printed in Sweden by Media-Tryck, Lund 2011

ACKNOWLEDGMENTS

There are many people who helped me during the research period of my doctoral study. First of all, Professor Kenneth M. Persson, who was my main supervisor for this thesis, and my co-supervisor Professor Lars Bengtsson for his valuable time and for assisting me with some of the papers. Kenneth and Lars always helped me to make this thesis as complete as possible.

I would like to thank Professor Magnus Larson, who was one of my important guides in the theoretical and several experimental suggestions. I thank my friends and colleagues at TVRL for their company and social activities. Many thanks go to all TVRL members the professors, PhDs and colleagues for their scientific and technical help and daily discussions. Many thank to Lennart Grahn for his help and time for technical and administrative supports at the Division.

I would like to express my gratitude to the international desalination association (IDA) for their help and support. They recently invited me to participate in the Environmental Task Force committee for the Environmental Conference on Desalination in the Arabian/Persian Gulf. I would also like to thank the Center for Middle East Study (CMES) at Lund University as my work was partly funded by them, primarily the experimental work conducted at the department. Some of my travelling expenses to conferences were also provided by the CMES.

I would like to thank my parents for providing me with the never ending opportunity to be where I am, it is thanks to them that I have been able to complete this work. Mama, you have always been my biggest fan, which I very much appreciate. Dad, your encouragement, input and constructive comments have been priceless. I would also like to thank my brothers and sisters. Extra special thanks go to my eldest brother, Associate Professor Tarek El Bashiti, who has always been ahead of his time and my greatest mentor.

Finally, I want to thank my friends who always remained close despite the distance. My greatest appreciation goes to my second Family, especially my Father- and Mother-in-law who always supported me in different aspects of life. Special thanks to my wife Hanan for her motivation and support. She is the main Family member who I wish to acknowledge.

Raed Abd Al Qader Ismaeil Bashiti alshaaer

رائد عبد القادر إسماعيل بشيتي الشاعر

Lund, Sweden, March, 2011

ABSTRACT

Seawater desalination constitutes an important water supply to the population bordering the Arabian Gulf, the Mediterranean Sea and the Red Sea. The three regions represent about 11.8% of the world land area and the countries hosted approximately 9% of the world population in 1950 and 2008 and are also projected to do so in 2050. The results obtained for desalination capacity in the study area were 62%, 58% and 60% of the world capacity for 1996, 2008, and 2050, respectively. The increase in the recovery ratio is considered an important factor in this study. In 1996 this ratio was about 30 to 35%, and in 2008 it was 40 to 45%, although in some plants it reached up to 50%. The gulf desalination capacities were obtained as 50, 40 and 45% of total world capacity at the end of 1996, 2008 and 2050 (prognosis) respectively.

All Middle Eastern countries suffer from a shortage of water along with increasing demand due to high population growth. Desalination can be a cost-effective way to produce fresh water and possibly electricity. A suggested solution for Sinai and the Gaza Strip involves the building of a joint power and desalination plant, located in Egypt close to the border with Gaza. This joint Egypt-Palestine project would increase the water supply by 500,000 m³/d and the power supply by 500MW. The result emerged from field work and the two experiments can also be applied to the design of this project. Water and salt mass balances for the Dead Sea were modelled by including and excluding the water from the proposed Red Sea Dead Sea Canal project, RSDSC. Precipitation, evaporation, river discharges, ground water flows, input/output from potash companies and salt production in addition to brine discharge were included in the models. The mixing time in the Dead Sea was modelled using a single-layer (well-mixed) and a two-layer (stratified) system.

An efficient method for increasing the dilution rate of brine water discharged into the sea is an inclined negatively buoyant jet of a single port or multi-diffuser. Two small-scale experimental studies were conducted to investigate the behaviour of a dense jet discharged into lighter ambient water. The first lab-scale experiment concerned the benefit of the initial angle of inclined dense jets, where the slope increased for the maximum levels as a function of this angle. An angle of 60 deg. led to a better result than 30 or 45 deg. An empirical prediction was found based on five geometric quantities to be considered in the future plan.

Field work measurements have been conducted in Cyprus, where the brine from a desalination plant and the Mediterranean Sea coastline has been investigated at the Eastern Mediterranean University. The result from the measured data demonstrates the need for more than one outfall (a series of outfalls) to the sea to avoid or minimize environmental impact on the coastline. The result also agreed well with simple, two dimensional mathematical models assuming Gaussian distribution. The calculated bottom slope is about 7.4%, which can explain the pollution that appears at the coast close to the discharge point. Thus small slope could be one reason.

The second lab-scale experiment studied the near and intermediate fields of negatively buoyant jets. The dilution along the flow was increased by about 10% and 40% with

bottom slope and bottom slope together with a 30 degree jet inclination, respectively. This method can be applied in brine discharge outlets to recipients to minimize concentration and facilitate faster and greater dilution. Over 16% bottom slope and more field work is needed for comparison with this result. It was found that an inclination of 30 degrees with 16 % bottom slope was more sustainable in designing brine discharge outfall. A Matlab code can be used to describe the lateral spreading and centerline dilution of buoyant jets and plumes in near and intermediate fields.

ABSTRACT (Swedish)

Avsaltning av havsvatten utgör en viktig källa för vattenförsörjning till befolkningen som bor vid Persiska viken, Medelhavet och Röda havet. De tre regionerna utgör ca 11,8 % av världens landyta och hade omkring 9 % av världens befolkning under 1950 och 2008, samt lika mycket enligt prognos för år 2050. Dessa områden är hemvist för 62 %, 58% och 60% av världens avsaltningskapacitet för år 1996, 2008 respektive 2050. Utbytet av dricksvatten ur havsvatten har identifierats som en viktig faktor i denna studie. Under 1996 uppgick utbytet till cirka 30-35 % och år 2008 var det cirka 40-45 %, medan vissa avsaltningsanläggningar nådde upp till hela 50 %. Runt Persiska viken fanns och finns 50 %, 40 % och 45 % av världens totala avsaltningskapacitet i slutet av 1996, 2008 respektive 2050 (prognos).

Alla länder i Mellanöstern lider av brist på vattenresurser samtidigt med en ökad efterfrågan av vatten på grund av den höga befolkningstillväxten. Avsaltning kan vara ett kostnadseffektivt sätt att producera färskvatten och möjligtvis också el. En lösning för Sinai och Gazaremsan föreslås som innebär att en gemensam kraft- och avsaltningsanläggning uppförs i Egypten nära gränsen till Gazaremsan. Detta gemensamma Egypten-Palestina projekt skulle öka vattenförsörjningen med 500 000 m³/d och kraftförsörjningen med 500 MW i regionen. Resultatet från fältarbete och två experiment i laboratorieskala redovisas. De kan även tillämpas för att utforma detta projekt. Massbalanser för vatten och salt för Döda havet modellerades genom att inkludera och exkludera vatten från ett föreslaget projekt att överföra vatten från Röda havet till Döda havet i en kanal (RSDSC). Nederbörd, avdunstning, ytvattenflöde, grundvattenflöden, samt uppgifter för tillflöde och avlopp från mineralutvinningsföretag runt Döda havet användes i modellen. Blandningstiden i Döda havet modellerades genom att använda två olika ekvationssystem, för väl omblandade respektive skiktade förhållanden.

En effektiv metod för att påskynda utspädningen av det salta rejektvattnet från avsaltningsverket i recipienten är att använda en vinklad utgångsstråle eller spridning med multipla utlopp. Två experimentella studier i laboratorieskala utfördes för att undersöka hur en tung/tät stråle fördelades i omgivande vatten. Den första studien gjordes med vinklade tunga/täta strålar för att studera betydelsen av utloppsstrålens vinkel, där lutningen ökade för de maximala nivåerna som funktion av denna vinkel. En utloppsvinkel på 60 grader ger snabbare inblandning än 30 eller 45 grader. En empirisk relation för effektiv inblandning togs fram som funktion av fem geometriska parametrar, vilken kan användas för framtida planering.

Fältundersökningar har gjorts på Cypern av hur rejektplymer från Eastern Mediterranean Universitys avsaltningsanläggning fördelas lokalt i Medelhavet. Mätningarna visar att det behövs mer än ett utlopp (multipla utlopp) ut till havet för att undvika eller minimera miljöpåverkan längs kusten. Resultatet överensstämde väl med en enkel två-dimensionell matematiska modell för spridning om plymen antas vara normalfördelad. Den beräknade bottenlutningen i fält var låg, omkring 7,4 %, vilket delvis kan förklara varför smuts från avsaltningen syntes på stranden i närheten av utsläppspunkten.

Ett andra laboratorieexperiment gjordes för att undersöka hur flödesfältet från tunga saltvattenplymer såg ut nära utloppet och i mellanzonen innan plymen fördelats ut i recipienten. Utspädningen längs plymen ökade med cirka 10 % och 40 % om botten lutade respektive om botten lutade och strålen riktades 30 grader upp från horisontalplanet. Resultat av denna studie kan användas för konstruktion av utlopp från avsaltningsverk för att minimera saltkoncentrationsskillnader och för att få plymen att spädas ut snabbare och mera i recipient. Mer än 16 % bottenlutning rekommenderas, liksom flera fältmätningar. En utloppsvinkel på 30 grader med 16 % bottenlutning ger mindre miljöpåverkan. De geometriska effekterna kan modelleras framgångsrikt i Matlab.

ABSTRACT (Arabic)

"وَجَعَلْنَا مِنَ الْمَاءِ كُلَّ شَيْءٍ حَيٍّ" (الأنبياء: ٣٠)

الملخص: تعد تحلية مياه البحر مصدرا مهما لتزويد سكان الدول المطلة على الخليج العربي والبحر الأبيض المتوسط والبحر الأحمر بالمياه الصالحة للشرب. تمثل هذه الدول نحو 11.8 % من إجمالي مساحة العالم وتعدادها السكاني ما يقارب 9.0 % من عدد سكان العالم وذلك في الفترة الواقعة بين 1950 ، 2008 ومن المتوقع أن تظل هذه النسبة حتى عام 2050. وأظهرت نتائج الدراسة أن قدرة تحلية مياه البحر في منطقة الدراسة تعادل 62 ، 58 ، 60 % من الإجمالي العالمي للأعوام 1996، 2008 ، 2050 على التوالي. في حين أن قدرة تحلية المياه في الخليج العربي تعادل 40 ، 50 ، 45 % فقط ، من الإجمالي العالمي في نهاية 1996 ، 2008 ، 2050 على التوالي. وتعتبر الزيادة في نسبة الاستعادة عاملا مهما في هذه الدراسة. ففي عام 1996 كانت هذه النسبة تتراوح ما بين 30 ، 35 % ، وفي عام 2008 كانت ما بين 40 ، 45 % في حين أنها وصلت إلى 50 % في بعض المحطات

وتعد تحلية المياه وسيلة فعالة أيضاً من حيث التكلفة لإنتاج المياه العذبة. وبعد إنشاء محطة لتحلية المياه بين مصر وفلسطين (تقع في الجانب المصري المجاور لقطاع غزة) الحل الأمثل لمواجهة نقص المياه في سيناء وقطاع غزة. والمشروع المقترح يمكن ان يوفر إمدادات المياه بما يزيد عن 500,000 متر مكعب يوميا وإمدادات الطاقة بمقدار 500 مليون واط للطرفين.

تم عمل نمذجة للموازنة المائية ولموازنة الأملاح بالبحر الميت مع الأخذ بعين الاعتبار مشروع القناة المقترحة بين البحر الأحمر و البحر الميت (RSDSC) ، مع الأخذ بعين الاعتبار كميات الأمطار والتبخرو تصريف الأنهار وجريان المياه الجوفية والمياه الناتجة و المستهلكة من قبل شركات إنتاج البوتاس والملح. وتم نمذجة زمن الخلط في البحر الميت باعتباره أحادي الكثافة مرة وثنائي الكثافة مرة أخرى. يعتبر النفط الطافي الموجه للأسفل عبر مخرج واحد أوعدة مخارج من أفضل الطرق لتمديد المياه المصروفة إلى البحر. تم إجراء تجربتين مخبريتين لدراسة سلوك تدفق مياه تركيزها أعلى من تركيز المياه المحيطة (ينطبق ذلك على عدم المياه المالحة الناتجة عن محطات التحلية). التجربة الأولى تم إجراؤها عبر نفث مائل وذلك لدراسة تأثير زاوية النفث المبدئية. فوجد ان ميل النفث بزاوية 60 درجة يعطي نتيجة أفضل من 30 أو 45 درجة. كما تم استنباط علاقات بين المتغيرات الخمس المختلفة والتي يمكن ان تؤخذ بعين الاعتبار في الدراسات المستقبلية.

وقد قمت بعمل قياسات حقليّة في قبرص للعدم الناتج من محطة تحلية المياه المالحة التابعة لجامعة شرق المتوسط الواقعة على ساحل البحر الأبيض المتوسط. وتحليل البيانات المقاسة وتوصلت الى وجوب استخدام أكثر من مصب للعدم لتجنب أو لتقليل الآثار البيئية على الساحل. وللتحقق من هذه النتائج تم عمل نموذج رياضي مبسط ثنائي الأبعاد والذي أوضح تقارب كبير مع القياسات الحقلية.

التجربة الثانية قمت بدراسة تأثير النفط الطافي المائل للأسفل على المجالات القريبة والمتوسطة المتولدة. فوجدت أن معدل التمديد قد زاد بنحو 10 و 40 في المئة في اتجاه الجريان مع ميل القاع و ميل القاع مصحوبا بنفث مائل بزاوية 30 درجة علي التوالي. ويمكن تطبيق هذا النوع لتقليل تركيز المياه المالحة المصروفة إلى وسط مائي. واستنتجت أيضا انه باستخدام نفث مائل بزاوية 30 درجة مع ميل قاع 16 % يعطي افضلية عند تصميم مصبات تفريغ العادم. وبمزيد من الدراسات الحقلية وبميل قاع أكثر من 16 % يمكن الحصول على نتائج أفضل. وقد تحققت من نتائج التجريبتين المعمليتين باستخدام نموذج رياضي بواسطة برنامج الماتلاب (Matlab).

APPENDED PAPERS

This thesis is submitted with the following appended papers, which will be referred to by their Roman numerals in the body text.

- I. Bashitialshaaer, R., and Persson K.M. 2011. Near and Intermediate Field Evolution of A Negatively Buoyant Jet. (Submitted to Ocean System Engineering)
- II. Bashitialshaaer, R., Larson M., and Persson K.M. 2011. An Experimental Investigation on Inclined Negatively Buoyant Jets. (Submitted to Journal of Hydraulic Research)
- III. Bashitialshaaer, R., Flyborg, L., and Persson, K.M. 2011. Environmental Assessment of Brine Discharge and Wastewater in the Arabian Gulf. *Desalination and Water Treatment*, (25) 276-285.
- IV. Bashitialshaaer, R., Persson, K.M., and Aljaradin, M. 2011. Estimated Future Salinity in the Arabian Gulf, the Mediterranean Sea and the Red Sea Consequences of Brine Discharge from Desalination. *International Journal of Academic Research*. Vol. 3. No. 1, Part I, 156-164.
- V. Bashitialshaaer, R., Bengtsson, L., Larson, M., and Persson, K.M. 2011. Sinuosity effects on Longitudinal Dispersion Coefficient. *Int. J. of Sustainable Water and Environmental Systems*, Volume 2, No. 2 (2011) 77-84.
- VI. Bashitialshaaer, R., and Persson K.M. 2009. Worldwide oil prize, desalination and population growth correlation study. *VATTEN* (65): 37-46.
- VII. Bashitialshaaer, R., and Persson K.M. 2010. Improving Water and Electricity Could Ease Border Tensions: A Case Study for Sinai-Gaza”. *Water policy* 2011 (submitted).
- VIII. Bashitialshaaer, R., and Persson K.M. 2011. The Dead Sea Future Elevation. *Int. J. of Sustainable Water and Environmental Systems*, Volume 2, No. 2 (2011) 67-76.
- IX. Bashitialshaaer, R., Persson, K.M., Larson, M., and Ergil, M. 2007. Impact on Seawater Composition from Brine Disposal at EMU Desalination Plant. *Proceedings 11th IDA World Congress-Maspalomas, Gran Canaria –Spain, October 21-26, 2007*.

Related publications

Papers, Magazine and newsletter

- Bashitialshaaer, R., Larson M., and Persson K.M. 2010. Mixing Time for the Dead Sea Based on Water and Salt Mass Balances. *VATTEN* (66): 55-66.
- Bashitialshaaer, R., and Persson K.M. 2007. Impact of Brine Disposal of small scale Desalination Plant on Seawater Composition. *International Desalination Association IDA-NEWS* Vol. 16, issue 5-6, May/June 2007, pp. 4-5.

- Bashitialshaaer, R., and Persson K.M. 2007. The Brine Impact. Everything about Water, Desalination Magazine. pp. 56-59, November 2007.

Conference papers and works

- Member and Facilitator of the IDA Environmental Task Force (ETF) Round Table in the Environmental Symposium, “*Desalination and the Gulf: The Relationship between the Environment and Meeting the Region’s Water Needs*”, Crowne Plaza, Manama, Kingdom of Bahrain (BHR2010), December 6-7, 2010.
- Bashitialshaaer, R., Persson, K.M., and Aljaradin, M. 2010. *The Dead Sea Future Elevation. International Conference on Energy, Water & Environment (ICEWE 2010)*. Amman, Jordan, December 12-15, 2010.
- Bashitialshaaer, R., Bengtsson, L., Larson, M., and Persson, K.M, Aljaradin, M., and Al-Itawi H., 2010. Sinuosity effects on Longitudinal Dispersion Coefficient. The International Conference on Energy, Water and Environment (ICEWE 2010) Ammam, Jordan 12 - 15 December 2010.
- Bashitialshaaer, R., and Persson K.M. 2010. Desalination and Power Plants Together for Water and Peace. A Case study of the Gaza-Strip, Palestine. Handshake across the Jordan: Water and understanding, 26-28, September, 2010. Pella, Jordan.
- Bashitialshaaer, R., Aljaradin, M., and Persson, K.M. The Environmental Impact of the Dead Sea Future Elevation. Handshake across the Jordan: Water and understanding, 26-28, September, 2010. Pella, Jordan.
- Bashitialshaaer, R., and Persson K.M. 2010. Environmental Effects of Large-scale Desalination Plant in the Middle East. WOCMES 2010, The World Congress for Middle Eastern Studies (WOCMES 2010) organized by the European Institute of the Mediterranean (IEMed), Barcelona, Spain, 19-24 July, 2010.
- Liu S., Bashitialshaaer, R., and Persson K.M. 2010. Prospects for Desalination as a Water Supply Method. Proceedings 9th Membranes in Drinking and Industrial Water Treatment (MDIW2010), 27-30 June, 2010, NTNU-Trondheim, Norway.
- Bashitialshaaer, R., and Persson K.M. 2010. Desalination and Economy Prospects as Water Supply Methods. Proceedings *ARWADEX-Water Desalination Conference in the Arab Countries. King Faisal Conference Hall Riyadh, KSA April 11-14, 2010*.
- Bashitialshaaer, R., Flyborg, L., and Persson, K.M. 2009. Environmental assessment of Brine Discharge including Wastewater Collection in the Arabian Gulf. Proceedings 12th IDA World Congress – Atlantis, The Palm – Dubai, UAE November 7-12, 2009.
- Bashitialshaaer, R., Persson, K.M., and Larson, M. 2009. Estimated Future Production of Desalinated Seawater in the MENA Countries and Consequences for the Recipients. Proceedings 12th IDA World Congress – Atlantis, The Palm – Dubai, UAE November 7-12, 2009.
- Bashitialshaaer, R., Persson, K.M., and Larson, M. 2008. Mixing Time for the Dead Sea Based on Water and Salt Mass Balances. Proceedings 5th EUROMED, Desalination Cooperation among Mediterranean Countries of Europe and the MENA Region, *European Desalination Society, Dead Sea, Jordan, November 9-13, 2008*.

Master Thesis and Supervision

- Jacopo Grazioli and Davide Aldo Noro “Evolution of a negatively buoyant jet in the near and intermediate field”. Laboratory experiments and Mathematical modeling. Water Resources Engineering Department of Building and Environmental Technology, Lund University, TVVR 10/0000, ISSN 0000-0000, Lund 2010.
- David Sánchez “Near-field evolution and mixing of a negatively buoyant jet consisting of brine from a desalination plant” Water Resources Engineering, Department of Building and Environmental Technology, Lund University, TVVR 09/5011, ISSN 1101-9824, Lund 2009.

ABBREVIATIONS & SYMBOLS

A	Cross-section area
ADCP	Acoustic Doppler Current Profiler
AG	Arabian Gulf (Persian Gulf)
AMTA	American Membrane Technology Association
APP	Atomic Power Project
B_o	Buoyancy flux at the nozzle
b	Width
b_T	Width of the concentration profile
BWRO	Brackish water reverse osmosis
c	Concentration
Ca	Calcium
Cl_2	Chlorine
c_a	Ambient concentration
c_m	Centerline concentration
c_{mo}	Initial centerline concentration
CORMIX	Cornell Mixing Zone Expert System
D	Mixing tank diameter
Dilution	Dilution is defined as initial concentration C_0 over dilution at a point C
d_0	Nozzle diameter
EC	Electric Conductivity
ED	Electrodialysis
EDS	European Desalination Society
Far-field	Region of the receiving water where buoyant spreading motions and passive diffusion control the trajectory and dilution of the effluent discharge plume
Fr	Densimetric Froude number
GCC	Gulf Cooperation council
g	Gravitational acceleration
g'	Effective gravitational acceleration
H	Mixing tank depth
h	Water depth
H_2SO_4	Sulfuric acid
IDA	International Desalination Association
IEA	International Energy Agency
K	Potassium
KCl	Potassium chloride
KSA	Kingdom of Saudi Arabia
kWh/m^3	Kilowatt hours per cubic meter
K_y	Trajectory relationship coefficients (K_{x_y} , K_{y_m} , $K_{x_{ym}}$, K_{x_e} & K_{x_i})
L	Mixing tank length
LA	Light attenuation system
LIF	Laser induced fluorescence system
l_M, l_Q	Characteristic length scale;
LOICZ	Land-Ocean Interactions in the Coastal Zone
M	Momentum flux at the nozzle
M_o	Initial momentum flux

M0	Measurements along the centerline
MED	Multi-effect distillation
MEDRC	Middle East Desalination Research Center
MENA	Middle East and North Africa
MF	Microfiltration
MFI	Modified fouling index
Mg	Magnesium
Mm ³ /d	Million cubic meters per day
MSF	Multi-stage flash distillation
MS	Mediterranean Sea
MW	Megawatt
MWh	Megawatt hours
Na	Sodium
Near-field	Region of a receiving water where the initial jet characteristic of momentum flux, buoyancy flux and outfall geometry influence the jet trajectory and mixing of an effluent discharge
NF	Nanofiltration
NGO	Non-governmental organization
O&M	Operation and maintenance costs
pH	Measure of the acidity or basicity of a solution
ppb	Parts per billion (e.g. $\mu\text{g/kg}$)
ppm	Parts per million (e.g. mg/kg)
ppt	Parts per thousand (e.g. g/kg)
psu	Practical salinity unit
Q	Volume flux at the nozzle
Q _{Brine}	Brine discharge volume (Q_B)
Q _E	Average annual evaporation
Q _{EX}	Mixing volume (exchange volume between system body and ocean)
Q _N	Residual volume transport associated with freshwater discharge
Q _F	Fresh water volume (Q_F)
Q _{Intake}	Intake seawater volume (Q_I)
Q _P	Average rainfall
Q _{RI}	Rivers' and springs' volume
Q _T	Total discharge (brine + wastewater)
Q _W	Wastewater discharge
r	Recovery ratio
RO	Reverse osmosis
RS	Red Sea
S	Salinity
S _b	Bottom slope
S _{Brine}	Brine salinity
S _F	Fresh water salinity (permeated water)
S _{Intake}	Intake salinity
S _L	Salinity at $x = L$
S*	Salinity for the case without seawater desalination
SO ₄	Sulfate
S _{ocn}	Adjacent ocean salinity

S_{sys}	System salinity
T	Temperature SWRO Seawater reverse osmosis
TDS	Total dissolved solids
TP	Thermal Processes
UAE	United Arab Emirates
u	Velocity
u_j	Nozzle velocity
u_o	Initial velocity
UF	Ultrafiltration
UK	United Kingdom
u_m	Centerline velocity
US	United States
VC	Vapour compression
W	Mixing tank width
WHO	World Health Organization
x	Coordinate directed offshore
X_e	Distance to edge point
X_y	Distance to maximum height
X_{Ym}	Distance to maximum jet edge height
y	Coordinate alongshore
Y	Maximum jet trajectory height
Y_m	Maximum jet edge height
α	Entrainment coefficient
δ	Dirac delta function
λ	Empirical coefficient of the spread of concentration and jet velocity
θ	Discharge angle
ρ	Tap water density
ρ_a	Ambient density
ρ_j	Effluent density
τ	Exchange time

CONTENTS

ACKNOWLEDGMENTS	i
ABSTRACT	ii
ABSTRACT (Swedish)	iv
ABSTRACT (Arabic)	v
APPENDED PAPERS	vi
ABBREVIATIONS & SYMBOLS	ix
1 Introduction	1
1.1 Background	1
1.2 Objectives and Procedures	2
1.3 Thesis structure	4
2 Desalination and Data	7
2.1 Background to Desalination	7
2.2 Desalination Intakes/Outfalls	9
2.3 Desalination Technologies and Raw Water	11
2.4 Cost of Desalination and Energy	12
2.5 Environmental Impacts of Brine Discharge	13
3. Jet Evolution and Mixing	15
3.1 Jet Flow	15
3.2 Flow Fields	15
3.2.1 Near-field	15
3.2.2 Intermediate-field	16
3.2.3 Far-field	16
3.3 Mixing	16
3.4 Mixing in Straight and Irregular Channels	17
4. Methodologies	19
4.1 Field Work and Experiments	19
4.1.1 Field Work	19
4.1.2 Experimental Work	20
4.2 Mathematical Modelling	21
4.2.1 Water and Salt Mass Balances	21
4.2.2 Simple Jet Model	22
4.2.3 One-D Advection-Diffusion Equation	23
5. Results and Recommendations	25
5.1 Field Work Procedure	25
5.2 Experimental Data Analysis	26
5.3 One-D Advection-Diffusion Equation	27
5.4.1 Recommendations	28
5.4.2 Future Studies	30
6. Conclusions	33
7. References	35

1 Introduction

1.1 Background

Desalination is an important source of fresh water in many countries around the world, especially in the Gulf area. High population growth and climate change have led to more severe water scarcity, causing several communities and researchers to propose the construction of desalination plants. Because virtually all seawater desalination plants will be located in the coastal zone, the construction and operation of the facilities will have to adapt to more or less strict environmental protection rules for coastal zones and other legislative issues related to brine discharge (Bahrain meeting 2010). The legal demands on desalination plants vary between countries. The increase in desalination capacity in countries with a shortage of water is a concern due to the environmental impact involved. Desalination leads to higher brine discharges that must be handled through stricter environmental regulations.

Impact on the environment from desalination plants can occur due to the high salt concentration in the brine discharge. The brine also contains some chemicals used in the pre- and post treatment of desalination that may negatively affect coastal areas and the marine ecosystem. Many plants use biocides such as chlorine to clean pipes or to pre-treat the water. These chemicals should be removed before the brine is discharged to the ocean, which is not always the case. Large-scale desalination plants use the latest technology but consume more energy than smaller plants. Three major driving forces have been identified mainly for oil countries in relation to new desalination plant projects, namely oil production, population growth and renewable water resources (see **paper VI**).

In this study, three important regions have been investigated; the Arabian/Persian Gulf, the Mediterranean Sea and the Red Sea plus the proposed Red Sea-Dead Sea canal (RSDSC) project including a large-scale desalination plant (see **paper IV, VIII**). Brine discharge to the sea is the main management approach for brines. The simplest method is to discharge at the coastline. Mixing was also proposed as a solution to reduce environmental impact, as was the reuse of wastewater for other purposes such as agriculture. The decision whether to mix wastewater with brine discharge or to reuse it is a difficult one (see **paper III**).

Some important criteria might influence the idea above, especially in a semi-enclosed recipient (Gulf region), such as changing brine concentration, exchange water with the Ocean and an increase in the amount of water discharged. The mixing of brine discharge has been practised in some countries, not only with wastewater but also with cooling water from power plants, e.g. in Australia. Many years ago, discharging the brine water through a longer pipe towards the sea was proposed as a simple method of reducing coastline salinity by increasing the volume of the recipient at the discharge point. Another idea is the evaporation pond, in which water is evaporated and chemicals extracted. The result of EMU field work clearly showed that building parallel brine discharge outlets and changing from one to the other can also minimize the impact (see **paper IX**). In order to find the best way (minimum impact) of carefully discharging brine water to the sea, more studies including field measurements and experimental work are necessary.

The shallowness of the Gulf makes it more important to study than the other two regions, as the maximum depth comprises less than 100 m over its entire area with a mean of only 35 m (Reynolds 1993). This leads to the formation of a very saline and dense water, with maximum salinities as high as 57 g/l along the southern coast (John et al. 1990). The Gulf covers an area of about 240,000 km², 1000 km in length and widths ranging from 185 km to 370 km, with a mean of 240 km and a volume of approximately 8,400 km³. The freshwater inflows from the Tigris, the Euphrates and the Karun at the Shatt al Arab delta are estimated at about 48 km³/yr (Reynolds 1993, Hunter 1986). The Gulf mean annual evaporation rate is approximately 1.5 m/yr compared to an average precipitation of 100mm/yr (Brewer and Dryssen 1985).

The Mediterranean Sea, including the Sea of Marmara, occupies an area of approximately 2,960,000 km². The Mediterranean is connected to the Atlantic Ocean by the narrow and shallow channel of the Strait of Gibraltar and to the Black Sea through the Dardanelles (Britannica <http> 2009). The typical values for the Mediterranean Sea comprise a mean width of about 800 km, a mean depth of approximately 1500 m, an extreme length of about 3,860 km, an average length of approximately 2700 km and an evaporation rate of approximately 1.3 m/yr (Moncef and Bernard 2000, Rahmstorf 1998). The maximum width of the Red Sea is about 225 km with mean depth of around 500 m and it's a gross length of about 2000 km. Its area approximately 450,000 km² and mean width of about 225 km, the Sea has an evaporation rate of approximately 2 m/yr (Purnama et al. 2005).

The Dead Sea is mainly fed by the Jordan River, which enters from the north. Several smaller streams also discharge into the Dead Sea, primarily from the east. The Dead Sea has no outlet and its water is transported away by evaporation, which is rapid in the hot desert climate. Gavrieli et al. (2005) reported a density and salinity of the Dead Sea of about 1237 kg/m³ and 342.4 g/l, respectively, whereas Vengosh and Rosenthal (1994) reported the Dead Sea salinity to be about 332.06 g/l. In 1997 the Dead Sea level was 390 bmsl, surface area 950 km² and volume 155 km³, while precipitation was 70-90 mm and evaporation 1300-1600mm/y (Gavrieli, & Bein, 2006; Gavrieli, 2000 and 1997).

1.2 Objectives and Procedures

The water intake to most of the world's desalination plants is located in the same place as the brine discharge. Some chemical and other parameters have to be considered as a function of the brine discharge from all desalination plant to assist people from an environmental and economic perspective, since fishing problems could increase in the future. More objectives were added to this study in order to find the relationships between an increase in desalination plant production and salinity increase in the recipient.

The first part of this study started in Cyprus with the small-scale desalination plant at the Eastern Mediterranean University, located on the Mediterranean Sea coastline. The idea was to investigate the brine discharge from this plant, how the brine plume spread out in the recipient and to assess any negative environmental impacts. Thus, the main objective was to study brine discharge from EMU desalination plant through field measurements. Looking more closely at the coastline near the discharge point revealed a different water colour to that of normal sea water. No swimming was allowed in this area. The most

important chemicals analysed were (Ca, Mg, Cl, SO₄, Na, pH, K, Electrical Conductivity, Alkalinity, and TDS), (see **paper IX**). It was decided to continue to perform the small-scale laboratory experiment. Two sets of experiments were studied for negatively buoyant jet, each with a total of 72 runs in order to:

- Understand jet behaviour when brine is discharged into a stagnant ambient and to find the maximum elevated level of the jet.
- Find the effect of the initial jet angle on mixing between a denser fluid comprising sodium chloride solution and tap water.
- Evaluate the importance of bottom slope with and without inclination and the effect of lateral spreading and centreline concentration.
- Compare with established hydraulic modelling software, e.g. CORMIX program.
- Compare with the Matlab code to see how the prediction of this code can be used in practical work; see (**Papers I, II**).

The continuous increase in desalination plant projects at the coasts of Seas and Oceans inspired me to study the environmental impacts of brine discharge by means of brine modelling, experimental work and measurement analysis. This increase in desalination production will lead to a greater amount of brine discharge in the world, particularly in the Arabian Gulf, the Red Sea and the Mediterranean Sea. Therefore, the following studies have been conducted (see **paper III**):

- Environmental assessment of brine discharge including wastewater mixing in the Arabian Gulf.
- Future salinity in the Arabian Gulf, the Mediterranean Sea and the Red Sea and consequences of brine discharge from desalination estimated by using 1D advection-diffusion equation.
- Water and salt mass balances were used for both studies.

Two more applications were included in the study. The first case, an infrastructure solution for Sinai and the Gaza Strip, is the suggested building of a joint power and desalination plant, located in Egypt close to the border with Gaza (see **paper VII**). This type of project improves the water and electricity supply and should ease border tensions. The second case concerns the effect of additional water coming from a proposed project on variations in the water level, surface area and volume of the Dead Sea (see **paper VIII**). In this investigation, the effect of brine discharge was evaluated from both a hydraulic and an environmental perspective. In this study, the mixing time for the Dead Sea was considered (i.e. theoretical time for Dead Sea surface water to mix with the entire water body).

1.3 Thesis structure

The thesis consists of desalination theory, experimental work including modelling, field measurements and some applications. In the first part, two different lab-scale experiments were performed and investigated (see **papers I, II**):

- Negatively buoyant jet and jet lateral spreading.
- Investigation of how a negatively buoyant jet develops in the near-field and mixes with the ambient water.
- Study of different initial jet inclination angles.
- Exploration of the behaviour of a dense jet and bottom plume in the near and intermediate fields.
- Inclined negatively buoyant jet with and without bottom slope.
- Experimental data were compared with the CORMIX package.
- This study also developed a Matlab code for describing lateral spreading.

Environmental impacts from large scale desalination plants have been discussed and summarized for the three regions (see **papers III, IV**). A number of parameters were evaluated:

- The amount of brine for each country with desalination plants.
- Inputs and outputs for each system such as fresh water from rivers, evaporation amount and precipitation.
- Allocations and mixing of wastewater, cooling water from power plants and brine discharge.
- Establishing water and salt mass balances to find residual flow, exchange flow and exchange time.
- Determining the long-term effects of brine discharge from desalination plants in the three regions for 1996 and 2008, and a prognosis for 2050.

Three major questions related to desalination plant projects were considered in this work as presented in **paper VI**, where the finding is helpful for new projects. The following questions were answered:

- What are the driving forces behind investment in desalination plant projects?

- What is the percentage of fresh water produced by desalination compared to renewable water resources?
- Where is the highest growth in population, desalination and oil production?

Four more studies were added related to desalination production, discharge mixing, water scarcity and the environmental impacts of brine discharge (see **papers V, VII, VIII, IX**).

- Analysing the variations in the water level, surface area and volume of the Dead Sea.
- Studying a joint power and desalination plant for Sinai and the Gaza Strip located in Egypt but close to the border with Gaza.
- Investigating sinuosity effects in the longitudinal dispersion coefficient.
- Field measurement from RO-plant in Cyprus.

2 Desalination and Data

2.1 Background to Desalination

Desalination has been a freshwater supply opportunity for a long time, especially in remote locations and on naval ships at sea. A British patent was granted for such a device in 1852 (Simson 1998). The island of Curaçao in the Netherlands Antilles has had desalination plants in operation since 1928. A major seawater desalination plant was built in 1938 in what is now Saudi Arabia and an early version of a modern distillation plant in Kuwait in the early 1960s (Cooley et al. 2006).

The concept of desalination refers to a wide range of processes designed to remove salts from brackish water, seawater and Oceans that may contain different salinities, thus providing fresh water. The TDS concentration in fresh or drinking water must be less than 400mg/l (WHO standard). Desalination is an important method for producing potable water in the world. Usually a country is considered at risk of water shortage if renewable water resources are below 1000 m³/capita/yr (Al-Gobaisi 1997). Desalination is a rapidly growing technology, as evidenced by the large number of regional and international organizations established during the last 30 years:

- International Desalination Association (IDA)
- Australian Desalination Association (AuDA)
- European Desalination Association (EDS)
- Indian Desalination Association (InDA)
- American Desalination Association (ADA)
- Middle East Desalination Research Center (MEDRC)

The amount of water in the hydrosphere is estimated to be about 1,400 Mkm³, 95.5 % of which is saltwater present in oceans and seas, and the remaining 4.5 % is fresh water (Ruiz and Gonzalez 2007). The world average renewable hydrological resources (excluding desalted and reused waters) are about 42,750 km³/yr, or 1 % of the total volume of superficial waters (fresh as well as salt). 50 % of the renewable water resources are contained in only nine country (i.e. Brazil, Canada, Russia, United States, China and India). Five great rivers discharge 27 % of these renewable resources to the sea (Amazon, Ganges-Brahmaputra, Congo, Yellow and Orinoco) (Valero et al. 2001, Ruiz and Gonzalez 2007).

Ninety-seven percent of the Earth's water is found in oceans with a salt content of more than 30,000 mg/L. Water with a dissolved solids (salt) content below about 1000 mg/L is considered acceptable for a community water supply (Buros 2000). Karagiannis and Soldatos (2008) reported that about 25% of the world's population does not have access to

satisfactory fresh water, more than 80 countries are facing severe water problems and only 3% of all water sources are regarded as potable. By 2002, over 10,000 industrial-scale desalination units with a total capacity of 32.4 million m³/d had been installed or contracted worldwide (Zhou and Tol 2005). Non-seawater desalination plants contributed 13.3 million m³/d, while the capacity of the seawater desalination plants reached 19.1 million m³/d (Wangnick 2002). The installed capacity increased rapidly worldwide, from 8000 m³/d (in 1970) to about 32 Mm³/d (by 2001), with seawater desalination plants accounting for 19.1 Mm³/d and Non-seawater for 13.3 Mm³/d (Wangnick 2002). Today, the global desalination capacity has grown to an output of more than 60 Mm³/d from over 13,500 desalination plants worldwide (IDA year book 2009-10).

Today's largest desalination capacity is found in Saudi Arabia, with a daily capacity of about 5, 7.75 and 39.7 million cubic meters in 1996, 2008 and 2050 respectively. The newly contracted desalination plant in Ras Azzour, KSA, will be the largest in the world, producing about 1,036,500 m³/d and is scheduled for completion at the end of 2014. It will be integrated into a 2,400 MW joint power plant costing a total of US\$ 1.46 billion (Desalination news, Sept. 2010).

The largest number of desalination plants can be found along the shores of the Arabian Gulf with a total seawater desalination capacity of approximately 45% of the worldwide daily production. The main producers in the Gulf region are the United Arab Emirates, Saudi Arabia (9% from the Gulf region and 13% from the Red Sea), Qatar and Kuwait (Lattemann and Höpner 2008, Wiseman 2006). In the Mediterranean, the total daily production from seawater is about 17% of the world total desalination capacity. Spain is the largest desalination producer in Europe with 7% of the worldwide capacity. The main process in Spain is reverse osmosis (RO) comprising 95% of all Spanish desalination plants (IDA 2006, Lattemann and Höpner 2008).

The third highest daily production of desalinated water can be found in the Red Sea region, with a combined capacity of 14% of the world total desalination capacity (IDA 2006, Lattemann and Höpner 2008). The exchange of water between the Red Sea and the Gulf of Aden occurs at the strait of Bab el Mandab. There is virtually no surface water runoff because no river enters the Red Sea (Shahin 1989, Morcos 1970). The results of brine discharge, Q_{Brine} (10⁶ m³/d) in the Arabian Gulf (AG), Mediterranean Sea (MS) and Red Sea (RS), in late 1996, 2008 and prognosis for 2050, are presented in Figure 2.1. The red arrows indicate the location of the exchange water, e.g. river inflow, inflow through the Dardanelle Strait from the Black Sea and exchange flow from the Gibraltar Strait etc, for the three systems.



Figure 2.1 Brine water Q_B results in $10^6 \text{ m}^3/\text{d}$ for the Arabian Gulf (AG), Mediterranean Sea (MS) and Red Sea (RS) in 1996, 2008 and 2050 (map from: Google Earth)

2.2 Desalination Intakes/Outfalls

There are three types of desalination method used throughout the world for a wide range of purposes, but mainly for potable water production for industrial and municipal use.

- Membrane Systems:** Reverse osmosis (RO) or Electrodialysis and Electrodialysis Reversal (ED) (Sedlak and Pinkston 2001, NAS 2004, Heberer et al. 2001).
- Thermal Processes (TP):** Multi-Stage Flash Distillation (MSF), Multiple-Effect Distillation (MED) and Vapor Compression (VC) (Birkett 1999, Wangnick 2005).

Other Desalination Processes: Different types of water can be desalinated through many other processes including small-scale ion-exchange resins, freezing and membrane distillation (MD) (Wangnick 2005).

The relation between intakes and outfalls of desalination plant is defined as the recovery ratio. Due to the development in desalination technology in recent years, the recovery ratio r has significantly increased in reverse osmosis plants. In the modern plants of today, recovery reaches about 40% and in some cases almost 50%. Figure 2.2 is a typical diagram

of a seawater desalination plant including pre and post treatment, where S_{Intake} and Q_{Intake} are salinity and volume of seawater intake, S_{Brine} and Q_{Brine} salinity and volume of brine discharge and S_F and Q_F salinity and volume of fresh water produced by the desalination plant. $S_{\text{Brine}} = S_{\text{Intake}}/(1-r)$ and $Q_{\text{Brine}} = (1-r)Q_{\text{Intake}}$, where r is the recovery ratio of 35-40% of the intake and $S_F \approx 0$ and $Q_F = rQ_{\text{Intake}}$.

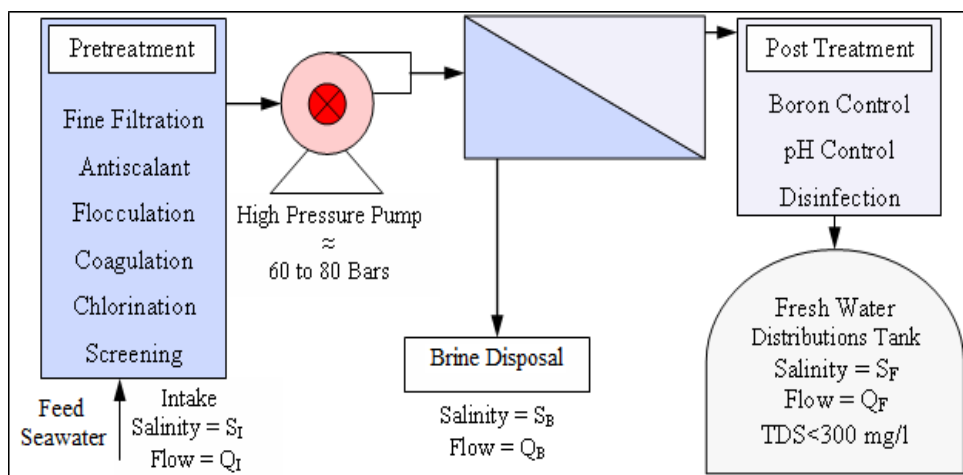


Figure 2.2 A typical reverse osmosis seawater desalination plant scheme showing input/output and different stages of treatment. Note that boron control involves a second RO stage (BWRO), which also produces brine with a low TDS (<3000mg/l).

Brines from thermal desalination plants can be mixed with cooling water to reduce the temperature or with wastewater to dilute the brine salinity, which may give the effluents a positive buoyant. If not mixed with cooling water or wastewater, the brines can still have a negative or neutral buoyant, depending on salinity and temperature. Table 2.1 presents the calculated salinities for brine from SWRO plant discharge, for feedwater salinities of 30-40‰ and recovery rates of 30-60%, assuming a permeate salinity of 0.3 (Lattemann 2010). The salinity values of brine discharge are derived by the equation $S_B = (Q_I * S_F - Q_F * S_F) / Q_B$.

Table 2.1 Calculated salinity of seawater reverse osmosis plant retentate brines (Lattemann, 2010)

Recovery r	Feedwater salinity, S_F										
	30	31	32	33	34	35	36	37	38	39	40
30%	43	44	46	47	48	50	51	53	54	56	57
35%	46	48	49	51	52	54	55	57	58	60	61
40%	50	51	53	55	56	58	60	61	63	65	66
45%	54	56	58	60	62	63	65	67	69	71	72
50%	60	62	64	66	68	70	72	74	76	78	80
55%	66	69	71	73	75	77	80	82	84	86	89
60%	75	77	80	82	85	87	90	92	95	97	100

2.3 Desalination Technologies and Raw Water

Since the early 1970s, the number of installed reverse osmosis plants has grown and they have some advantages and disadvantages compared to thermal systems. Thermal desalination systems produce water quality of less than 25 parts per million (ppm) as total dissolved solids (TDS) compared to membrane systems of less than 500 ppm TDS (USBR 2003). The main thermal processes include multistage flash evaporation (MSF), multiple effect evaporation (ME) and vapour compression (VC).

The membrane processes contain reverse osmosis (RO), electrodialysis (ED) and nanofiltration (NF). The MSF and RO processes dominate the market for both seawater and brackish water desalination, sharing about 88% of the total installed capacity (Wangnick 2002). Distribution can be seen in Figure 2.3, compiled at the end of 2001. The installed capacity by technology is as follows: reverse osmosis (RO) 58 %, multi-stage flash evaporation (MSF) 27 %, multi-effect distillation (MED) 9 %, electrodialysis (ED) 4 % and 1% hybrid (GWI Desalination data IDA 2008–09). The difference in the two references is due to different years of compiling this percentage, of which 2008–09 is the most recent and accurate.

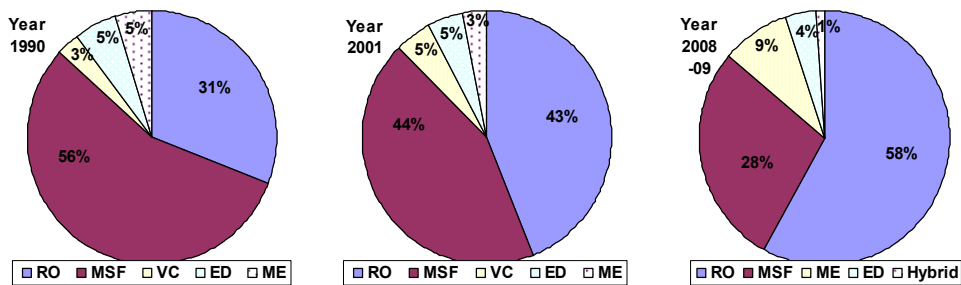


Figure 2.3 Global distributions of fresh water production by desalination technology in the years 1990, 2001 and 2008-09.

Six different input water sources were used to produce fresh water (seawater, brackish water, wastewater, rivers, brines and pure water). The proportions of different water sources seem to have almost the same percentages over the last 30 years. Saline raw water from the sea ranges from 56 to 65% of all feed waters and brackish waters range from 20 to 24% over the years. Wastewater gradually seems to be becoming more important, although in 2009 only 5% of all raw waters had their direct origin from wastewater systems. The potential in reusing wastewater is thus very large, see Figure 2.4.

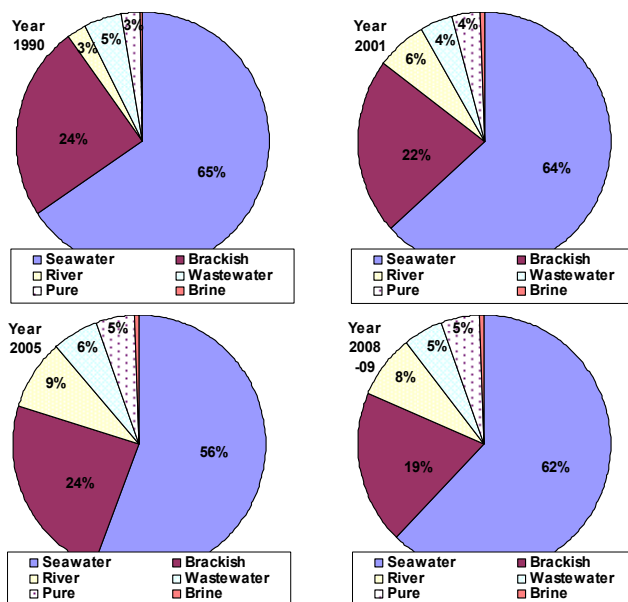


Fig. 2.4 Global distributions by raw water for desalination in the years 1990, 2001, 2005 and 2008-09

2.4 Cost of Desalination and Energy

According to Karagiannis and Soldatos (2008), the energy needed for desalination is divided into two categories 1) conventional mainly fossil energy (gas, oil, nuclear power) and 2) renewable energy (wind, solar, etc). The cost of fresh water produced from desalination using conventional sources of energy is at present much lower (Karagiannis and Soldatos 2008). Desalination powered by renewable energy sources may be an attractive solution in terms of induced environmental impact due to lower conventional energy consumption and reduced gas emissions. In some cases these systems are connected with a conventional source of energy (e.g. local electricity grid) in order to minimize the variations in the level of energy production and consequently water production (Karagiannis and Soldatos 2008).

The specific energy needed for desalination of seawater reverse osmosis (SWRO) has decreased with the development of energy reuse systems. At present, 1 cubic meter of desalinated water consumes 3.7 kWh of energy, mainly electricity (Gary 2006). Although the investment and operational costs of desalination plants depend on location, total production costs decreased from roughly \$2.5/m³ in the late 1970s to \$1.5/m³ in the early 1990s to around \$0.50/m³ in 2003 (Pankratz 2004). Dore stated that the current costs associated with brackish water lie in the range 0.07 - 0.08\$ per m³ and for seawater 0.50 - 0.70\$ per m³, including capital and operating costs (Dore 2005). According to (AMTA 2003), the cost of brackish water desalination ranges between 0.38 and 0.75\$ per m³ and seawater varies between 0.75 and 2.0\$ per m³.

The production unit cost of seawater desalination dropped significantly between 1955 and 2009 and will probably fall to less than 0.5 \$/m³ in 2020. This result was presented by Bashitialshaer and Persson (2010) and data were extracted from the International Desalination Association (IDA) yearbooks 2006-07, 2007-08, 2008-09 and 2009-10 pertaining to 18 different projects, some with similar intake salt concentration, mainly in Middle Eastern countries. The desalination plant capital cost for the production of 1 m³ a day was found to be about 1080 \$ (approx. 1 million \$ to produce 1000 m³/d). It was also found that the average cost of producing 1 Watt from the power plant was equal to about 1 \$ (approx. 1 million \$ to produce 1 MW) (Bashitialshaer and Persson 2010).

2.5 Environmental Impacts of Brine Discharge

The concentration of brine discharge from desalination plants is always higher than that of natural seawater. Brines are normally returned to the sea. The major concerns for the marine environment are the construction of intake and outfall from the desalination plant and the coastal area, the impingement and entrainment of marine organisms with the intake water, which may have an effect on ecosystem population dynamics. Other concerns are the concentrate and chemical discharges into the sea (Lattemann and Höpner 2008, 2009, 2010). The salt concentrations of the brines are usually found to be double or close to double that of natural seawater (Vanhems 2001). The total dissolved solids (TDS) in the three main regions are about 38.6, 45 and 41 g/l for the Mediterranean, the Arabian Gulf and the Red Sea respectively, compared to typical seawater of about 34.5g/l (Magazine 2005).

The reject streams of SWRO and desalination plants generally affect different realms of the marine environment. The SWRO concentrate, if not dissipated, will spread over the sea floor and may affect benthic communities, whereas the reject streams of desalination plants will likely affect the whole water column for two reasons: the outfalls are usually located directly on the shoreline, i.e., in shallow water, and the plants have large discharge flow rates. A more detailed review of the scientific literature concerning monitoring and bioassay studies of desalination projects has been carried out and published in (Lattemann et al. 2008). The aforementioned study used a wide range of approaches and methods to investigate the environmental impacts of desalination plant discharges.

Cleaning chemicals from the desalination plants are also an issue and may impact on the environment, especially in the vicinity of the coastline. The cleaning frequencies depend on the raw water quality. Cleaning is typically carried out at 1-2 year intervals in SWRO plants operating on beachwell water and more frequently, often several times per year, in SWRO plants operating on surface seawater (Wilf et al. 2007). Chemical cleaning is often performed in two stages, first with an acidic and then an alkaline solution (Mauguin and Corsin 2005). More information can be found in Table 2.2, where some properties of the effluents of SWRO, MSF and MED plants with conventional process design are summarized.

Table 2.2 Some properties of the effluents of SWRO, MSF and MED plants with conventional process design (from: WHO 2010, Lattemann and Höpner 2008).

	Seawater reverse osmosis (SWRO)	Multi-stage flash evaporation (MSF)	Multi-effect distillation (MED)
Physical parameters	SWRO: no use of cooling water in the process, but RO plants may receive their intake water from cooling of power plants.	MSF/MED: it is assumed that the two waste streams from the desalination process are typically combined, i.e., the brine is diluted with major amounts of cooling water from the desalination process. Further dilution with cooling water from power plants may occur but is not considered.	
Salinity (S) depending on ambient salinity and recovery	SWRO: 65-85 BWRO: 1-25	Cooling water S: ambient. Brine S: typically 60-70. Combined S: typically 45-50.	Cooling water S: ambient. Brine S: typically 60-70. Combined S: typically 50-60.
Temperature (T) depending on ambient temperature	If surface intakes are used: may be below ambient T due to a lower T of the source water. If open intakes are used: close to ambient. If power plant cooling waters are used as source: above ambient.	Brine T: 3-5 °C above ambient. Cooling water T: 8-12 °C above ambient. Combined T: 5-10 °C above ambient.	Brine T: 5-25 °C above ambient. Cooling water T: 8-12 °C above ambient, up to 20°C possible. Combined T: 10-20 °C above ambient.
Plume density (ρ)	Higher than ambient (negatively buoyant)	MSF/MED: plume can be positively, neutrally or negatively buoyant depending on the process design and mixing with the cooling water before discharges; typically positively buoyant due to large cooling water flows.	
Cleaning solutions (if discharged into surface water)			
Cleaning chemicals (used intermittently)	Alkaline (pH 11-12) or acidic (pH 2-3) solutions containing cleaning additives, e.g.: Detergents (e.g., dodecylsulfate) Complexing agents (e.g., EDTA) Oxidants (e.g., sodium perborate) Biocides (e.g., formaldehyde)	Acidic (low pH) washing solution may contain corrosion inhibitors such as benzotriazole.	

3. Jet Evolution and Mixing

3.1 Jet Flow

In this chapter, the jet flow is described to improve understanding of the behaviour of negatively buoyant jet. The discharge of fluid from small nozzles or a slot into a large ambient of the same or a similar fluid composition is the so called jet flow. Most of the discharges in our environmental cases are classified as buoyant jets, which differ from sources of momentum and force of buoyancy, e.g. brine discharge from a desalination plant and discharge of untreated wastewater. The initial flow can be derived from the momentum of the fluid flow, but the effluent may be less or denser than the ambient and the resulting jet acts as a buoyant force. There are two different types of jet flows namely simple jet and buoyant jet.

Jet and similar flow problems have previously been studied and analysed by several authors (Pincince and List 1973, Fischer et al. 1979, Roperts and Toms 1987, Turner 1966, Cipollina et al. 2005). More details can also be found in the user's manual by Jirka et al. (1996), where a hydrodynamic mixing zone model and decision support system for pollutant discharges into surface waters are described. These authors characterize the discharge by its kinematic fluxes of volume Q_o , momentum M_o and buoyancy B_o :

$$Q_o = \frac{\pi d_o^2}{4} u_o; M_o = \frac{\pi d_o^2}{4} u_o^2; B_o = g \frac{\rho_o - \rho_a}{\rho_a} Q_o = g' Q_o \quad (3.1)$$

The jet is discharged at an initial velocity of u_o through a round nozzle with a diameter d_o , yielding ρ_o = effluent density, ρ_a = ambient density, g = acceleration due to gravity and $g' = g(\rho_o - \rho_a)/\rho_a$ = the modified acceleration due to gravity. The most common non-dimensional number used in this study is the densimetric Froude number Fr_d .

$$Fr_d = \frac{u_o}{\sqrt{g' d_o}} \quad (3.2)$$

3.2 Flow Fields

3.2.1 Near-field

Jet behaviour in the near field has been the object of many studies in recent years, mainly because the jet properties are governed by the discharge arrangements, such as the depth of discharge, the type and number of any diffusers, as well as the initial flux of volume, momentum and buoyancy. It is thus possible to control the dilution in the near field, where the dilution and mixing of brines are due to entrainment of ambient water into the jet. In this study, the near field was investigated to determine where the flux was mainly influenced by buoyant forces and where the buoyant jet wited into a bottom plume.

Olsson and Fuchs (1996) conducted a study on a large eddy simulation (LES) of the near-field from a round jet, this region was found to be in the range of ($3 \leq x/d_0 \leq 9$).

3.2.2 Intermediate-field

The intermediate-field is where the initial near-field jet flux properties slowly change into a bottom density plume subject to passive diffusion, the main process that governs jet evolution at a certain distance from the source point. This extension of the mixing zone is difficult to define as it is greatly dependent upon the initial conditions of the jet and the ambient influences. Christoudoulou (1991) suggested the point of interaction between the negatively buoyant jet and bottom as the start of the intermediate field and stated that the total length of the field is inversely proportional to the drag coefficient. In our experiment, the absence of any ambient forces, for example, wind or current, combined with a glass bottom with a low drag coefficient, prevented the far field from developing completely. As a near-field and intermediate-field property of negatively buoyant jets, the transitional (intermediate) zone is assumed to extend along the entire length of the tank.

3.2.3 Far-field

This study only provides a brief description of the far-field for the sake of completeness. Few brine disposal studies have been conducted in the far-field due to the nature of the transport and mixing processes, which are mainly dominated by advection from ambient currents and mixing from ambient diffusion processes. Ambient currents can be generated by wind, waves and tides. However, advection may appear as “spreading processes due to the buoyant forces caused by the density difference of the mixed flow relative to the ambient density” (Doneker and Jirka 2007).

3.3 Mixing

The term mixing refers to the mechanisms behind the intermingling of parcels of water as they move from one location to another due to freshwater flows, tidal flows and secondary current effects. Discharges with high concentrations of brine and other dissolved substances are transported along estuaries, rivers and open channels by the longitudinal advection associated with large-scale water movements and secondary currents, and by the longitudinal dispersion associated with shear velocity (NSW 2001). Mixing rate or time required for mixing has been extensively used in the calculation of the future Dead Sea elevation. The Dead Sea example illustrates the mixing of different waters entering and leaving the Dead Sea, such as the River Jordan, and brine discharge from the proposed desalination project in the Dead Sea basin. This mixing takes a specific time. The freshwater does not immediately mix with the saltwater and can float for a considerable time on the surface. Until mixing takes place, the excess of less dense water can continuously accumulate and float on the surface of the Dead Sea (see **paper VIII**). Three different types of mixing, namely vertical, lateral and longitudinal, are always present in the case of water movement for different concentrations.

Vertical Mixing: The basic mechanism is the velocity shear caused by the bed of the estuary (surface and mid-depth velocities are faster than bed velocities). In most recipients, vertical mixing is responsible for well-mixed salinity regimes (NSW 2001). Compared with longitudinal mixing, it develops very quickly in most streams and estuaries, especially in shallow places, which may be due to the force of gravity (Jeon et al. 2007).

Longitudinal Mixing: Longitudinal mixing depends on a number of processes, the most important being longitudinal water exchange in response to tidal and freshwater discharges along estuaries and rivers. Velocity shear is also associated with the lateral and vertical variations of longitudinal velocities. Extensive shoals, peripheral bays and channels generate strong velocity shear between fast-moving main channel flows and the slow waters that move in and out of shoal areas, acting on rising and falling tides. Shoals are also considered as roughness in the channel. In general, mixing will be greatest in those estuaries where lateral and vertical velocity gradients are large (NSW, 2001).

Lateral mixing: The mechanisms of lateral mixing of waters across estuaries and rivers are the velocity shear, lateral velocity gradients, wind shear, lateral tidal flows, meanders and bends in the main channels. Water depth is also important (deeper waters flow faster). These mechanisms cause lateral variations in velocity, which result from the presence of the banks of the estuary. The presence of bends and meanders in the channel cross-section is due to water flows from one side to the other and associated with mixing across the channel (NSW 2001).

3.4 Mixing in Straight and Irregular Channels

The flow in straight channels of a great width is one example of a flow which meets all of the requirements for use of turbulent mixing coefficient. This turbulence is considered as homogeneous and stationary in the straight and uniform channels. The natural channels are differing from the straight ones in three important respects: depth irregularity, the shape channel is likely to curve and sidewall irregularities such as groins or accumulation sediment.

The shape of the channel affects the mixing and in nature most channels are irregular or sinuous. The most common definition of sinuosity in rivers and streams is the ratio between the length measured along the flow and the length of the channel, which is always larger than one. The flow velocity is also important as the bank closest to the zone of highest velocity is usually eroded, resulting in a cut-bank leading to sinuous or irregular behaviour (see **Paper V**).

4. Methodologies

4.1 Field Work and Experiments

4.1.1 Field Work

Field work is required at desalination plants to investigate the area surrounding the discharge point where brine is released. The RO-system utilized for the Eastern Mediterranean University EMU desalination plant is located on the Mediterranean Sea coastline. This plant is fed by about 3000m³/d of seawater obtained via three parallel pipes 30m from the coastline at an average depth of 15m. The seawater contains 36,000-40,000 ppm TDS. In this way, 1000 m³ of seawater per day is released as a high quality output (the EMU desalination plant produces water quality of less than 400 ppm TDS, which can be used as drinking water), while approximately 2000m³/d is released from the system as a brine with a salt concentration of about 56,000 ppm TDS (Mukaddas 2004).

Some chemicals (Ca, Mg, Cl, SO₄, Na, pH, K, Electrical Conductivity, Alkalinity, and TDS) and other factors were analysed as a function of the brine disposal from the desalination plant. The sampling locations were selected with respect to an x and a y axis; x is the location of each point in relation to seawater and perpendicular to the coastline and y is the location parallel to the coastline. The analysis was carried out by the State Laboratory of North Cyprus. Samples were collected and recorded twice a month in calm weather (see **paper IX**).



Photo 4.1 Taking samples and recording them

4.1.2 Experimental Work

The idea behind this work was to construct an experimental lab-scale model of the brine discharge from a desalination plant to be used in the field work measurements. Two sets of experiments were carried out separately, each with a total of 72 runs. The first investigated the inclined negatively buoyant jet discharged from the denser tank to the fresh water tank (tap water). Four initial jet parameters were changed, namely nozzle diameter, initial jet inclination, jet density (or salinity) and flow rate (or exit velocity). The measurements of the jet evolution in the tank included five geometric quantities describing the jet trajectory that is useful for the design of brine discharge systems. Thus, the collected data encompassed the maximum elevation of the jet (Y_m) and its horizontal distance (X_{ym}), the maximum level of the jet centerline (Y) and its horizontal distance (X_y) as well as the distance to the edge point (X_e) (where the jet returns to the discharge level) (see **Paper I**).

The second experiment was also carried out for negatively buoyant jet but includes some changes due to the introduction of bottom slope as most of the receiving coastline has a natural bottom slope. The purpose of this study was to explore the behaviour of a dense jet and bottom plume composed of brine water, discharged into a receiving body of lighter tap water. The model was divided into two sub-models, describing the near and the intermediate field properties, respectively, of the discharge for different inclinations and bottom slope. The lateral spreading and electrical conductivity were also described by generalization of measured data. This type of measurement can improve our knowledge of brine discharge when building a new desalination plant or enlarging some of the existing ones (see **Paper II**).

The apparatus and materials used in the lab-scale negatively buoyant jet experiment is presented in (Figure 4.1). These included five different tanks; three small tanks for mixing tap water with salt and colour to obtain the salty water necessary to create the negatively buoyant jet and two large tanks filled with tap water, into which the salty water with the dye was introduced to observe the jet. The large glass tanks had capacities of about 500 and 600 litres. Their dimensions (L x W x H) were (150 x 60 x 60) and (200 x 50 x 60) centimetres. The water temperature was about 20 to 22 C° in all experiments. The frequency-meter was important to be able to test and calibrate prior to regulating the flow-meter and reading the flow in l/min (± 0.01).

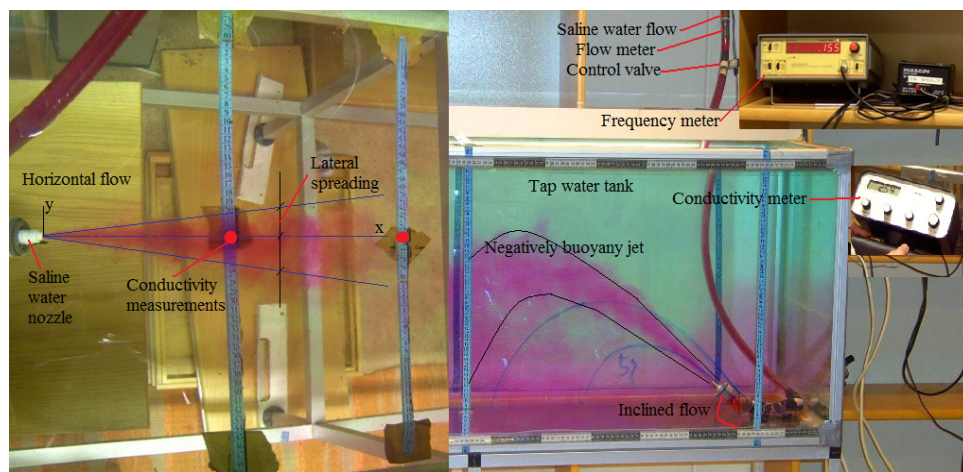


Fig. 4.1 Lab-scale experiment on a negatively buoyant jet and major contents

Sodium chloride solution was mixed with tap water to create denser water in the jet. A conductivity meter was employed to measure conductivity in the three different concentrations. The density measurement was obtained by the weighted method for four concentrations 2, 4, 6 and 8% (20, 40, 60 and 80 g/l) respectively. The density result used in the calculation was an average of five different measurement trials. Small differences in density measurements were reported between the saltwater used in this study and natural seawater. Potassium permanganate (KMnO_4) served to colour the saline water. The dye coloured the transparent water when 0.1g/liter was added. The result of a jar test for (KMnO_4) concentration revealed that at 0.3 mg/l it was still pink but at 0.195 mg/l no pink was visible.

4.2 Mathematical Modelling

4.2.1 Water and Salt Mass Balances

A generalized diagram summarizing water and salt budgets for coastal ecosystems is described in (Figure 4.2). It was essential to use water and salt mass balance in this thesis to determine the changes in the study area of the Mediterranean Sea, the Arabian Gulf, the Red Sea and the Dead Sea. This method worked according to LOICZ biogeochemical modelling (Gordon et al. 1996). The total water received from rivers and springs is denoted (Q_{RI}), average rainfall (Q_P), average annual evaporation (Q_E), the mixing volume (exchange volume between system body and ocean) across the open boundary of the system (Q_{EX}) and the residual volume transport associated with freshwater discharge (Q_N). Q_{Brine} is the brine discharge to the sea and Q_{Intake} the amount of feed water intake to the desalination plant from the open sea or from wells located about 20 to 30 meters away from the coastline. S_{sys} is the system salinity, S_{ocn} the adjacent ocean salinity. All other terms with the exception of precipitation and evaporation have salinity values approximated to zero. The units for all output and input are usually in (m^3/s) and all

concentrations will be assumed to be (g/l). This section was used in three papers (see **Papers III, IV and VIII**).

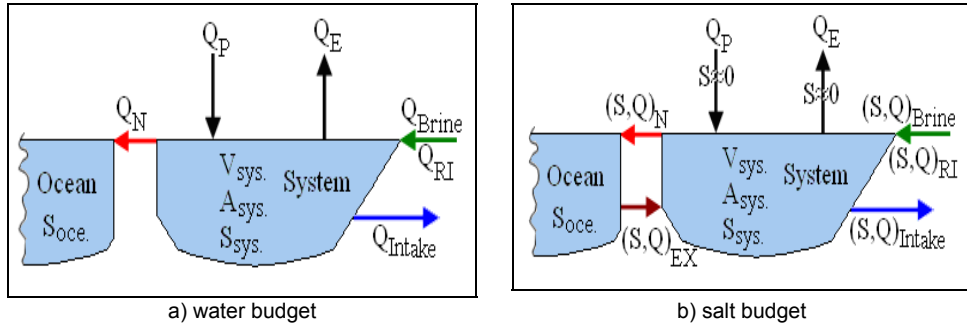


Fig. 4.2 Generalized diagram summarizing water and salt budgets for coastal ecosystems.

In order to keep the volume constant, the same amount of water must flow into and out of the system. This flow known as the "residual flow, Q_N ", or net residual volume. For the salt budget, we assigned related salinity to each of the water inputs and outputs. The inputs and outputs then became each flow multiplied by the appropriate salinities (designated S) for most of the important terms. In this method, the terms with low salinity (having no effect on the system) like evaporation and precipitation, it is sufficient to assume their salinity to be (Zero) and exclude it from the calculations. In which salinity of the exchange volume is the difference between ocean salinity S_{ocn} and system salinity S_{sys} , and the net volume Q_N salinity is equal to the average of ocean and system salinities.

4.2.2 Simple Jet Model

A mathematical model of the brine discharge from the desalination plant and its spread in the nearshore zone was developed based on simple jet theory. The result was compared with field work measurements from the EMU desalination plant. It was assumed that the conditions were uniform throughout the water column and that the discharge behaved like a plane jet that expanded primarily due to entrainment of ambient water at the sides. The assumption of vertical uniformity will clearly be violated some distance from the discharge point and the brine will spread as a gravity current along the bottom, although observations in the study area indicated that the conditions did not vary significantly in the water column. Friction along the bottom was also neglected in the model discussed here. Three equations govern the evolution of the jet, i.e. conservation of water flow, momentum flux and flux of the constituent of interest, expressed as (compare with Fischer et al. 1979):

$$c_m - c_a = (c_{mo} - c_a) \left(1 + 2\sqrt{2}\alpha \frac{\rho u_o^2}{M_o} \int_0^x h(x) dx \right)^{-1/2} \quad (4.1)$$

where u_o is the velocity and M_o the momentum flux (conserved during jet evolution) at $x=0$, c_{mo} is the centerline concentration at $x=0$, c the concentration, h the water depth, x a

coordinate directed offshore, ρ a representative density, α an entrainment coefficient, while subscripts m and a denote conditions at the centerline and in the ambient, respectively.

4.2.3 One-D Advection-Diffusion Equation

The present mathematical model is simple. It was designed to fit a situation where channel geometry data are limited. It should be used to check trends rather than accurately predict surface salinity distribution. Thus, if we are to develop a mathematical model, it is necessary to make many simplifications. Figure 4.3 is a channel characterised by square-root increasing width of parabolic cross-sections and uniformly descending with a slope $2H_L/L$. It was assumed that the water exchange with the open sea at $x = L$ is the main source of water (Purnama et al., 2005). The mass flux of water equation is the difference between the inputs and outputs and the seawater intake at a desalination plant located at $x = a$.

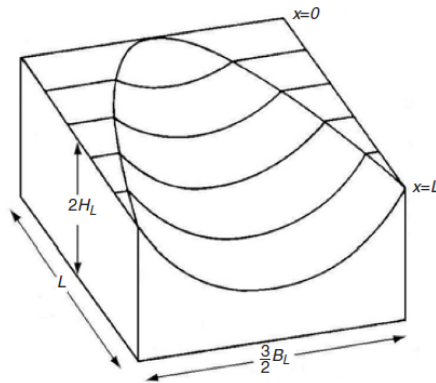


Fig. 4.3 Parabolic cross sections with a square-root increasing width and uniformly descending depth (Purnama et al., 2005)

One of the major aims of this study is to determine the level of short and long term salinity changes in the study area. Therefore, water mass balance and desalination capacities as well as the characteristics of each recipient were established. The modelling of the Arabian Gulf, Mediterranean Sea and Red Sea is accordance with (Purnama et al., 2005). These authors assumed that the water exchange with the open sea at $x = L$ is the main source of water, in which $A = BH$ is the cross-sectional area, U the incoming tidally averaged current and U_L the tidally averaged value of the rate of change of water depth (Purnama et al. 2005). The equation of mass flux of water is the difference between the incoming current and the freshwater input from rivers Q_{RI} , with continuous depletion by evaporation at the rate E :

$$\frac{d}{dx}(AU - Q_{RI}) = -EB - rQ_i\delta(x - a) \quad (4.2)$$

where rQ is the rate of the plant's water production and δ is the Dirac delta function. Seawater of salinity s is removed at the volumetric rate Q_i (intake water), so that a one-dimensional advection-diffusion approach can be adopted (Largier et al. 1996, 1997):

$$\frac{d}{dx}(AU_s) - \frac{d}{dx}\left(AD_L \frac{ds}{dx}\right) = Q_i s \delta(x - a) \quad (4.3)$$

where D_L is the tidally averaged shear dispersion coefficient that can be estimated numerically from field observations of surface salinity. By integrating and matching the salinity with s_L at $x = L$, we obtain the logarithm of relative salinity (Purnama et al. 2005). For a description of the method, see **Paper IV**.

5. Results and Recommendations

5.1 Field Work Procedure

The discharge of brine from the first desalination plant built in Northern Cyprus belonging to the Eastern Mediterranean University was investigated in the field. The measurements of M0 along the centerline of the brine discharge were compared with the simple jet theoretical solution given by Eq. (4.1). Figure 5.1 presents the results of a comparison between calculated and measured concentrations for the studied constituents. In general, satisfactory agreement was obtained between the simple model and the measurements, although over- or under-prediction was observed depending on the constituent studied.

The TDS result was measured at the discharge point (M0) to about 74.2 g/l and 53 g/l at (M30), 30 m away along the flow. During non desalination periods on the coast of Cyprus, the TDS of the recipient was about 40 g/l. An additional solution was suggested that could minimize the differences in concentration between the local area at the discharge point and the ambient (see **paper IX**).

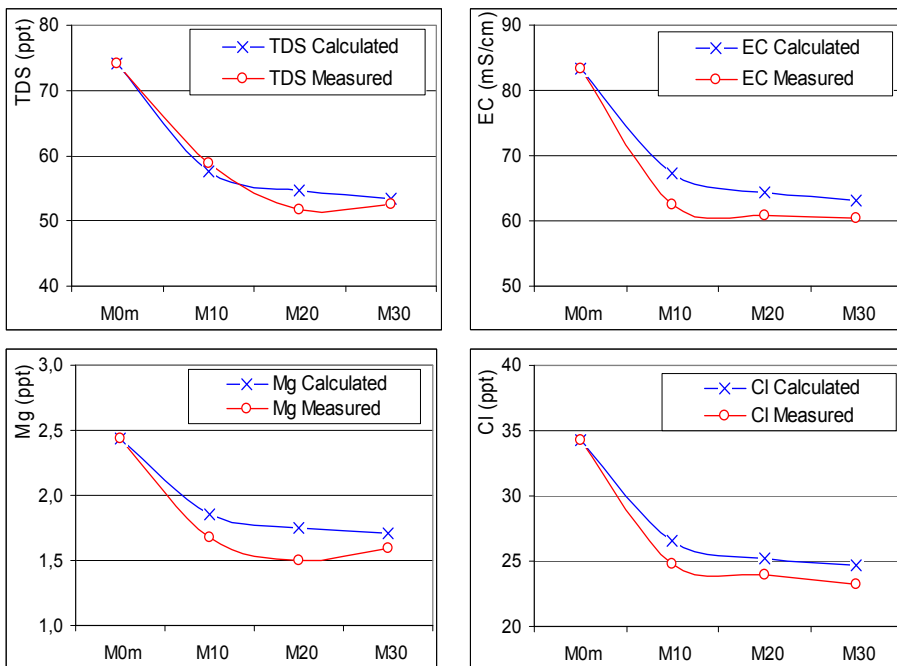


Fig. 5.1 Sample comparison between calculated and measured spatial evolution of the concentration along the centerline of a brine discharge (see **paper IX**)

5.2 Experimental Data Analysis

Results of different coefficients (k_y , k_{ym} , kx_y , kx_{ym} , and kx_e) from the first set of lab experiments as presented in **Paper II**, were compared with the two previous studies (Cipollina *et al.* (2005) (C) and Kikkert *et al.* (2007) (K)). The values produced by their analytical model were measured by the light attenuation system (LA) and laser-induced fluorescence system (LIF). The value of all coefficients was compared with regard to the three initial jet angles (30, 45 and 60 degrees). For example, the value obtained for k_{ym} at 30 degrees was 0.92 compared to those reported by Cipollina *et al.* (2005) of 1.08 and Kikkert *et al.* (2007) of 1.02 (see Figure 5.2). Thus, in this case the agreement is good; however, for larger angles the deviation between the coefficient values obtained in this and previous studies is larger than in the case of smaller angles. Differences in experimental setups and procedures may be one reason for the discrepancies between the compared experiments. There may also be marked differences in some of the input parameters that are not described by the non-dimensional quantities employed such as tank dimensions. Other reasons could include the method of density measurements and temperature difference between discharge solution and the tap water tank.

Some geometric quantities describing the jet trajectory showed strong correlations with experimental output, for example, Y_m versus Y , X_{ym} versus X_y , and X_e versus X_{ym} . Thus, if the vertical and horizontal distance to the maximum centerline level (or, alternatively, the maximum jet edge level) can be predicted, other geometric quantities can also be calculated. The relationship between the maximum levels and their horizontal distances exhibited more scatter (see Figure 5.3) and included a dependence on the initial jet angle. However, a general linear type equation could be fitted through the data points with reasonable accuracy, for example $X_y = k_\theta Y$, where k_θ is an empirical coefficient that takes on the values 2.3, 1.5 and 1.0 for the initial jet angle of 30, 45 and 60 degrees, respectively. A similar equation could be developed for X_{ym} and Y_m .

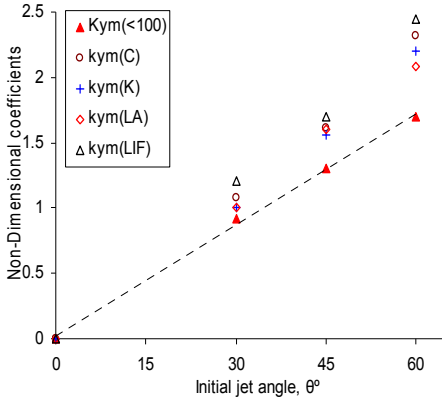


Fig. 5.2 Slope coefficient for maximum jet edge level (k_{ym}) as a function of initial jet angle

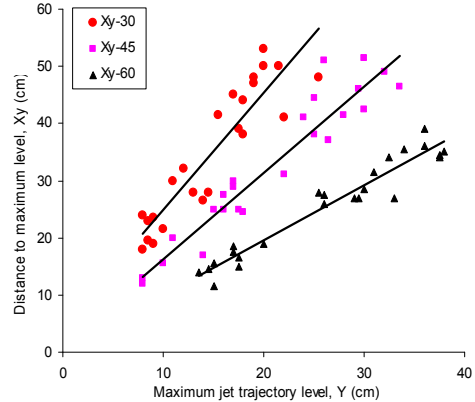


Fig. 5.3 Maximum jet centerline level versus its horizontal distance with respect to initial jet angle

In second experiment, the bottom slope S_b was introduced by tilting the receiving tank. Most beaches and coastlines have a natural bottom slope as has been observed on the Cyprus coast, where the brine discharge point is located (see **paper IX**). Different types of effect should first be observed in a lab-scale experiment for lateral spreading of the dense effluent and concentration along the flow. Both spreading and concentration are important for designing a new desalination plant discharge point, especially for a large-scale project that may discharge about 3 MCM of brine water per day.

The result was compared with Matlab code models and it was found that the code could be applied successfully to model experimental runs. The best results were obtained for the run without the bottom slope, as highlighted by the lower average error calculated. Another comparison was made between the measured data and CORMIX software. CORMIX was developed for hydrodynamic modelling of real (field) cases. The result revealed that the CORMIX program is not suitable for describing lateral spreading in small scale cases. The result for concentration percentage measured at three distances along the flow was compared with and without bottom slope for densimetric Froude numbers smaller and larger than 40, as presented in Figure 5.4. The concentration along the flow was improved by about 10% with the bottom slope for Froude numbers less than 40. When localising an appropriate outlet, the bottom slope is of importance. A high bottom slope allowed the brine discharge to dilute faster. More results and comparisons can be found in **Paper I**.

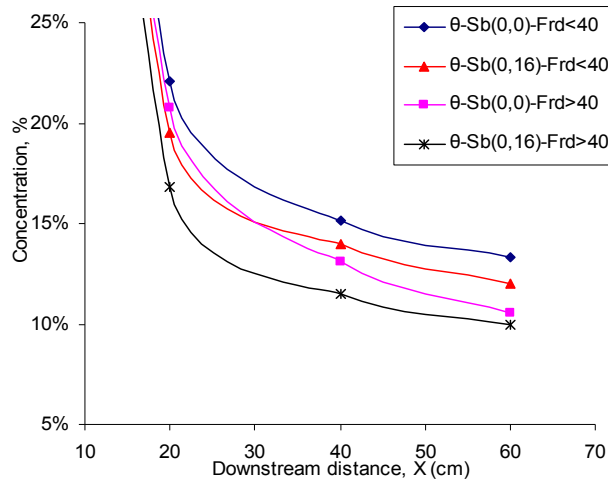


Fig. 5.4 Concentration percentage along the flow with and without bottom slope

5.3 One-D Advection-Diffusion Equation

Three recipients, the Arabian Gulf, Mediterranean Sea and Red Sea, were focused upon, as they constitute the study area in most of this research. Using desalination capacity data from IDA year books, a prognosis was made for 2050 assuming a continuous increase in

desalination plant capacities. This result was useful for providing an idea of the changes in salinity concentration at the brine points as illustrated in Figure 5.5. These results represent the logarithm of relative salinity increase due to seawater desalination in the Arabian Gulf, Mediterranean Sea and Red Sea. The salinity increase due to desalination plant brine discharge in 2050 will reach about 2.24, 0.81 and 1.16 ppt in the Arabian Gulf, Mediterranean Sea and Red Sea respectively. This increase was calculated over the entire volume of each studied area and will be much greater closer to the discharge point.

The mathematical method from Purnama et al. (2005) used to determine the results in Figure 5.5 is very important when applied locally, for example on the coastline between Kuwait and Bahrain, which includes the largest desalination plant in Saudi Arabia. The coastline is about 600 km long and total desalination production exceeds 7 millions m^3/day , leading to a local increase in salinity due to low flushing rates in major embayments, such as the Gulf of Salwah south of Bahrain, with salinities exceeding 70 g/l. It has been assumed that propagules of corals, fishes etc. from outside the Gulf reach the Iranian shoreline first and then circulate towards the Arabian States (Sheppard et al., 1992).

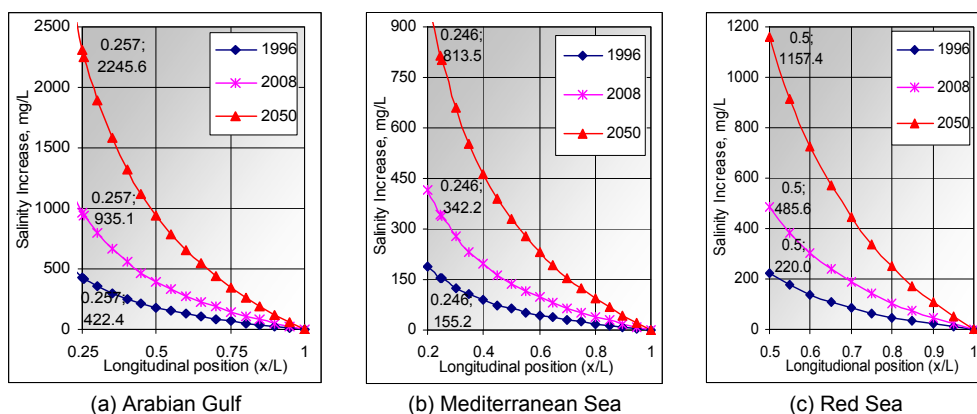


Fig. 5.5 Results of the logarithm of relative salinity increase in the Arabian Gulf, Mediterranean Sea and Red Sea due to a desalination plant located at $a/L = 0.5$ in 1996, 2008 and 2050 (see **paper IV**)

5.4 Recommendations and Future Studies

5.4.1 Recommendations

It was shown that in **paper IX**, the distance required for the brine discharge concentration to become similar to the ambient concentration was about 70 m from the discharge point along the centreline downstream, see (Figure 5.6). The suggested idea of changing the discharge location and building more than one outfall for the brine discharge could reduce the impact (see **paper IX**). This solution has a similar outcome to the suggestion provided earlier concerning discharge from a longer outfall pipe in order to increase the volume of ambient water that can be mixed with the brine discharge.

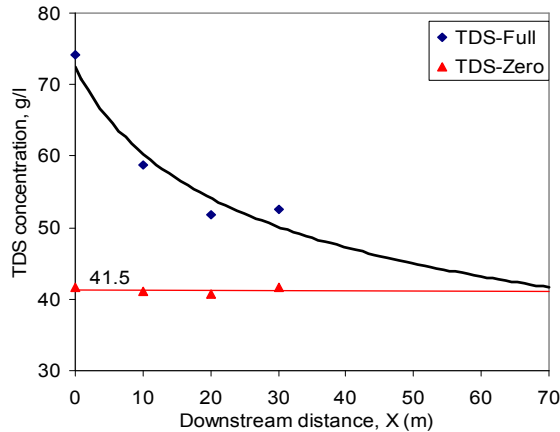


Fig. 5.6 Concentration percentage along the flow with and without bottom slope

The result of **Paper II** recommends the use of 60 degrees for the initial jet angle to ensure maximum level of the jet centreline. Having reached its maximum level, it drops due to the effect of negatively buoyant force but more gradually than at 30 and 45 degrees, which allows a greater opportunity for the jet to mix with the ambient. Some geometric jet quantities had strong correlations that could help with predictions. Some important recommendations are presented in **Paper I** based on the second experiment, as shown in Figure 5.7. The concentration percentage measured at three distances along the flow was compared for four cases with and without bottom slope, an initial jet angle of 30 degrees and a densimetric Froude number less than 40.

More results and recommendations can be found in **Papers I and II**. The two experiments were valuable and could be used in design of desalination plants such as in **Paper VII**. Some countries, for example Bahrain, are trying to limit the allowable increase in concentration at the coastline where desalination plant discharge points are located to 55 g/l of TDS (Alawadhi 2010). It is known that the average concentration in Gulf water is about 45g/l. One good example comes from Sydney desalination plant, where brine discharge is mixed with ambient water in a small /harbour-like area (semi-enclosed receiving area) and then the whole volume is released from the opening. This volume will be much less concentrated than the brine itself. Nowadays, many countries are building combined desalination and power plants to mix brine water from desalination with cooling water from power plants before discharging it back to the sea.

The concept of mixing including its different effects was studied in **Paper V** to find a better mixing rate and effective time as shown for sinuous and/or irregular channels. The calculation of mixing time is important in all of the studies, especially these three papers (**III, IV and VIII**) that discuss the Arabian Gulf, Mediterranean Sea, Red Sea and Dead Sea. The recommendation of a joint desalination and power plant is important for

cooperation between Gaza and Egypt. In my view such projects can increase peace and security on the border between Egypt and Gaza. This project has been compared among five different alternatives. In the divided country Cyprus, a wastewater treatment plant was built in 1996 to treat wastewater from both sides (40 and 60 percent), although it is located in the Northern part.

The concentration percentage along the flow is much better with a bottom slope of 16% and a 30 degree initial jet angle compared to the other three cases. The concentration in this case rapidly drops below 10% at a distance of 37 cm from the discharge point, while the other cases are still above 15% at the same distance. A comparison of the two cases with and without bottom slope reveals that the one with slope is slightly better. My first recommendation is to have a minimum of 16% bottom slope at the discharge point because up to this value little difference has been found. The second is to have both inclination and bottom slope as shown in Figure 5.7. The idea behind these recommendations is to increase the water column and water depth at the discharge point to enable rapid mixing with the ambient.

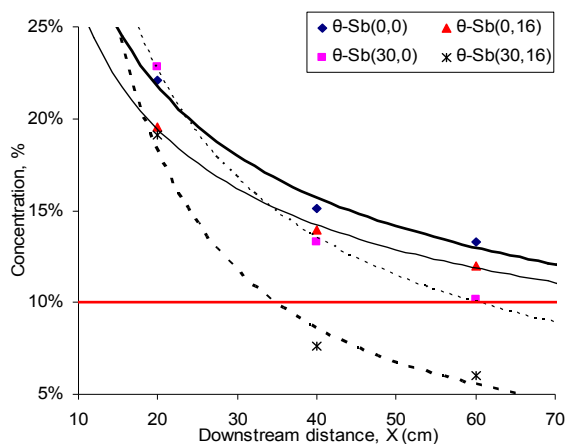


Fig. 5.7 Concentration percentage along the flow with and without bottom slope

5.4.2 Future Studies

The main issue for future research is the rapid development of desalination technology and how to increase fresh water production capacity. In this thesis, three important aspects were studied and discussed from different perspectives; field work, experimental work and modelling. In my opinion, more investigations using each of these perspectives should be performed to improve some of the results, taking account of different regions and countries.

Field work is essential for providing baseline data in which elevated TDS in recipient sea water is acceptable for the A) technical, B) economic and C) ecological operation of the desalination plant. Other important aspects of brine discharge discussed in this thesis are related to modelling and field work, such as measuring different chemicals at the discharge point and the effects on fishing and marine life.

Further work and research should take the form of large-scale experiments on a negatively buoyant jet and involve, for example, increasing receiving tank size and bottom slope with different inclinations to determine the limitations of changing bottom slope. In the second experiment, the jet flow touched the walls of the receiving tank after reaching the intermediate field, which should be avoided in future work especially for lateral spread measurements. It is advisable to consider some comments from the first and second experiments regarding new instrumentation, such as a conductivity meter and the latest probe measurement technology to enable quicker reading, especially when measuring the far-field.

In practice, there are three major parameters that need to be studied before starting any desalination plant project, namely population growth, available water resources and the economy of the country. The location of the project is also important for designing and operating the plant so as to reduce environmental impacts by better compliance with operator guidelines. Some of these guidelines can be found in this study but more should be developed for the design of plant outfall in order to achieve sustainable desalination plant discharge.

Mixing and mixing zones is very important for brine discharge in order to avoid changes in the composition of seawater. The Red Sea-Dead Sea canal project is an example of complex mixing due to great differences in densities and composition between the brine discharge from the planned desalination plant and the Dead Sea water. Dead Sea mixing is critical and more studies need to be carried out prior to the start of the project. The relation between near, intermediate and far-field zones should be considered in future work. These zones are normally connected, as the effluent initially rises to start the near field and then drops to the bottom due to jet impingement to start the intermediate field. At the end of the intermediate field, the far-field starts due to irregularities at the bottom.

6 Conclusions

This thesis has two important aims, which in most cases are contradictory. The first is to raise the water supply by increasing desalination production and the second to protect the receiving area from environmental impacts. Many countries suffer from a shortage of fresh water and therefore build new desalination plants to increase their production to cope with population growth, especially around the Arabian Gulf, which accounts for about 45% of world desalination production, see **papers III and IV**.

The slope of the best-fit straight line through the data points was a function of the initial jet angle (θ), where the slope increased in line with θ for the maximum levels studied, as observed in some previous investigations, which recommend the use of a 60 degree initial jet angle. A general linear type equation could be fitted through the data points with reasonable accuracy for five geometric quantities, for example $X_y = k_\theta Y$, where k_θ is an empirical coefficient 1.0 for the initial jet angle. This can be applied in future desalination plant design, see **paper I**.

In the second experimental the concentration along the flow was improved by about 10% with the bottom slope and by about 40% with bottom slope and an inclination of 30 degrees. Thus, this type of improvement is recommended for brine discharge outlets to the recipients to minimize the concentration and enable it to dilute faster and go further. More than 16% bottom slope is recommended, see **paper II**. In the Cyprus EMU case, the calculated bottom slope was about 7.4% and the coastal area was dirty/polluted because of this small incline, see **paper IX**.

An inclination of 30 degrees with a 16 % bottom slope is more sustainable for the design of brine discharge outfall. The result was also compared with the Matlab code, as the former could be applied successfully to model the experimental runs. The best results were obtained for the run without bottom slope but the CORMIX software was inadequate for describing the lateral spread in small scale cases.

The potential benefits of seawater desalination are great, since fresh water production can become independent of precipitation if national and international help is provided. It was found that oil and desalination come in pairs in the oil producing countries. However, desalination requires a high energy input and produces not only freshwater but also brines with high salt concentration, see **paper VI**. The mixing of wastewater and brine discharge is an important method for minimizing salinity in the coastal waters of the Arabian Gulf. It was difficult to decide whether to use the wastewater for mixing with brine or for other purposes after treatment, see **paper III**. The flow in straight and irregular channels for mixing was theoretically described in **paper V**. The characteristics and the shape of the channels can effects the mixing in the channels.

The result of the present study can be applied to real projects such as a combined desalination, power and wastewater treatment plant. The study proposes one such project for Sinai and the Gaza Strip as a joint power and desalination plant solution. A good reason for having a joint power and desalination project is the mixing of brine water from

desalination with cooling water from the power plant to minimize the negative effects of brine discharge, which is already in operation in some countries. Such a project would also enhance peaceful cooperation between Egypt and Gaza, which should lead to increased security in the border area, see **paper VII**.

7 References

- Alawadi A. A. 2010. Environmental Assessment of the Kingdom of Bahrain Desalination Plants Discharges. DESALINATION AND THE GULF. International Desalination Association, IDA-BHR2010, DECEMBER 6-7, 2010.
- Al-Gobaisi, A. D. M. 1997. Sustainable augmentation of fresh water resources through appropriate energy and desalination technology". IDA World Congress on Desalination and Water Reuse, Madrid, Spain.
- AMTA-American Membrane Technology Association, Desalting Facts: How Much Does Desalted Water Cost? 2001a, [Online]. Available: <http://www.membranes-amta.org/media/pdf/desaltingcost.pdf>. [2003, October 28].
- Bahrain meeting, 2011. Desalination and the Gulf. Bahrain symposium, International Desalination Association, IDA-BHR2010, December 6-7.
- Bashithalshaaer, R., and Persson K.M. 2010. Desalination and Economy Prospects as Water Supply Methods. Proceedings *ARWADEX-Water Desalination Conference in the Arab Countries. King Faisal Conference Hall Riyadh, KSA April 11-14, 2010*.
- Birkett, J. "Cooley H., Personal communication" (1999).
- Brewer P.G., Dryssen, D., 1985. Chemical oceanography of the Persian Gulf. Progress in Oceanography, (14) 41–55.
- Britannica. <http://www.britannica.com> (last update January 26, 2009)
- Buros, O. K. 2000. The ABCs of desalting, report, 2nd ed., Int. Desalination Assoc., Topsfield, Mass (2000).
- Christoudoulou G. C. 1991. Dilution of dense effluents on a sloping bottom. Journal of Hydraulic research 29, 329-339.
- Cipollina A., Brucato A., Grisafi F. and Nicosia S. 2005. Bench-Scale Investigation of Inclined Dense Jets. J. of Hydraulic Engineering, (ASCE) 131 (11), 1017–1022.
- Cooley, H. P., Gleick, H., and Wolff. G. 2006. Desalination, With A Grain Of Salt: A California Perspective.
- Desalination news, http://www.desalination.biz/news/news_story.asp?src=nl&id=5480 (15SEP, 2010)
- Doneker, R.L. and Jirka, G.H. 2007. A Hydrodynamic Mixing Zone Model and Decision Support System for Pollutant Discharges into Surface Waters. Cormix User Manual 6.0E.
- Dore, M. H. I. 2005. Forecasting the economic costs of desalination technology. Desalination, (172) 207–214.

- Fischer, H.B., List, J.E., Koh, R.C.Y., Imberger, J., and Brooks, N. 1979. Mixing in inland and coastal waters. Academic Press, New York, NY.
- Gary, C. 2006. Desalination in Australia, IDA News, September/October.
- Gavrieli, I. and Bein, A. (2006). Formulating A Regional Policy for the Future of the Dead Sea - The "Peace Conduit" Alternative, Geological Survey of Israel.
- Gavrieli, I., Amos B. and Aharon, O. 2005. The Expected Impact of the Peace Conduit Project (The Red Sea-Dead Sea Pipeline) On the Dead Sea, Mitigation and Adaptation Strategies for Global Change 10: 3–22.
- Gavrieli, I. (1997). Halite deposition from the Dead Sea: 1960-1993: In book “The Dead Sea: the lake and its setting”, edited by Tina M. Niemi, Zvi Ben-Avraham, Joel R. Gat. Oxford University Press, Oxford, pp. 161-170.
- Gordon, Jr., D. C., Boudreau, Mann, P. R. K., J.-E. Ong, H. W., Silvert, L., Smith, S. Wattayakorn, V. G., Wulff, F., and Yanagi, T. 1996. LOICZ Biogeochemical Modelling Guidelines. LOICZ Reports & Studies No 5, 1-96.
- GW/Desalination data and IDA International Desalination Association year book and CD (2008–2009).
- Heberer, T. D. Feldman, K. Redderson, H. Altmann, and T. Zimmermann. 2001. Removal of Pharmaceutical Residues and Other Persistent Organics from Municipal Sewage and Surface Waters Applying Membrane Filtration”. Proceedings of the National Groundwater Association, 2nd International Conference on Pharmaceuticals and Endocrine Disrupting Chemicals in Water. Minneapolis, Minnesota and Westerville, Ohio: National Groundwater Association, October 9-11.
- Hunter, J. R., 1986. The physical oceanography of the Arabian Gulf: A review and theoretical interpretation of previous observations. In: Halwagy, Clayton, and Bebehabi, eds., Proceedings of the 1st Gulf Conference on Environment and Pollution, KISR, Kuwait. (KISR is the Kuwait Institute for Scientific Research), pp. 1–23.
- IDA, 2009-10. International Desalination Association Yearbook.
- IDA, 2008-09. International Desalination Association Yearbook.
- IDA, 2006-07. International Desalination Association Yearbook.
- IDA, 2007-08. International Desalination Association Yearbook.
- IDA, 2006. IDA Worldwide Desalting Plant Inventory, No. 19 in MS Excel format, Media Analytics Ltd., Oxford, UK.
- Jeon T. M., Kyong, O. B., and Seo, I. W. 2007. Development of an empirical for the transverse dispersion coefficient in natural streams. Environmental Fluid Mech (7) 317–329.

- Jirka, G.H., Doneker, R.L. & Hinton, S.W. 1996. User's Manual for CORMIX: A Hydrodynamic Mixing Zone Model and Decision Support System for Pollutant Discharges into Surface Waters, U.S. Environmental Protection Agency, Tech. Rep., Environmental Research Lab, Athens, Georgia, USA.
- John, V. C., Coles, S. L., and Abozed, A. I. 1990. Seasonal cycle of temperature, salinity and water masses of the Western Arabian Gulf. *Oceanol. Acta*, (13) 273-281.
- Karagiannis, I. C. and Soldatos, P. G. 2008. Water desalination cost literature: review and assessment. *Desalination* 223, 448-456.
- Kikkert G. A., Davidson M. J., and Nokes R. I. 2007. Inclined Negatively Buoyant Discharges. *J. of Hydraulic Engineering*, (ASCE) 133 (5), 545-554.
- Largier, J.L. Hearn, C.J. and Chadwick, D.B. 1996. Density structures in low inflow estuaries". *Coastal and Estuaries Studies*, 53, 227-241.
- Largier, J.L. Hollibaugh, J.T. and Smith, S.V. 1997. Seasonally hypersaline estuaries in Mediterranean climate regions. *Estuarine, Coastal and Shelf Science*, 45, 789-797.
- Lattemann, S., PhD Thesis, 2010. Development of an Environmental Impact Assessment and Decision Support System for Seawater Desalination Plants. February 2010, Delft, the Netherlands.
- Lattemann, S. Mancy, K. Khordagui, H. Damitz, B. and Leslie, G. 2008. *Desalination: Resource and guidance manual for environmental impact assessments*. United Nations Environment Programme (UNEP), Nairobi, Kenya, www.unep.org/bh/Publications/Type7.asp (last accessed on 12.09.2009).
- Lattemann, S., Höpner, T., 2008. Environmental impact and impact assessment of seawater desalination, *Desalination* (220) 1-15.
- Lattemann, S. 2009. Protecting the marine environment. In A. Cipollina, G. Micale and L. Rizzuti, editors. *Seawater desalination, green energy and technology*, pages 271-297, Springer-Verlag, Berlin Heidelberg.
- Magazine, Water Condition & purification, January, (2005): <http://www.lenntech.com/WHO-EU-water-standards.htm>.
- Mauguin G. and Corsin, P. 2005. Concentrate and other waste disposals from SWRO plants: characterization and reduction of their environmental impact". *Desalination*, 182(1-3): 355-364.
- Moncef B., and Barnier, B. 2000. Seasonal and inter-annual variations in the surface freshwater flux in the Mediterranean Sea from the ECMWF re-analysis project, *Journal of Marine Systems* (24) 343-354.
- Morcos, S.A. 1970. Physical and chemical oceanography of the Red Sea. *Oceanography Marine Biology Annual Review*, (8) 73-202.

- Mukaddes O. 2004. A comparative Study for MSF & MEE Desalination Systems using Alternative Energy Sources, M. Sc. thesis, July.
- NAS-National Academy of Sciences. 2004. Review of the Desalination and Water Purification Technology Roadmap. Water Science and Technology Board. Washington, D.C.:National Academies Press.
- NSW-New South Wales. 2001. Department of Natural Resources: (last update, June 2010), <http://www.dnr.nsw.gov.au/estuaries/factsheets/physical/mixing.shtml>.
- Olsson, M. & Fuchs, L. 1996. Large eddy simulation of the proximal region of a spatially developing circular jet. *Phys. Fluids* 8.
- Pankratz, T. 2004. An overview of Seawater Intake Facilities for Seawater Desalination, The Future of Desalination in Texas Vol 2: "Biennial Report on Water Desalination, Texas Water Development Board.
- Pincince, A. B., and List, E. J. 1973. Disposal of brine into an estuary. *J. Water Pollut. Control Fed.*, 45, 2335–2344.
- Purnama, A., Al-Barwani, H. H. and Smith R. 2005. Calculating the Environmental Cost of Seawater Desalination in the Arabian Marginal Seas. *Desalination* 185, 79–86.
- Rahmstorf, S. 1998. Influence of Mediterranean outflow on climate, *EOS Trans., AGU* 79, (24) 281–282.
- Reynolds, R.M. 1993. Physical oceanography of the Gulf, Strait of Hormuz, and the Gulf of Oman-Results from the Mt Mitchell expedition. *Mar. Pollut. Bull.*, (27) 35–59.
- Roberts, P. J. W., and Toms, G. 1987. Inclined dense jets in flowing current. *J. Hydraul. Eng.*, 113(3), 323–341.
- Ruiz-Mateo M., and J. Gonzalez. 2007. Discharges to the sea from desalination plants. MEDCOAST-07, 13–17 November, Alexandria, Egypt.
- Sedlak, D. L. and K.E. Pinkston. 2010. Factors Affecting the Concentrations of Pharmaceuticals Released to the Aquatic Environment. Proceedings of the National Groundwater Association, 2nd International Conference on Pharmaceuticals and Endocrine Disrupting Chemicals in Water. Minneapolis, Minnesota and Westerville, Ohio:National Groundwater Association, October 9–11.
- Shahin, M., 1989. Review and assessment of water resources in the Arab region. *Water Int.*, (14) 206–219.
- Sheppard, C., Price, A., Roberts, C., 1992. Marine Ecology of the Arabian Region: Patterns and Processes in Extreme Tropical Environments. Academic Press, London.
- Simon, P. 1998. Tapped Out: The Coming World Crisis in Water and What We Can Do About It. New York: Welcome Rain Publishers.

- Turner, J.S. 1996. Jets and plumes with negative or reversing buoyancy. *J. Fluid Mech.* 26, 779–792.
- USBR. 2003-United States Bureau of Reclamation. Desalting Handbook for Planners. 3rd Edition. Desalination and Water Purification Research and Development Report #72. Denver, Colorado. Water Treatment Engineering and Research Group.
- Valero, A. Uche, J. and Serra, L. 2001. Desalination as an Alternative to Spanish National Hydrology Plan. Technical Report, CIRCE and University of Zaragoza.
- Vanhems, C. 2001. Critical Review of Desalination Concentrate Disposal to Surface Water (2001), USA, 1992. (UNEP, 2001).
- Vengosh, A., and Rosenthal, E. 1994. Saline groundwater in Israel: it's bearing on the water crisis in the country. *J. Hydrol* 156: 389–430.
- Wangnick/GWI. 2005. Worldwide Desalting Plants Inventory. Oxford, England: Global Water Intelligence. Data provided to the Pacific Institute.
- Wangnick, K. 2002. IDA worldwide desalting plants inventory”, Rep.17, Int. Desalination Assoc., Topsfield, Mass (2002).
- WHO. 2010-World Health Organization. *Desalination technology: Health and environmental impacts*. Taylor and Francis (CRC Press).
- Wilf, M. Awerbuch, L. Bartels, C. Mickley, M. Pearce, G. and Voutchkov, N. 2007. The guidebook to membrane desalination technology. Balaban Desalination Publications, L'Aquila, 2007.
- Wiseman R. 2006. Editor's corner, *Desal. Water Reuse*, 16 (3) 10–17.
- Zhou, Y. and R. S. J. Tol. 2005. Evaluating the costs of desalination and water transport, *Water Resour. Res.*, 41, W03003.

Paper I

Near and Intermediate Field Evolution of A Negatively Buoyant Jet

Bashithalshaaer, R., and Persson K.M. 2011

Ocean System Engineering (under review)

Near and Intermediate Field Evolution of A Negatively Buoyant Jet

Raed Bashitialshaer^a, Kenneth M. Persson^{ab}

^aDepartment of Water Resources Engineering, Lund University, PO Box 118, SE-221 00 Lund, Sweden
Tel. +46462224367; Fax: +46462224435; Raed.Alshaar@tvrl.lth.se; Kenneth_M.persson@tvrl.lth.se

^bSYDVATTEN AB, Skeppsgatan 19, SE 211 19 Malmö, Sweden. Tel. +46 46 222 9470

Abstract. The purpose of this study is to explore the behavior of a dense jet and bottom plume, composed of brine water of heavier effluent into a quiescent homogeneous ambient, discharged into a receiving body of lighter fresh water (tank). This situation is common in connection with freshwater production from sea water (desalination), which produces a brine waste stream, usually discharged back into sea water. In this study, a mathematical model was developed to simulate the jet and plume behavior in order to determine the optimum discharge conditions for different scenarios. The model was divided into two sub-models, describing respectively the near and intermediate field properties of the discharge for different inclinations and bottom slope. The lateral spreading and electrical conductivity was also described through a generalization of measured data.

The predictions of the model were compared with experimental data collected in lab as well as results obtained with a commercial software simulation package (CORMIX). After the calibration of the main parameters, the model satisfactorily reproduced the experimental data, although the simulations are not able to adequately describe the effects of the bottom slope. To overcome this problem separate calibrations are done with and without the bottom slope (tank tilting).

A Matlab code developed describing the lateral spreading and centerline dilution of buoyant jet and plumes for near and intermediate field was developed. The model produces results in acceptable agreement with data and observations, even though some improvements should be made in order to give the correct weight to the bottom slope parameter and to reduce the need for user calibration. An overall assessment of the CORMIX software behavior cannot be made; in our case (i.e. small scale) the software was not giving simulation results that reproduced the data.

This study has limited result for only 16% bottom slope and 30 degrees inclination. Concentration was improved with the bottom slope by 10% than the horizontal bottoms and improved by about 40% with bottom slope together with inclination of 30 degrees. The suggestion in the practical applications concerning desalination brines and similar discharge of heavy wastes is to have inclination and bottom slope together.

Keywords: Experimentation; Inclined dense jets; Tank tilting; Negatively buoyant; CORMIX; MATLAB; Desalination; Salinity.

1. Introduction

1.1. General

The usage of sea water as a source for water supply (intakes) has constantly been increasing, due to the development of desalination processes. The desalination process brings as output fresh water from one side and brine water (outfalls) on the other side. The

disposal of brines directly into the sea can increase the salinity level in the proximity of the output, alter the ecosystem equilibrium, and bring losses in efficiency of the desalination plant, if the sea water uptake is influenced by this change. The brine discharge devices are usually positioned at the lowest point of the receiving water which can be either ocean or deep water sea outfalls. The discharged fluid density is generally different from that of the surrounding, due to either different temperature or chemical composition. The resulting buoyancy forces can have a great effect on both the mean flow and mixing. Brine discharge from desalination plants is the common and best example; this type is the so-called negatively buoyant or dense discharges, which have relatively high-salinity concentrations.

A particular discharge should be considered as "shallow" or "deep" depending on the relative dynamic impact of this flow and recipients, notably its fluxes of momentum and buoyancy. In total 72 runs were performed at the Department of Water Resources Engineering (TVRL) laboratory at an appropriate scale to ensure turbulent jet behaviour. We are focusing in particular on releases where the initial vertical momentum flux of the discharge is in the opposite direction of the buoyancy generated momentum flux as the Boussinesq assumption is applicable.

1.2. Concept of Jet Flow

In general, there are three regions of the jet flow can in general be identified as: the near-field, the intermediate-field and the far-field flow. The near-field is the initial flow or development region (named the potential core for a top-hat exit profile); it is usually found within $(0 \leq x/d_0 \leq 6)$. The far-field is the fully-developed region where the thin shear layer approximations can be shown (with appropriate scaling); jet flows generally become self-similar beyond $(x/d_0 \geq 25)$ (Christopher, 2007). The intermediate-field, or transition region, lies between the near- and far-fields of the jet. Method of understanding mixing in intermediate-field or transition was well defined qualitatively by flow visualization in Dimotakis et al. (1983) and in Dimotakis (2000). In the intermediate region of a round jet there was only Reynolds dependence of shear stress distributions as shown from Matsuda & Sakakibara (2005). They used method of a stereo particle image velocity (PIV) system. The mean and fluctuating velocity curves were plotted for $Re = 1,500; 3,000; 5,000$.

It was possible to investigate the effects of turbulent energy on the initial development and large scale instabilities of a round jet by placing grids at the nozzle outlet to alter the jet initial conditions because the grids causes small scale injection of turbulent energy (Burattini et al., 2004). The jet lateral spreading and consequent dilution at the bottom is of considerable practical importance in assessing the environmental impact of the effluent on the receiving water at the discharge point (Christodoulou, 1991). The behaviour of laterally confined 2-D density current has been considered in past (Ellison and Turner, 1959; Benjamin, 1968; Simpson, 1987) but the number on 3-D study was very limited. Hauenstein and Dracos (1984) proposed an integral model based on similarity assumptions, which was supported by their laboratory experimental data of the radial spreading of a dense current inflow into a quiescent ambient.

Previous studies mainly focussed on the separate analysis of near-field and intermediate-field properties of buoyant jets and plumes. Some hypotheses on how to connect the two different zones have also been proposed. Turner (1966) and Abraham (1967) were the first to analyse this kind of problem of a vertical negatively buoyant jet. Many investigations

and experimental works has been previously done by Anderson et al. (1973), Chu (1975), Pincince and List (1973), Shahrabani and Ditmars (1976), Zeitoun et al. (1970), Tong and Stolzenbach (1979), Roberts and Toms (1987) for the near-field of vertical and inclined dense jets. They have proposed an empirical solution and theoretical expressions mainly for the maximum rise level and the centreline dilution. Many studies investigated the main properties of submerged jets using non-dimensional numbers and developed empirical relationships based on such numbers. The dense layer spreads in all directions at a rate proportional to the entrainment coefficient (Alavian, 1986). His result was obtained by flowing salt solution on a sloping surface in a tank of freshwater and his experimental result was based on three different inflow buoyancy fluxes on three angles of incline of 5°, 10°, and 15°. The starting salt concentration was constant at 4 g/l for all runs.

Akiyama and Stefan (1984) developed an expression for the depth at the plunge point as a function of inflow internal Froude number, mixing rate, bed slope, and total bed friction. Cipollina et al. (2004) presented a model based on the conservation of mass, volume flux, momentum and buoyancy flux, describing the evolution of a buoyant jet in the near field of the discharge, validating the model against laboratory data. Sanchez (2009) developed a similar model, and for the model testing data collected in the laboratory were employed, as well as data from Cipollina et al. (2004). He employed a range of entrainment coefficients in the model obtained from previous studies. Christoudoulou (1991) described theoretically the main factors affecting near-, intermediate-, and far-field properties, suggesting appropriate length scales for each zone. Bleninger and Jirka (2007a,b) developed the software CORMIX to calculate jet trajectories and dilutions rates for general purpose applications in engineering projects. Suresh et al. (2008) investigated the lateral spreading of plane buoyant jets and how they depend on the Reynolds number, suggesting and demonstrating that a reduction of the spreading occurs with an increase in the Reynolds number. Table 1 is the summary of different sizes that have been used for laboratory mixing tank dimensions (L x W x H) as found in literature.

Table 1: Dispersion tanks with different sizes used in earlier experiments

Previous study	Cross-section (m)	Depth (m)
Turner, 1966	0.45 x 0.45	1.40
Demetriou, 1978	1.20 x 1.20	1.55
Alavian, 1986	3.0 x 1.50	1.50
Lindberg, 1994	3.64 x 0.405	0.508
Roberts et al., 1997	6.1 x 0.91	0.61
Zhang & Baddour, 1998	1.0 x 1.0	1.0
Pantzlaff & Lueptow, 1999	D = 0.295	0.89
Bloomfield and Kerr, 2000	0.40 x 0.40	0.70
Cipollina et al., 2005	1.50 x 0.45	0.60
Jirk G.H., 1996,2004,2006	CORMIX, CorJet	
Kikkert et al. 2007	6.22 x 1.54	1.08
Papanicolaou & Kokkalis, 2008	0.80 x 0.80	0.94
Shao & Law, 2010	2.85x0.85	1.0
This study	1.50 x 0.60	0.60
	2.0 x 0.50	0.60

1.3. Objective

The present study focuses on the discharge of the residue brine water and on the modeling of its evolution in space downstream the discharge area. The overall objective of this work is the investigation of the behavior of a negatively buoyant jet, and the following bottom plume ideally composed of brine water from a desalination plant, with focus on the lateral spreading (perpendicular to jet or plume axis) and the evolution of the salinity concentration on the centerline. This kind of analysis will help to find the most effective parameters influencing spreading and mixing, in order to design a proper discharge system. The detailed objectives can be summarized as to:

- Run a set of laboratory experiments, simulating discharge conditions in bench scale
- Develop a mathematical model to describe lateral spreading and centerline dilution of buoyant jet and plumes for near and intermediate field
- Find out possible correlation of measured values with non-dimensional numbers, e.g. densimetric Froude and Reynolds numbers
- Observe the effect of main parameters variation on spreading and dilution properties
- Calibrate the mathematical model with data collected in the laboratory, and test it on a different set of data
- Compare measured data and modeled data with simulation results obtained using the software CORMIX and Matlab programme

2. Laboratory and experimental work

2.1. General descriptions

The apparatus and major materials used in the experiments at the laboratory were named as water tanks, flow-meter, digital frequency-meter, digital conductivity meter, pump, pipes, valves, nozzles and nozzles' support, salt and dye (Photo 1). Five different tanks were used in the experiments; three small tanks for mixing tap water with salt and colour to obtain the salty water necessary to create the negatively buoyant jet and two large tanks used to fill with tap water and introduce the salty water with the dye to observe the jet inside it. The small tanks were made of plastics with capacities of about 45, 70 and 90 liters. The large tanks were in glass with capacities of about 500 to 600 liters. Their dimensions (L x W x H) were (150 x 60 x 60) and (200 x 50 x 60) each in centimetres.

Fine pure sodium chloride was used to create the saline water in the jet by mixing it with tap water. The water quantity was measured using a bucket and the salt was measured using a balance to obtain the correct salt concentration. A conductivity meter was used to measure the conductivity in the three different concentrations. The density measurement for the three concentrations presented in this study was found as 1025, 1039 and 1051 kg/m³ for 4, 6 and 8% (40, 60 and 80 g/l) respectively. Each of the density was averaged of five different measurements from the weight method. Small differences in density measurements were reported between saltwater used in this study and natural seawater. The chemical composition of seawater is different from sodium chloride solutions, but the density varies only slightly compared with the pure sodium chloride solutions.

Potassium permanganate (KMnO_4) was used to colour the saline water. The dye colours the transparent water into purple by adding 0.1 g/liter. The use of a purple jet was made to facilitate the observation of the behaviour of the jet in the tap water tank. The result of jar test for (KMnO_4) concentration showed that at 0.3 mg/l, the solution is still pink but at concentration of 0.195 mg/l no pink colour is visible.

2.2. Preliminary measurements

Preliminary measurements were conducted after calibrating all apparatus in order to obtain reference data and to check if our measurement tools (i.e. flow meter, conductivity meter) were reliable and coherent with literature data. These measurements are flows, water salinity, density, and conductivity, diving information about water density and conductivity variation as a function of salinity at a constant room temperature of $20^\circ\text{C} \pm 1^\circ\text{C}$. Each experimental run was characterized by a set of parameters, and the first step of each run was used to find the proper combination of parameter values. The parameters of interest were:

- Diameter of nozzle, d_0 (4.8; 3.3; 2.3 mm)
- Initial jet angle, θ to the horizontal line (0; 30°)
- Bottom slope S_b (0; 16 %), the tank tilting
- Salinity of brine discharge S (4; 6; 8 %)

The two parameters submerged discharge angle θ and bottom slope S_b effecting the lateral spreading of the dense effluent. Lateral spreading is shown in Figure 1 in two dimensions x-axis and y-axis, in which $b(x)$ was measured at three locations b_1 , b_2 and b_3 at horizontal distances X_1 , X_2 and X_3 for 20, 40 and 60 cm respectively. Similarly, $EC(x)$ was also measured three times at the centreline of the x-axis. Nozzle parameters are denoted with zero (0) while ambient parameters are denoted as (a). The parameters along the centreline and flow direction are functions of x-axis and denoted as (x). In Figure 2, the experimental strategies for submerged negatively buoyant for four cases are presented, changing in inclination and bottom angle: ($\theta=0$, $S_b=16\%$; $\theta=0$, $S_b=0$; $\theta=\text{inclined}$, $S_b=16\%$; $\theta=\text{inclined}$, $S_b=0$). Each part of this figure was measured for 18 experiments with respect to three different salinities.

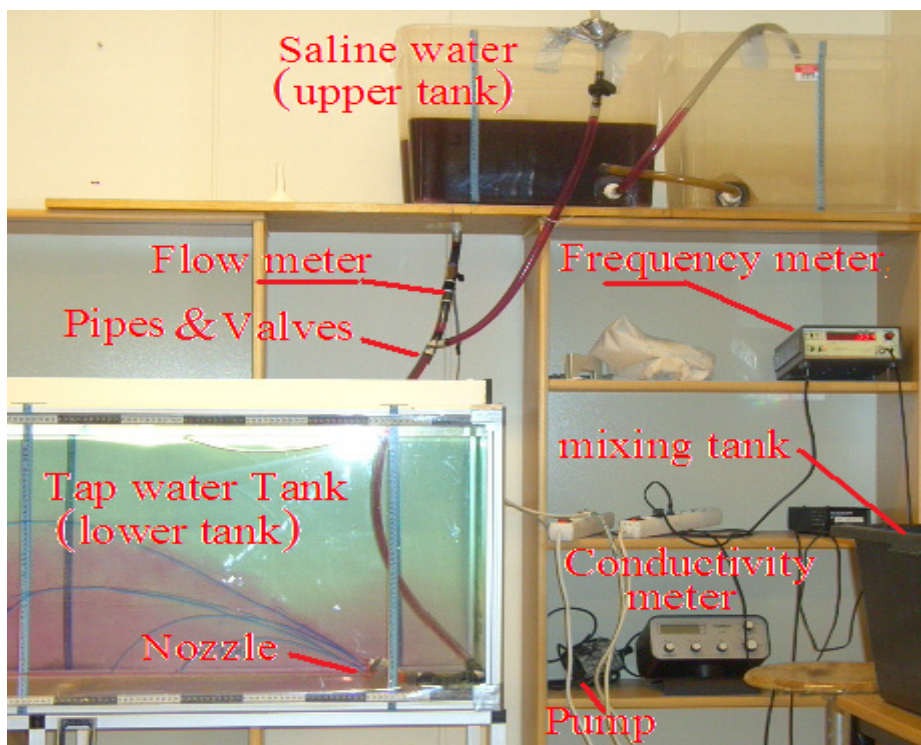


Photo. 1. Terminology for experimental apparatus used

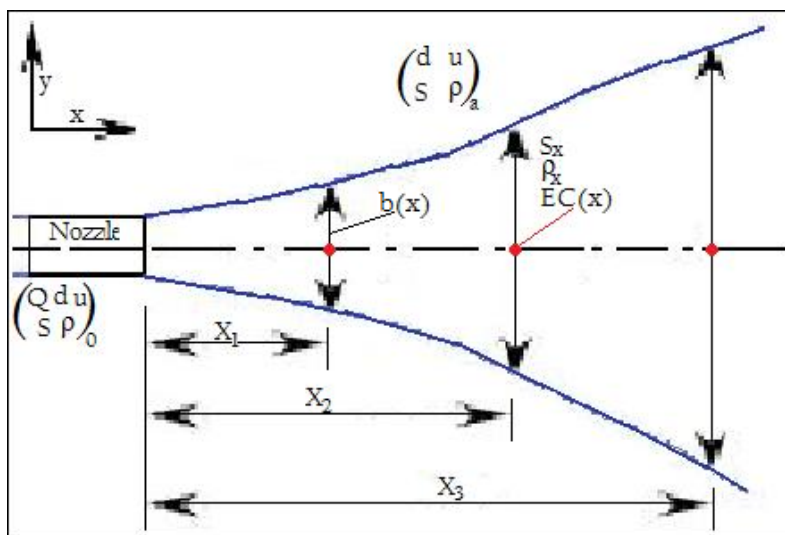


Fig. 1. Plan view of lateral spreading measurements along the flow

2.3. Data and observations

Experimental data for inclined dense jets with major parameters for this study are listed (see Table 2) for the 72 runs. The jet lateral spreading width b was measured at three distances 20, 40 and 60cm (see Figure 1) and EC is the electrical conductivity reading at the same location of the three distances but only at the centreline; one set during the experiment in operation and another set after experiment stops.

Table 2: Experimental results of major parameters for the inclined dense jet

Run	Angle	S	d_0	S_b	$\Delta\rho_0/\rho_a$	Q_0	u_0	Fr_d	Spreading			EC during experiment ($\mu S/cm$)		
									(cm)			EC ₁	EC ₂	EC ₃
	θ°	%	(mm)	%		(l/min)	(m/s)		b_1	b_2	b_3			
1	0	4	2.3	16	0.027	0.68	2.73	111.3	15.5	32.5	43.5			
2	0	4	2.3	16	0.027	0.4	1.61	65.5	18.0	37.5	50.0			
3	30	4	2.3	16	0.027	0.7	2.81	114.6	4.0	15.5	29.0			
4	30	4	2.3	16	0.027	0.48	1.93	78.6	5.0	16.5	31.0			
5	0	4	2.3	0	0.027	0.62	2.49	101.5	6.0	12.5	27.0	3900	2500	2300
6	0	4	2.3	0	0.027	0.4	1.61	65.5	7.5	14.5	29.0	3400	2300	1600
7	30	4	2.3	0	0.027	0.57	2.29	93.3	5.0	11.0	16.0	3800	1900	1300
8	30	4	2.3	0	0.027	0.34	1.36	55.7	6.0	13.5	19.5	3900	1300	1200
9	0	4	3.3	16	0.027	1.3	2.53	86.3	6.0	19.0	36.0			
10	0	4	3.3	16	0.027	0.7	1.36	46.5	9.0	20.0	45.0			
11	30	4	3.3	16	0.027	1.3	2.53	86.3	5.0	9.0	31.0			
12	30	4	3.3	16	0.027	0.7	1.36	46.5	6.0	16.0	43.0			
13	0	4	3.3	0	0.027	1.01	1.97	67.1	6.0	16.5	30.0	4000	2600	2300
14	0	4	3.3	0	0.027	0.6	1.17	39.8	8.0	21.0	33.0	3900	2700	2300
15	30	4	3.3	0	0.027	1.04	2.03	69.1	4.0	14.0	26.0	4500	2300	1900
16	30	4	3.3	0	0.027	0.61	1.19	40.5	5.5	15.5	31.0	3900	2200	1400
17	0	4	4.8	16	0.027	1.14	1.05	29.7	33.0	45.0	53.0			
18	0	4	4.8	16	0.027	0.65	0.60	16.9	26.0	37.0	50.0			
19	30	4	4.8	16	0.027	1.13	1.04	29.4	39.0	46.0	53.0			
20	30	4	4.8	16	0.027	0.68	0.63	17.7	35.0	43.0	51.0			
21	0	4	4.8	0	0.027	1.24	1.14	32.3	10.0	24.0	35.5	5100	2900	2300
22	0	4	4.8	0	0.027	0.79	0.73	20.6	13.0	27.0	37.0	3800	2600	2300
23	30	4	4.8	0	0.027	1.3	1.20	33.8	7.5	20.0	30.0	5200	5100	2400
24	30	4	4.8	0	0.027	0.72	0.66	18.7	10.5	25.0	36.0	4600	2100	1600
25	0	6	2.3	16	0.041	0.77	3.09	104.2	16.0	25.5	38.0	4500	3200	2800
26	0	6	2.3	16	0.041	0.53	2.13	71.7	22.0	32.0	42.0	3120	2000	1450
27	30	6	2.3	16	0.041	0.77	3.09	104.2	11.0	20.0	32.5			
28	30	6	2.3	16	0.041	0.55	2.21	74.5	17.0	30.5	44.0			
29	0	6	2.3	0	0.041	0.63	2.53	85.3	9.5	21.0	28.5	4500	3100	2600
30	0	6	2.3	0	0.041	0.37	1.48	50.1	13.0	26.5	35.5	4100	2600	2400
31	30	6	2.3	0	0.041	0.6	2.41	81.2	5.0	11.0	14.0	3800	2500	1300
32	30	6	2.3	0	0.041	0.41	1.65	55.5	7.0	10.0	16.0	3100	2200	1300
33	0	6	3.3	16	0.041	1.19	2.32	65.3	25.0	38.0	46.0			
34	0	6	3.3	16	0.041	0.8	1.56	43.9	23.0	42.0	48.0			
35	30	6	3.3	16	0.041	1.07	2.09	58.7	21.0	33.0	42.0			
36	30	6	3.3	16	0.041	0.78	1.52	42.8	25.0	37.0	46.0			
37	0	6	3.3	0	0.041	0.93	1.81	51.1	13.0	22.0	32.5	6300	3300	3100
38	0	6	3.3	0	0.041	0.63	1.23	34.6	15.0	25.5	37.5	5300	3600	1300
39	30	6	3.3	0	0.041	1.04	2.03	57.1	5.5	16.0	22.0	5500	3300	1100
40	30	6	3.3	0	0.041	0.58	1.13	31.8	7.0	19.0	25.5	4900	2000	1800
41	0	6	4.8	16	0.041	1.43	1.32	30.8	40.0	48.0	53.0			
42	0	6	4.8	16	0.041	0.85	0.78	18.3	36.0	43.0	50.0			
43	30	6	4.8	16	0.041	1.17	1.08	25.2	31.5	43.0	53.0			
44	30	6	4.8	16	0.041	0.87	0.80	18.7	33.0	41.0	53.0			
45	0	6	4.8	0	0.041	1.27	1.17	27.3	13.0	26.0	33.5	7500	5000	3500
46	0	6	4.8	0	0.041	0.89	0.82	19.1	21.0	30.0	40.0	4000	3600	2700
47	30	6	4.8	0	0.041	1.01	0.93	21.7	15.0	23.0	32.0	6300	3000	2900
48	30	6	4.8	0	0.041	0.87	0.80	18.7	17.0	26.0	35.0	5800	3100	2500

49	0	8	2.3	16	0.053	0.64	2.57	76.2	19.5	30.5	34.5	6500	4300	3900
50	0	8	2.3	16	0.053	0.43	1.73	51.2	22.5	34.5	40.0	3400	2400	2000
51	30	8	2.3	16	0.053	0.7	2.81	83.4	8.5	20.0	30.0	6000	3600	2300
52	30	8	2.3	16	0.053	0.48	1.93	57.2	12.0	25.5	36.5	4900	1500	1000
53	0	8	2.3	0	0.053	0.67	2.69	79.8	11.0	19.5	30.0	6200	4300	2700
54	0	8	2.3	0	0.053	0.42	1.69	50.0	14.5	23.5	32.0	5200	3000	2300
55	30	8	2.3	0	0.053	0.61	2.45	72.6	8.0	14.0	20.0	5200	2600	1800
56	30	8	2.3	0	0.053	0.43	1.73	51.2	11.0	19.0	27.0	4400	1900	1300
57	0	8	3.3	16	0.053	1.05	2.05	50.7	19.5	30.0	38.0	7500	5100	4500
58	0	8	3.3	16	0.053	0.63	1.23	30.4	24.0	36.0	43.0	4500	3400	2400
59	30	8	3.3	16	0.053	1.15	2.24	55.5	11.0	21.0	28.0	4900	3000	2400
60	30	8	3.3	16	0.053	0.67	1.31	32.4	21.0	36.0	42.0	3800	1400	1200
61	0	8	3.3	0	0.053	1.05	2.05	50.7	20.0	32.5	40.0	9300	5400	3900
62	0	8	3.3	0	0.053	0.7	1.36	33.8	28.5	40.5	47.0	6600	3200	2600
63	30	8	3.3	0	0.053	1.06	2.07	51.2	9.0	23.5	36.0	7400	2900	1900
64	30	8	3.3	0	0.053	0.71	1.38	34.3	16.5	30.0	42.0	5000	3400	2100
65	0	8	4.8	16	0.053	1.21	1.12	22.9	28.0	37.5	39.0	7500	5200	4800
66	0	8	4.8	16	0.053	0.91	0.84	17.2	32.0	40.0	48.0	4900	3500	3100
67	30	8	4.8	16	0.053	1.43	1.32	27.1	25.0	35.0	44.0	6900	3100	2700
68	30	8	4.8	16	0.053	0.97	0.89	18.4	29.0	39.0	50.0	5300	2000	1900
69	0	8	4.8	0	0.053	1.17	1.08	22.1	27.0	36.5	35.0	7900	5500	6100
70	0	8	4.8	0	0.053	0.9	0.83	17.0	36.5	43.5	48.0	6000	4300	5300
71	30	8	4.8	0	0.053	1.25	1.15	23.7	23.0	32.5	39.5	8500	5800	4800
72	30	8	4.8	0	0.053	0.89	0.82	16.8	27.0	39.0	46.5	4800	2400	2300

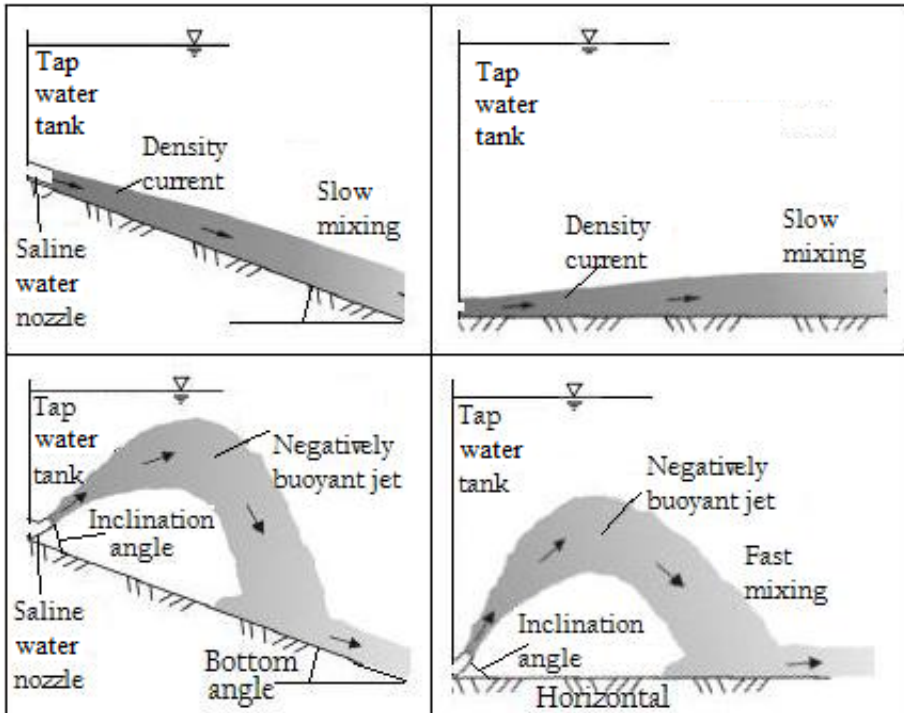


Fig. 2. Experimental strategies for submerged negatively buoyant for four cases, changing in inclination and bottom angle (After: Bleninger et. al, 2006)

3. Mathematical modelling and data analysis

3.1. Dimensional analysis

Brine discharge from a desalination plant is an example of denser fluid discharge to a stagnant ambient from a single port or a multiport at angle θ , with bottom slope S_b . This flow is conceptually divided into three connected regimes, the near-field, the intermediate field and the far-field. Considering a negatively buoyant jet, the dilution at the impact point S_d in the near-field from a single port into a stagnant ambient comes with some assumptions. For the jet to retain its identity, the discharge angle should be small to avoid attachment to the bottom, or too large to avoid falling on itself (Christodoulou, 1991). From this assumption, the terminal minimum dilution at the impact point can be written as:

$$S_d = f(Q_o, M_o, B_o, \theta) \quad (1)$$

The jet is discharged at a flow rate Q_o through a round nozzle with a diameter d_o , yielding an initial velocity of u_o , with an inclination angle θ to the horizontal plane. Most previous studies employ the discharge as initial volume flux Q_o , kinematic momentum flux M_o , and buoyancy flux B_o as leading variables in the dimensional analysis. The three main parameters are given in the form as:

$$Q_o = \frac{\pi d_o^2}{4} u_o \quad (2)$$

$$M_o = \frac{\pi d_o^2}{4} u_o^2 \quad (3)$$

$$B_o = g \frac{\rho_o - \rho_a}{\rho_a} Q_o = g' Q_o \quad (4)$$

where g = acceleration due to gravity, and $g' = g(\rho_o - \rho_a)/\rho_a$ = the modified acceleration due to gravity. The initial density of the jet is ρ_o and the density of the receiving water (ambient) ρ_a , where $\rho_o > \rho_a$, giving an initial excess density in the jet of $\Delta\rho = \rho_o - \rho_a$. The effect of the discharge is normally small and negligible, after simple dimensional analysis the initial dilution can be given by:

$$S_d = f_1(\theta, Fr_d) \quad (5)$$

where Fr_d is a Froude densimetric number defined as:

$$Fr_d = \frac{u_o}{\sqrt{g' d_o}} \quad (6)$$

A Froude number of 10 or larger simplifies the above equation to:

$$\frac{S_d}{Fr_d} = c(\theta) \quad (7)$$

Where the constant c is a function of inclined angle θ . Previously this constant was determined experimentally by many peoples e.g. Roberts and Tom (1987) for 60° inclined angle as a value of $c = 1.03$, for the same angle Zeitoun et al. (1970) has an earlier estimation of c value of about 1.12.

In the description of the intermediate field lateral spreading of the dense plume along a mildly sloping bottom, one should take into account that at small slopes, the entrainment is small and negligible (Alavian 1986; Britter and Linden, 1980; Ellison and Turner, 1959). Therefore, the width of the plume should depend mainly on the buoyancy flux, the bottom roughness (drag coefficient C_d) and the geometrical characteristics of the problem (Christodoulou, 1991). Thus, the lateral spreading width b at the downstream at distance x can be written as:

$$b = f(x, b_0, B_0, S_b, C_d, g) \quad (8)$$

With simple dimensional analysis eq. (8) can be written as:

$$\frac{b}{b_0} = f_1\left(\frac{x}{b_0}, \frac{B_0}{g^{3/2}b_0^{5/2}}, S_b, C_d\right) \quad (9)$$

Alavian (1986) suggested that the terminal to initial width ratio b_n/b_0 is essentially independent of the slope for $5^\circ \leq S_b \leq 15^\circ$, although the rate of approach to the normal state is faster for smaller slopes. From the above statement the determination of the terminal width b_n for relatively small slopes (less than about 15°), the explicit inclusion of S_b in, equation (9) can be omitted:

$$\frac{b_n}{b_0} \approx f_2\left(\frac{B_0}{g^{3/2}b_0^{5/2}}, C_d\right) \quad (10)$$

A power law form of equation (10) could be simplifies to:

$$\frac{b_n}{b_0} = K\left(\frac{B_0}{g^{3/2}b_0^{5/2}}\right)^a \quad (11)$$

Where $K = K(C_d)$. Equation (11) has been tested against limited experimental data by Alavian (1986) and numerical results by Tsihrintzis and Alavian (1986). They referred to a distance $x = 100b_0$, where the spreading width had not yet strictly reached a constant value, apparently due to the low drag coefficient employed. The value of the exponent was estimated by Christodoulou, 1991, as $a = 0.183$, while k exhibits an increasing trend with decreasing C_d .

3.2. Model assumption

In this paper, mathematical modeling of the jet and plume evolution was essentially divided into two sub-models the near field and the intermediate field. The near field is the proximity of the nozzle, where jet and plume development is driven by the initial conditions; i.e. the initial momentum flux, volume flux, and buoyancy flux, and there is no interaction with the bottom. In the intermediate field, the buoyant jet essentially becomes a plume and it is interacting with the bottom. The main forces to be taken into account are bottom drag force and bottom slope effects. The “intermediate field” begins when the buoyant jet reaches the bottom. In order to develop a simple model describing the situation in the proximity of the discharge nozzle, some assumptions are made following Jönsson (2004):

- Density differences are too small to affect inertia forces, but are important for the buoyancy force (the Boussinesque approximation). This assumption implies that the continuity equation can be described in terms of volume instead of mass
- Horizontal momentum of the jet is constant along the jet trajectory.
- Jet is symmetrical in a plane perpendicular to the jet axis.
- There is no influence from the boundaries of the receiving water.
- The section of the plume is not anymore round shaped but rectangular
- Plume is moving attached to the bottom; drag effect is taken into account by C_d .
- There is a linear relationship between concentration and density.
- Slope of the bottom is constant.
- There is a similarity for velocities and concentrations (or density deficit) in planes perpendicular to the jet axis (Gaussians distributions) see Figure 3.

The Gaussian distribution profile was assumed in this study as shown in Figure 3, where C_c is the concentration along the centerline, and B is the jet width or, as in our case the spreading (Doneker & Jirka, 2007).

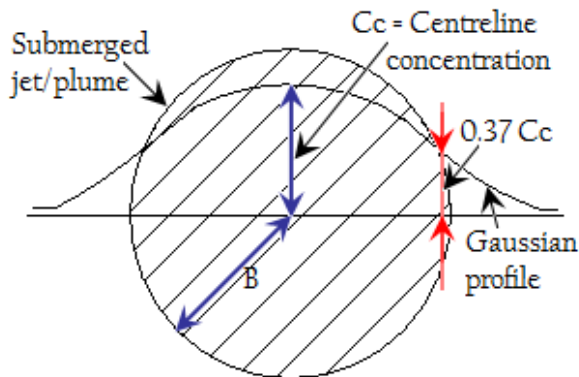


Fig. 3. Submerged jet/plume Gaussian profile used to calculate the salt concentration (after Doneker & Jirka, 2007)

3.3. Validation of the model

The validation of the model is one of the most important phases in the model building sequence. A completely independent set of parameters from the one used during the calibration must be used. For each experimental run three errors are calculated:

$$\varepsilon_{EC,i} = \left| \frac{EC_{model,i} - EC_{experiment,i}}{EC_{experiment,i}} \right| \quad (12)$$

$$\varepsilon_{b,i} = \left| \frac{b_{model,i} - b_{experiment,i}}{b_{experiment,i}} \right| \quad (13)$$

$$\varepsilon_i = \left| \frac{\varepsilon_{EC,i} - \varepsilon_{b,i}}{2} \right| \quad (14)$$

Where, $\varepsilon_{EC,i}$ is the error estimated in modeling of electrical conductivity (EC, $\mu\text{S}/\text{cm}$), in the i -th point of measurement ($i = 0.2; 0.4; 0.6 \text{ m}$), $\varepsilon_{b,i}$ is the error in modeling of lateral spreading b , in the i -th point of measurement and ε is the overall average error, in the i -th point of measurement. The validation process was done considering the two different cases with and without the bottom slope as done before for the calibration. In Figure 4 the graphical visualizations of the error made in the modeling of the half width spreading and the concentration for the test without the bottom slope are reported. The best results are for the values closer to the trendline where the perfect correspondence between the model and the measures is. The sum of these two errors committed in the modeling is used to obtain an average error.

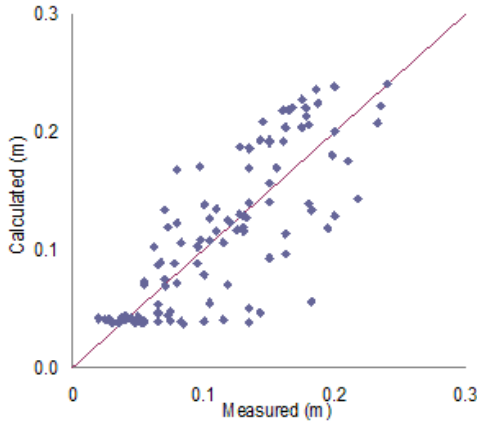


Fig. 4a. Evaluation of the $\varepsilon_{b,i}$ error between measured and calculated half width spreading ($b/2$)

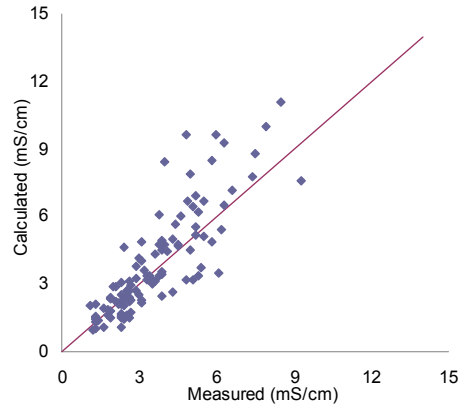


Fig. 4b. Evaluation of the $\varepsilon_{EC,i}$ error between measured and calculated Electrical Conductivity (EC)

4. Results and Discussions

4.1. Froude and Reynolds number

Some limitations can be noted with the experimental setup, but these limitations were eliminated to a large extent by reproducing the experiments. The measurement of the lateral spreading, recorded on the bottom glass, was influenced by the visual impressions of the person who drew it, which created some difficulties to estimate the accuracy of the measurements. An alternative methodology was applied by Cipollina et al. (2005) and Suresh et al. (2008), who used techniques based on image processing, capable of recording the jet with more accuracy, also at the lowest levels of tracer concentration. The measurement of electrical conductivity EC through a portable device is quite fast, but brings with it uncertainties concerning the exact location of the measurement point. Also, the introduction of a probe during the test can disturb the flow regime downstream the measurement point. It was also difficult to estimate the error associated with the probe measurements. Non-dimensional lateral spreading measured at the plan view along the flow at horizontal distances 20, 40 and 60cm was drawn versus densimetric Froude and compared with Reynolds number figures. The figures exhibit the different behaviour of the measured data at the horizontal initial jet angle with and without bottom slope. The data vary with the densimetric Froude number in both cases with and without bottom slope while it exhibits the same trendline versus Reynolds number.

4.2. Comparisons with Matlab and CORMIX

The Matlab model could be applied successfully to model the experimental runs and the best results were obtained for the run without the bottom slope, as highlighted by the lower average error was previously calculated. The average error ε_i obtained in this case was around 28 %. Analyzing the experimental runs without bottom slope, an effort can be made to determine where more of the errors are found regarding the spreading and the concentration. Spreading values above the average are found for the runs with a salinity of 8 %, where an average error ε_i of 46 % was calculated. For all other salinities the average spreading error ε_i is around 28 %. From the comparison of the Matlab model with the experimental results is that the error for the lateral spreading is within the range of 30 % for all the measurements, slightly above the error without bottom slope. Things became different considering the Electrical Conductivity, as a matter of fact the error made in this case is definitely larger and in particular for the measurements with θ equal to zero, where the error was around 60 %, twice the error made for θ equal to 30°. The Matlab model in general is less accurate in predicting the values when a bottom slope is present, but in this case the error is definitely larger than expected. In discussing these results, one must take into account the difficulty in measuring the conductivity at the same point every time and the variability in the readings obtained with the probe used.

CORMIX was developed as software for hydrodynamic modeling of real (field) cases. In this study, the model was used to test its ability to describe results from small-scale laboratory experiments. However CORMIX merely provided exactly the same results in both cases; this unexpected behavior was revealed only when the values were compared to each other. From these results it is clear that the CORMIX program is not suitable in

describing the lateral spreading in cases involving small scales. To verify the effectiveness of CORMIX in real case simulations, such an example has to be carried out and compared with the results obtained with Matlab model. The Electrical conductivity error $\epsilon_{EC,i}$ is more widely spread; above ϵ_i average values are found independently from the geometrical configuration or salinity used in the experimental run, but the errors are comparable with the one found for lateral spreading.

4.3. Bottom slope effects

Electrical conductivity ratio and lateral spreading compared with and without bottom slope at three horizontal distances 20, 40 and 60cm are presented in Figure 5. The figures presented for electrical conductivity give an expression that there are small variations between flow on horizontal and with bottom slope. The correlations between the two cases are between 86-89%, which means the sloping bottom does not affect the flow regime. For the lateral spreading, it also showed that the correlation is 88-91%, much better than in electrical conductivity.

Normalized lateral spreading (b/d_0) and thickness of the dense layer (z/d_0) are drawn in Figure 6, and compared for four cases at horizontal distances 20, 40 and 60cm along the x-axis with respect to inclined angle (θ) and bottom slope (S_b). Different comparison was made for interrelation between measured parameters to see the effect of initial angle and bottom slope. First we compare normalized lateral spreading in three different positions, inclined angle ($\theta = 0^\circ$) and bottom slope ($S_b = 0^\circ$) versus ($\theta = 30, S_b = 0$); ($\theta = 0, S_b = 16$); ($\theta = 30, S_b = 16$). As it can be seen, for the lateral spreading all figures and trendline have shown good correlation and it is above 80% except one of them. Comparing the second part of Figure 6, the normalized dense layer thickness showed that for two cases is not so good and it is below 70% and for one case with ($\theta = 30, S_b = 0$) showed bad correlation which indicates that inclined and initial angle is much important than bottom slope.

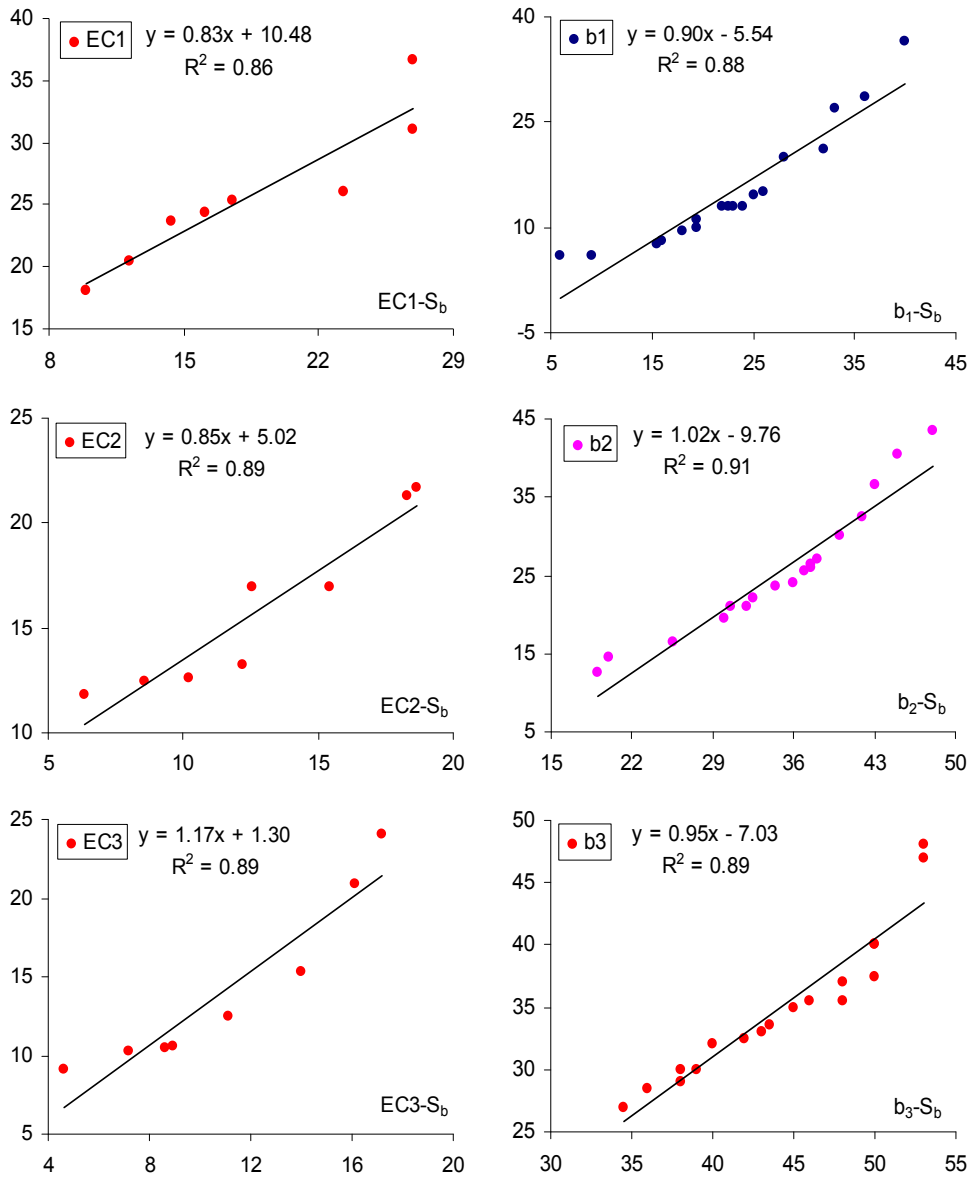


Fig. 5. Electrical conductivity (EC as a ratio) and lateral spreading (b in cm) comparisons with and without bottom slope (S_b) at horizontal distances 20, 40 and 60cm

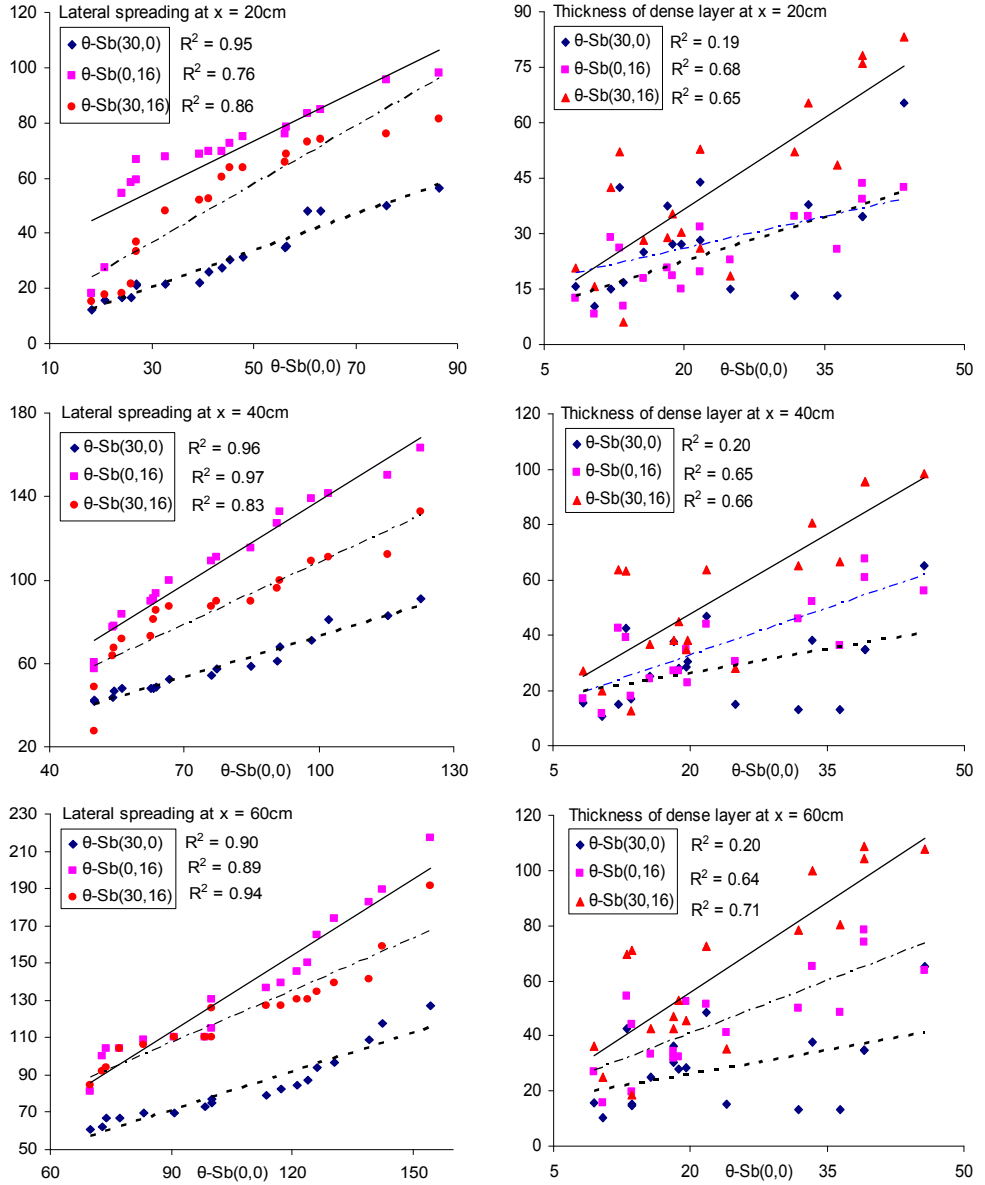


Fig. 6. Normalized lateral spreading (b/d_0) and thickness of dense layer (z/d_0) comparison for four cases at horizontal distances 20, 40 and 60cm, with respect to inclined angle θ and bottom slope (S_b)

The concept of dilution spreading up to the attainment of a normal state is correlated in normalized form with and without the bottom slope (Christodoulou, 1991). The estimation of lateral spreading and electrical conductivity comparisons will be useful in practical

applications concerning the disposal of heavy industrial wastes or brines into coastal or inland waters. The result derived may allow us to understand and estimate overall dilution and final plume width up to the far field. This estimation will be more useful in discharging brines from desalination plant. Based on the findings in this study in the near- and intermediate the flow geometry depends on the angle of incline and the rate of supply of the dense fluid. After an initial spreading, the flow geometry becomes relatively constant with the horizontal distance down the slope (Alavian, 1986). For a given buoyancy flux, the normal layer width seems to weakly depend on slope.

The use of this study originally was made to be able to distinguish between different discharges at bottom slopes to the recipients including jet inclination angle. Desalination brine is the real case to consider in studying environmental impact and assessment when building new projects. In real life most of the recipient e.g. Seas and Oceans are naturally having bottom slope, this can be vary from coast to another. Therefore, an experimental result for concentration percentage that was measured at three distances along the flow was compared with and without bottom slope for densimetric Froude number smaller and larger than 40, as presented in Figure 7. The concentration along the flow was improved by about 10% with the bottom slope for Froude number smaller than 40 as real discharge cases does. Thus, this type of improvement can be used for brine discharge outlet to the recipients to minimize the concentration and let it dilute faster and goes farther. Another comparisons presented in Figure 8, with and without bottom slope but this time including jet inclination angle of 30° . It also showed better improvement in the concentration of about 40% with bottom slope and inclination for Froude number smaller than 40, but small difference for Froude number larger than 40 which is not the case.

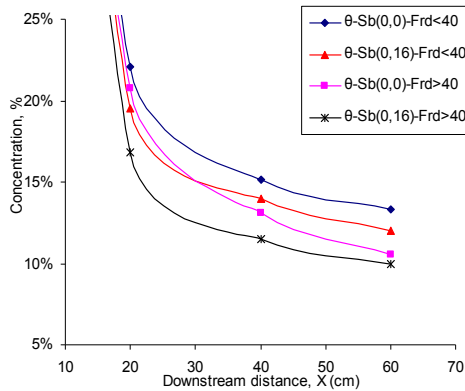


Fig. 7. Concentration percentage along the flow with and without bottom slope

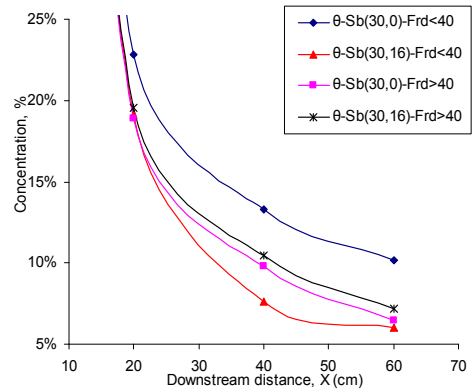


Fig. 8. Concentration percentage along inclined flow with and without bottom slope

5. Conclusions

The results achieved with the mathematical simulation model are satisfactory, considering the different behavior of the buoyant jet in the near and intermediate field. The Matlab model could be applied successfully to model the experimental runs and the best results were obtained for the run without the bottom slope, as highlighted by the calculation at lower average error. An average error ϵ_i of 0.28 and 0.37 was found, respectively, for the test with and without the presence of an inclined bottom. The model failed to give a proper description of the influence of the bottom slope through the parameter employed, and a new hypothesis is needed for modeling the entrainment process. The commercial software CORMIX did not properly reproduce the experimental results, giving inaccurate results for the bench scale simulations. Non-dimensional analysis showed how the dilution and lateral spreading of brine discharge in the near and intermediate field is not related to the initial hydraulic properties, as represented by the densimetric Froude and Reynolds numbers. It is anyway important to underline that is not under discussion the fact that in the near field, the jet properties are strongly dependent by the initial condition, but in the present study the presence of near and intermediate field is considered together, without trying to divide the two different zones.

The concept of spreading up to the attainment of a normal state is correlated in normalized form with and without the bottom slope. The estimation of lateral spreading and electrical conductivity comparisons will be useful in practical applications concerning the disposal of heavy industrial wastes or brines into coastal or inland waters. The result derived may allow us to understand and estimate overall dilution and final plume width up to the far field. This estimation will be more useful in discharging brines from desalination plant. Based on the findings in this study in the near- and intermediate the flow geometry depends on the angle of incline and the rate of supply of the dense fluid. After an initial spreading, the flow geometry becomes relatively constant with the horizontal distance down the slope. For a given buoyancy flux, the normal layer width seems to weakly depend on slope. Concentration was improved with the bottom slope by 10% than the horizontal bottoms and improved by about 40% with bottom slope together with inclination of 30 degrees. The suggestion in the practical applications concerning desalination brines and similar discharge of heavy wastes is to have inclination and bottom slope together. This study has limited result for only 16% bottom slope and 30 degrees inclination, subject to further experimental study.

Acknowledgments

Authors would like to thank Center for Middle Eastern Studies (CMES) at Lund University because the project was partly funded by them, primarily the experimental work. Also Jacopo Grazioli and Davide Noro are acknowledged for assistance in the valuable work.

Notations

A	= cross-sectional area;
B_o	= buoyancy flux the nozzle;
b	= lateral spreading
D	= mixing tank diameter;
d_o	= nozzle diameter;
C_c	= centerline concentration
C_d	= drag coefficient
EC	= electrical conductivity
Fr_d	= jet densimetric Froude number;
g	= acceleration due to gravity;
g'	= effective acceleration due to gravity;
H	= mixing tank depth;
L	= mixing tank length;
M_o	= momentum flux at the nozzle;
Q_o	= volume flux at the nozzle;
PIV	= particle image velocity
S	= nozzle salinity;
S_b	= bottom slope
S_d	= dilution at the impact point
u_o	= nozzle velocity;
W	= mixing tank width;
θ	= initial jet angle;
ρ_o	= effluent density; and
ρ_a	= ambient density;
ε	= error

References

- [1] Abraham, G. (1967), "Jets with negative buoyancy in homogeneous fluids", J. Hydr. Res., 5, 236-248.
- [2] Akiyama, J. and Stefan, H. G. (1984), "Plunging Flow into a Reservoir: Theory", Journal of Hydraulic Engineering, ASCE, Vol. 110, No. 4, Apr., pp. 484-499.
- [3] Alavian V. (1986), "Behavior of density currents on an incline", J. of Fluid Mechanics, ASCE, 112, (1) 27-42.
- [4] Anderson, J.L. Prker, F.L. and Benedict, B.J. (1973), "Weakly depositing turbidity current on a small slope", J. Hydr. Res., 28, (1) 55-80.
- [5] Benjamin, T.B. (1968), "Gravity currents and related phenomena", J. Fluid Mech, 31, (2) 209-248.
- [6] Bleninger, T. and Jirka, G. H. (2007a), "Modelling and environmentally sound management of brine discharges from desalination plants", Accepted for EDS Congress, April 22-25, Halkidiki, Greece.
- [7] Bleninger, T. and Jirka, G. H. (2007b), "Towards Improved Design Configurations for Desalination Brine Discharges into Coastal Waters", IDA World Congress-Maspalomas Gran Canaria -Spain October 21-26, REF: IDAWC/MP07-139.
- [8] Bleninger T. Jirka, G.H. and Weitbrecht, V., 2006, "Optimal discharge configuration for brine effluents from desalination plants", Proc. DME (Deutsche MeerwasserEntsalzung) - Congress, 04.-06.04.2006, Berlin.

- [9] Bloomfield, L.J. & Kerr, R.C. (2000), "A theoretical model of a turbulent fountain" *J. Fluid Mech.* 424, 197–216.
- [10] Britter, R.E. and Linden, P.E. (1980), "The motion of the front of a gravity current travelling down an incline", *J. of Fluid Mechanics*, 99, (3) 531-543.
- [11] Burattini, P. Antonia, R. A. Rajagopalan, S. and Stephens, M. (2004), "Effect of initial conditions on the near-field development of a round jet", *Expt. Fluids* 37, 56–64.
- [12] Christopher, G. B. and Andrew, P. (2007/01), "A Review of Experimental and Computational Studies of Flow from the Round Jet", Queen's University, Kingston, Ontario, Canada, INTERNAL REPORT No. CEFDL.
- [13] Christodoulou, G. C. (1991), "Dilution Of dense effluents on a sloping bottom", *Journal of Hydraulic Research*, Vol. 29 (3) 329-339.
- [14] Chu, V.H. (1975), "Turbulent dense plumes in a laminar cross flow", *J. Hydr. Res.*, 13, 253-279.
- [15] Cipollina, A. Brucato, A. Grisafi, F. And Nicosia, S. (2005), "Bench scale investigation of inclined dense jets", *J. Hydraulic Eng.* 131(11), 1017–1022.
- [16] Cipollina, A. Bonfiglio, A. Micale, G. and Brucato, B. (2004), "Dense jet modelling applied to the design of dense effluent diffusers", *Desalination* 167, 459-468.
- [17] Demetriou, J.D., (1978). Turbulent diffusion of vertical water jets with negative buoyancy (In Greek), Ph.D. Thesis, National Technical University of Athens.
- [18] Dimotakis, P. E. (2000), "The mixing transition in turbulent flows", *J. Fluid Mech.* 409, 69–98.
- [19] Dimotakis, P. E. Miake-Lye, R. C. and Papantoniou, D. A. (1983), "Structure and dynamics of round turbulent jets", *Phys. Fluids* 26, 3185–3192.
- [20] Doneker, R.L. and Jirka, G.H. (2007), "A Hydrodynamic Mixing Zone Model and Decision Support System for Pollutant Discharges into Surface Waters" *Cormix User Manual 6.0E*.
- [21] Ellison, T.H. Turner, J.S. (1959), "Turbulent entrainment in stratified flows", *J. Fluid Mech*, 9, 423-448.
- [22] Hauenstein, W. and Dracos, TH. (1984), "Investigation of plume density currents generated by inflows in lakes", *J. Hydr. Res.*, 22, (3) 157-179.
- [23] Jirka, G.H. (2006), "Integral model for turbulent buoyant jets in unbounded stratified flows", Part 2: Plane jet dynamics resulting from multiport diffuser jets". *Environ. Fluid Mech.*, (6) 43-100.
- [24] Jirka, G.H. (2004), "Integral model for turbulent buoyant jets in unbounded stratified flows", Part 1: The single round jet". *Environ. Fluid Mech.*, (4) 1-56.
- [25] Jirka G. H. Robert L. Doneker, and Steven W. H. (1996), "User's Manual for CORMIX: A Hydrodynamic Mixing Zone Model And Decision Support System For Pollutant Discharges Into Surface Waters" DeFrees Hydraulics Laboratory School of Civil and Environmental Engineering, Cornell University.
- [26] Jönsson, L. (2004), "Receiving Water Hydraulics", *Water Resources Engineering*, Lund University.
- [27] Kikkert, G.A. Davidson, M.J. and Nokes, R.I. (2007), "Inclined negatively buoyant discharges", *J. Hydraulic Eng.* 133(5), 545–554.
- [28] Lindberg, W.R. (1994), "Experiments on negatively buoyant jets, with and without cross-flow, in: P.A. Davies", M.J. Valente Neves (Eds.), *Recent Research Advances in the Fluid Mechanics of Turbulent Jets and Plumes*, NATO, Series E: Applied Sciences, vol. 255, Kluwer Academic Publishers, pp. 131–145.
- [29] Matsuda, T. and Sakakibara, J. (2005), "On the vortical structure in a round jet", *Phys. Fluids* 17.
- [30] Pantzlauff, L. and Lueptow, R.M. (1999), "Transient positively and negatively buoyant turbulent round jets", *Exp. Fluids* 27, 117–125.

- [31] Papanicolaou, P.N. and Kokkalis, T.J. (2008), "Vertical buoyancy preserving and non-preserving fountains, in a homogeneous calm ambient", *International Journal of Heat and Mass Transfer* 51, 4109–4120.
- [32] Pincince, A.B. & List, E.J. (1973), "Disposal of brine into an estuary", *J. Water Pol. Contr. Fed.*, 45, 2335-2344.
- [33] Roberts, P.J.W. Ferrier, A. and Daviero, G. (1997), "Mixing in inclined dense jets", *J. Hydraulic Eng.* 123(8), 693–699.
- [34] Roberts, P.J.W. and Toms, G. (1987), "Inclined dense jets inflowing current", *J. Hydr. Engrg.*, ASCE, 113, (3) 323-341.
- [35] Sanchez D. (2009), "Near-field evolution and mixing of a negatively buoyant jet consisting of brine from a desalination plant", Thesis work at Water Resources Engineering, Department of Building and Environmental Technology, Lund University.
- [36] Shahrabani, D.M. and Ditmars, J.D. (1976), "Negative buoyant slot jets in stagnant and flowing environments, *Ocean Engrg. Rep. No. 8*, Dept. Civil Engrg., Univ. of Delaware, Newark, Del., U.S.A.
- [37] Shao, D., and Law, A.W.-K. (2010), "Mixing and boundary interactions of 30° and 45° inclined dense jets", *Environmental Fluid Mechanics*, 10 (5) 521-553.
- [38] Simpson, J.E. (1987), "Density Currents: In the environment and the laboratory", Ellis Horwood Ltd, Chichester, U.K.
- [39] Suresh, P. R. Srinivasan, K. Sundararajan, T. and Sarit, Das, K. (2008), "Reynolds number dependence of plane jet development in the transitional regime", *Physics of fluids* 20, 044105 1-12.
- [40] Tong, S.S. and Stolzenbach, K.D. (1979), "Submerged discharges of dense effluent", R. M. Parsons Lab., Rept. No. 243, Mass. Inst. Of Tech, Cambridge, Mass., U.S.A.
- [41] Tsihrintzis V.A. and Alavian, V. (1986), "Mathematical modeling of boundary attached gravity plumes", *Proceedings Inter. Symp. On Buoyant Flows*, Athens, Greece, 289-300.
- [42] Turner, J.S. (1966), "Jets and plumes with negative or reversing buoyancy", *J. of Fluid Mechanics*, 26, 779-792.
- [43] Zhang, H. Baddour, R.E. (1998), "Maximum penetration of vertical round dense jets at small and large Froude numbers", *J. Hyd. Eng.*, ASCE 124 (5) 550–553, Technical Note No. 12147.
- [44] Zeitoun, M.A. et al., (1970), "Conceptual design of outfall systems for desalination plants", *Res. and Devel. Progress Res. No. 550*, Office of Saline Water, U.S. Dept. of the Interior.

Paper II

An Experimental Investigation on Inclined Negatively Buoyant Jets

Bashithalshaaer, R., Larson M., and Persson K.M. 2011

Journal of Hydraulic Research (under review)

An Experimental Investigation on Inclined Negatively Buoyant Jets

Raed Bashitialshaaer^a, Magnus Larson^a, Kenneth M. Persson^{ab}

^aDepartment of Water Resources Engineering, Lund University, PO Box 118, SE-221 00 Lund, Sweden
Tel. +46462224367, 8729; Fax: +46462224435; Raed.Alshaaer@tvrl.lth.se, magnus.larson@tvrl.lth.se

^bSYDVATTEN AB, Skeppsgatan 19, SE 211 19 Malmö, Sweden. Tel. +46 46 222 9470; email:
Kenneth_M.persson@tvrl.lth.se

ABSTRACT

An experiment was performed to investigate the behavior of inclined negatively buoyant jets. Such jets arise when brine is discharged from desalination plants and improved knowledge of their behavior is required for designing discharge systems that cause a minimum of environmental impact on the receiving waters. In the present experiment, a turbulent jet with a specific salinity was discharged through a circular nozzle at an angle to the horizontal into a tank with fresh water and the spatial evolution of the jet was recorded. In total, 72 experimental cases were carried out where four different initial jet parameters were changed, namely the nozzle diameter, the initial jet inclination, the jet density (or salinity), and the flow rate (or exit velocity). The measurements of the jet evolution in the tank included five geometric quantities describing the jet trajectory that are useful in the design of brine discharge systems. Thus, the collected data encompassed the maximum rise level of the jet (Y_m) and its horizontal distance (X_{ym}), the maximum level of the jet centerline (Y) and its horizontal distance (X_y), and the distance to the edge point (X_e) (where the jet returns to the discharge level). Several of the geometric jet quantities showed strong correlation, for example, Y_m versus Y , X_{ym} versus X_y , and X_e versus X_{ym} , and regression relationships could be developed where one quantity can be predicted from another. If maximum levels were correlated with the corresponding horizontal distances, the angle must be taken into account when developing predictive relationships. Dimensional analysis demonstrated that the geometric jet quantities studied, if normalized with the jet exit diameter, should be related to the densimetric Froude number (Fr_d). Analysis of the collected data showed that this was the case for $Fr_d < 100$, whereas for larger values on Fr_d the scatter in the data increased significantly, simultaneously as the studied jet quantities did not increase at the same rate. As has been observed in some previous investigations, the slope of the best-fit straight line through the data points was a function of the initial jet angle (θ), where the slope increased with θ for the maximum levels studied, but had a more complex behavior for horizontal distances.

Keywords: Laboratory experiment; turbulent jet; mixing; negative buoyancy; desalination; brine.

1 Introduction

1.1 Background, objectives, and procedure

In desalination, high-salinity brine is produced that needs to be discharged to a receiving water with a minimum of environmental impact. The brine is typically discharged as a turbulent jet with an initial density that is significantly higher than the density in the

receiving water, where the difference in salinity between the jet and the ambient may be up to 4-5%. Thus, a rapid mixing of the discharged brine is desirable to ensure minimum impact, which requires detailed knowledge of the jet development. Since the density of the jet is larger than the density of the receiving water, the jet is negatively buoyant and it will impinge on the bottom some distance from the discharge point depending on the initial momentum, buoyancy, and angle of the discharge, as well as the bathymetric conditions. After the jet encounters the bottom it will spread out as a gravity current with a low mixing rate, making it important to achieve the largest possible dilution rate when the jet moves through the water column.

However, relatively few studies have been conducted on negatively buoyant jets, especially with regard to experimental work. The present investigation focuses on collecting data through a laboratory experiment on the evolution of a negatively buoyant jet with the purpose of: (1) increasing our understanding of the behavior of such jets, (2) developing empirical relationships for predictive purposes, and (3) calibrating and validating numerical models. Only the two first aspects are discussed in the present paper (for numerical modelling of the collected data, see Sanchez 2009).

The experiment was performed to investigate the behavior of inclined negatively buoyant jets. A turbulent jet with a specific salinity was discharged through a nozzle at an angle to the horizontal into a tank with fresh water and the evolution of the jet was recorded. In total, 72 experimental cases were carried out where four different initial jet parameters were changed, namely the nozzle diameter, the jet inclination, the jet density (or salinity), and the flow rate (or exit velocity). The measurements of the jet evolution in the tank included five geometric quantities describing the jet trajectory that are useful in the design of brine discharge systems. Thus, the collected data encompassed the maximum rise level of the jet and its horizontal distance, the maximum level of the jet centerline and its horizontal distance, and the distance to the edge point (where the jet returns to the discharge level).

First, a general survey is made of previous studies on negatively buoyant jets of relevance for the present investigation. Existing data on jet evolution and mixing properties are compiled from the literature and subsequently used for comparison in the analysis of the collected data. Dimensional analysis is carried out to determine the main parameters governing the jet development, focusing on the properties of the jet trajectory. The experimental work is then described, including experimental setup, procedure, and cases performed. The new data from this study are analyzed based on the results from the dimensional analysis, and empirical relationships are formulated to predict the quantities of interest. These results are then compared with previous studies. Finally the conclusions are given.

1.2 Previous relevant studies

Dense jets, being a particular type of negatively buoyant flows, have been studied by several authors (*e.g.*, Turner, 1966; Abraham, 1967; Tong and Stolzenbach, 1979; James *et al.*, 1983; McLellan and Randal, 1986; Baines *et al.*, 1990; Roberts and Toms, 1987, 1988; Roberts *et al.*, 1997; Zhang and Baddour, 1998). In an early study, Zeitoun *et al.* (1972) investigated an inclined jet discharge, focusing on an initial jet angle of 60 deg because of the relatively high dilution rates achieved for this angle. Roberts and Toms (1997) and Roberts *et al.* (1997) also focused on the 60 deg discharge configuration, where both the

trajectory and dilution rate were measured. A jet discharge into a moving ambient has also been investigated (Pincince and List, 1973). Negatively buoyant jets are known as fountains when they are injected upwards into a less dense environment (*e.g.*, Turner, 1966; Abraham, 1967; Baines *et al.*, 1966). Measurements of the penetration height of fountains were reported by Demetriou (1978) and Zhang and Baddour (1998) for a wide range of initial densimetric Froude numbers. The stable stratification formed by a fountain was studied and discussed by Baines *et al.* (1990), whereas the effects of cross flows and angle of injection on fountains were investigated by Lindberg (1994). Cipollina *et al.* (2005) extended the work performed in previous studies on negatively buoyant jets discharged into calm ambient by investigating flows at different discharge angles, including 30, 45, and 60 deg, and for three densities 1055, 1095 and 1179 kg/m³. Kikkert *et al.* (2007) developed an analytical solution to predict the behavior of inclined negatively buoyant jets and reasonable agreement was obtained with measurements for initial discharge angles ranging from 0 to 75 deg and initial densimetric Froude numbers from 14 to 99. The dimensions of the experimental tank (mixing tank or lighter density tank) may be important to take into account when comparing results from different studies. Boundary effects could be present and for smaller tanks recirculation may influence the jet behavior. Table 1 summarizes key experimental studies on negatively buoyant jets and the size of the tank used in the experiment (dimensions given for the tanks in terms of bottom area and height).

Table 1 Previous experimental studies on negatively buoyant jets and the size of the tanks employed in the experiments (if a circular tank was used, D denotes diameter)

Previous study	Bottom area (m ²)	Depth (m)
Turner, 1966	0.45 x 0.45	1.40
Demetriou, 1978	1.20 x 1.20	1.55
Lindberg, 1994	3.64 x 0.405	0.508
Roberts <i>et al.</i> , 1997	6.1 x 0.91	0.61
Zhang & Baddour, 1998	1.0 x 1.0	1.0
Pantzlaff & Lueptow, 1999	$D = 0.295$	0.89
Bloomfield and Kerr, 2000	0.40 x 0.40	0.70
Cipollina <i>et al.</i> , 2005	1.50 x 0.45	0.60
Kikkert <i>et al.</i> (2007)	6.22 x 1.54	1.08
Papanicolaou & Kokkalis, 2008	0.80 x 0.80	0.94
Shao & Law, 2010	2.85 x 0.85	1.0
This study	1.50 x 0.60	0.60

Bleninger and Jirka (2007a,b) suggested that smaller discharge angles of about 30 to 45 deg may have higher dilution rates at the impingement location and better offshore transport of the mixed effluent during weak ambient currents than larger angles. Submerged negatively buoyant jet discharging over a flat or sloping bottom, covering the entire range of angles from 0 to 90 deg, were investigated in Jirka (2006) for desalination brine discharges into coastal waters in order to improve design configurations.

As a complement to experimental studies, and as a user of data from such studies, numerical modelling of the evolution of negatively buoyant jets may be performed. For example, Jirka (2004) employed simulation results from the CORMIX submodel CorJet, which includes a numerical jet integral model, to study negatively buoyant jets. This model has been validated with data on the jet trajectory development for a limited set of

experimental data (e.g., Bleninger and Jirka, 2007a,b), all for flat bottom. For high-capacity desalination, producing large volumes of brine, it may be necessary to distribute the initial discharge over several ports, *i.e.*, using a multiport diffuser. This situation can be simulated employing a numerical model such as CorJet (Jirka, 2006). A model for a multiport diffuser discharge in an ambient coflow was presented earlier by Lee *et al.* (1977) and Jirka (1982). If higher dilution rates or smaller mixing zones are required at a particular site, the use of multiport diffusers may be necessary (e.g., Lee and Jirka, 1980; Jirka, 1982).

2 Dimensional considerations and review of main jet properties

2.1 Dimensional analysis of negatively buoyant jet

An inclined negatively buoyant jet discharged upwards at an angle towards the horizontal is shown in Fig. 1, representing the typical case of a brine jet being discharged to a receiving water. The jet describes a trajectory that reaches a maximum level, after which the jet changes its upward movement and plunges towards the bottom. Since the jet is negatively buoyant, the initial vertical momentum flux driving the flow upwards is continuously reduced by the buoyancy until this flux becomes zero at the maximum level and the jet turns downwards.

Knowledge of the shape of the jet trajectory is important in the design of brine discharge. Major variables that previously have been employed to describe the jet trajectory (with respect to the location of the jet origin) are: the maximum level of the jet centerline Y and its horizontal distance X_y , the maximum level of jet flow edge Y_m , and its horizontal distance X_{ym} , and the maximum horizontal distance to the jet flow edge point X_e (that is, where the jet returns to the discharge level). Fig. 1 illustrates the definition of these five geometric quantities. The location of the jet edge may be defined based on a certain reduction of the centerline concentration. However, laboratory experiments have often been performed with colored jets and the jet edge is then often arbitrarily defined as a location where the color is no longer visible (or has been reduced to a specific value). This could make it difficult to compare absolute values obtained in different experiments, but as long as a consistent definition is applied during a specific set of experiments, quantities such as spreading angles yields comparable values.

In order to establish possible relationships between the geometric quantities of interest and the main governing variables, a dimensional analysis was carried out. The jet is discharged at a flow rate Q_o through a round nozzle with a diameter d_o , yielding an initial velocity of u_o , and at an angle θ to the horizontal plane. The initial density of the jet is ρ_o and the density of the receiving water (ambient) ρ_a , where $\rho_o > \rho_a$, giving an initial excess density in the jet of $\Delta\rho = \rho_o - \rho_a$. Similar flow problems were previously analyzed through dimensional analysis by Turner (1966), Pincince and List (1973), Fischer *et al.* (1979), Roperts and Toms (1987), and Cipollina *et al.* (2005). In general, the jet will be turbulent and the Reynolds number (Re) high, so viscous effects are negligible and Re is not included in the analysis.

Most previous studies employ the initial volume flux Q_o , kinematic momentum flux M_o , and buoyancy flux B_o as leading variables in the dimensional analysis (the initial angle of

The diagram illustrates the trajectory of a projectile, showing the centerline and the edge of the projectile. The trajectory is defined by the centerline and the edge. The centerline is the path of the center of the projectile, and the edge is the path of the edge of the projectile. The trajectory is shown in a 2D coordinate system with a horizontal x-axis and a vertical y-axis. The origin is at the launch point. The trajectory starts at the origin and ends at the impact point. The centerline is a solid line, and the edge is a dashed line. The trajectory is labeled with various parameters: θ is the launch angle, g is the acceleration due to gravity, Y_m is the maximum height of the centerline, Y is the height of the centerline at a given horizontal distance X_Y , X_{Ym} is the horizontal distance to the maximum height of the centerline, X_e is the horizontal distance to the impact point, and X_{em} is the horizontal distance to the maximum height of the edge. The impact point is labeled "Impact point" and the edge point is labeled "Edge point".

$$Q_o = \frac{\pi d_o^2}{4} u_o \quad (1)$$

$$B_o = g \frac{\rho_o - \rho_a}{\rho_a} Q_o = g' Q_o \quad (3)$$

$$l_M = \frac{M_o^{3/4}}{B_o^{1/2}} \quad (4)$$

By using the bulk quantities Q_o , M_o , and B_o , the nozzle shape and the initial velocity distribution is implicitly taken into account. For a uniform velocity distribution, $l_O = \sqrt{A_o}$ and if the nozzle is circular $l_O = \sqrt{\pi/4}d_o$.

The length scale l_Q quantifies the distance over which the initial volume flux constitutes a significant portion of the local jet volume flux, or in other words, where the entrained ambient water and Q_o is of the same order (Wright, 1984). Thus, for distances from the nozzle much larger than l_Q , Q_o will not be of significance. The length scale l_M represents the distance over which the buoyancy generates a momentum flux similar to the initial momentum flux (M_o). At distances from the nozzle much greater than l_M the effect of M_o becomes negligible and the buoyant jet has essentially become a plume. For a negatively buoyant jet discharged upwards, the initial momentum flux will always be an important parameter during the phase when the jet is moving upwards, because M_o and the buoyancy are not acting in the same direction (Roberts *et al.*, 1997). The importance of these length scales has been discussed by several authors, including Wright (1984) and Fischer *et al.* (1979).

Thus, since any dependent variable describing the jet flow will be a function of Q_o , M_o , and B_o only, the maximum level of the jet centerline (Y), for example, can be expressed in terms of the two length scales (Roberts and Toms, 1988; Roberts *et al.*, 1987, 1997 and 2007):

$$\frac{Y}{l_M} = f\left(\frac{l_M}{l_Q}\right) \quad (6)$$

For $l_m \gg l_Q$, the effects of Q_o becomes negligible, and Eq. (6) simplifies to:

$$\frac{Y}{l_M} = K \quad (7)$$

where K is a constant. For a circular jet, the length scale l_M may be written,

$$l_M = \frac{M_o^{3/4}}{B_o^{1/2}} = \left(\frac{\pi}{4}\right)^{1/4} d_o Fr_d \quad (8)$$

where Fr_d is a Froude densimetric number defined as:

$$Fr_d = \frac{u_o}{\sqrt{g' d_o}} \quad (9)$$

Thus, Eq. (7) can be rewritten as:

$$\frac{Y}{d_o} = k \cdot Fr_d \quad (10)$$

where $k = K \left(\pi/4\right)^{1/4}$. Similar equations may be developed for the other geometric jet quantities Y_m , X_y , X_{ym} , and X_e , but with different values on the coefficient k .

2.2 Previous results for geometric jet quantities

A relationship similar to Eq. (10) was first developed by Turner (1966) for the case of a heavy jet injected vertically upwards ($\theta = 90$ deg) and a value of $k = 1.74$ was obtained (for the initial jet height). Subsequently, Abraham (1967), Fan and Brooks (1968), and Zeitoun *et al.* (1970) arrived at k -values of 1.95, 1.9, and 1.74 respectively, also based on experimental investigations. The case of an inclined dense jet in a stagnant ambient was first studied by Zeitoun *et al.* (1970), followed by Roberts and Toms (1987), and Roberts *et al.* (1997,2007). For an initial jet angle of $\theta = 60$ deg these three studies obtained k -values of 2.04, 2.08, and 2.2, respectively. In the study by Cipollina *et al.* (2005), the k -value was obtained for different geometric quantities and initial jet angles, as summarized in Table 2. No significant effects of viscosity on the k -value was observed, which was also found by Roberts *et al.* (1997). Kikkert *et al.* (2007) employed a light attenuation system (LA) and a laser-induced fluorescence system (LIF) to collect data in their experiment on inclined negatively buoyant jets. They also obtained other k -values through analytical modeling, which was validated with the data collected from the LA and LIF systems. The k -values obtained with their model are also given in Table 2.

Table 2 Coefficient values describing the linear dependence of normalized geometric jet quantities on the densimetric Froude number reported in previous investigations (Kikkert *et al.*, 2007; and Cipollina *et al.*, 2005).

References	θ°	Coefficients			
Kikkert <i>et al.</i> (2007)		ky	kx_y	ky_m	kx_i
	30	0.65	1.69	1.02	2.95
	45	1.11	1.83	1.61	3
LA data	60	1.7	1.77	2.2	2.71
	30	0.55	1.77	1.0	3.1
	45	1.05	1.82	1.6	3.25
LIF data	60	1.48	1.58	2.08	2.8
	30	0.7	1.83	1.2	3.43
	45	1.11	2.1	1.7	3.5
Cipollina <i>et al.</i> (2005)	60	1.75	1.77	2.45	2.9
	30	0.79	1.95	1.08	3.03
	45	1.17	1.8	1.61	2.82
	60	1.7	1.42	2.25	2.25

The subscript of k in the table corresponds to the specific geometric quantities previously discussed, with the exception of x_i , which is the distance to the jet impact point (where the jet centerline encounters the level of the jet nozzle; see Fig. 1). The values of the constants k vary depending on the investigation. This may partly be due to differences in flow geometry and tank size used in the experiments (compare Table 1), measurement errors, and different definitions and procedures for determining the geometric quantities. Also, there may be some effects from differences in the basic input jet parameters selected that the normalization does not capture.

3 Laboratory experiments

3.1 Experimental setup

The experiment on inclined negatively buoyant jets was carried out in the laboratory of Water Resources Engineering at Lund University. The apparatus and major equipment used in the experiment included water tanks, a flow meter, a digital frequency recorder, a digital conductivity meter, pump, pipes, valves, nozzles and nozzle support, salt, and dye (see Fig. 2). Several different tanks were used in the experiment: (1) a small tank to mix tap water with salt and a coloring dye to obtain saline water for generating an easily visualized negatively buoyant jet, (2) two elevated small tanks used to create the hydraulic head for generating the jet, and (3) a large tank made with glass walls filled with tap water (fresh water) where the jet was introduced through a nozzle. The small tanks were made of plastics and their volumes were 45, 70, and 90 liters, whereas the maximum volume of the large tank was 540 liters with the bottom area dimensions of 150 x 60 cm² and a height of 60 cm. Two of the smaller tanks were placed at a higher elevation compared to the large tank to create the necessary hydraulic head for driving the jet. These two tanks were connected by a pipe and together they had a sufficiently large capacity (*i.e.*, surface area) to keep the water level approximately constant in the two tanks during the experiment to ensure a constant flow. The water temperature was in the range 20 to 22 C° in all experimental cases.

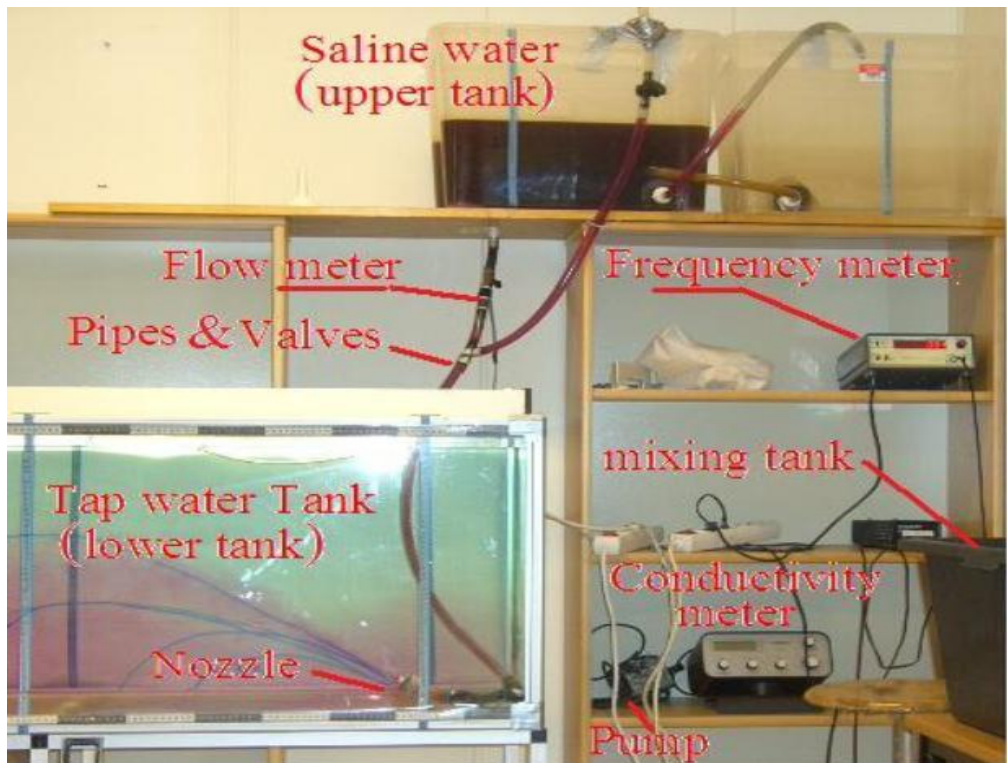


Fig. 2 Experimental setup and major components

The difference in elevation between the water levels of the upper tank and the lower tank was about 100 cm. The colored saltwater from the upper tanks was discharged through a plastic, transparent pipe directly connected to the jet nozzle, which was fixed at the bottom of the large water tank. Between the elevated tanks and the nozzle there was a valve to control the flow to the nozzle. A flow meter was installed in the pipe between the valve and the outlet from the upper tanks in order to record the initial jet flow. This meter was connected to a digital frequency recorder, from which the readings were converted into flow rates based on a previously derived calibration relationship. The employed nozzle diameters were 1.5, 2.3, 3.3, and 4.8 mm (inner diameter), and the initial jet inclination angles 30, 45, and 60 deg to the horizontal (see Fig. 1).

3.2 Experimental procedure and data collected

Before starting an experimental case, it was crucial to empty the pipe leading from the upper tanks from air. This was done by attaching a special pipe to the flow meter and discharging tap water through this pipe, bringing out the air from the system. After each experimental case a submersible water pump was used to completely empty the large tank, so that each case started with water that was not contaminated by salt. With the capacity of the pump, it took about 12 minutes to empty the tank. Also, the whole system was regularly washed to avoid accumulation of salt, which would cause disturbances to the experiment.

Fine pure sodium chloride was used to create the saline water in the jet by mixing it with tap water. The water quantity was measured using a bucket and the salt was measured using a balance to obtain the correct salt concentration.

A conductivity meter was used to measure the conductivity for the three different concentrations. The density measurements for the three concentrations investigated in this study yielded 1011, 1024 and 1035 kg/m³ for 2, 4 and 6%, (20, 40, and 60 g/l), respectively. Each of the densities was the average of five different measurements based on the weight method.

Differences in the density were observed between the saltwater used in this study and natural seawater. The chemical composition of seawater is different from the sodium chloride solutions used here, although the density varies only slightly in seawater compared with the pure sodium chloride solutions.

Potassium permanganate (KMnO₄) was used to color the saline water and make the jet visible during the experiment. The dye gives the transparent water a distinct purple color by adding 0.1g/liter. The use of a colored jet facilitated the observation of the jet trajectory and the mixing behavior in the larger water tank. The results of jar test for different (KMnO₄) concentrations showed that at a concentration of 0.3 mg/l the water is still colored, whereas at concentration of 0.2 mg/l no color was visible to the eye.

During a specific case, the jet was discharged for a sufficiently long time to allow steady-state conditions to develop, but short enough to avoid unwanted feedback from saline water accumulating in the tank (the duration of an experimental case was normally about 3-5 min). The jet trajectory and its geometric properties were determined by tracing the observed trajectory on the glass wall of the flume. The outer edges of the jet were traced and the center line was determined as the average between these two lines. In order to minimize the influence of the subjective element in tracing the jet, several different people were involved in this procedure to ensure that the results were consistent, in agreement,

and repetitive. Also, the experimental cases was recorded with a video camera and subsequently viewed. Three cases did not produce satisfactory data due to malfunctioning, and here the results from 69 cases are reported. As previously mentioned, five different quantities describing the jet trajectory were recorded (Y , X_y , Y_m , X_{ym} , and X_e). Table 3 gives a complete listing of the data, including the main input parameter values and the measured geometric quantities.

Table 3 Summary of results for inclined negatively buoyant jet experiment

Case	θ°	S	d_0	Q_0	$Q_0 \times 10^{-5}$	u_0	ρ_0	Fr_d	Y	X_y	Y_m	X_{ym}	X_e
	%		(cm)	(l/min)	(m ³ /s)	(m/s)	(kg/m ³)		(cm)	(cm)	(cm)	(cm)	(cm)
1	30	4	0.48	0.97	1.6	0.9	1023.7	25	8.5	19.5	11	25	51
2	30	6	0.48	1.20	2.0	1.1	1034.8	26	10	21.5	13.5	25.5	47
3	30	2	0.48	1.00	1.7	0.9	1011.1	34	8	18	11	23	37
4	30	6	0.33	0.88	1.5	1.7	1034.8	49	11	30	15.5	35	57
5	30	6	0.48	2.37	4.0	2.2	1034.8	52	17	45	23.5	50	82
6	30	4	0.48	2.05	3.4	1.9	1023.7	53	17.5	39	22	49	83
7	30	2	0.48	1.75	2.9	1.6	1011.1	60	19	47	27.5	59	85.5
8	30	4	0.33	1.02	1.7	2.0	1023.7	67	15.5	41.5	20	50	71
9	30	6	0.23	0.58	1.0	2.3	1034.8	80	14.5	28	18.5	32	53.5
10	30	6	0.33	1.45	2.4	2.8	1034.8	81	18	44	25	49	84
11	30	4	0.33	1.41	2.4	2.7	1023.7	92	19	48	25.5	57	90
12	30	4	0.23	0.60	1.0	2.4	1023.7	97	9	19	11.5	22	41
13	45	6	0.48	0.96	1.6	0.9	1034.8	21	10	15.5	14	18.5	36
14	45	4	0.48	1.25	2.1	1.2	1023.7	32	16	27.5	20.5	31.5	52
15	45	2	0.48	1.00	1.7	0.9	1011.1	34	8	12	11	12.5	22.5
16	45	6	0.48	2.38	4.0	2.2	1034.8	52	25	38	33.5	48	75
17	45	4	0.33	0.82	1.4	1.6	1023.7	54	17	29	21.5	37	54
18	45	4	0.48	2.10	3.5	1.9	1023.7	54	25	44.5	33	52	81
19	45	6	0.33	0.98	1.6	1.9	1034.8	55	17.5	25	23	31	57
20	45	2	0.48	1.75	2.9	1.6	1011.1	60	28	41.5	37	45	77.5
21	45	2	0.33	0.80	1.3	1.6	1011.1	70	8	13	11	15.5	23.5
22	45	6	0.23	0.52	0.9	2.1	1034.8	71	16	25	20.5	28.5	50
23	45	6	0.33	1.46	2.4	2.8	1034.8	81	29.5	46	37	56.5	91
24	45	4	0.23	0.51	1.0	2.0	1023.7	82	17	30	21	34.5	55
25	45	4	0.33	1.40	2.3	2.7	1023.7	92	26	51	34.5	62	94
26	45	6	0.15	0.24	0.4	2.3	1034.8	96	15	25	19	26	42.5
27	60	4	0.48	1.00	1.7	0.9	1023.7	26	14.5	14.5	18	16	32
28	60	6	0.48	1.22	2.0	1.1	1034.8	27	17.5	15	23.5	19	35
29	60	6	0.33	0.70	1.2	1.4	1034.8	39	17	18.5	21.5	21.5	39
30	60	2	0.48	1.25	2.1	1.2	1011.1	43	17	17.5	25	23.5	36.5
31	60	4	0.48	1.75	2.9	1.6	1023.7	45	29	27	37	34.5	63
32	60	6	0.48	2.20	3.7	2.0	1034.8	48	33	27	41	31.5	58
33	60	4	0.33	0.86	1.4	1.7	1023.7	56	26	26	34.5	31.5	53
34	60	2	0.48	1.70	2.8	1.6	1011.1	58	34	35.5	43	42.5	69
35	60	2	0.33	0.80	1.3	1.6	1011.1	70	13.5	14	16	16.5	29.5
36	60	6	0.33	1.27	2.1	2.5	1034.8	71	31	31.5	40	36	47
37	60	4	0.33	1.10	1.8	2.1	1023.7	72	38	35	45	40	75
38	60	6	0.23	0.60	1.0	2.4	1034.8	82	25.5	28	31.5	31	52
39	60	4	0.23	0.57	1.0	2.3	1023.7	92	26	27.5	31	33	56
40	30	2	0.33	1.20	2.0	2.3	1011.1	105	14	26.5	17	31	59
41	30	6	0.23	0.82	1.4	3.3	1034.8	113	22	41	27.5	48	79
42	30	6	0.15	0.30	0.5	2.8	1034.8	120	8	24	12	29	50
43	30	2	0.33	1.80	3.0	3.5	1011.1	158	25.5	48	35.5	66.5	96.5
44	30	4	0.23	1.00	1.7	4.0	1023.7	162	20	50	25	58	89.5
45	30	6	0.15	0.42	0.7	4.0	1034.8	168	12	32	15	39	63.5
46	30	2	0.23	0.85	1.4	3.4	1011.1	184	9	23.5	11.5	27.5	55
47	30	2	0.23	1.00	1.7	4.0	1011.1	216	20	53	25.5	58	102
48	30	2	0.15	0.35	0.6	3.3	1011.1	220	8.5	23	11	28	41
49	30	4	0.15	0.65	1.1	6.1	1023.7	306	13	28	16	33	53
50	30	4	0.15	1.00	1.7	9.4	1023.7	471	18	38	22.5	44.5	72

51	30	2	0.15	0.85	1.4	8.0	1011.1	535	21.5	50	27.5	56	92.5
52	45	6	0.23	0.76	1.3	3.0	1034.8	104	24	41	27.5	48	82
53	45	2	0.33	1.45	2.4	2.8	1011.1	127	30	42.5	40	52.5	88.5
54	45	2	0.23	0.60	1.0	2.4	1011.1	130	11	20	16	26	40.5
55	45	4	0.23	0.90	1.7	3.6	1023.7	145	30	51.5	36.5	57	98
56	45	6	0.15	0.38	0.6	3.6	1034.8	152	22	31	28	36	59
57	45	2	0.23	0.85	1.4	3.4	1011.1	184	32	49	41	57	97
58	45	2	0.15	0.38	0.6	3.6	1011.1	239	14	17	17.5	19	37
59	45	4	0.15	0.65	1.1	6.1	1023.7	306	18	24.5	24	30	49
60	45	4	0.15	1.00	1.7	9.4	1023.7	471	26.5	37	33	44.5	67.5
61	45	2	0.15	0.80	1.3	7.5	1011.1	504	33.5	46.5	40	53	90
62	60	2	0.23	0.50	0.8	2.0	1011.1	108	17.5	16.5	23	22	36
63	60	6	0.15	0.28	0.5	2.6	1034.8	112	20	19	26	21	37
64	60	6	0.23	0.82	1.4	3.3	1034.8	113	36	36	45	41	70
65	60	2	0.33	1.35	2.3	2.6	1011.1	118	32.5	34	43	42.5	29.5
66	60	4	0.23	0.87	1.5	3.5	1023.7	141	36	39	45	47.5	86.5
67	60	2	0.23	0.70	1.2	2.8	1011.1	151	37.5	34.5	43.5	45	87
68	60	6	0.15	0.49	0.8	4.6	1034.8	196	29.5	27	37	32	53
69	60	2	0.15	0.38	0.6	3.6	1011.1	239	15	11.5	18.5	15.5	31
70	60	4	0.15	0.60	1.0	5.7	1023.7	282	15	15.5	20	17	33
71	60	4	0.15	0.85	1.4	8.0	1023.7	400	30	28.5	38.5	34.5	50
72	60	2	0.15	0.90	1.5	8.5	1011.1	567	37.5	34	45.5	41.5	72

4 Results and discussion

4.1 General jet development

After the dense jet is discharged from the exit, less heavy water is entrained from the ambient and the density in the jet decreases. However, since the density in the jet always will be larger than the density in the ambient, the negative buoyancy will divert the jet from its original upward paths towards the bottom, which it will eventually impinge upon. Thus, the jet trajectory will be similar to what simple ballistics theory describe for a solid particle in air, with the major exception that an effective acceleration due to gravity controls the jet evolution and it varies depending on the entrainment. The latter implies that the jet trajectory is not symmetric, as for the ballistics case, but has a longer rising phase compared to the declining phase. Since ambient water is entrained into the jet, the salinity of the jet decreases. An important design parameter for brine discharge systems is the maximum dilution rate that can be achieved, which is directly related to the length of the jet trajectory before it encounters the bottom and continues to spread as gravity current. The densimetric Froude number (Fr_d) quantifies the relative importance of the momentum and buoyancy force. A small Fr_d -value indicates that the buoyancy force controls the jet behavior, shortening the trajectory length. On the other hand, a large Fr_d -value signifies initial dominance of momentum and a longer trajectory, although eventually the buoyancy forces will still prevail and deflect the jet towards the bottom.

Analysis of the video films taken during the experiment showed that small Fr_d -values were associated with less fluctuation in the jet behavior and a more stable trajectory compared to jets with large Fr_d -values. It is expected that smaller density differences between the jet and the ambient (corresponding to larger Fr_d values) will produce a jet more prone to instability behavior resulting in a less stable trajectory (compare with Bleninger and Jirka, 2007a,b). However, this observation was not as clear for the experimental cases with the smaller salinity.

4.2 Jet trajectory analysis

As previously mentioned, in total 72 experimental cases were carried out with different jet quantities for which Y and X_y (maximum level of the jet centerline and its horizontal distance, respectively), Y_m and X_{ym} (maximum level of jet flow edge and its horizontal distance, respectively), and X_e (maximum horizontal distance to the jet flow edge point) were measured (in three cases no reliable measurements were obtained). As an example, Figure 2a illustrates the relationship between Y_m and Y for all the cases. A very strong correlation between the two quantities is found, lending some confidence to the accuracy of the measurements. The least-square fitted line through the origin yields a slope of about 1.25, implying that Y_m on the average is about 25% larger than Y .

Figure 2b shows the relationship between X_y and X_{ym} , which also indicates a strong correlation with limited scatter around the least-square fitted straight line through origo. The slope of this line was about 1.20, which is somewhat lower than what the relationship between Y and Y_m yielded. Furthermore, the horizontal distance to edge point of the jet (X_e) showed rather good correlation with X_{ym} (or X_y), as displayed in Figure 2c, although the scatter was larger than for the previously discussed relationships (*e.g.*, Figures 2a and 2b). The slope of the least-square fitted line was approximately 1.65.

Figure 2d shows Y as a function of X_y with respect to the initial jet angle (θ). Since Y is closely dependent on θ , the analysis for the different angles should be performed individually. Thus, in the figure, separate lines are least-square fitted to the data for the three investigated initial jet angles (30, 45 and 60 deg).

The slopes of the fitted straight lines were 2.3, 1.5, and 1.0 for 30, 45, and 60 deg, respectively. If a simple ballistics model was employed to describe the jet trajectory (*i.e.*, constant g'), the ratio between X_y and Y would be given by $2/(\tan \theta)$, which yields the following slopes for the lines: 3.5, 2.0, and 1.2.

Thus, the simple ballistics model would overestimate X_y/Y , but progressively less for larger angles. The spread of the data in Figure 2d around the regression line for each angle indicates that the trajectories are not simply scale copies of each other, but other factors influence the shape of the trajectories. However, as the angle increases the effect of these factors become smaller.

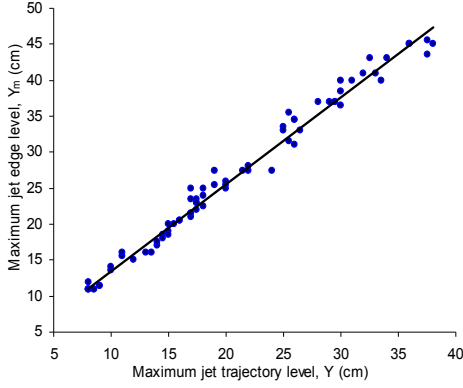


Fig. 2a Relationship between maximum level of jet centerline (Y) and maximum edge level (Y_m) for all experimental cases

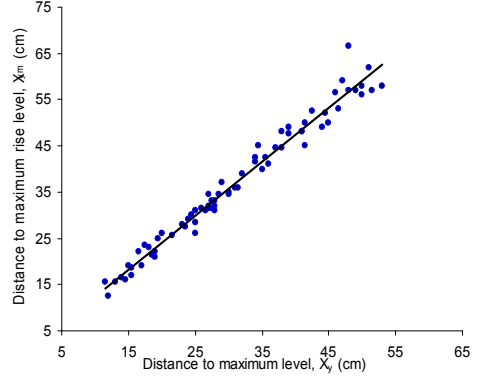


Fig. 2b Relationship between horizontal distance to maximum jet centerline level (X_y) and maximum edge level (X_{ym}) for all experimental cases

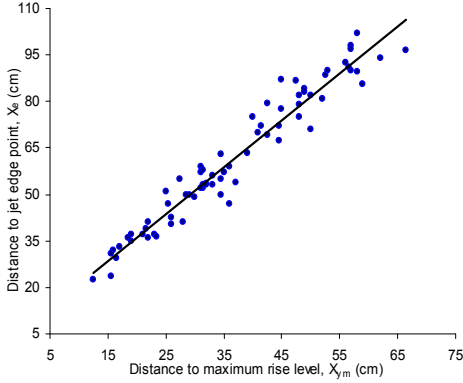


Fig. 2c Relationship between horizontal distance to maximum jet edge level (X_m) and jet edge point (X_e) for all experimental cases

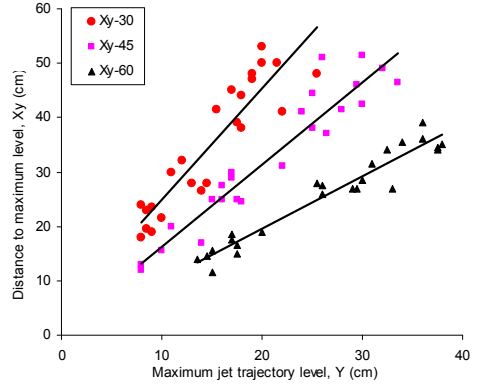


Fig. 2d Maximum jet centerline level versus its horizontal distance with respect to initial jet angle

4.3 Densimetric Froude number dependence

The dimensional analysis carried out in section 2.1 showed that the geometric quantities characterizing the jet trajectory should be a function of the densimetric Froude number (Fr_d). Thus, Y , X_y , Y_m , and X_{ym} were normalized with the exit jet diameter (d_o) and plotted versus Fr_d separately for the three initial jet angles in order to investigate possible relationships (compare Cipollina *et al.*, 2007). For all jet quantities studied there seemed to be a change in behavior at approximately $Fr_d = 100$; below this value the data points followed a linear trend well, displaying little scatter around the least-square fitted line. For $Fr_d > 100$, the data points exhibited much more scatter. However, if a straight line was still fitted through the data the slope of the line was significantly smaller than for $Fr_d < 100$. Figures 3a and 3b illustrates Y/d_o , X_y/d_o and Y_m/d_o , X_{ym}/d_o , respectively as functions of Fr_d for the three initial jet angles, where straight lines were least-square fitted separately for the data points above and below $Fr_d = 100$. The quantity X_e showed the same behavior as

X_y and X_{ym} , and no plots with this quantity are presented here. Equation 7 indicates a linear relationship between the normalized quantities to describe the jet trajectory and the Fr_d . However, this is built on the assumption that $l_m \gg l_Q$, otherwise Eq. 6 should be employed. Developing Eq. 6 by introducing the definition of the length scales yields,

$$\frac{Y}{d_o} = k \cdot Fr_d \cdot \Psi(Fr_d) \quad (11)$$

where Ψ = function and Y is used as an example of a geometric jet quantity. If Fr_d is small $\Psi(Fr_d) \rightarrow 1$, whereas for large Fr_d values $Y \rightarrow \infty$. The data indicates a relationship where $Y/d_o \propto Fr_d^n$, with $n < 1$. Based on the theoretical constraints and the empirical observations, the following equation was proposed to describe Y/d_o as a function of Fr_d over the entire range of experimental data,

$$\frac{Y}{d_o} = \frac{k \cdot Fr_d}{(1 + \alpha Fr_d)^m} \quad (12)$$

where α and m are empirical coefficients obtained from fitting against data. Equation 12 can be approximated with a straight line in accordance with Eq. 10 for small values on αFr_d .

Figure 4 shows an example of least-square fitting Eq. 12 against the data for the maximum jet centerline level (Y) and an initial jet angle of 30 deg, where the optimum values on k , α , and m were determined (1.35, 0.008, and 0.8, respectively). Overall the trend of the data points is well described, but the significant scatter for $Fr_d > 100$ is still present, which degrades the agreement. The other initial angles for Y and the other jet quantities could be fitted about equally well.

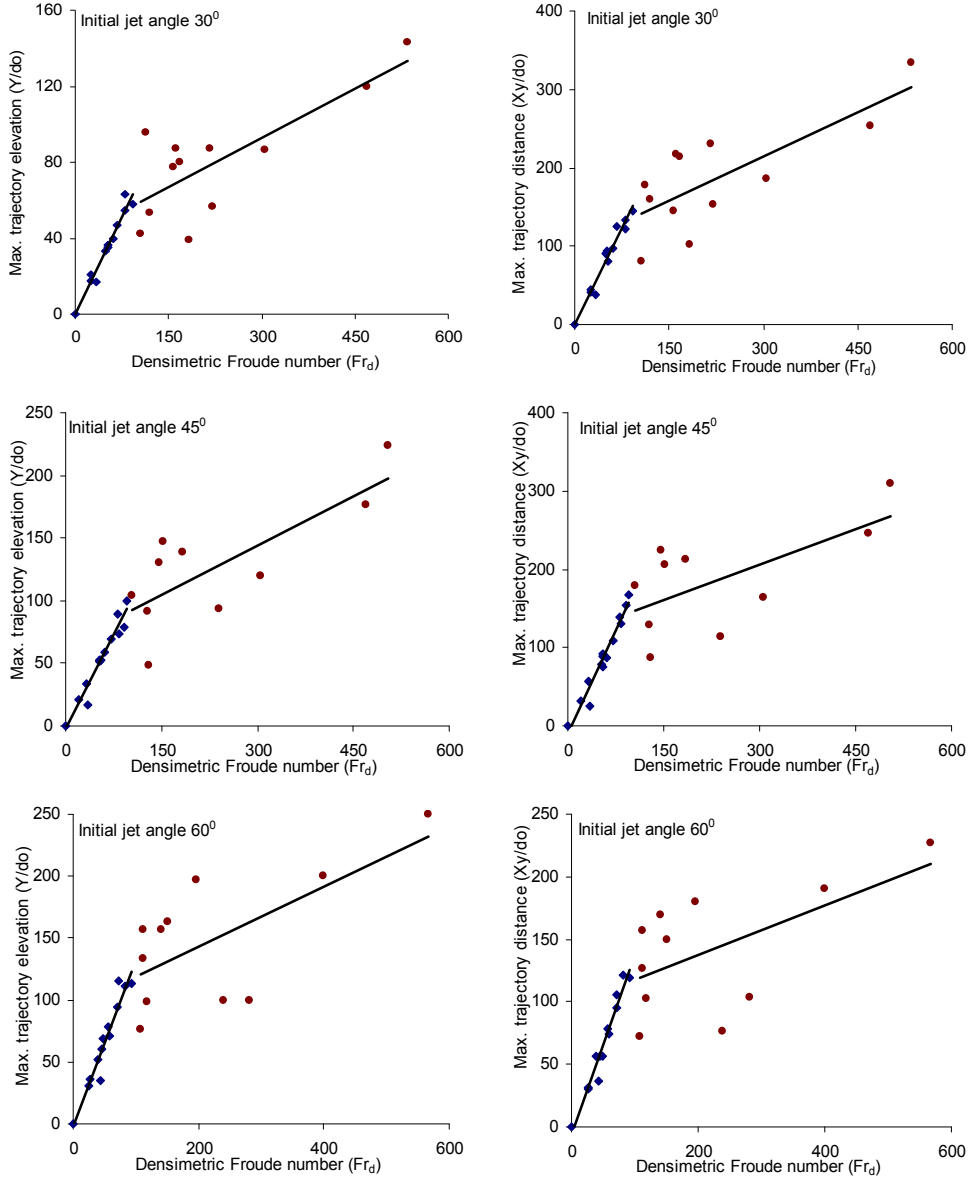


Fig. 3a Non-dimensional jet quantities Y/d_o and X_y/d_o as a function of Fr_d for different initial jet angles together with linear regression lines fitted for Fr_d -values smaller and larger than 100

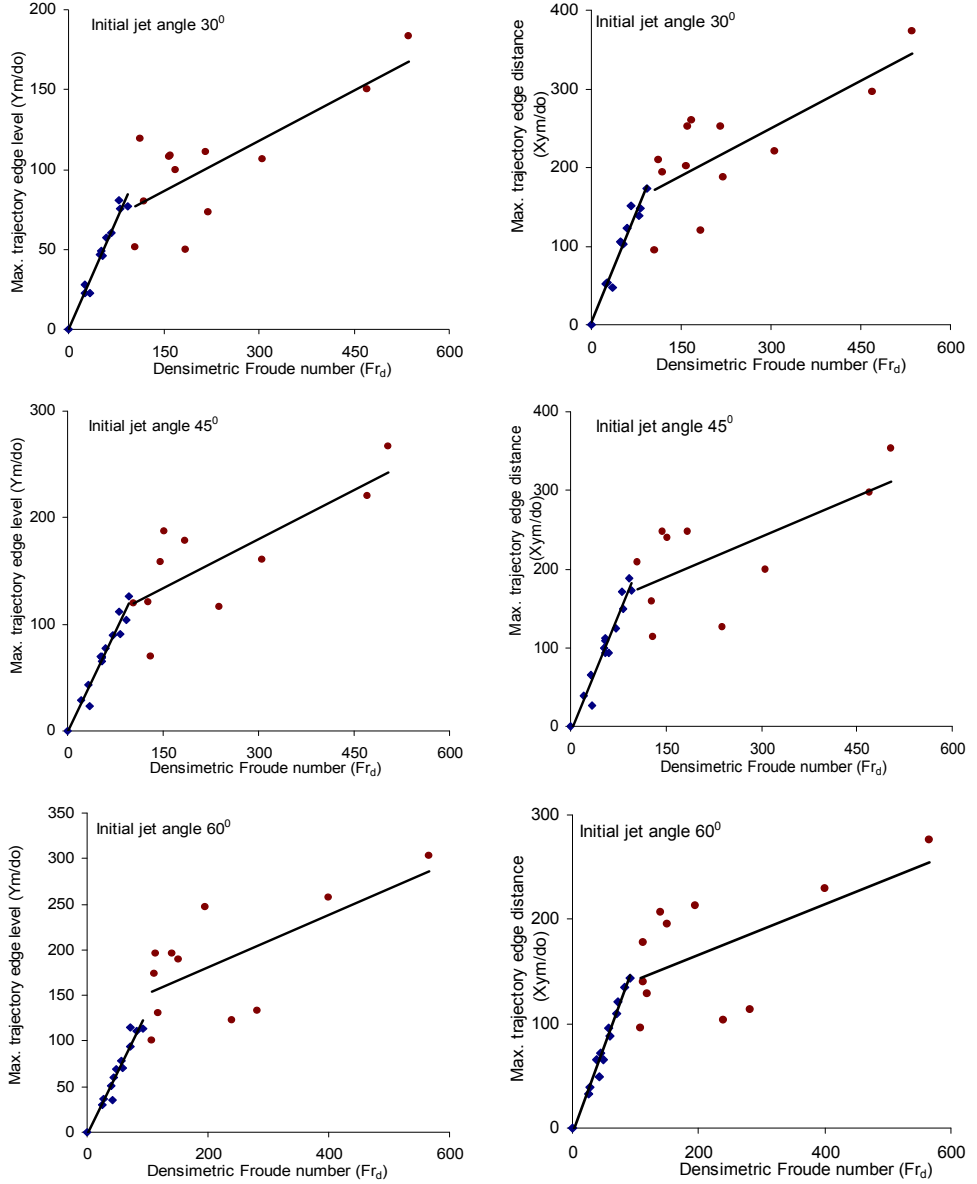


Fig. 3b Non-dimensional jet quantities Y_m/d_o and X_{ym}/d_o as a function of Fr_d for different initial jet angles together with linear regression lines fitted for Fr_d -values smaller and larger than 100

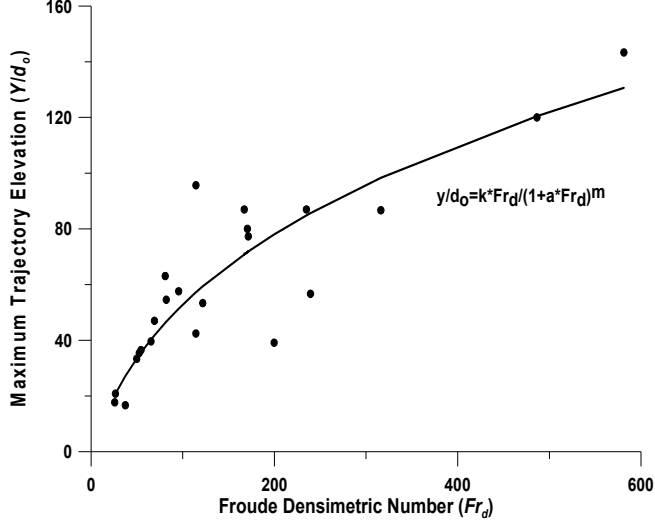


Fig. 4 Normalized maximum jet centerline level as a function of the densimetric Froude number for an initial jet angle of 30 deg.

4.4 Relationships for jet quantities

The slopes of the least-square fitted straight lines discussed in the previous section were determined for the different jet quantities, separating data points below and above $Fr_d = 100$. The obtained slope coefficients for the normalized maximum jet levels $Y(ky)$ and $Y_m(ky_m)$ as a function of Fr_d are shown in Figure 5. The coefficient values seem to increase with the initial jet angle in a linear manner, although the number of points was limited. Figure 5 also includes corresponding coefficient values found in earlier studies, which have reported the same trend. These values originate from four different sources, namely Cipollina *et al.* (2005) (C), Kikkert *et al.* (2007) (K) with values predicted from their analytical model and measured by the light attenuation system (LA), and laser-induced fluorescence system (LIF). The values for ky and ky_m are listed in Table 4 with respect to the three initial jet angles (30, 45, and 60 deg). For example, the values obtained for ky_m at 30 deg were 0.92 ($Fr_d < 100$) and 0.21 ($Fr_d > 100$) compared to the value reported by Cipollina *et al.* (2005) of 1.08, which was obtained for $Fr_d < 100$. Thus, for this case the agreement is good; however, for the larger angles the deviation between the coefficient values (ky and ky_m) obtained in this study and in previous studies is larger than for the smaller angles.

As mentioned before, besides differences in experimental setups and procedures, a reason for the discrepancies between experiments may be marked differences in some of the input parameters not described by the non-dimensional quantities employed. For example, Cipollina *et al.* (2005) used densities in the jet much larger than in the present experiment, and also much larger than what is expected in brine jets. The slope coefficients for the horizontal distance to the maximum jet centerline level (kx_y), to the maximum jet edge level (kx_{ym}), and to the edge point (kx_e) were also determined with regard to the initial jet angle and whether Fr_d was above or below 100 (see Figure 6). Furthermore, previously obtained corresponding values reported by Cipollina *et al.* (2005) and Kikkert *et al.* (2007)

were included for comparison. The dependence of the coefficients for the horizontal distances on the initial jet angle are quite different from the vertical distances, and two extra points may be added on theoretical grounds, namely at $\theta = 0$ and 90 deg for which the distance should be zero (Cipollina *et al.*, 2005). Over the range of studied initial jet angles, the variation in the coefficient values with θ is limited, but there is a tendency for these values to decrease with θ (from 30 to 60 deg).

A polynomial was fitted through the data five points, but the shape of the curve outside the measurement points has little support. In general, the coefficient values obtained in the present study are somewhat lower than what was recorded in previous studies. Table 4 summarizes the coefficient values found for the vertical and horizontal distances investigated for Fr_d above and below 100 (corresponding values from previous studies are shown in Table 2).

Table 4 Coefficient values linearly relating different vertical and horizontal distances to the densimetric Froude number obtained in the present study

Based	θ°	Coefficients				
$Fr_d < 100$		ky	kx_y	ky_m	kx_{ym}	kx_e
	30	0.69	1.64	0.92	1.89	3.12
	45	1.0	1.74	1.30	2.0	2.90
	60	1.40	1.44	1.70	1.65	2.66
$Fr_d > 100$		ky	kx_y	ky_m	kx_{ym}	kx_e
	30	0.17	0.38	0.21	0.40	0.65
	45	0.26	0.42	0.31	0.35	0.53
	60	0.24	0.20	0.29	0.24	0.36

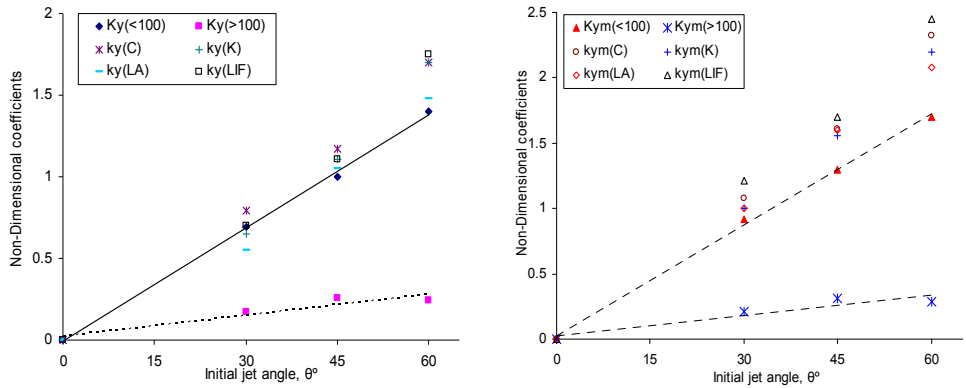


Fig. 5 Slope coefficient for maximum jet centerline level (ky) and maximum jet edge level (kym) as a function of initial jet angle for densimetric Froude number below and above 100 , together with results from previous studies

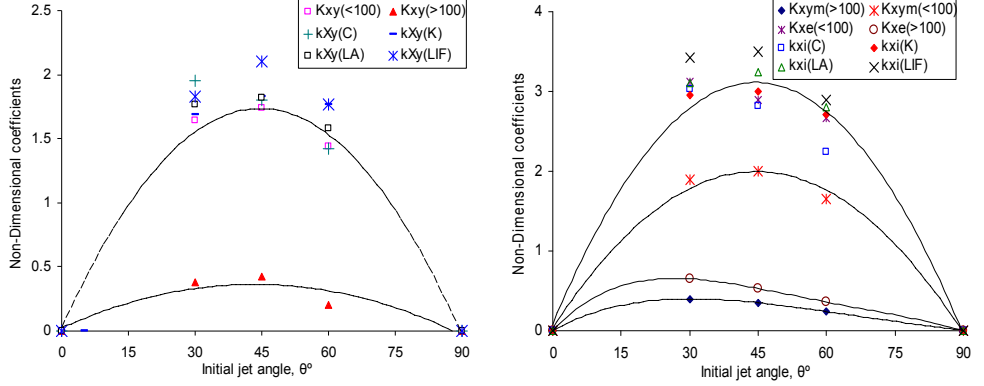


Fig. 6 Slope coefficient for horizontal distance to maximum jet centerline level (kx_y) and maximum jet edge level (kx_{ym}) as a function of jet angle for densimetric Froude number below and above 100, together with results from previous studies

5 Discussion

Some geometric quantities describing the jet trajectory showed strong correlations, for example, Y_m versus Y , X_{ym} versus X_y , and X_e versus X_{ym} . Thus, if the vertical and horizontal distance to the maximum centerline level (or, alternatively, the maximum jet edge level) can be predicted, other geometric quantities can be calculated from the following regression relationships:

$$\left. \begin{aligned} Y_m &= 1.25Y \\ X_{ym} &= 1.20X_y \\ X_e &= 1.65X_{ym} \end{aligned} \right\} \quad (13)$$

The relationship between the maximum levels and their horizontal distances displayed more scatter (see Figure 2d) and included a dependence on the initial jet angle. However, a general equation of linear type could be fitted through the data points with reasonable accuracy,

$$X_y = k_0 Y \quad (14)$$

where k_0 is an empirical coefficient that takes on the value 2.3, 1.5, and 1.0 for the initial jet angle 30, 45, and 60 deg, respectively. A similar equation could be developed for X_{ym} and Y_m .

Normalized jet quantities could also be related to Fr_d , although it was difficult to develop any equations for $Fr_d > 100$ because of the significant scatter observed. However, for $Fr_d < 100$ a straight line, as predicted by dimensional analysis, provided a good fit between normalized geometric jet quantities and Fr_d . The slope coefficient for the least-square

fitted line showed a dependence on the initial jet angle, where the coefficient seemed to grow linearly with the angle for Y and Y_m . For the horizontal distances X_y and X_{ym} the relationship was more complex and the limited number of angles investigated prevented the development of an equation. Assuming a linear relationship between ky and θ (in deg), and substituting the resulting empirical equation into Eq. 10 yields:

$$\frac{Y}{d_o} = 0.022 \cdot \theta Fr_d \quad (15)$$

A similar equation can be developed for Y_m/d_o , but Eq. 13 may be employed instead to obtain Y_m from Y . Equation 6 indicates a more complex dependence on Fr_d than the simple linear one under certain conditions. Thus, an alternative equation was proposed that exhibited more flexibility to describe the observed variation in the various geometric quantities with Fr_d . An application to Y/d_o indicated the potential for this equation, but because of the scatter recorded for $Fr_d > 100$, it did not seem worthwhile to proceed and carry out a comprehensive analysis with the objective to determine the coefficient values in Eq. 12. It is not clear why the scatter increased markedly for $Fr_d > 100$. As pointed out before, the jet displayed a tendency to be less stable for larger Fr_d values which may have affected the measurement accuracy somewhat. However, this can only explain a limited portion of the large variation obtained.

6 Conclusions

A laboratory experiment was conducted to investigate the behavior of negatively buoyant jets discharged at an angle to the horizontal into a quiescent body of water. The jet was made denser than the surrounding water by adding salt (sodium chloride) at specific concentrations, which increased the density. In total 72 experimental cases were carried out with the initial angles 30, 45, and 60 deg for different exit jet diameters, velocities, and densities. The jet trajectory was recorded by measuring certain geometric quantities, including the maximum rise level of the jet (Y_m) and its horizontal distance (X_{ym}), the maximum level of the jet centerline (Y) and its horizontal distance (X_y), and the distance to the edge point (X_e) (where the jet returns to the discharge level).

Several of the geometric jet quantities showed strong correlation, for example, Y_m versus Y , X_{ym} versus X_y , and X_e versus X_{ym} , and regression relationships could be developed where one quantity can be predicted from another. If maximum levels were correlated with the corresponding horizontal distances, the angle must be taken into account when developing predictive relationships. Dimensional analysis demonstrated that the geometric jet quantities studied, if normalized with the jet exit diameter, should be related to the densimetric Froude number (Fr_d). Analysis of the collected data showed that this was the case for $Fr_d < 100$, whereas for larger values on Fr_d the scatter in the data increased significantly, simultaneously as the studied jet quantities did not increase at the same rate. As has been observed in some previous investigations, the slope of the best-fit straight line through the data points was a function of the initial jet angle (θ), where the slope increased with θ for the maximum levels studied, but had a more complex behavior for horizontal distances. A more complex, nonlinear relationship between normalized geometric jet

quantities and Fr_d was developed based on semi-empirical observations as an alternative to a simple linear fit. Although this more complex equation could better describe the data over the entire range of Fr_d -numbers studied, the scatter was still marked for $Fr_d > 100$, and from a practical point of view it was worthwhile to develop predictive relationships. It is believed that the empirical relationships developed in this study have a potential for being used in practical design where the trajectory of brine jets needs to be estimated, if $Fr_d < 100$. Equations were proposed to relate levels or horizontal distances to each other, that is, Y_m to Y , X_{ym} to X_y , and X_e to X_{ym} . In order to relate a level to the corresponding horizontal distance, Fr_d may be employed in non-dimensional equations where the initial jet angle is included as well. For example, knowledge of the initial jet parameters yields the Fr_d value, from which the maximum level of the jet centerline can be calculated. From this value the other jet quantities discussed in this paper can be estimated from Eqs. 13 and 14.

Acknowledgments

This study was partially funded by Center for Middle East Study (CMES) at Lund University, Sweden. David Sanchez, Master student at Water Resources Engineering, Lund University, provided invaluable assistance during the laboratory experiments.

Notations

The following symbols are used in this paper:

- A = cross-sectional area;
- B_o = buoyancy flux the nozzle;
- D = mixing tank diameter;
- d_o = nozzle diameter;
- Fr_d = jet densimetric Froude number;
- g = acceleration due to gravity;
- g' = effective acceleration due to gravity;
- H = mixing tank depth;
- $k_y, kx_y, ky_m, kx_{ym}, kx_e$ &
- kx_i = slope coefficients;
- L = mixing tank length;
- LA = light attenuation system;
- LIF = laser induced fluorescence system;
- l_M, l_m = characteristic length scale;
- m = empirical coefficient;
- M_o = momentum flux at the nozzle;
- Q_o = volume flux at the nozzle;
- S = nozzle salinity;
- u_o = nozzle velocity;
- W = mixing tank width;
- X_e = edge point horizontal distance;
- X_y = horizontal distance to jet centerline maximum level;
- X_{ym} = horizontal distance to maximum jet edge level;

Y = trajectory centerline maximum;
 Y_m = maximum jet edge level;
 α = empirical coefficient;
 θ = initial jet angle;
 ρ_o = effluent density; and
 ρ_a = ambient density;
 Ψ = function.

References

- Abraham, G., (1967). Jets with negative buoyancy in homogeneous fluid. *J. Hyd. Res.* 5 (4) 235–248.
- Baines, W.D., Turner, J.S., Campbell, I.H. (1990). Turbulent fountains in an open chamber. *J. Fluid Mech.* 212, 557–592.
- Bleninger, T., Jirka, G.H., (2007a). Modelling and environmentally sound management of brine discharges from desalination plants. Accepted for EDS Congress, April 22–25, Halkidiki, Greece.
- Bleninger, T., Jirka, G.H., (2007b). Towards Improved Design Configurations for Desalination Brine Discharges into Coastal Waters. IDA World Congress-Maspalomas Gran Canaria –Spain October 21-26, REF: IDAWC/MP07-139.
- Bloomfield, L.J., Kerr, R.C., (2000). A theoretical model of a turbulent fountain. *J. Fluid Mech.* 424, 197–216.
- Cipollina, A., Brucato, A., Grisafi, F., Nicosia, S. (2005). Bench scale investigation of inclined dense jets. *J. Hydraulic Eng.* 131(11), 1017–1022.
- Demetriou, J.D., (1978). Turbulent diffusion of vertical water jets with negative buoyancy (In Greek), Ph.D. Thesis, National Technical University of Athens.
- Fan, L.-N., Brooks, N.H., (1968). Dilution of waste gas discharge from campus buildings. Tech. Memo. 68-1. W. M. Keck Laboratory of Hydraulics and water Resources, California Institute of Technology, Pasadena, Calif.
- Fischer, H.B., List, E.J., Koh, R.C.Y., Imberger, J., Brooks, N.H., (1979). *Mixing in Inland and Coastal Waters*. Academic Press.
- James, W.P., Vergara, I., Kim, K., (1983). Dilution of a dense vertical jet. *J. Environ. Eng.*, 109 (6) 1273–1283.
- Jirka, G.H., (2006). Integral model for turbulent buoyant jets in unbounded stratified flows. Part 2: Plane jet dynamics resulting from multiport diffuser jets“. *Environ. Fluid Mech.*, (6) 43-100.
- Jirka, G.H., (2004). Integral model for turbulent buoyant jets in unbounded stratified flows. Part 1: The single round jet“. *Environ. Fluid Mech.*, (4) 1-56.
- Jirka, G.H. (1982). Multiport diffusers for heat disposal-a summary. *J. Hydraul. Div., Proc. ASCE*, 108, HY12.
- Kikkert, G.A., Davidson, M.J., Nokes, R.I. (2007). Inclined negatively buoyant discharges. *J. Hydraulic Eng.* 133(5), 545–554.
- McLellan, T.N., Randall, R. (1986). Measurement of brine jet height and dilution. *J. Waterw., Port, Coast, Ocean Eng.* 112(2), 200–216.

- Lee, J.H., Jirka, G.H., Harleman, D.R.F., (1977). Modeling of unidirectional diffusers in shallow water. R.M. Parsons Laboratory for Water Resources and Hydrodynamics, Tech. Rept. 228, Massachusetts Institute of Technology.
- Lee, J.H., Jirka, G.H., (1980). Multiport diffuser as line source of momentum in shallow water. *Water Resources Research*, 16, 4.
- Lindberg, W.R., (1994). Experiments on negatively buoyant jets, with and without cross-flow, in: P.A. Davies, M.J. Valente Neves (Eds.), *Recent Research Advances in the Fluid Mechanics of Turbulent Jets and Plumes*, NATO, Series E: Applied Sciences, vol. 255, Kluwer Academic Publishers, pp. 131–145.
- Pantzlaff, L., Lueptow, R.M., (1999). Transient positively and negatively buoyant turbulent round jets. *Exp. Fluids* 27, 117–125.
- Papanicolaou, P.N., Kokkalis, T.J., (2008). Vertical buoyancy preserving and non-preserving fountains, in a homogeneous calm ambient. *International Journal of Heat and Mass Transfer* 51, 4109–4120.
- Pincince, A.B., List, E.J., (1973). Disposal of brine into an estuary. *J. Water Pollut. Control Fed.*, 45 2335–2344.
- Roberts, P.J.W., Ferrier, A., Daviero, G., (2007). Mixing in inclined dense jets. *J. Hydr. Engrg.*, ASCE, 123 (8) 693–699.
- Roberts, P.J.W., Toms, G. (1987). Inclined dense jets in flowing current. *J. Hydraulic Eng.* 113(3), 323–341.
- Roberts, P.J.W., Toms, G. (1988). Ocean outfall system for dense and buoyant effluents, *J. Environ. Eng.*, 114(5) 1175–1191.
- Roberts, P.J.W., Ferrier, A., Daviero, G. (1997). Mixing in inclined dense jets. *J. Hydraulic Eng.* 123(8), 693–699.
- Sánchez, D., (2009). Near-field evolution and mixing of a negatively buoyant jet consisting of brine from a desalination plant. Master Thesis at the dept. Water Resources Engineering, Lund University.
- Shao, D., Law, A.W.-K., (2010). Mixing and boundary interactions of 30° and 45° inclined dense jets. *Environmental Fluid Mechanics*, 10 (5) 521–553.
- Tong, S.S., Stolzenbach, K.D., (1979). Submerged discharge of a dense effluent. Rep. No. 243, Ralph M. Parsons Laboratory, Massachusetts Institute of Technology, Cambridge, Mass.
- Turner, J.S., (1966). Jets and plumes with negative or reversing buoyancy. *J. Fluid Mech.* 26 779–792.
- Wright, S.J., (1984). Buoyant jets in density-stratified crossflow. *J. of Hydraulic Engineering*. ASCE. 110, (5) 643–656.
- Zeitoun, M.A., Reid, R.O., McHilheny, W.F., Mitchell, T.M. (1972). Model studies of outfall systems for desalination plants. Res. and Devel. Progress Rep. 804. Office of Saline Water, U.S. Dept. of the Interior, Washington DC.
- Zeitoun, M.A. et al., (1970). Conceptual designs of outfall system for desalination plants.” Res. And Devel. Progress Rep. No. 550, Office of Saline Water, U.S. Dept. of Interior, Washington, D.C.
- Zhang, H., Baddour, R.E., (1998). Maximum penetration of vertical round dense jets at small and large Froude numbers. *J. Hyd. Eng.*, ASCE 124 (5) 550–553, Technical Note No. 12147.

Paper III

Environmental Assessment of Brine Discharge and Wastewater in the Arabian Gulf

Bashithalshaaer, R., Flyborg, L., and Persson, K.M. 2011

Desalination and Water Treatment, (25) 276-285



Environmental assessment of brine discharge and wastewater in the Arabian Gulf

Raed Bashitialshaaer^{a*}, Lena Flyborg^a, Kenneth M. Persson^{a,b}

^aDepartment of Water Resources Engineering, Lund University, PO Box 118, SE-221 00 Lund, Sweden
Tel. +46 (46) 222-4367, -8729; Fax +46 (46) 222-4435; email: Raed.Alshaaer@tvrl.lth.se

^bSydvatten AB, R&D, Skeppsgatan 19, SE 211 19 Malmö, Sweden

Received 19 April 2010; Accepted in revised form 6 July 2010

ABSTRACT

This study assesses the environmental effects of brine discharge into the Arabian/Persian Gulf and the option of mixing with wastewater to reduce the salt content in the discharge. The Arabian Gulf region occupies about 3.3% of the world area and has 1.0, 2.0 and 2.2% of the total world population in the years 1950, 2008 and 2050 (prognosis) respectively. The study area desalination capacities were obtained as 50, 40 and 45% of total world capacity at the end of 1996, 2008 and 2050 (prognosis) respectively. The trend towards increased recovery ratio in the desalination plants was considered as one important environmental factor. This will significantly increase the brine salt concentration from 1.5 to more than 2 times the seawater. The allocation of wastewater and brine is important for the Arabian Gulf. Straightforward water and salt mass balances were used to calculate residual flow, exchange flow and exchange time in the Arabian Gulf. For example, at zero wastewater discharge from 1996 to 2008, the net volume in the Arabian Gulf decreased by 7.4 million m³/d, the exchange volume increased by 69 million m³/d, and the mixing time decreased by 22.5 d. Discharging a mix of brine and wastewater in the Arabian Gulf reduces the water and salt exchange between the Gulf and the Indian Ocean. Nutrients in wastewater may cause problems such as eutrophication in the Gulf if the exchange of water is low or if wastewater is discharged to the Gulf with insufficient treatment.

Keywords: Arabian Gulf; Desalination; Wastewater; Population; Water–salt balance; Environmental impacts; Salinity

1. Introduction

1.1. General

Desalination is an important source of potable water in arid areas. Six percent of all desalination plants are located in the Asia-Pacific region, 7% in the Americas, 10% in Europe, and 77% in the Middle East and North Africa [10,11]. The largest number of desalination plants can be

found in the Arabian Gulf with a total seawater desalination capacity of approximately 11 million m³/d, which means a little less than half (45%) of the worldwide daily production. The main producers in the Gulf region are the United Arab Emirates (26% of the worldwide seawater desalination capacity), Saudi Arabia (23%, of which 9% can be attributed to the Gulf region and 13% to the Red Sea), and Kuwait (<7%) [11,28]. The water sources are 58% seawater, 22% brackish water and 5% tertiary treated wastewater. The mineral content of brine is usually found to be double or close to double that of natural seawater

* Corresponding author.

[12]. The total dissolved solids (TDS) in the three main regions are higher, 38.6, 45 and 41 g/l for the Mediterranean, the Arabian Gulf, and the Red Sea respectively, compared to typical seawater of about 34.5 g/l [9].

Usually a country is considered to face a water shortage if renewable fresh water resources are below 1000 m³/cap/y [1]. This is the case for all Middle East countries. To solve this problem, more desalination plants are being built all over the world. However, the increasing number of desalination plants along the coast lines as well as the higher capacity recovery ratio, from 30 up to 50% in some countries, increases the brine discharge concentration from 1.5 to 2 times of the intake concentration. A higher brine concentration results in weaker mixing, stronger stratification, and a longer traveling time that affects and may harm the coastal area.

In this paper, a comparison between the world and the Arabian Gulf region was made for: 1) Average annual population growth rate (PGR) in three periods (1950, 2008 and 2050), 2) Average annual desalination growth ratio (DGR) during two periods (at the end of 1996 and 2007–08), 3) Coverage area ratio, and 4) Desalination recovery ratio related to freshwater production (Q_f), brine discharge (Q_{Brine}), and seawater intake (Q_{Intake}).

The Arabian Gulf (AG) area has a very high evaporation rate, between 1200–2000 mm annually, and a very low annual precipitation, between 90–150 mm. The AG is semi-enclosed and the arid climate characterized by a higher salt content due to the high rate of evaporation [2]. Although the existing amount of water resources on our planet is substantial, it is generally saline and unevenly distributed [3]. For instance, only five great rivers capture about 27% of the global renewable fresh water resources (Amazon, Ganges-Brahmaputra, Congo, Yellow and Orinoco) [4,5].

1.2. Dispersion of the concentrated salts

One major environmental problem associated with a desalination plant is disposal of and/or minimization of the brine concentration. A natural and easy way is to discharge the brine to the sea, but an appropriate design is required in order to ensure proper dispersion of the brine. Different alternatives have been suggested in previous studies such as discharge by a long pipe, direct discharge of the brines at the coastline, mixing of the brine via the outlet of power stations' cooling water or wastewater, using the brines for a salt production evaporation pond, and having more than one outlet to the sea.

The forces of buoyancy in wastewater and brine discharge are important in the dilution process of water jets [13]. For saline waters, brine discharges have normally negative buoyancy and wastewater have positive buoyancy. Negatively buoyant brine discharge is also important and requires submerged discharge location in form of jet that ensures a high dilution in order to minimize harmful

impacts on the marine environment. The process of brine dilution is a combination of two physical processes: 1) the primary (jet) dilution and 2) the natural dilution process. A co-location of a power station and a desalination plant (joint project) offers many advantages when handling the brine discharge, although most of these are relevant to plants that are based on the various evaporation systems as opposed to reverse osmosis plants [14–18]. A co-location will give a chance of mixing brine water with water from power station and discharge together back to the sea in order to reduce salinity.

The data presented in Table 1 were adopted from International Desalination Association (IDA) yearbooks 2006–07, 2007–08, 2008–09 and 2009–2010. The data are collected to help us to find better and accurate result regarding future calculations. These data were collected from different projects mainly in the Middle East countries. In Table 1, eight co-location projects and available data for recovery ratios of the desalination plants are also presented. The results from the Ashkelon and Hadera desalination plants indicate that the total salinity of the water in the vicinity of the outlet of the discharge pipe would increase by 1–5%. This result was based on the available models for dispersion. The effect of the concentrated brine will disappear at a distance of a few meters from the outlet [19,20].

1.3. Objectives

This study was initiated for assessing the effects of brine discharge into recipients. A large number of desalination plants that have been built around the Arabian Gulf using its water both for intake and as recipient for brines. Population increase and economical growth are also considered as main driving forces in this area. They are directly related to fresh water consumption, brine production and wastewater production and possible reuse. The main objective of this study is to analyze the effects of increasing desalination in the AG area on the AG seawater quality. Therefore, the following studies have been executed:

- The effects of discharge of brines of desalination plants and wastewater to the Arabian Gulf are calculated for 1996 and 2008, and assessed for the year 2050.
- Water and salt mass balances were employed to find residual flow, exchange flow, and exchange time for the Gulf for the same years.
- The allocations of wastewater and brines have been assessed. Mixing brine with wastewater has been calculated on the basis of a recycling percentage of 0, 25, 50, 75 and 100%. Many countries around the Arabian Gulf already reuse wastewater or have plans to do so in the future. With very high evaporation rate in the area, reuse of wastewater will reduce the flow of low-salinity waters to the Gulf.

Table 1

Data from different desalination plants including eight power plant projects, desalinated water output and recovery ratio

Project name	Date	Total capacity (m ³ /d)	Intake TDS (mg/l)	Production recovery ratio (%)	Output TDS (mg/l)	Within project (MW)	Technology type
IDA year book (2006–2007)							
Ashkelon SWRO, Israel	2005	326144	40679	40.7	300		RO
Carboneras SWRO, Spain	2002	120000	39000	45	<500		RO
Fujairah, UAE*	2003	454000	40000	NA	<180	500	MSF
Shuweihat, UAE*	2004	454000	44000	NA	<250	1500	MSF
IDA year book (2007–2008)							
Dhekelia, Cyprus	1997	40000	40570	50	<500		RO
Larnaca, Cyprus	2001	54000	40300	50	<500		RO
Perth, Australia	2007	143700	36500	42.6	30		RO
Wadi Ma'in, Jordan	2006	128767	2000	85–90	250		RO
IDA year book (2008–2009)							
Hidd (IWPP), Bahrain*	07–08	408780	44000	45	<50	910	MED
Taweelah B: Extension, UAE*	2008	315000	44000	40	<25	1000	MSF
Ras Laffan B (IWPP), Qatar*	2008	272520	42000	40	<25	1025	MSF
Hamma (SWRO), Algeria	2008	200000	39000	42	<500		RO
Palmachim SWRO, Israel	2007	110000	40233	45	<300		RO
IDA year book (2009–2010)							
Barcelona-Liobregat, Spain	2009	200000	44800	44	400		
Marafiq IWPP-Jubail, KSA*	2009	800000	42000	45	<25	2745	MED
Barka 2 IWPP, Oman*	2009	123000	39300	39	45	678	RO
Alicant 1 and 2, Spain	03–08	130000	40000	42	400		RO
Rabigh IWSPP, KSA *	2007	218000	39600	35	<10	360	RO

IDA — International Desalination Association Yearbook; SWRO — seawater reverse osmosis; WEB — Water Energiebedrijf; APP — atomic power project; IWPP — independent water power project; IWSPP — integrated water steam and power project; KSA — Kingdom of Saudi Arabia; UAE — United Arab Emirates; MSF — multistage flash; MED — multi-effect distillation.

* indicates a co-location plant

- In all studies above, the increase in population and population growth rate was considered.

2. Study area: background and characteristics

2.1. General

The countries bordering the Arabian Gulf are: Iran, Iraq, Kuwait, Saudi Arabia, Qatar, Bahrain, and the United Arab Emirates (as shown in Fig. 1). The Arabian Gulf is a shallow semi-enclosed marginal sea, with maximum depth less than 100 m over its entire extent and a mean depth of only 35 m [21]. It covers an area of about 240,000 km², with 1000 km in length and widths ranging from 185 km to 370 km, with a mean of 240 km. The total water volume in the Gulf is approximately 8,400 km³. There are freshwater inflows from the Tigris, the Euphrates, and the Karun at the delta of the Shatt al Arab, estimated at 0.2 m/y over the gulf cross-sectional area, in which fresh water and river inflow equals 48 km³/y

(131.5×10⁶ m³/d) [21,22]. The mean annual evaporation rate is estimated at approximately 1.5 m/y [23]. Most brines are discharged to the AG directly, with exception for Iraq. The total brine discharge from Iraqi desalination plants is about 715,000 m³/d. Of this amount 5% is estimated to be discharged to the Arabian Gulf and the rest to be discharged to other places such as rivers or lakes upstream. The same percentage is also used for Iraqi wastewater. The total discharge Q_t to the Gulf is estimated as the sum of brine discharge Q_b and wastewater discharge Q_w . The values presented for Q_t includes the discharge of 100% wastewater, which will be mixed with brine water (Fig. 1).

The shallowness and humidity lead to the formation of saline, dense water, with maximum salinities as high as 57 g/l in the AG [24]. Ahmad and Sultan (1991) employed the Knudsen relations to estimate the annual mean Gulf water outflow transport at 14.7×10⁹ m³/d [25] and compared it with the observation from an Acoustic Doppler Current Profiler (ADCP) moored in the Strait of Hormuz,

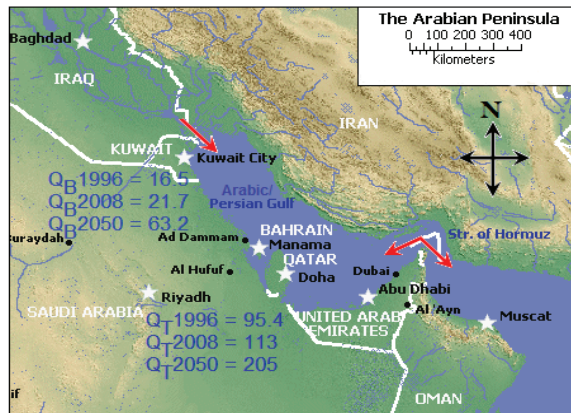


Fig. 1. Results of water discharged to the Arabian Gulf (in $10^6 \text{ m}^3/\text{d}$) in 1996, 2008 and 2050 (Map from Google).

which indicated no strong seasonal variation outflow transport and an annual mean of $(17.3\text{--}21.6) \times 10^9 \text{ m}^3/\text{d}$ [26]. Bidokhti and Ezam estimated a typical mass transport of the outflow from the Arabian Gulf at about $34.5 \times 10^9 \text{ m}^3/\text{d}$, which was larger than previously reported [27].

2.2. Population and area

A comparison of population, area, and population growth rate for the world and the study area is presented in Table 2 for a span of 100 years. The total population in the study area is approximately 1.0 and 2.0% of the world's population in the years 1950 and 2008 and prognoses to increase to 2.2% by the year 2050 [29]. The area around the Arabian Gulf occupies approximately 3.3% of the world area. Population growth ratio is high in the AG area. The annual population growth rate in the world

and study area in the 100 year period from 1950 to 2050 was found to be 1.30 and 2.07 respectively.

The growth rates were calculated using the formula: $R(t) = \ln [P_{t+1} / P_t]$, in which $t = \text{year}$; P_{t+1} = population at mid-year $t+1$, P_t = population at mid-year t , and \ln = natural log [29]. The growth rate is normally calculated from mid-year to mid-year.

3. Long-term data

3.1. Desalination capacities distribution

An estimate of desalination capacity and capacity per capita up to 2050 was made with available and calculated data. Fig. 2 is a typical diagram of a seawater desalination plant including pre and post treatment, where S_{Intake} and Q_{Intake} are salinity and volume of seawater intake, S_{Brine} and

Table 2

Comparison of area and population growth rate in the world and study area in 1996, 2008 and 2050 [29]

Country or area	Population			Area (km^2)	Population growth rate (PGR)
	1950	2008	2050		
World	2,555,948,654	6,677,602,292	9,392,797,012	130,772,667	1.30
Bahrain	114,840	718,306	973,412	665	2.14
Iran	16,357,000	65,875,223	81,490,039	1,636,000	1.61
Iraq	5,163,443	28,221,181	56,360,779	432,162	2.39
Kuwait	144,774	2,596,799	6,374,800	17,820	3.78
Qatar	25,101	928,635	1,239,216	11,437	3.90
KSA	3,859,801	28,161,417	49,706,851	2,149,690	2.56
UAE	71,520	4,621,399	8,018,904	83,600	4.72
Total	25,736,479	131,122,960	204,164,001	4,331,374	2.07
Percentage	1.0	2.0	2.2	3.3	0.77

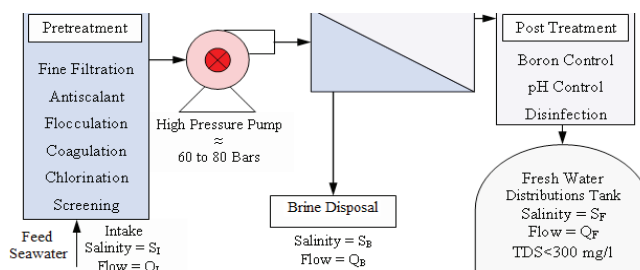


Fig. 2. A typical reverse osmosis seawater desalination plant scheme showing input/output and different stages of treatment. Note that boron control involves a second RO stage (BWRO), which also produces brine with a low TDS (< 3000 mg/l).

Q_{Brine} salinity and volume of brine discharge, and S_F and Q_F salinity and volume of fresh water produced by the desalination plant. $S_{\text{Brine}} = S_{\text{Intake}} / (1 - r)$ and $Q_{\text{Brine}} = (1 - r) Q_{\text{Intake}}$, where r is the recovery ratio between 35–45% of the intake and $S_F \approx 0$ and $Q_F = r Q_{\text{Intake}}$. The high concentration brine is discharged back to the open sea through pipes and in some cases in an open channel. The cooling water flows in MSF and MED are disregarded, since they do not affect salinity.

Over the last ten years of desalination development, the recovery ratio r has been significantly increased in reverse osmosis plants. For example, Raed et al. demonstrated that seawater intake salinity, S_{Intake} , is equal to 41.7 ppt, and the brine directly in front of the output pipeline is equal to 74 ppt. The recovery ratio will be $S_{\text{Brine}} = S_{\text{Intake}} / (1 - r)$, or $r = 44\%$ recovery ratio [30]. Table 3 pres-

ents desalination capacities in 1,000 m³/d globally as well as for the studied area at the end of 1996 and 2008, and estimated values for 2050. The operation temperature in a multistage flash desalination plant (MSF) can reach up to 120°C. In multi-effect distillation plants (MED), the plants operate at temperatures below 70°C. Brines from thermal desalination plants can be mixed with cooling water to decrease the temperature or mixed with wastewater to dilute the brine salinity. This may give the effluents a positive buoyant. If not mixed with cooling water or wastewater, the brines can also have negative or neutral buoyant, depending on salinity and temperature. More and recent examples for recovery ratio can be found in Table 1. These data contain the major desalination technologies RO membrane and thermal desalination.

Three types of water in the typical desalination plant

Table 3

Comparison between the world and study area for desalination capacity at the end of 1996, 2008, and predictions for the year 2050 [4,10,11,15–18,28]

Country	Desalination capacity in 1,000 m ³ /d								
	1996			2008			2050		
	Q_F	Q_B	Q_I	Q_F	Q_B	Q_I	Q_F	Q_B	Q_I
World	20000	46667	66667	47709	71564	119273	192211	192211	384422
Bahrain	283.0	660	943	825.2	1238	2063	3022	3022	6044
Iran	423.4	988	1411	547.8	822	1370	3138	3138	6276
Iraq	324.5	757	1082	476.6	715	1192	2519.3	2519	5039
Kuwait	1284.3	2997	4281	2308.7	3463	5772	10822	10822	21644
Qatar	560.8	1308	1869	1026.3	1539	2566	4762	4762	9524
KSA	5006.2	11681	16687	7750.8	11626	19377	39669	39669	79339
UAE	2134.2	4980	7114	6094.7	9142	15237	22533	22533	45065
Total	10016	23372	33388	19030	28545	47575	86465	86465	172931
Percentage	50.1	50.1	50.1	39.9	39.9	39.9	45.0	45.0	45.0
Total*	7078	16515	23592	14480	21720	36201	63179	63179	126359

Q_F = freshwater production; Q_B = brine discharge; Q_I = seawater and brackish water intake

*Total for the KSA with 41.3% of the flows reaching the AG

(freshwater production Q_p , brine discharge Q_{Brine} , and seawater intake Q_{Intake}) were defined and compared in the last twelve years between early 1996 and 2008 and estimated for the year 2050 for the total desalination capacity in the world and the study area. Calculations made by Lattemann and Höpner and the IDA year books (2006–07; 2007–08 and 2008–09) show that Saudi Arabia (KSA) has approximately 41.3% of its desalination capacity along the shores of the Arabian Gulf and 58.7% along the Red Sea [8,11,17,31]. In this study, just 41.3% of the total daily brine discharge of Saudi Arabia will be considered and the same will apply to the wastewater calculations. The results describe the relation between the three water types in three different time periods.

3.2. Wastewater collection

In recent decades, the water demand in the Gulf Cooperation Council (GCC) countries has more than doubled compared to the increase in population, due to more water supply, higher living standards, expansion of agriculture, and green land irrigation [32]. The water consumption around the millennium was over 700 l/person/d (255 m³/cap/y) in the UAE and in Kuwait and Qatar over 400 l/person/d (145 m³/cap/y) [32]. In Europe, the corresponding figure for 2005 was 920 m³/cap/y [33]. The USA has the largest consumption of 1720 m³/cap/y and Denmark the lowest with 130 m³/cap/y [33]. These figures include also agricultural demand. An increase in water consumption in the AG — area caused by an expansion of agriculture has not been considered in this study because this sector uses groundwater as the main source [32].

With the increase in population and associated increase in water consumption, the amount of wastewater that has to be treated increases as well. More wastewater treatment plants must be built to protect the environment. The amount of wastewater that will be recycled to agriculture, green land irrigation, and augmentation of aquifers will most probably increase due to the shortage of water [32]. Many countries around the Arabian Gulf already reuse the wastewater or have plans to do so, for example Kuwait, where treated wastewater is used for irrigation and landscaping [34], while the UAE has initiated a nation-wide program for reuse of treated wastewater in landscaping [35].

4. Methodology and modeling

4.1. Wastewater calculation

In order to estimate the amount of wastewater generated in 2050, the following assumptions were made:

- Population increase calculated on the basis of the increase between 1996 and 2050.
- Water produced by desalination is only distributed

for domestic and industrial use. Therefore all the produced freshwater will end as potential wastewater.

- Leaks in pipes transporting potable water and wastewater are assumed to be equal to other potable water sources.

Due to the general water stress situation in the AG-area, the amount of treated wastewater that will be reused will probably be high. An analysis of mixing brine with wastewater was also made, assuming four different scenarios:

- All wastewater is reused; 0% of produced desalinated water is discharged with brine
- 25% of produced desalinated water is discharged with brine
- 75% of produced desalinated water is discharged with brine, or
- 100% of produced desalinated water is discharged with brine

4.2. Water and salt mass balances

A generalized diagram summarizing water and salt budgets for coastal ecosystems is presented in Fig. 3. The Arabian Gulf is considered to be a one-layer system (non-stratified) to easily modify and describe such a budget in terms of a simple mass balance equation. In accordance with LOICZ biogeochemical modeling, it is important to estimate the mixing volume Q_{EX} (exchange volume between system body and ocean) across the open boundary of the system. Q_{EX} is estimated from the water and salt budgets [36].

In Fig. 3, the total water received from rivers and springs is denoted Q_{RP} , average rainfall Q_p , average annual evaporation Q_{E} , the amount of wastewater that will be added to the system and can be mixed with brine water Q_{W} , and the residual volume (net volume) transport associated with freshwater discharge Q_{N} . Q_{Brine} is brine discharge to the sea surface from a desalination plant with a high salt concentration and Q_{Intake} the amount of water intake to the desalination plant from the open sea or wells located about 20–30 m away from the coastline. S_{sys} is the system salinity, S_{ocn} the adjacent ocean salinity, and all other terms have salinity values except precipitation and evaporation, which were approximated to zero. The units for all output and input are usually in m³/s and all concentrations will be assumed to be g/l.

5. Results and recommendations

5.1. Study area characteristics

The water mixing across the open boundary of the water system is governed by the dispersion process [37]. The following criteria are used to decide how the system will be treated in shape, shear, and mixing. A system is considered to be “narrow and deep” if $L_c/B > 2$ and B/H

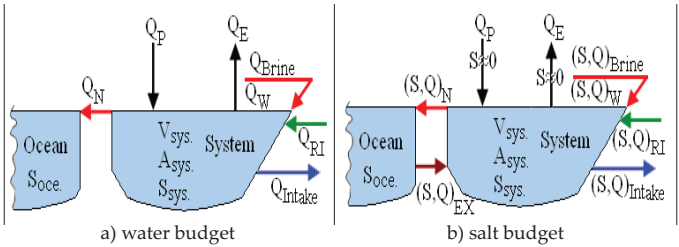


Fig. 3. Generalized diagram summarizing water and salt budgets for coastal ecosystems.

< 500 (vertical shear dominant). A system is considered “wide and shallow” if $L_c/B < 2$ and $B/H > 500$ (horizontal shear dominant) as defined by Taylor [38]. L_c (m) is the distance from the center of the system to its mouth, H (m) the average depth of the system, and B (m) the width of the system.

The typical and calculated parameters related to the Arabian Gulf are presented in Table 4. From Table 4 it can be concluded that the Arabian Gulf system should be considered “wide and shallow” and dominated by horizontal shear. This result will help us to understand the circulation and mixing in the system.

5.2. Results from desalination and wastewater discharge

The result of net volume, exchange volume, exchange time, calculation of brine and wastewater discharge to

the Arabian Gulf in late 1996 and 2008, and a prediction for the year 2050 are presented in Table 5. The amount of wastewater is added stepwise to the brine discharge from 0 to 100% in order to find differences in exchange time and the mixing behavior in the whole system. These percentages are also derived from the wastewater used per capita per year in the countries in the study area, where zero percent in the table means that all wastewater is treated and used for different purposes on land, while 100% implies that all wastewater is mixed with the brine and discharged to the Arabian Gulf.

The differences from zero to 100% were calculated for net volume, exchange volume, and exchange time for the entire Arabian Gulf in order to separately evaluate and understand the conditions in each period and changes between the three periods. The net volume increased by 79 million m^3/d in 1996 when changing the wastewater discharge to the Gulf from zero to 100%, decreasing the exchange volume by about 524 million m^3/d and increasing the mixing time by about 203 d.

Correspondingly, the net volume increased by 92 million m^3/d in 2008, decreasing the exchange volume by 608 million m^3/d and increasing the mixing time in the system by about 233 d. In the forecast for 2050 after desalination and wastewater capacity calculations, the difference in net volume increased to 143 million m^3/d , the exchange volume decreased to 947 million m^3/d , resulting in an increase in the mixing time of about 328 d.

The different years presented in Table 5 can first be compared without wastewater discharge. From 1996 to 2008, the net volume decreased by 7.4 million m^3/d , the exchange volume increased by 69 million m^3/d , and the mixing time decreased by 22.5 d. For the next 42 years from 2008 until 2050, the calculation shows a decrease in net volume of 48.7 million m^3/d , an exchange volume increase of 424 million m^3/d , and a mixing time decrease of about 126 d. And within the 54 years from 1996 to 2050, the net volume decreased by 56 million m^3/d , the exchange volume increased by 493 million m^3/d , and the mixing time decreased by 149 d. Obviously, the more desalinated water that is collected from the Gulf, the higher is the remaining salinity. With higher salinity in the Gulf,

Table 4
The typical and calculated parameters for the Arabian Gulf [36–39]

Categories	Arabian Gulf
Parameters	
L_{ave} ($\times 10^3$ m)	1,000
L_c ($\times 10^3$ m)	450
B ($\times 10^3$ m)	240
H (m)	35
A ($\times 10^6$ m ²)	240,000
V ($\times 10^9$ m ³)	8,400
Input/output, 10^6 m ³ /d	
Average ppt., P_{ave}	65.8
Evaporation rate, E	986.3
River discharge, Q_{RI}	131.5
Average outflow, Q_O	25,918
Classifications	
L_c/B ratio	$1.9 < 2$
B/H ratio	$6857 > 500$
Shape	Wide and shallow
Shear	Horizontal shear dominant

Table 5

Results of brine and wastewater discharge to the Arabian Gulf in 1996 and 2008 and the prediction for 2050

Parameters	Brine and wastewater discharges (10 ⁶ m ³ /d)					Difference (0 compared with 100% wastewater)
Wastewater discharge in %	0	25	50	75	100	
Total discharge in 1996	16.5	36.2	55.9	75.7	95.4	
Q_N (10 ⁶ m ³ /d)	–796	–776.4	–756.7	–737.0	–717.3	79
Q_{EX} (10 ⁶ m ³ /d)	4507	4376	4245	4114	3 983	–524
τ (time in y)	4.34	4.46	4.60	4.74	4.89	0.56
τ (time in d)	1584	1630	1679	1732	1787	203
Total discharge in 2008	21.7	44.6	67.5	90.4	113.3	
Q_N (10 ⁶ m ³ /d)	–804	–780.6	–758	–734.9	–712	92
Q_{EX} (10 ⁶ m ³ /d)	4576	4 424	4272	4120	3968	–608
τ (time in y)	4.28	4.42	4.57	4.74	4.91	0.64
τ (time in d)	1561	1614	1670	1730	1795	233
Total discharge in 2050	63.2	98.8	134.4	170.1	205.7	
Q_N (10 ⁶ m ³ /d)	–852	–816.6	–781.0	–745.3	–709.7	143
Q_{EX} (10 ⁶ m ³ /d)	5000	4763	4527	4290	4 053	–947
τ (time in y)	3.93	4.12	4.33	4.57	4.83	0.90
τ (time in d)	1435	1505	1583	1668	1764	328

the exchange with the Indian Ocean will increase (S_{EX} and Q_{EX} in Fig. 3).

The various years can also be compared by means of 100% wastewater discharge mixed with brine. From 1996 to 2008, the net volume increased by 5.3 million m³/d, the exchange volume decreased by 15 million m³/d and the mixing time increased by 7.8 d. For the next 42 years from 2008 until 2050, the calculation shows a net volume increase of 2.3 million m³/d, the exchange volume increased by 85 million m³/d, and the mixing time decreased by 31 d. Within the next 54 years from 1996 to 2050, the net volume increased by 7.6 million m³/d, the exchange volume increased by 70 million m³/d, and the mixing time decreased by 23.5 d. Mixing brine with wastewater reduces the water and salt exchange between the Gulf and the Indian Ocean.

Overall, the result from 1996 to 2008 revealed that the net volume amounted to 13 million m³/d, the exchange volume decreased by 84 million m³/d, and the mixing time increased by 30 d. For the next 42 years from 2008 until 2050, the calculation shows an increase in the net volume of 51 million m³/d, in exchange volume by 339 million m³/d, and in the mixing time by 95 d.

According to the above comparisons, the higher percentage of wastewater added to the system, i.e. discharged back to the Arabian Gulf, the greater the net volume flow and the lower the exchange volume due to the mixing of high saline brine. Thus, the exchange volume from the ocean will become gradually smaller due to reduced water flow from low to higher saline concentration. On a local scale, the mixing of wastewater with brine will help to reduce the salinity gradients in the coastal areas.

So is it positive or negative to increase the mixing of wastewater with brine? This is a difficult question. The environmental effects depend on all inputs and outputs as defined by water and salt mass balance, population growth and the increase in desalination. Mixing times are attributed to the net and exchange volume. When comparing 1996 with 2050, it is obvious that mixing times will decrease due to increasing desalination. Salinity will increase even more if the wastewater discharge goes down, reducing the exchange volume.

Exchange time or mixing time calculations for these different water concentrations demonstrate that the higher the amount of wastewater mixed with brine discharge, the longer the mixing time. However, if untreated, the wastewater will contribute to an increasing eutrophication of the Gulf. The management of the Arabian Gulf needs to be studied thoroughly. Other conditions contribute to the system performance. For instance, the amount of natural evaporation is huge when compared to the total amount extracted from the Arabian Gulf. However, while the water is locally extracted, the evaporation occurs all over the surface area of the Gulf and thus has less impact than local extraction.

6. Conclusion

Desalination and wastewater treatment plants are needed in all countries of the study area due to the scarcity of fresh water. The mixing of wastewater and brine discharge is an important method for minimizing the salinity increase in the coastal waters of the Arabian Gulf. Therefore, it will be possible to minimize the impact

and reduce the salt concentration in the future when adding wastewater to the brine discharge. This method will, however, also minimize the water that comes from the ocean to the Gulf. It will be very difficult to decide whether to use the wastewater for mixing with brine or reuse for other purposes after treatment.

Some points must be taken into account in the future, such as:

- The building of wastewater treatment plants to take care of increased wastewater production in urban areas.
- The extra cost of advanced treatment compared with the costs of the extra production of desalinated water, damaged groundwater aquifers, and potential environmental problems will probably promote water recycling.
- In some cases there might be no appropriate space close enough to irrigate with treated wastewater, which therefore may be discharged with brine.
- The content of nutrients in wastewater is positive for irrigation, but with only secondary treatment, problems such as eutrophication in the Gulf may increase if the exchange of water is low.
- Considering the concentration of dissolved solids in the Gulf water, simultaneous discharge of wastewater with brine conserves the salt (reduces the salt concentration of the brine when discharged back to the sea). This may actually be one argument for not recycling the wastewater on land.

The higher the percentage of wastewater added to the system, the greater the net volume flow and the smaller the exchange volume due to the mixing of high saline brine and low saline wastewater. Thus, the exchange volume from the ocean will be progressively minimized due to a reduced flow from low saline to high saline concentration waters. On a local scale, the mixing of wastewater with brine will help to reduce the salinity gradients in the coastal areas. It will be possible to minimize the impact and reduce the salt concentration in the future by adding wastewater to the brine discharge.

Abbreviations and symbols

ADCP	—	Acoustic doppler current profiler
APP	—	Atomic power project
BWRO	—	Brackish water reverse osmosis
DGR	—	Desalination growth ratio
GCC	—	Gulf Cooperation Council
IWPP	—	Independent water power project
IWSP	—	Integrated water steam and power project
MED	—	Multi-effects distillation
MSF	—	Multistage flash distillation
PGR	—	Population growth rate
RO	—	Reverse osmosis
TDS	—	Total dissolved solids

WEB	—	Water Energiebedrijf
Q_{Brine}	—	Brine discharge
Q_{EX}	—	Exchange volume
Q_{F}	—	Freshwater production
Q_{Intake}	—	Intake seawater or brackish water
Q_{N}	—	Residual volume (net volume)
Q_{RI}	—	River flow
Q_{T}	—	Total discharge (brine + wastewater)
Q_{W}	—	Wastewater discharge
S_{Brine}	—	Salinity of brine
S_{F}	—	Salinity of produced fresh water
S_{Intake}	—	Intake salinity
S_{ocn}	—	Adjacent ocean salinity
S_{sys}	—	System salinity
τ	—	Mixing time

References

- [1] D.M.A. Al-Gobaisi, Sustainable augmentation of fresh water resources through appropriate energy and desalination technology. IDA World Congress on Desalination and Water Reuse Madrid, Spain, 1997.
- [2] A. Purnama, H.H. Al-Barwani and S. Ronald, Calculating the environmental cost of seawater desalination in the Arabian marginal seas, *Desalination*, 185 (2005) 79–86.
- [3] I. Shiklomanov, *World Water Resources: Modern Assessment and Outlook for 21st century*. Hydrological Institute, Saint Petersburg, 1999.
- [4] M. Ruiz-Mateo Antequera and J. Gonzalez, Discharges to the sea from desalination plants. MEDCOAST-07, Alexandria, Egypt, 13–17 November 2007.
- [5] A. Valero, J. Uche and L. Serra, Desalination as an Alternative to Spanish National Hydrology Plan. Technical Report, CIRCE and University of Zaragoza, 2001.
- [6] A.A. Akkad, Conservation in the Arabian Gulf countries: Management and operations, *J. AWWA*, May (1990) 40–50.
- [7] O.K. Buros, *The ABCs of Desalting*, 2nd ed., 1998.
- [8] IDA — International Desalination Association Yearbook, 2007–2008.
- [9] Magazine Water Condition and Purification, January, 2005, <http://www.lennetech.com/WHO-EU-water-standards.htm>.
- [10] IDA Worldwide Desalting Plant Inventory in MS Excel format, Media Analytics Ltd., Oxford, UK, 2006, No. 19.
- [11] S. Lattemann and T. Höpner, Environmental impact and impact assessment of seawater desalination, *Desalination*, 220 (2008) 1–15.
- [12] C. Vanhems, Critical Review of Desalination Concentrate Disposal to Surface Water, USA, 1992 (after UNEP, 2001).
- [13] UNEP, Assessment of the State of Pollution of the Mediterranean Sea by Zinc, Copper and their Compounds. Document UNEP (OCA)/MED WGer it&, 1995, pp. 121.
- [14] S. Barak, *Water & Watering*, 4 (2000) 406–411 [in Hebrew].
- [15] M. Perla, The Israel Electric Corporation Ltd, 2000 [in Hebrew].
- [16] Worldwater: <http://www.worldwater.org/data.html>. Last update January 2009.
- [17] IDA — International Desalination Association Yearbook, 2006–2007.
- [18] S. Ghabayen, M. McKee and M. Kemblowski, Characterization of uncertainties in the operation and economics of the proposed seawater desalination plant in the Gaza Strip, *Desalination*, 161 (2004) 191–201.
- [19] A. Glazer and M. Dadon, The Israel Electric Corporation Ltd, 2000 [in Hebrew].

- [20] M. Sladkevich, E. Kit and M. Gluzman, Numerical simulation of cooling water recirculation for the Rutenberg power station. Prepared for the Israel Electric Corporation Ltd., Technion, Haifa, PN 371194, 1994.
- [21] R.M. Reynolds, Physical oceanography of the Gulf, Strait of Hormuz, and the Gulf of Oman — Results from the Mt Mitchell expedition. *Mar. Pollut. Bull.*, 27 (1993) 35–59.
- [22] J.R. Hunter, The physical oceanography of the Arabian Gulf: A review and theoretical interpretation of previous observations. In: *Marine Environment and Pollution, Proc. 1st Gulf Conference on Environment and Pollution*, KISR, Kuwait, 7–9 February 1982, pp. 1–23.
- [23] P.G. Brewer and D. Dryssen, Chemical oceanography of the Persian Gulf. *Progr. Oceanography*, 14 (1985) 41–55.
- [24] V.C. John, S.L. Coles and A.I. Abozed, Seasonal cycle of temperature, salinity and water masses of the Western Arabian Gulf, *Oceanol. Acta*, 13 (1990) 273–281.
- [25] E. Ahmad and S.A. Sultan, Annual mean surface heat fluxes in the Arabian Gulf and the net heat transport through the Strait of Hormuz, *Atmos. Ocean.*, 29(1) (1991) 45–61.
- [26] A.S. Bower, H.D. Hunt and J.F. Price, Character and dynamics of the Red Sea and Persian Gulf outflows, *J. Geophys. Res.*, 105(C3) (2000) 6387–6414.
- [27] A.A. Bidokhti and M. Ezam, The structure of the Persian Gulf outflow subjected to density variations, *Ocean Sci. Discuss.*, 5 (2008) 135–161.
- [28] R. Wiseman, Editor's corner, *Desal. Water Reuse*, 16(3) (2006) 10–17.
- [29] US Census Bureau International: Data Base; World Bank, 2004. Data updated 01-05-2009, <http://www.census.gov/ipc/www/idb/idbprint.html>
- [30] A.I.B. Raed, M.P. Kenneth, L. Magnus and E. Mustafa, Impact of brine disposal from EMU desalination plant on seawater composition, IDA World Congress, Maspalomas, Gran Canaria, Spain, October 2007, pp. 21–26.
- [31] IDA — International Desalination Association Yearbook, 2008–2009.
- [32] F. Al-Rashed Muhammad and M.S. Mohsen, Water resources in the GCC countries: An overview, *Wat. Resources Manage.*, 14 (2000) 59–75.
- [33] OECD Factbook, 2005, ISBN 92-64-01869-7.
- [34] M.A. Jasem, S.B. Haider and T.H. Abdullah, Wastewater reuse practices in Kuwait, *Environmentalist*, 23 (2003) 117–126.
- [35] UAE, United Arab Emirates Yearbook 2008: http://viewer.zmags.co.uk/showmag.php?mid=stfrs&preview=1&_x=1#/page158/.
- [36] D.C. Gordon, Jr., P.R. Boudreau, K.H. Mann, J.-E. Ong, W.L. Silvert, S.V. Smith, G. Wattayakorn, F. Wulff and T. Yanagi, LOICZ Biogeochemical Modelling Guidelines. LOICZ Reports & Studies, 5 (1996) 1–96.
- [37] T. Yanagi, *Coastal Oceanography*. Kluwer, Dordrecht, 2000, 162 p.
- [38] G.I. Taylor, Dispersion of soluble matter in solvent slowly flowing through a tube. *Proc. Royal Soc. London*, A219 (1953) 186–203.
- [39] M. Masahiro, *Managing Water for Peace in the Middle East: Alternative Strategies*, United Nations University Press, Tokyo – New York – Paris, The United Nations University, 1995, 319 p.

Paper IV

Estimated Future Salinity in the Arabian Gulf, the Mediterranean Sea and the Red Sea Consequences of Brine Discharge from Desalination

Bashithalshaaer, R., Persson, K.M., and Aljaradin, M. 2011

International Journal of Academic Research. Vol. 3. No. 1, Part I, 156-164

Estimated Future Salinity in the Arabian Gulf, the Mediterranean Sea and the Red Sea Consequences of Brine Discharge from Desalination

Raed Bashitialshaer^{a*}, Kenneth M. Persson^{ab}, Mohammad Aljaradin^a

^aDepartment of Water Resources Engineering, Lund University, PO Box 118, SE-221 00 Lund, Sweden

*Tel.: +46 46 222 4367; Fax: +46 46 222 4435; email: Raed.Alshaer@tvrl.lth.se

^bSydvatten AB, R&D, Skeppsgaten 19, SE 211 19-Malmö, Sweden

ABSTRACT

Seawater desalination constitutes an important source for water supply to the population bordering the Arabian Gulf, the Mediterranean Sea, and the Red Sea. The three regions represent about 11.8% of the world land area and the countries hosted approximately 9% of the world population in 1950 and 2008 and are projected to do so again in 2050. Population statistics for a 100-year period has been used including a prognosis from 2010 to 2050. Data on desalination plant capacity covering 12 years from 1996 to 2008 has been summarized and a prognosis of the increase in desalination for the three regions until 2050 developed. The results obtained for desalination capacity in the study area were 62%, 58%, and 60% of the world capacity for 1996, 2008, and 2050, respectively.

The increase in the recovery ratio is considered an important factor in this study. In 1996 this ratio was about 30 to 35%, and in 2008 it was 40 to 45%, although in some plants it reached up to 50%. Brine discharge will increase the salinities of the Arabian Gulf, Mediterranean Sea, and Red Sea, by some extra 2.24, 0.81 and 1.16 g/l in the year 2050.

Keywords: Arabian Gulf; Mediterranean Sea; Red Sea; Desalination; Water-Salt balance; 1D advection diffusion; Salinity.

1. INTRODUCTION

1.1. An overview

Water and salt mass balances were both employed to calculate residual flow, exchange flow, and exchange time in each of the receiving water systems in order to understand system dynamics, water movement, and mixing times. The effects of desalination plant and brine discharge in the Arabian Gulf, the Mediterranean Sea and the Red Sea were mathematically modeled and evaluated for the years 1996, 2008 and 2050. The calculations presented here focus on salinity changes in three receiving water systems due to brine from seawater desalination plants. The three regions, the Arabian Gulf (AG), the Mediterranean Sea (MS) and the Red Sea (RS) have very high evaporation rates, from 1.2 to 2 m annually, and very low annual precipitations, from 90 to 150 mm. The salinity in the recipients may increase in the long term if larger and larger amounts of desalinated water are removed from the water bodies. Due to their semi-enclosed nature and arid climate, AG, MS, and RS waters are naturally characterized by a higher salt content due to the accelerated rate of evaporation (Anton et al., 2005).

Desalination is considered an important source of fresh water that should proportionally follow the increase in populations. Any country with water resources of less than 1000 m³/capita/yr is considered in trouble (Al-Gobaisi, 1997). Thus, increasing water resources mainly from desalination through improving the recovery ratio from 30 to 50 percent in some countries will increase the brine salt concentration. The existing amount of water resources on our planet is enormous compared with the population increments (Shiklomanov, 1999). Almost 95% is in oceans and seas that contain a high degree of salinity, thus it is impossible to directly use the water resources for any purpose (e.g. agriculture, industry or domestic) unless they have been previously treated (Ruiz et al., 2007). Six countries receive nearly 50% of the total freshwater resources (Brazil, Canada, Russia, United States, China and India) and five great rivers transport 27% of the renewable resources (Amazon, Ganges-Brahmaputra, Congo, Yellow and Orinoco) (Ruiz et al., 2007; Valero et al., 2001).

The amount of desalinated water in the Arabian Gulf accounts for over 60% of the world's total production (Akkad, 1990). The installation capacity was counted at the end of 1999 as follows: 60% in the Middle East, 16% in the United States; 10% in the European Union, 6% in the Arabian Mediterranean countries, and 8% in the rest of the world (Ruiz et al., 2007). The desalination capacities in 1998 were distributed as 60% in West Asia and the Middle east, 11% in the United States; 7% in the European Union, 7% in North Africa, 4% in South and Central America, and 11% in the rest of the world (Magazine, 2005). About six percent of all desalination plants are located in the Asia-Pacific region, 7% in the Americas, 10% in Europe and 77% in the Middle East and North Africa (IDA, 2006; Lattemann & Höpner, 2008).

The total daily capacity of installed desalination plants worldwide was 22.7 million cubic meters (MCM), an increase of about 70% from that previously reported in the Desalting ABCs in 1990 (Buros, 1998; IDA, 2006-07). The energy demand for reverse-osmosis seawater desalination has decreased, leading to a reduction of production cost from about 2.5 to 0.5 US \$/m³ in some places, partly depending on the intake

raw water quality. The cost of desalination plants may also depend on their location as well as on the local unit costs and operations, in which prices have decreased from roughly \$1.5/m³ in the early 1990s to around \$0.50/m³ in 2003 (Pankratz, 2004), for example, according to Crisp, the Perth desalination plant consumes only 3.7 kWh/m³ of fresh water (Gary, 2006).

1.2. Brine discharge and dispersion of salt

All desalination brines, the concentration of which is higher than that of natural seawater, are normally returned to the sea. The salt concentrations of the brines are usually found to be double or close to double that of natural seawater (Vanhems, 2001). In the reverse osmosis desalination plants (RODP), the total water is taken from the sea and the brine is discharged back to the same medium, where salinity will increase by 70% (Ruiz et al., 2007). Constructions close to the coastline give opportunities for one or more outfalls to the sea and can thus minimize or reduce the environmental impact of brine discharge (Raed et al., 2007).

The total dissolved solids (TDS) in the three main regions are higher, 38.6, 45 and 41 g/l for the Mediterranean, the Arabian Gulf, and the Red Sea respectively, compared to typical seawater of about 34.5g/l (Magazine, 2005). These values help us to understand each region separately in terms of the intake water and how the brine water will act on the recipient. The recovery ratio is also related to these values as well as the quality of fresh water production and the desalination cost.

1.3. Objectives

This study was initiated to estimate the effects of brine discharge into recipients such as changing in salinity. A large number of desalination plants that have been built around the three regions mainly Arabian Gulf and using same water for both for intake and for brine. Population increase and economical growth are also considered as main driving forces in these areas. They are directly related to fresh water consumption and amount of brine discharge. The main objective of this study is to analyze the effects of future increasing in desalination capacity. Therefore, the following studies have been executed:

- The effects of brines discharge from desalination plants in the three regions for 1996 and 2008, and prognosis for the year 2050.
- Water and salt mass balances were employed to find residual flow, exchange flow, and exchange time for the Gulf for the same years.
- Future salinity and changes from the past, today and for year 2050.

2. STUDY AREA: BACKGROUND & CHARACTERISTICS

The water scarcity in the Middle East regions (MENA), especially the Arabian Gulf countries, has reached unprecedented crisis levels. Desalination is the most important source in these countries and the largest capacity is also located in these regions. The results of brine water Q_{Brine} (10⁶ m³/d) from the three regions, the Arabian Gulf (AG), Mediterranean Sea (MS) and Red Sea (RS), in late 1996, 2008 and 2050 are presented in (Figure 1). The red arrows indicate the location of the exchange water, e.g. river inflow, inflow through the Dardanelle Strait from the Black Sea, and exchange flow from the Gibraltar Strait etc, all related to the three systems.

The countries bordering the Arabian Gulf are: Iran, Iraq, Kuwait, Saudi Arabia, Qatar, Bahrain, the United Arab Emirates and Oman. The countries bordering the Mediterranean Sea are: Spain, France, Monaco, Italy, Malta, Slovenia, Croatia, Bosnia and Herzegovina, Montenegro, Albania, Greece, Turkey, Cyprus, Syria, Lebanon, Palestine, Israel, Egypt, Libya, Tunisia, Algeria and Morocco. The countries bordering the Red Sea are: Egypt, Israel, Jordan, Sudan, Eritrea, Saudi Arabia, Yemen and Djibouti.

2.1. Arabian Gulf (AG)

The Arabian Gulf is a shallow semi-enclosed marginal sea, with less than 100 m in depth over its entire extent and with a mean of only 35 m (Reynolds R.M., 1993). It covers an area of about 240,000 km², with 1000 km in length and widths ranging from 185 km to 370 km, with a mean of 240 km. The volume is approximately 8,400 km³. There are freshwater inflows from the Tigris, the Euphrates, and the Karun at the delta of the Shatt al Arab, estimated at 0.2 m/yr, in which fresh water and river inflow equals 48 km³/yr (Reynolds, 1993; Hunter, 1986). The mean annual evaporation rate is estimated at approximately 1.5 m/yr (Brewer & Dryssen, 1985).

The shallowness of the Arabian Gulf water leads to the formation of a very high saline and dense water, with maximum salinities as high as 57 g/l along the southern coast (John et al., 1990). Typical mass transport by the outflow from the Arabian Gulf has been estimated to be about 34.5 x10⁹ m³/day, which is larger than that reported by other studies (Bidokhti & Ezam, 2008). Ahmad and Sultan (1991) employed the

Knudsen relations and estimated that the annual mean Gulf water outflow transport was about $14.7 \times 10^9 \text{ m}^3/\text{day}$, compared to the observation of an annual mean of $(17.3\text{--}21.6) \times 10^9 \text{ m}^3/\text{day}$ from an Acoustic Doppler Current Profiler (ADCP) in the Strait of Hormuz (Bower et al., 2000).

The largest number of desalination plants can be found along the shores of the Arabian Gulf with a total seawater desalination capacity of approximately (45%) of the worldwide daily production. The main producers in the Gulf region are the United Arab Emirates, Saudi Arabia (9% from the Gulf region and 13% from the Red Sea), Qatar and Kuwait (Lattemann & Höpner, 2008; Wiseman, 2006). There are about 1,500 desalination units operating in the Arabian Gulf countries, which account for 58% of the world desalination production (Al-Mutaz et al, 1989). The brine percentage discharged to the Arabian Gulf from the Iraq desalination plant is not clear to me but I estimate it to be about 5%.

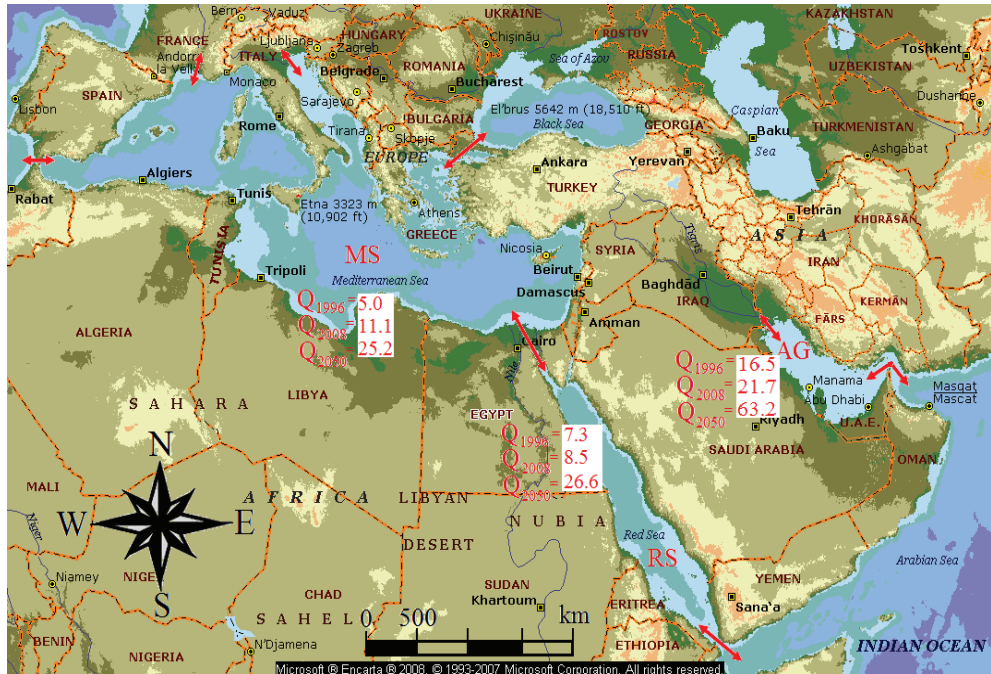


Fig. 1. Brine water Q_B results in $10^6 \text{ m}^3/\text{d}$ for the Arabian Gulf (AG), Mediterranean Sea (MS), and Red Sea (RS) in 1996, 2008, and 2050 (map from: Google Earth)

2.2. Mediterranean Sea (MS)

The Mediterranean Sea in (Figure 1), including the Sea of Marmara, occupies an area of approximately $2,960,000 \text{ km}^2$. The Mediterranean is connected to the Atlantic Ocean by the narrow and shallow channel of the Strait of Gibraltar and to the Black Sea through the Dardanelles (Britannica http, 2009). The typical values for the Mediterranean Sea comprise a mean width of about 800 km, a mean depth of approximately 1500 m, an extreme length of about 3,860 km, an average length of approximately 2700 km and an evaporation rate of approximately 1.3 m/yr (Moncef & Bernard, 2000; Rahmstorf, 1998).

Along the North African coast from Gabis in Tunisia to Egypt, precipitation of more than 250 mm per year is rare, whereas on the Dalmatian coast of Croatia there are places that receive 2,500 mm. Maximum precipitation is found in mountainous coastal areas (Mediterranean Sea, 2008). Precipitation on the coastal plain near Tel Aviv (on the MS coast) is 200 mm near Beersheba and less than 50 mm at Eilat in the south (on the RS coast) (Gisser & Pohoryles, 1977). Large volumes of sewerage are dumped directly into the Mediterranean Sea (http://en.wikipedia, 2009). Several important desalination plants are located along the Mediterranean coast. Ashkelon desalination plant is an example with a maximum production of 110 MCM/yr, with an intake salinity of 40,679 ppm TDS and brine concentration of $<80 \text{ ppm TDS}$ (Sauvet, 2007). The construction of the Hadera desalination plant was expected to begin during late 2007 and it has a planned production capacity of up to 100 MCM/year (Gustavo, 2007). In the Mediterranean, the total daily production from seawater is about 17% of the world total desalination capacity. Spain is the largest desalination producer in Europe with 7% of the worldwide capacity. The main process in Spain is reverse osmosis (RO) comprising 95% of all desalination plants (IDA, 2006; Lattemann & Höpner, 2008).

2.3. Red sea (RS)

The maximum width of the Red Sea is about 225 km, its greatest depth 3,040 m, and its area approximately 450,000 km². The typical values for the Red Sea are a mean width of about 225 km, a mean depth of around 500 m, a gross length of about 2000 km, and an evaporation rate of approximately 2 m/yr (Anton et al., 2005). In the Red Sea region, the third highest daily production of desalinated water can be found, with a combined capacity of 14% of the world total desalination capacity (IDA, 2006; Lattermann & Höpner, 2008). The exchange of water between the Red Sea and the Gulf of Aden occurs at the strait of Bab el Mandab. There is virtually no surface water runoff because no river enters the Red Sea (Shahin, 1989; Morcos, 1970).

The winter (November–May) exchange value is about 0.5 MCM/sec, which occurs at the surface and bottom layers, whereas in summer (June–October) this figure is about 0.16 MCM/sec (Thompson, 1939; Murray & Johns, 1997). Murray and Johns (1997) also estimated that the annual mean Red Sea outflow transport is about 0.37 MCM/sec, which roughly agrees with Siedler's (1969) estimated amount of 0.33 MCM/sec, based on the Knudsen relation. The rainfall over the Red Sea and its coasts is extremely low, averaging 60–100 mm/y with an average volume of about 233,000 km³. The renewal of water in the Red Sea is estimated to take 20 years (Red Sea, 2008).

3. LONG TERM DATA COLLECTION AND CALCULATION

3.1. Desalination parameters

Desalination plant capacity, annual population growth rate, and recovery ratio for the years 1996 to 2008 have been summarized in this study in order to compare world and study area data. From the available calculated data, desalination capacity and capacity per capita up to the year 2050 have been extrapolated. (Figure 2) is the typical diagram for a seawater desalination plant including details of pre and post treatment. S_{Intake} and Q_{Intake} are the salinity and volume of seawater intake, S_{Brine} and Q_{Brine} are the salinity and volume of brine discharge, and S_F and Q_F are the salinity and volume of fresh water produced by desalination plants. Moreover, $S_{\text{Brine}} = S_{\text{Intake}}/(1-r)$ and $Q_{\text{Brine}} = (1-r)Q_{\text{Intake}}$, where r is the recovery ratio, generally between 35 and 45% of the intake, $S_F \approx 0$ and $Q_F = rQ_{\text{Intake}}$. The cooling water flows in MSF and MED are disregarded, since they do not affect salinity. Brine is discharged back to the open sea through pipes and in some cases in open channels. During the past ten years of desalination development, the recovery ratio r has been significantly increased in reverse osmosis plants. For example, Raed et al. (2007) stated that seawater intake salinity, S_{Intake} , is equal to 41.7 ppt and the brine outlet is 74 ppt. According to the relation $S_{\text{Brine}} = S_{\text{Intake}}/(1-r)$, the recovery ratio $r = 44\%$. If the recovery ratio increases, the brine concentration also increases.

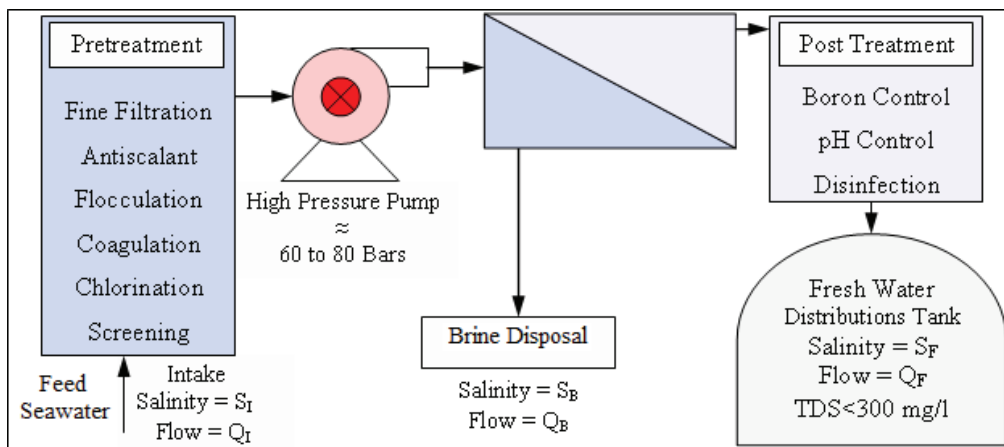


Fig. 2. A typical reverse osmosis seawater desalination plant scheme showing input/output and different stages of treatment. Note that boron control involves a second RO stage (BWRO), which also produces brine with a low TDS (<3000mg/l).

3.2. Population growth rate

In total, 25 countries (approximately 90% of the countries) in the three regions were studied in respect of area and population. There are about 35 countries in the regions but some of them e.g. Oman and Iraq

are not directly connected to the coasts of these three regions. Comparisons for the population, area, and population growth rate for the world and the study area are used in this study for 100 years. Data was collected for the period 1950-2008 and calculated for the period 2009-2050. The growth rate from the mid year of the whole period is the most common way of expressing population growth as a rate. The growth rates for the 24 countries were calculated using the formula: $R(t) = \ln [P_{t+1} / P_t]$, in which t = year; $R(t)$ = growth rate from mid year t to mid year $t+1$; $P(t)$ = population at mid year t and \ln = natural log (from: U.S. Census Bureau, 2008). The total population in the study area is approximately 9.4% of the world population during the 100 years and the land area occupies approximately 11.8% of the world total land area. The population growth rates over 100 years from 1950 to 2050 were found to be 1.30 and 1.35 in the world and the study area respectively.

3.3. Desalination production

Desalination capacities expressed as 1,000 m³/day in the world and study area for the year 1996 and the estimated values for the year 2050 are listed and compared in (Table 1). The three types of water in the typical desalination plant (freshwater production Q_F , brine discharge Q_{Brine} , and seawater intake Q_{Intake}) were compared for 1996 and 2008 and calculated for 2050 for both the world and study area desalination capacity. These results describe the relation between three water types in three different time steps for each country as well as the whole study area. They were also compared with the world capacities. It was important to estimate the fresh water in 2050 in order to calculate the increase in desalination in the studied area compared with the increase in world capacity.

The final result suggests that in 1996, 2008 and 2050, the study area represents about 62%, 58%, and 60% of the overall world capacity. (Table 1) also presents the results in terms of desalination capacity in cubic meters per capita per year in 1996, 2008 and 2050. For example, in this calculation, Bahrain's capacity per capita in 1996 was 164 m³, increasing to 409 m³ in 2008 and reaching 718 m³ in 2050.

Table 1. Comparisons between the world and study area desalination capacity and amount in cubic meters per capita per year at the end of 1996, 2008 and 2050 (Magazine, 2005; IDA, 2006; Lattemann & Höpner, 2008; IDA, 2007-08; IDA, 2008-09; Worldwater, 2009; IDA, 2006-07; Ghabayen et al., 2004)

Country or area	Brine Location	Desalination capacity in 1,000 m ³ /day						Desalination capacity in m ³ /capita/year		
		1996		2008		2050		1996	2008	2050
		Q_F	Q_B	Q_F	Q_B	Q_F	Q_B	Q_F	Q_F	Q_F
WORLD		20000	46667	47709	71564	192211	192211	1.19	2.54	4.74
Algeria	MS	190.8	445	1055.9	1584	3044.1	3044	2.30	11.13	16
Bahrain	AG	283.0	660	825.2	1238	3022.0	3022	164	409.0	718
Cyprus	MS	6.275	15	183	275	399.0	399	3.01	82.3	110
Egypt	MS,RS	102.1	238	491.1	737	1479.6	1480	0.51	2.14	2.68
France	MS	29.1	68	230.3	345	603.7	604	0.17	1.28	2.00
Greece	MS	36.0	84	50.0	75	273.7	274	1.26	1.66	6.31
Iran	AG	423.4	988	547.8	822	3138.2	3138	2.63	2.96	8.91
Iraq	AG!	324.5	757	476.6	715	2519.3	2519	4.76	6.01	10.3
Israel	MS,RS	90.4	211	630.1	945	1703.6	1704	5.27	31.54	36.4
Italy	MS	483.7	1129	824.3	1237	3984.7	3985	3.06	5.05	18.3
Jordan	RS	7.0	16	173.0	260	382.1	382	0.48	9.94	7.51
Kuwait	AG	1284.3	2997	2308.7	3463	10822	10822	210	316.5	393
Lebanon	MS	17.0	40	27.0	41	136.1	136	1.72	2.42	6.34
Libya	MS	638.4	1490	940.0	1410	4961.1	4961	43.1	54.2	106
Malta	MS	145.0	338	248.4	373	1197.3	1197	133.2	219	700
Morocco	MS	20.0	47	36.0	54	168.6	169	0.24	0.37	0.76
Palestine	MS	9.0	21	10.0	15	63.4	63	0.89	0.86	1.50
Qatar	AG	560.8	1308	1026.3	1539	4761.9	4762	258	393	889
KSA	AG,RS	5006	11681	7750.8	11626	39669	39669	74.4	98.0	184.7
Spain	MS	492.8	1150	3420.7	5131	9258.7	9259	4.58	30.1	60.2
Sudan	MS,RS	1.0	2	23.0	35	51.1	51	0.01	0.20	0.13
Tunisia	MS	47.4	111	98.8	148	426.7	427	1.83	3.39	7.89
Turkey	MS	6.0	14	39.0	59	107.4	107	0.03	0.19	0.29
UAE	AG	2134	4980	6094.7	9142	22532	22533	198	469.5	650
Yemen	RS	37.0	86	47.0	71	272.5	272	0.66	0.73	0.88
Total		12375	28876	27558	41337	114979	114979	7.86	15.61	29.54
Percentage		62		58		60				

Where, Q_F = Freshwater production from desalination and Q_{Brine} =Brine Discharge.

4. METHODOLOGY AND MODELING

4.1. Water and salt mass balances

A generalized diagram summarizing water and salt budgets for coastal ecosystems is described in (Figure 3). This diagram assumes a one-layer system for the Arabian Gulf, Mediterranean Sea, and the Red Sea. From this, budgets for water mass and salt mass can be calculated through a simple mass balance equation. The general definitions of the input/output in the system are presented in (Figure 3). The total water received from rivers and springs is denoted (Q_{RI}), average rainfall (Q_P), average annual evaporation (Q_E), the mixing volume (exchange volume between system body and ocean) across the open boundary of the system (Q_{EX}), and the residual volume transport associated with freshwater discharge (Q_N). Q_{Brine} is the brine discharge to the sea and Q_{Intake} the amount of feed water intake to the desalination plant from the open sea or from wells located about 20 to 30 meters away from the coastline. S_{sys} is the system salinity, S_{ocn} the adjacent ocean salinity, and all other terms have salinity values except precipitation and evaporation approximated to zero. The units for all output and input are usually in (m^3/s) and all concentrations will be assumed to be (g/l). According to LOICZ biogeochemical modeling, it is important to estimate the mixing volume Q_{EX} (exchange volume between system body and ocean) across the open boundary of the system (Gordon et al., 1996).

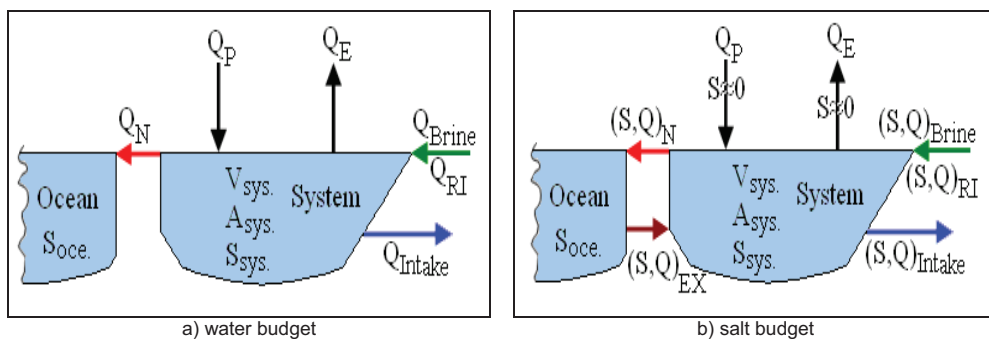


Fig. 3. Generalized diagram summarizing water and salt budgets for coastal ecosystems

5. RESULTS AND DISCUSSIONS

It is necessary to calculate desalination capacity in the three different periods in order to estimate it in cubic meters per capita per year in each country and the whole region to determine the amount of fresh water collected from desalination. The aim here is to determine the total brine water in each region for the past and future as accurately as possible in order to avoid or minimize some of the impacts. The calculated desalination capacities in the world and the three regions for fresh water Q_F , brine water Q_{Brine} , intake water Q_{Intake} , and percentages from world production at the end of the years 1996, 2008 and 2050. Corresponding desalination capacities of about 35.4, 10.7 and 15.7% have been found in the Arabian Gulf, Mediterranean Sea and Red Sea respectively at the end of 1996.

5.1. Results for recipients

Comparison between the world and the study area (AG, MMS and RS) for: 1) Average annual population growth rate (PGR) in three periods (1950, 2008 and 2050), 2) Average annual desalination growth rate (PGR) in two periods (late 1996 to 2008), 3) Coverage area ratio, 4) Desalination recovery ratio related to: Freshwater production (Q_F), Brine discharge (Q_{Brine}), Seawater intake (Q_{Intake}), and 5) Desalination capacity estimation, $m^3/capita$ in 2008 and 2050.

The mixing of different inputs across the open boundary of the recipient is governed by the dispersion process (Yanagi, 2000b). The following criteria are used to decide how to classify the water body. The recipient is considered to be "narrow and deep" if $L_c/B > 2$ and $B/H < 500$ (vertical shear dominant). The recipient is considered "wide and shallow" if $L_c/B < 2$ and $B/H > 500$ (horizontal shear dominant) (Taylor, 1953). Where L_c is the distance in meters from the center of the water system to its mouth, H (m) is the system average depth and B (m) the width of the system.

The typical and calculated parameters are related to the Arabian Gulf, the Mediterranean Sea and the Red Sea water systems. (Table 2) presents the summary results of water and salt mass balances and salinity results for the Arabian Gulf, the Mediterranean Sea, and the Red Sea based on desalination data from 1996. The result also contains the net volume, the exchange volume, and the exchange time in late

1996 and 2008 and predictions for 2050. The exchange time calculation in the three water systems was found to have insignificant changes over 54 years but significant differences between the three systems that are proportional to the system area and the total amount of desalination capacities.

Table 2. Water and salt mass balances and salinity results for the three regions (^aMasahiro, 1995; ^bRajar et al., 2007)

Parameters	Region								
	Arabian Gulf			Mediterranean Sea			Red Sea		
Input/Output at the end of year 1996 (MCM/day)									
Average Ppt., P_{ave}	65.8 ^b			1,825			100		
Evaporation Rate, E	986.3			10,543			2,466		
River Discharge, Q_{RI}	(48km ³ /yr) = 131.5			(347km ³ /yr) = 950.4 ^a			-----		
Average Outflow, Q_O	25,918			3198 ^a			34,560		
Brine Discharge, Q_B	16.5			5.0			7.3		
Seawater Intake, Q_I	23.6			7.2			10.5		
Results:	1996	2008	2050	1996	2008	2050	1996	2008	2050
Q_N (x10 ⁶ m ³ /day)	-796	-804	-852	-7770	-7775	-7793	-2369	-2372	-2393
Q_{EX} (x10 ⁶ m ³ /day)	4507	4576	5000	479963	480267	481695	31154	31208	31564
τ (days)	1584	1561	1435	8919	8913	8887	6712	6700	6626
τ (years)	4.34	4.28	3.93	24.42	24.40	24.33	18.4	18.3	18.1
Salinity, g/L, ppt	0.42	0.93	2.24	0.16	0.34	0.81	0.22	0.49	1.16

5.2. Salinities modeling

The results in (Figure 4) for cases (a) and (b) are the logarithm and peak logarithm of relative salinity due to seawater desalination in the Arabian Gulf and the Mediterranean Sea respectively. This is due to the fact that seawater desalination activities in the two regions were calculated for 1996, 2008 and 2050. The Arabian Gulf and Mediterranean Sea were both defined as wide and shallow and thus horizontal shear dominant, which means that the logarithm of relative salinity with Q_B = brine discharge from desalination production 10 years before 1996 and Q_B = brine discharge in 1996, 2008 and 2050. Anton Purnama et al. (2005) found that the peak salinity in the Arabian Gulf occurs at $(X_{max}/L) \approx (X'/L) (1-q)^{(2/3)}$, where (X'/L) is the brine discharge location.

Thus, the effect of the desalination plant in the Arabian Gulf with Q_B = brine discharge in 1996 is equivalent to the peak salinity increased by 0.42 ppt, in 2008 increased by 0.93 ppt, and in 2050 by 2.24 ppt. The result for the Mediterranean Sea with Q_B = brine discharge in 1996 is also equivalent to the peak salinity increased by 0.16 ppt, in 2008 increased by 0.34 ppt, and in 2050 by 0.81 ppt. Case (c) in (Figure 4) presents the result of applying the logarithms of relative salinity and salinity increase in the Red Sea due to a desalination plant located at $a/L = 0.5$, in 1996, 2008 and 2050. Thus, the effect of the desalination plant in the Red Sea with Q_B = brine discharge in 1996 is equivalent to the peak salinity increased by 0.22 ppt, in 2008 increased by 0.49 ppt and in 2050 by 1.16 ppt.

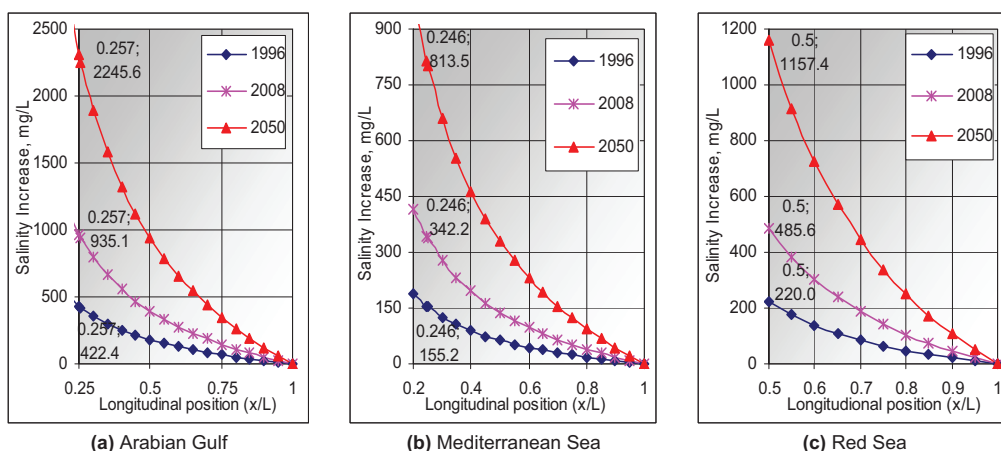


Figure 4. Results from (a) and (b) are the logarithm and peak logarithm of relative salinity due to seawater desalination in the Arabian Gulf and the Mediterranean Sea, and (c) is the logarithm of relative salinity and salinity increase in the Red Sea due to a desalination plant located at $a/L = 0.5$ in 1996, 2008 and 2050.

The results by Anton Purnama et al. (2005) are that the effect of brine discharge in the Arabian Gulf is equivalent to the peak increased by 0.06 ppt and by 0.23 and 0.47 ppt for 5 and 10 times the amount of present brine discharge. In the Red Sea, the effect of brine discharge is equivalent to the peak increased by 0.14 and 0.28 ppt corresponding to 10 and 50 times of present brine discharge. The amount of natural evaporation in the three regions is huge compared to the total amount of water that is extracted by desalination. Evaporation takes place all over the surface area of the three regions but the amount extracted by desalination is local and has a greater effect than evaporation.

6. CONCLUSION

Population and desalination growth were considered as two equally important parts of this research in terms of the result. Estimated desalinated production from seawater and population prognoses also help us to take care of the impact from salinity increments, desalination activities, and amount of brine discharge on coastal receiving water. Desalination capacity in cubic meters per capita per year for each country was also calculated for comparison with the world standards and to understand the shortage of fresh water.

The purpose of this study was to evaluate how the coasts of the Arabian Gulf, the Mediterranean Sea and the Red Sea are and will be affected by seawater desalination brine discharge. For example, the results reveal significant volumes of brine discharge to the sea. In 1996 about 14 million m³/day was discharged into the Arabian Gulf, 4.6 million m³/day into the Mediterranean Sea, and 6.4 million m³/day into the Red Sea. In 2008, these figures had increased to 18.4, 9.8, and 6.8 million m³/day respectively.

Thus, the increase in brine discharge significantly raises the salt concentration in the recipients as shown in this study. This increase must be observed from an environmental point of view, as well as technically and economically. As seawater salinity increases, the recovery ratio decreases, which raises the cost of desalinated water. This can already be partly observed in the Arabian Gulf area.

REFERENCES

1. Ahmad, E., Sultan, S. A., (1991). Annual mean surface heat fluxes in the Arabian Gulf and the net heat transport through the Strait of Hormuz, *Atmos. Ocean*. 29(1), 45-61.
2. Al-Gobaisi, D.M.A., (1997). Sustainable augmentation of fresh water resources through appropriate energy and desalination technology. IDA World Congress on Desalination and Water Reuse, Madrid, Spain.
3. Al-Mutaz, I.S., Soliman, A.M., Daghtem, M.A., (1989). Optimum Design for a Hybrid Desalting Plant. Fourth World Congress on Desalination and Water Reuse, Kuwait. International Desalination Association. *Desalination* 76 (4): 177-88.
4. Anton, P., Al-Barwani, H. H., Smith, R., (2005). Calculating the Environmental Cost of Seawater Desalination in the Arabian Marginal Seas, *Desalination* (185) 79-86.
5. Akkad, A.A., 1990. Conservation in the Arabian Gulf countries. Management and Operations, Journal of the American Water Works Association, 40-50.
6. Bidokhti, A., Ezam, M., (2008). The structure of the Persian Gulf outflow subjected to density variations, *Ocean Sci. Discuss.*, (5) 135-161.
7. Bower, A. S., Hunt, H. D., Price, J. F., (2000). Character and dynamics of the Red Sea and Persian Gulf outflows, *J. Geophys. Res.*, 105(C3), 6387-6414.
8. Brewer P.G., Dryssen, D., 1985. Chemical oceanography of the Persian Gulf. *Progress in Oceanography*, (14) 41-55.
9. Britannica. <http://www.britannica.com> (last update January 2009)
10. Buros, O.K., 1998. The ABCs of Desalting, Second Edition
11. Gary, C., 2006. Desalination in Australia, IDA News, September/October.
12. Ghabayen, S., McKee, M., Kemblowski, M., 2004. Characterization of uncertainties in the operation and economics of the proposed seawater desalination plant in the Gaza Strip, *Desalination* (161) 191-201.
13. Gisser, M., and S. Pohoryles. (1977). Water Shortage in Israel: Long-Run Policy for the Farm Sector. *Water Resources Research* 13 (6): 865-72.
14. Gordon, Jr. D. C., Boudreau, P. R., Mann, K. H., Ong, J.-E., Silvert, W. L., Smith, S. V., Wattayakorn, G. F., Wulff, Yanagi, T., (1996). LOICZ Biogeochemical Modelling Guidelines. LOICZ Reports & Studies No 5, 1-96.
15. Gustavo K., (2007). Hadera 100mcm/year BOT Project, IDA World Congress-Maspalomas, Gran Canaria -Spain October 21-26.
16. Hunter, J.R., (1986). The physical oceanography of the Arabian Gulf: A review and theoretical interpretation of previous observations. In: Halwagy, Clayton, and Bebehabi, eds., *Proceedings of the 1st Gulf Conference on Environment and Pollution*, KISR, Kuwait. (KISR is the Kuwait Institute for Scientific Research), pp. 1-23.
17. http://en.wikipedia.org/wiki/Mediterranean_Sea: (January 2009)
18. <http://www.worldwater.org/data.html> (latest information January 2009).
19. IDA, 2008-09. International Desalination Association Yearbook.
20. IDA, 2006-07. International Desalination Association Yearbook.
21. IDA, 2007-08. International Desalination Association Yearbook.

22. IDA, 2006. IDA Worldwide Desalting Plant Inventory, No. 19 in MS Excel format, Media Analytics Ltd., Oxford, UK.
23. John, V. C., Coles, S. L., Abozed, A. I., (1990). Seasonal cycle of temperature, salinity and water masses of the Western Arabian Gulf, *Oceanol. Acta*, (13) 273-281.
24. Lattemann, S., Höpner, T., (2008). Environmental impact and impact assessment of seawater desalination, *Desalination* (220) 1–15.
25. Magazine - Water Condition & purification, Januray 2005:
26. <http://www.lenntech.com/WHO-EU-water-standards.htm>
27. Masahiro, M., 1995. Managing Water for Peace in the Middle East: Alternative Strategies, United Nations University Press, TOKYO - NEW YORK – PARIS, The United Nations University (ISBN 92-808-0858-3) pp. 319.
28. Mediterranean Sea, (2008). In *Encyclopædia Britannica*. Retrieved June 11, 2008, from Encyclopedia Britannica Online 2009:
29. <http://www.britannica.com/EBchecked/topic/372694/Mediterranean-Sea>
30. Moncef B., Barnier, B., (2000). Seasonal and inter-annual variations in the surface freshwater flux in the Mediterranean Sea from the ECMWF re-analysis project, *Journal of Marine Systems* (24) 343–354.
31. Morcos, S.A., (1970). Physical and chemical oceanography of the Red Sea. *Oceanography Marine Biology Annual Review*, (8) 73–202.
32. Murray, S. P., Johns, W., 1997. Direct observations of seasonal exchange through the Bab El Mandab Strait, *Geophys. Res. Lett.*, (24) 2557-2560.
33. Pankratz, T., 2004. An overview of Seawater Intake Facilities for Seawater Desalination, The Future of Desalination in Texas Vol 2: Biennial Report on Water Desalination, Texas Water Development Board.
34. Raed A.I.B., Kenneth M. P., Magnus L., Mustafa E., (2007). Impact of Brine Disposal from EMU Desalination Plant on Seawater Composition, IDA World Congress-Maspalomas, Gran Canaria –Spain October 21-26.
35. Rahmstorf, S., 1998. Influence of Mediterranean outflow on climate, *EOS Trans.*, AGU 79, (24) 281–282.
36. Rajar, R., Cetina, M., Širca, A., Horvat, M., Žagar, D., (2007). Mass balance of mercury in the Mediterranean Sea. *Marine chemistry* (107) 89–102.20.
37. Red Sea, 2008. In *Encyclopædia Britannica*. Retrieved June 11, 2008, from Encyclopædia Britannica Online: <http://www.britannica.com/EBchecked/topic/494479/Red-Sea>
38. Reynolds, R.M., (1993). Physical oceanography of the Gulf, Strait of Hormuz, and the Gulf of Oman—Results from the Mt Mitchell expedition. *Mar. Pollut. Bull.*, (27) 35–59.
39. Ruiz-Mateo, Antequera, M., Gonzalez, J., (2007). Discharges to the sea from desalination plants. MEDCOAST-07, 13-17 November, Alexandria, Egypt.
40. Sauvet-Goichon, B., (2007). Ashkelon desalination plant-A successful challenge, *Desalination* (203) 75–81.
41. Shahin, M., (1989). Review and assessment of water resources in the Arab region. *Water Int.*, (14) 206–219.
42. Shiklomanov, I., (1999). World Water Resources: Modern assessment and outlook for 21st century. Hydrological Institute, Saint Petersburg.
43. Siedler, G., (1969). General circulation of water masses in the Red Sea, in hot brines and recent heavy metals deposits in the Red Sea, edited by E. T. Degens and D. A. Ross, pp 131-137, Springer Verlage, New York.
44. Taylor, G. I., (1953). Dispersion of soluble matter in solvent slowly flowing through a tube. *Proceedings of the Royal Society of London A*219, 186-203.
45. Thompson, E.F., (1939). Chemical and physical investigations. The exchange of water between the Red Sea and Gulf of Aden over the “sill”. *John Murray Expedition 1933–34 Scientific Report*, vol. 2 (3), pp. 83–103.
46. U.S., 2004. Census Bureau International: Data Base; World Bank. <http://www.census.gov/ipc/www/idb/idbprint.html>
47. Valero, A., Uche, J., Serra, L., 2001. Desalination as an Alternative to Spanish National Hydrology Plan. Technical Report, CIRCE and University of Zaragoza.
48. Vanhems, C., (2001). Critical Review of Desalination Concentrate Disposal to Surface Water, USA, 1992. (After: UNEP, 2001).
49. Wiseman, R., (2006). Editor's corner, *Desal. Water Reuse*, 16 (3) 10–17.
50. Yanagi, T., (2000b). *Coastal Oceanography*. Kluwer Publishers., Dordrecht, 162 pages.

Paper V

Sinuosity effects on Longitudinal Dispersion Coefficient

Bashitalshaaer, R., Bengtsson, L., Larson, M., and Persson, K.M. 2011

Int. J. of Sustainable Water and Environmental Systems, Vol. 2, No. 2 (2011) 77-84

Sinuosity effects on Longitudinal Dispersion Coefficient

Raed Bashitialshaer^{a*}, Lars Bengtsson^a, Magnus Larson^a, Kenneth M. Persson^a

^a*Department of Water Resources Engineering, Lund University, PO Box 118, SE-221 00 Lund, Sweden*

Abstract

A method for reaching longitudinal dispersion coefficient accounting sinuosity effects is suggested. The proposed method was verified using 43 sets of measured field data from previous study were collected from 30 streams and these data were chosen depends on characteristics availability (flow parameters, fluid properties and Sinuosity). Statistical programs namely MINITAB and SPSS were used to derive the relationship between measured longitudinal dispersion coefficient and geometric parameters were used. The new predicted formulas of the longitudinal dispersion coefficient, were correlated with a high coefficient compared to the measured data (i.e. $R^2 = 0.92$ and 0.94) excluding and including sinuosity in the calculations respectively. Comparisons made among 16 other studies of over long period of measured, experimental, and predicted longitudinal dispersion coefficient from different cross-sectional areas (e.g. triangle, rectangular, full and half full circular pipe, parabolic, narrow and deep and, wide and shallow).

The correlation coefficients increased when including irregularities (Sinuosity) term of the natural streams of different cross section in the calculations. Also, the second equation which including sinuosity is more precisely describing the longitudinal dispersion in the rivers and streams. Thus, we strongly prefer and recommend using the second equation for better result than the one not including sinuosity especially for mixing in the case of brine and wastewater discharge. The two results were compared for RMSE (30.1, 24.0, 51.0, 48.9, 90.6, and 70.0) to previous studies e.g. Kashefipour and Falconer (2002), Deng et al. (2001), Seo and Cheong (1998), and Iwasa and Aya (1991) respectively.

Keywords: Longitudinal dispersion coefficient; Flow parameters; Fluid properties; Sinuosity; MINITAB; SPSS; Statistical Analysis.

1. Introduction

1.1. General

The continued mixing of an instantaneously released pollutant is as longitudinal dispersion caused by the non-uniform velocity in the cross section. The common of all flows is that spreading of contaminants in the direction of flow is caused primarily by the velocity profile in the cross section. This spreading causes the shear flow and dispersion into a receiving water and considered as dispersion of dissolved of contaminants flow which can be divided into five categories: 1) Dispersion in laminar shear flow; 2) Dispersion in turbulent shear flow; 3) Dispersion in unsteady shear flow; 4) Dispersion in two dimensions and; 5) Dispersion in unbounded shear flow Fischer et al. (1979). The effects of the cross-sectional shape and velocity distribution on dispersion coefficient have been found by Sooky (1969) assuming a logarithmic velocity profile and power-function velocity profile. He also assumed that the dispersion coefficient increases as the width-to-hydraulic radius ratio increases Sooky (1969). Meredith

and Chris (2007) used an Acoustic Doppler Current Profiler (ADCP) method for estimating the longitudinal dispersion coefficient (D_L) from velocities and bathymetry measured with. They observed that if shear dispersion controls the mixing, the dispersion coefficient can be estimated from measurements of velocity and depth in a cross section. Both the comparison of field data and an analysis with theoretical velocity profiles suggest that the error in (D_L) will be largest when the velocity profile is nearly uniform.

In reality there are three stages in the mixing of an effluent into any receiving water system; 1) initial momentum and buoyancy determine mixing near the outlet, 2) turbulent and currents the receiving water determine further mixing after initial momentum and buoyancy are dispersed and, 3) after cross-sectional mixing is complete, longitudinal dispersion erases longitudinal gradients caused by changes in effluent or recipient discharge Fischer et al. (1979). The term dispersion coefficient expresses the diffusivity of the velocity distribution and is generally known as "Longitudinal dispersion coefficient LDC (D_L) and it's given by:

*Raed Bashitialshaer, Tel.: +46 46 222 4367

Fax: ++46 46 222 4435; E-mail: Raed.Ashaer@tvrl.lth.se

© 2010 International Association for Sharing Knowledge and Sustainability
DOI:10.5383/swes.02.02.002

$$D_L = -\frac{1}{hD} \int_0^h u' \int_0^y \int_0^y u' dy dy dy \quad (1)$$

where D is the molecular diffusion coefficient, the distance between two plates or the depth $h = h(y)$; u' is the deviation of the velocity from the cross-sectional mean velocity

$$u'(y) = u(u) - \bar{u}; \text{ and the mean velocity } \bar{u} = \frac{1}{h} \int_0^h u dy; y$$

is the Cartesian coordinate in the lateral direction and an overbar is used as a cross-sectional average. The net advection balances the transverse diffusion and derived a triple integrals leads to Fischers equation. Fischer et al. (1979) has developed this integral as an expression from the above to the following form for the longitudinal dispersion coefficient as:

$$D_L = -\frac{1}{A} \int_0^B hu' \int_0^y \frac{1}{D_T h} \int_0^y hu' dy dy dy \quad (2)$$

where A = cross-sectional area; B = channel width; and $D_T = D_T(y)$ = local transverse mixing coefficient. Eq. (3) has been employed as the basis of various empirical methods determining the longitudinal dispersion coefficient.

This study is important for understanding mixing for different type of pollutant flow into the water receiving such as rivers and estuaries such as wastewater discharge, denser fluid (brines), and flow from industrial area. The paper will discuss different type of mixing namely vertical mixing, lateral mixing and longitudinal mixing and to distinguish between mixing in straight and irregular channels (sinuous channels). The main part of this study will start with literature preview and previous study mainly for longitudinal dispersion coefficient in straight and in sinuous channels. The discussion covers more than 16 different studies from (Taylor, 1954; Elder, 1959; Fischer, 1966, 1968, 1975; Seo et al. 2008) in which method of dimensional analysis and statistical analysis are used to determine the new equations.

1.2 Characteristics of mixing

Mixing in straight and in irregular channels: The different between the two types, straight and irregular channels is important for mixing behaviour. Mixing is an important phenomenon between two different densities of flow for example the brine discharge is denser than the recipient is so called negatively buoyant. Wastewater discharge is also another problem for mixing and this is called positively buoyant. To have straight channels are not common and usually controlled by a linear zone of weakness in the underlying rock as seen in Figure 1. The velocity of flow also important as the bank closest to the zone of highest velocity is usually eroded and results in a cut-bank in which will be sinuous or irregular behaviour.

The most common definition of sinuosity in rivers and streams can be stated as the ratio of the length measured along the flow (F_L) divided by the length of the channel (C_L) and always greater than one as it appear in Figure 1. The effect of sinuosity is added to the left side of eq. (3) considered as irregularities of the revivers and estuaries.

$$hv' \frac{\partial \bar{c}}{\partial x} + hv' \frac{\partial \bar{c}}{\partial y} = \frac{\partial}{\partial y} h D_T \frac{\partial c'}{\partial y} \quad (3)$$

where c' is the deviation from the mean of local depth mean concentration from the cross-sectional mean concentration. For complete vertical mixing ($v \approx 0$), then eqn. (3) will be reduced to a new equation can be still valid describing the sinuosity.

$$hv' \frac{\partial \bar{c}}{\partial x} = \frac{\partial}{\partial y} h D_T \frac{\partial c'}{\partial y} \quad (4)$$

2. Review of previous studies

Turbulence is important in distributing a tracer along the longitudinal axis, because longitudinal dispersion results primarily from motions of larger scale Fischer (1976) and may causes lateral mixing. In a vertical Mixing and homogeneous pen-channel flow the vertical-mixing coefficient is approximately $\varepsilon_v = 0.07 du_*$ Elder (1959), where d is depth and u_* is the Shear velocity. Transverse mixing in straight, rectangular channels the mixing coefficient $\varepsilon_T \approx 0.15 du_*$ Fischer (1973), but in natural channels much higher values are sometimes observed. Transverse mixing in estuaries is probably caused in part by large-scale horizontal circulations induced by shoreline irregularities and secondary circulations Taylor (1931). The advantage of Fischer et al. (1979) is that the dimensionless dispersion coefficient $D_L/(Hu_*)$ can be estimated from readily available bulk hydraulic variables, width-to-depth ratio B/H , and friction term U/u_* .

The role of non-uniform flow on the longitudinal dispersion (D_L) of pollutants was first investigated by Taylor (1931). He showed that a pipe the D_L was proportion to the shear velocity and the hydraulic radius. Elder (1959) extended Taylor's method for uniform flow in an open channel of infinite width and he derived a dispersion equation assuming that the mixing coefficients for momentum transfer and mass transfer in the vertical direction are the same ($D_L = 5.93 hu_*$) in which h is the depth of flow. Fischer et al. (1975) developed an important formula for estimating the value of the longitudinal dispersion coefficient from the readily measurable hydraulic quantities depth, width, mean velocity, and surface slope, which he structured after the theoretical result of D_L for constant depth channel, Fischer equation can be written as:

$$D_L = 0.011 \left(\frac{U}{u_*} \right)^2 \left(\frac{B}{H} \right)^2 (Hu_*) \quad (5)$$

If the effects of buoyancy, radius of curvature and rotation are neglected then for parabolic channels Smith (1977), $D_L = 0.096 (B^3 U/H)$, where D_L is the longitudinal dispersion coefficient; B is the width or breadth; U is a cross-sectional mean velocity and; H is mean depth. Christensen (1977) arrived at this form of D_L in correcting Liu's (1977) empirical formula by dimensional analysis. In which yield $u_* = \sqrt{(gRS)}$, where g is the gravitational acceleration constant; R hydraulic radius (flow area/wetted perimeter); Φ is the experimental coefficient and can be calculated from the data and but in the equation and S the friction slope ($S \approx \partial h / \partial x \approx \text{bed slope}$).

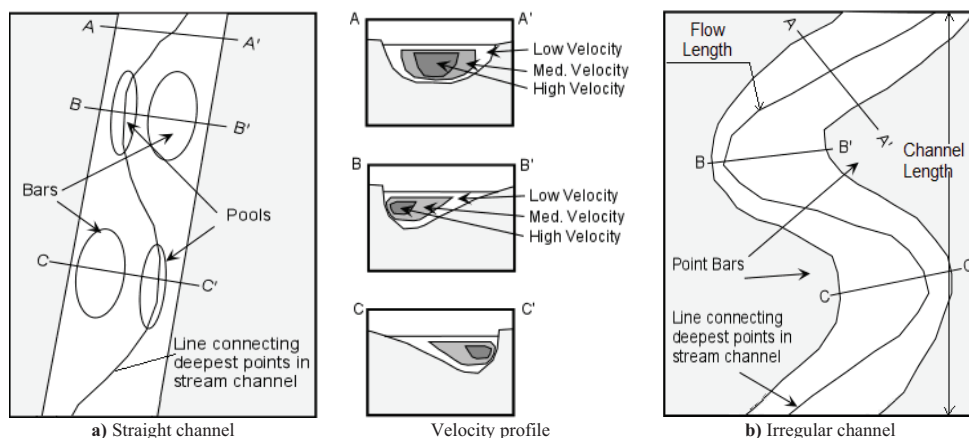


Fig. 1: Straight and irregular channel showing velocity profile (after Earth science)

Abd El-Hadi and Daver (1976) performed experiments in a recirculating flume with different bed roughness simulations, and reported that the dimensionless longitudinal dispersion coefficient is a function of relative roughness height and the relative roughness spacing. They also showed that the relation between longitudinal dispersion coefficient and (hu_*) is nonlinear. Liu (1977) derived a dispersion coefficient equation after Fischer's equation (1966, 1968) taking into account the role of lateral velocity gradient in dispersion in natural streams $D_L = \delta (U^2 B^2 / Hu_*)$. This coefficient δ is considered a parameter which represents a function of the channel cross section shape and the velocity distribution across the stream as in Fischer et al. (1975). He suggests that this parameter can be determined by considering sinuosity, sudden contractions and extractions in a natural stream by least-square fitting to the field data obtained by Godfrey and Frederick (1970) and they obtained at $\delta = 0.18(u_* / U)^{1.5}$.

Iwasa and Aya (1991), they used their laboratory data and previous field data from Nordin and Sabol (1974) and others derived an equation to predict the dispersion coefficient in natural streams and canals. Seo and Cheong (1998) used the one-step Huber method, which is one of the nonlinear multi-regression methods, to derive a new longitudinal dispersion coefficient. Some rivers are shallow and wide, and some are deep and narrow, so, this equation assumed to be valid for local flow depth assuming that the Manning equation could be used to determine relation velocity depth Deng et al. (2001). Deng et al. (2002) derived a new triple integral expression for the longitudinal dispersion coefficient and developed of an analytical method for prediction of this coefficient in natural streams. The proposed method is verified by

using straight manmade canals to sinuous natural rivers. Kashefpour and Falconer (2002) developed an equation for predicting the longitudinal dispersion coefficient in river in-flows, based on 81 sets of measured data, and obtained from 30 rivers in the USA. The best fit of a simple equation they derived was $D_L = 10.612 Hu_* (U/u_*)^2$ with $R^2 = 0.84$, then by trial and error find $[7.428 + 1.775(u_*/U)^{0.572} (B/H)^{0.62}]$ resulting the most appropriate equation as seen in Table 1. Seo and Baek (2004), has developed a theoretical method for predicting the longitudinal dispersion coefficient is developed based on the transverse velocity distribution in natural streams. Equations of the transverse velocity profile for irregular cross sections of the natural streams were analyzed.

Seo et al. (2008) worked for two types of dispersion coefficient tensor for meandering channels were examined. They provided that D_L decreases when local depth of flow (h) increases, while D_T increases. (D_L/hu_*) has relatively uniform distribution, compared to the transverse coefficient (D_T/hu_*) and comes in the ranges from 1.5–4.5, which is less than $(D_L/hu_*) = 5.93$ that Elder 1959, proposed. Table 1 presented several empirical and semi-empirical formulas have been developed to explain the longitudinal dispersion coefficient (D_L) in natural streams, rivers, estuaries, channels and canals. The general form for the longitudinal dispersion coefficient can be written as:

$$D_L = a \left(\frac{U}{u_*} \right)^b \left(\frac{B}{H} \right)^c (S_n)^d (Hu_*) \quad (6)$$

Table 1. Previous study formulas for longitudinal dispersion coefficient following the general form

	Formula\Constant	a	b	c	d
1	Taylor (1954)	10.1 δ	0.0	0.0	0.0
2	Elder (1959)	5.93	0.0	0.0	0.0
3	Parker (1961)	20.2 ϕ	0.0	0.0	0.0
4	Godfrey and Frederick (1970)	0.18	0.5	2.0	0.0
5	McQuivery and Keefer (1974)	0.058 λ	1.0	0.0	0.0
6	Fischer (1975)	0.011	2.0	2.0	0.0
7	Smith (1977)	0.096	1.0	2.0	0.0
8	Christensen (1977)	0.41	0.0	2.0	0.0
9	Liu (1977)	0.18	0.5	2.0	0.0
10	Iwasa and Aya (1991)	2.00	0.0	1.5	0.0
11	Seo and Cheong (1998)	5.92	1.43	0.62	0.0
12	Koussis and Rodriguez-Mirasol (1998)	0.60	0.0	2.0	0.0
13	Magazine et al. (1988)	338 α	-0.63	0.0	0.0
14	Deng et al. (2001)	0.15 ϵ	2.0	1.67	0.0
15	Kashefipour and Falconer (2002)	10.6	2.0	0.0	0.0
16	Seo and Baek (2004)	γ_1, γ_2	2.0	2.0	0.0
	This study: Excluding Sinuosity, D_{L1}	20.95	0.87	0.5	0.0
	Including Sinuosity, D_{L2}	20.95	0.87	0.5	0.3

3. Developing and predicting of a new equation

The longitudinal dispersion coefficient is generally affected by many factors such as flow properties; and channel geometry parameters; and varies within a large range for different sizes and types of channels. The data used for this study were selected from 70 sets in 30 rivers and streams in the USA were all collected from published papers by Tayfur and Singh (2005); Deng et al. (2001, 2002); Meredith & Chris (2007) and; Seo and Cheong (1998). The selection was depending on the availability of their parameters such as geometric, hydraulic and fluid properties especially of sinuosity.

3.1 Method of dimensional analysis

The main factors can influence the dispersion of pollutants in the natural receiving water system were divided into three groups: geometric flow properties, hydraulic flow properties and, fluid flow properties. In which B = channel width; H = mean channel depth; g = acceleration due to gravity; S_f = bed shape factor; S_n = sinuosity and; S = channel slope are considered as geometric flow properties; U = cross-sectional mean velocity; u_* = shear velocity are hydraulic flow properties and; ρ = fluid density and μ = fluid viscosity are the fluid flow properties. Thus, the parameters mentioned above are related to the longitudinal dispersion coefficient and written as:

$$D_L = f_1(\rho, \mu, U, u_*, H, B, S_f, S_n, g, S) \quad (7)$$

Using Buckingham's π -theorem to determine longitudinal dispersion coefficient, a new functional relationship between normalized terms is derived as:

$$\frac{D_L}{HU} = f_2\left(\frac{UH\rho}{\mu}, \frac{U}{\sqrt{gH}}, \frac{U}{u_*}, \frac{B}{H}, S_f, S_n, S\right) \quad (8)$$

where $(UH\rho/\mu)$ = Reynolds number; (U/\sqrt{gH}) = Froude number; (B/H) = width-to-depth ratio; and (U/u_*) = friction term. Bed shape factor, S_f , and sinuosity, S_n , indicate horizontal and longitudinal irregularities, respectively. The terms have been excluded in some study because of collection difficulties in natural streams; therefore the effect of the vertical irregularities can be negligible because it is already included in the friction term. In this study, one solution has been made to determine whether sinuosity for available data sets as stated in equation (9b) or not. For fully

turbulent flow in rough open channels, such as natural streams, the effect of the Reynolds number is also negligible and very small Froude number too ($Fr \ll 0.5$), there was no significant effects from the slope. Thus equation (8) reduces to:

$$\left. \begin{aligned} \frac{D_{L1}}{Hu_*} &= f_3\left(\frac{U}{u_*}, \frac{B}{H}\right) \text{ and} \\ \frac{D_{L2}}{Hu_*} &= f_4\left(\frac{U}{u_*}, \frac{B}{H}, S_n\right) \end{aligned} \right\} \quad (9a,b)$$

In which D_{L1} and D_{L2} are the new predicted longitudinal dispersion coefficient without and with sinuosity. The function was derived from the relation between left and right side in a multi regression of non-linear analyses as:

$$\left. \begin{aligned} \frac{D_{L1}}{Hu_*} &= a\left(\frac{U}{u_*}\right)^b \left(\frac{B}{H}\right) \text{ and} \\ \frac{D_{L2}}{Hu_*} &= a\left(\frac{U}{u_*}\right)^b \left(\frac{B}{H}\right)^c (S_n) \end{aligned} \right\} \quad (10a,b)$$

To be able to derive relationship between longitudinal dispersion coefficient and hydraulic and geometric parameters hypothesizes to a logarithmic function. Taking logarithmic function in both side and considering the normalized longitudinal dispersion coefficient, then equations (10a and b), reduces to:

$$\begin{aligned} \ln\left(\frac{D_{L1}}{HU}\right) &= \ln(a) + b \ln\left(\frac{U}{u_*}\right) + c \ln\left(\frac{B}{H}\right), \text{ and} \\ \ln\left(\frac{D_{L2}}{HU}\right) &= \ln(a) + b \ln\left(\frac{U}{u_*}\right) + c \ln\left(\frac{B}{H}\right) + d \ln(S_n) \end{aligned} \quad (11a,b)$$

The relationships presented here and with the measured data available from previous study were not following normal distribution and found to be lognormal distribution as fitted by MINITAB and SPSS. Plots presented in Figure 2 shows that the non-dimensional measured longitudinal dispersion coefficient appears to have some dependency on the other parameters (e.g. width-to-depth ratio, friction term and sinuosity), even though the data are somewhat scattered in some observations. The non-dimensional longitudinal dispersion coefficient is increasing as width-to-depth ratio and friction term are increasing; and increasing as sinuosity slightly decreasing. In which M is the measured longitudinal dispersion coefficient (LDC).

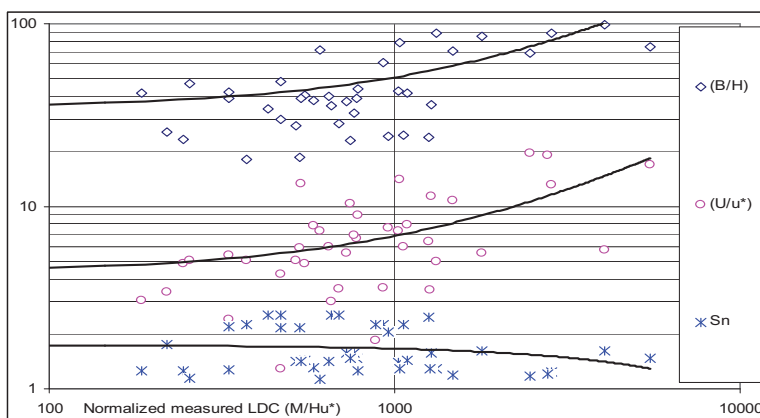


Fig. 2: Plots of normalized measured LDC versus (width-to-depth ratio, friction term and sinuosity)

3.2 Regressions analysis

Regression and statistical analysis has been made between normalized measured longitudinal dispersion coefficients and width-to-depth ratio, friction term and sinuosity in order to establish the best fit relationship. In this study, the form of function from MINITAB and SPSS statistical programs was used to derive this relationship. This method was not the correct one because the data were found to be in a non-linear response. This is because the slope of this line is expressed as the product of two parameters. The results for the new formulas D_{L1} and D_{L2} were compared to the measured longitudinal dispersion coefficient as shown in Figure 3 and 4. The two figures showed very high correlation and good agreement compared to the measured data. In which D_{L1} and D_{L2} or (LDC_1 & LDC_2) are the new predicted longitudinal dispersion coefficient without and with sinuosity as shown below. The new derived formulas without and with sinuosity are written as:

$$\left. \begin{aligned} D_{L1} &= 20.95 \left(\frac{U}{u_*} \right)^{0.87} \left(\frac{B}{H} \right)^{0.5} (Hu_*) \quad \text{and} \\ D_{L2} &= 20.95 \left(\frac{U}{u_*} \right)^{0.87} \left(\frac{B}{H} \right)^{0.5} (S_n)^{0.3} (Hu_*) \end{aligned} \right\} \quad (12a,b)$$

Sinuosity term is added to the second equation to help us in describing the flow and mixing behaviour in estuaries and rivers that is applied to sinuous channels that can show a certain degree of irregularity. In the main time, the flow travels slower than that in straight from one point to another that may also help mixing to take place and longer chance. As the most common definition of sinuosity in rivers and streams, it can be stated that the ratio of the length measured along the flow over the length of the channel.

Figure 5 is the plots of the selected previous study and new formulas compared to the measured longitudinal dispersion coefficient, it is clearly shown that the best result is how close to the measured data. The same way comparisons of predicted and previous study values versus measured longitudinal dispersion coefficient presented in Figure 6. This figure showed good agreement between the new and measured value when compared to previous study as much closer to the measured trend-line. The previous studies presented in the two figures were selected as the best of 16 formulas discussed in this paper.

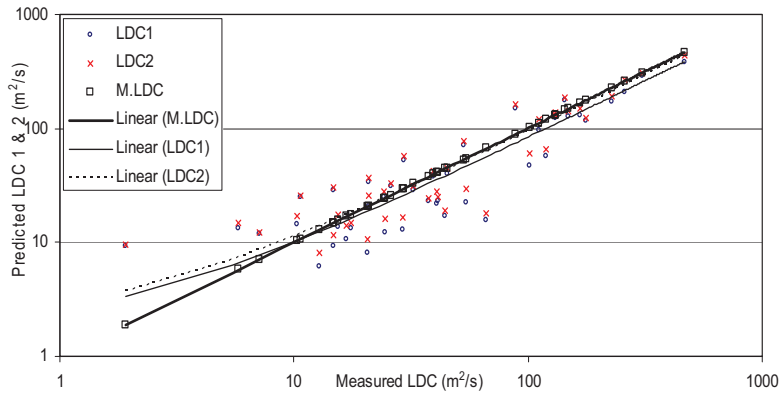


Fig. 3: Predicted results versus measured longitudinal dispersion coefficient (M = Measured longitudinal dispersion coefficient, LDC₁ & LDC₂ = New predicted longitudinal dispersion coefficient without and with sinuosity)

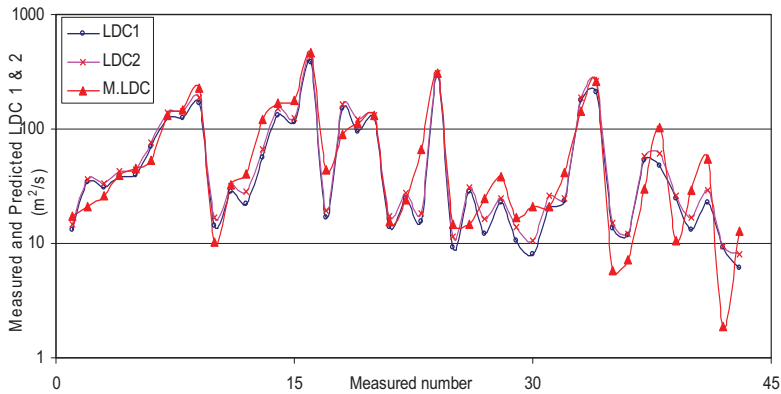


Fig. 4: Predicted results compared to measured longitudinal dispersion coefficient (M = Measured longitudinal dispersion coefficient, LDC₁ & LDC₂ = New predicted longitudinal dispersion coefficient without and with sinuosity)

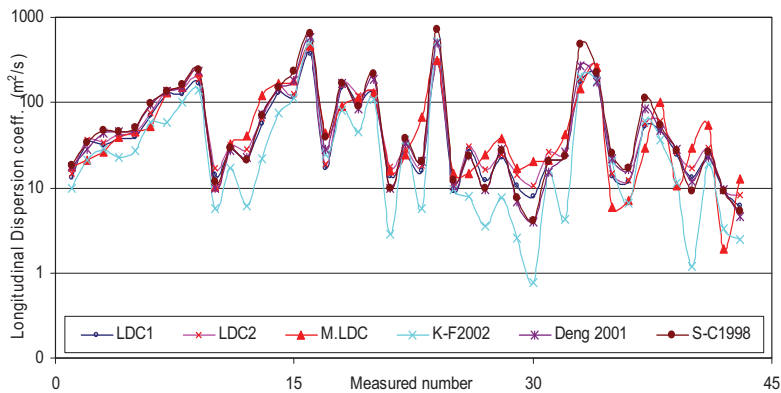


Fig. 5: Predicted formulas and previous study results compared to measured longitudinal dispersion coefficient (M = Measured longitudinal dispersion coefficient, LDC₁ & LDC₂ = New predicted longitudinal dispersion coefficient without and with sinuosity, Kashefipour and Falconer (2002), Deng et al. (2001), Seo and Cheong (1998)

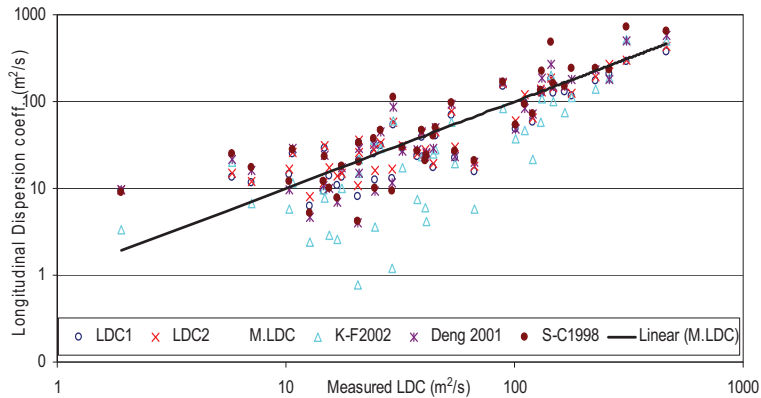


Fig. 6: Comparisons of predicted and previous study results versus measured longitudinal dispersion coefficient (M = Measured longitudinal dispersion coefficient, LDC₁ & LDC₂= New predicted longitudinal dispersion coefficient without and with sinuosity, Kashefipour and Falconer (2002), Deng et al. (2001), Seo and Cheong (1998)

4. Validation & comparison of the predicted equations

Five different types of statistical comparisons made between new results and measured longitudinal dispersion coefficient and the existing study:

1. The root mean square error (RMSE), defined as Dolling and Varas (2002) was computed for each model. In which N = number of observations:

$$RMSE = \sqrt{\frac{\sum_{i=1}^N (D_{L,obs_i} - D_{L,pre_i})^2}{N}}$$

2. There are two approaches: normalize the RMSD to the range of the observed data, or normalize to the mean of the observed data. Normalized root mean squared deviation: The normalized root mean squared deviation or error (NRMSE or NRMSE) is the RMSD divided by the range of observed values, or:

$$NRMSE = \frac{RMSE}{D_{L,max} - D_{L,min}}$$

3. The coefficient of variation (CV) of (RMSE): The CV, or more commonly CV (RMSE), is defined as the RMSD normalized to the mean of the observed values (Montgomery, 2001):

$$Cv, RMSE = \frac{RMSE}{D_{L,ave}}$$

4. The mean of the absolute error (ME) is defined by:

$$ME = \frac{1}{N} \sum_{i=1}^N |DR_i|$$

5. The root mean square (RMS) with this index is written as:

$$RMS = \frac{1}{N} \sqrt{\sum_{i=1}^N (DR_i)^2}$$

where N is the total number of data. To obtain good model predictions, the resulting values for comparisons should be as close as possible, to zero. Therefore, the difference between the calculated values for ME and RMS and zero can help in establishing the relative accuracy of each model in predicting the dispersion coefficient. The adjusted R^2 is the variation of the ordinary R^2 statistic that reflects the number of factors in the model and it is important when we wish to evaluate the impact of increasing or decreasing the number of model terms (Montgomery, 2001). Different results are compared and presented in Table 2.

Table 2. Comparison of the new formulas among selected previous study using different statistical methods

Statistical quantities	LDC ₁ D _{L1}	LDC ₂ D _{L2}	K-F 2002	Deng 2001	S-C 1998	I-A 1991
R²	0.923	0.936	0.809	0.870	0.778	0.561
R²adj.	0.921	0.933	0.804	0.866	0.772	0.550
corr	0.961	0.967	0.899	0.933	0.882	0.749
mean	66.3	74.7	60.9	85.8	102.6	53.6
max	378.7	432.8	512.3	577.2	723.1	203.1
min	6.2	8.1	0.8	4.0	4.2	3.6
RMSE	30.1	24.0	51.0	48.9	90.6	70.0
NRMSE	0.081	0.056	0.100	0.085	0.126	0.351
CV	0.45	0.32	0.84	0.57	0.88	1.31

5. Conclusions

Verifying the new predicted longitudinal dispersion equations (LDC), five different types of statistical comparisons were used. The final results and comparisons clearly shown in Table 1 and 3 as well as in Figure 3-6 with higher accuracy for the predicted value among selected study and measured longitudinal dispersion coefficient. The new formulas were correlated with the measured sets (i.e. $R^2 = 0.92$ and 0.94) when excluding and including sinuosity term respectively. The two results were compared for RMSE (30.1, 24.0, 51.0, 48.9, 90.6, and 70.0) to previous studies e.g. Kashefipour and Falconer (2002), Deng et al. (2001), Seo and Cheong (1998), and Iwasa and Aya (1991). These results mean that the correlation coefficients increased due including irregularities (Sinuosity) term of the natural streams of different cross section in the calculations. The second equation which including sinuosity is more precisely describing the longitudinal dispersion in the rivers and streams. Thus, we strongly prefer and recommend using the second equation for better result than the one not including sinuosity especially for mixing in the case of brine and wastewater discharge. In this study the accuracy of normal and adjusted R^2 were both increased when adding sinuosity term, it improves the accuracy by amount of 2%. The proposed methodology performs better than all previous study over long period for longitudinal dispersion coefficient from different cross-sectional areas (e.g. triangle, rectangular, full and half full circular pipe, parabolic, narrow and deep and, wide and shallow). These formulas were tested and fitted smoothly for larger data size, it was much better than the existing study.

References

- [1] Abd El-Hadi, N. D. and Daver, K. S. (1976), "Longitudinal dispersion for flow over rough beds." *J. Hydr. Div. (ASCE)*, 102(4), 483–498.
- [2] Christensen, B. A. (1977). "Discussion of predicting dispersion coefficients of streams, by H. Liu." *J. Env. Eng. Div., ASCE*, 103(6), 1144–1146.
- [3] Deng, Z.-Q., Singh, V. P., and Bengtsson, L. (2001). "Longitudinal dispersion coefficient in straight rivers." *J. Hydraul. Eng.*, 127(11), 919–927.
- [4] Deng, Z.-Q., Bengtsson, L., Singh, V. P. and Adrian, D. D. (2002). "Longitudinal Dispersion Coefficient in Single-Channel Streams." *J. Hydraul. Eng.*, 128(10), 901–916.
- [5] Dolling, O. R., and Varas, E. A. (2002). "Artificial neural networks for streamflow prediction." *J. Mater. Sci. Technol.*, 40(5), 547–554.
- [6] Earth science: (updated Jan. 2010) http://earthsci.org/flood/J_Flood04/stream/stream.html.
- [7] Elder, J. W. (1959). "The dispersion of a marked fluid in turbulent shear flow." *J. Fluid Mech.*, 5(4), 544–560.
- [8] Fischer, B. H. (1966). "Longitudinal dispersion in laboratory and natural streams." Rep. KH-R-12, Keck Lab. of Hydr. and Water Resour. California Institute of Technology, Pasadena, Calif.
- [9] Fischer, B. H. (1968). "Dispersion predictions in streams." *J. Sanit. Eng. Div. ASCE*, 94(5), 927–943.
- [10] Fischer, H. B. (1973), "Longitudinal dispersion and turbulent mixing in open-channel flow." *Ann. Rev. Fluid Mech.* (5): 59-78.
- [11] Fischer, B. H. (1975). "Discussion of 'Simple method for predicting dispersion in streams,' by R. S. McQuivey and T. N. Keefe." *J. Environ. Eng. Div. (Am. Soc. Civ. Eng.)*, 101(3), 453–455.
- [12] Fischer H. B. (1976), "Mixing and Dispersion in Estuaries." *Rev. Fluid Mech.* 1976.8:107-133.
- [13] Fischer, H. B., List, E. J., Koh, R. C. Y., Imberger, J., and Brooks, N. H. (1979). "Mixing in inland and coastal waters." Academic, New York.
- [14] Godfrey, R. G. and Frederick, B. J. (1970), "Stream dispersion at selected sites." U.S. Geological Survey Prof. Paper 433-K, Washington, D.C.
- [15] Iwasa, Y., and Aya, S. (1991). "Predicting longitudinal dispersion coefficient in open-channel flows." *Proc., Int. Symp. on Environmental Hydrology*, Hong Kong, 505–510.
- [16] Kashefipour, S. M. and Falconer, R. A., (2002). "Longitudinal dispersion coefficients in natural streams", *Water Research*, 36, 1596-1608.
- [17] Koussis, A. D. and Rodriguez-Mirasol, J. (1998). "Hydraulic estimation of dispersion coefficient for streams." *J. Hydr. Engrg., ASCE*, 124(3), 317–320.
- [18] Liu, H. (1977). "Predicting dispersion coefficients of streams, by H. Liu." *J. Env. Eng. Div., ASCE*, 103(1), 59–69.
- [19] Magazine, M. K, Pathak, S. K., and Pande, P. K. (1988). "Effect of bed and side roughness on dispersion in open channels." *J. Hydraul. Eng.*, 114(7), 766–782.
- [20] McQuivey, R. S., and Keefe, T. N. (1974). "Simple method for predicting dispersion in streams." *J. Environ. Eng. Div. (ASCE)*, 100(4), 997–1011.
- [21] Meredith, L. C. and Chris, R. R. (2007). "Measuring the Dispersion Coefficient with Acoustic Doppler Current Profilers." *J. Hydraul. Eng.*, 133(8), 977–982.
- [22] Montgomery D. C. (2001), "Design and Analysis of Experiments" 5th edition. Wiley, New York.
- [23] Nordin, C. F. and Sabol, G. V. (1974), "Empirical data on longitudinal dispersion in rivers." U.S. Geological Survey of Water Resources Investigation 20-74, Washington, D.C.
- [24] Parker, F. L. (1961). "Eddy diffusion in reservoirs and pipelines." *J. Hydr. Div., ASCE*, 87(3), 151–171.
- [25] Seo, I. W., and Cheong, T. S. (1998). "Predicting longitudinal dispersion coefficient in natural streams." *J. Hydr. Engrg., ASCE*, 124(1), 25–32.
- [26] Seo, I. W., and Baek, K. O. (2004). "Estimation of the longitudinal dispersion coefficient using the velocity profile in natural streams." *J. Hydraul. Eng.*, 130(3), 227–236.
- [27] Seo, I. W. Myung, E. L., and Kyong, O. B. (2008). "2D Modeling of Heterogeneous Dispersion in Meandering Channels." *J. Hydr. Engrg., ASCE*, 134(2), 196–204.
- [28] Smith R., "Long-term dispersion of contaminants in small estuaries." *J. Fluid Mech.*, 82 (1977) 129–146.
- [29] Sooky, A. A. (1969). "Longitudinal dispersion in open channels." *J. Hydr. Div., Am. Soc. Civ. Eng.*, 95(4), 1327–1346.
- [30] Tayfur, G. and Singh, V. P. (2005). "Predicting Longitudinal Dispersion Coefficient in Natural Streams by Artificial Neural Network." *J. Hydraul. Eng.*, 131(11), 991–1000.
- [31] Taylor, G. I. (1931), "Internal waves and turbulence in a fluid of variable density." *Rapp. P.-V. Rbun. Con. Int. Explor. Mer* 76:35-42; 1960. *Sci. Pap.* 2:240-46. London: Cambridge Univ. Press.
- [32] Taylor, G. I. (1954). "The dispersion of matter in turbulent flow through a pipe." *Proc. R. Soc. London, Ser. A*, 223, 446–468.

Notation

A	= cross-sectional area of river channel;	P	= generalized roughness parameter;
B	= channel width;	r	= tube radius;
b	= exponent of flow depth in generalized local velocity equation;	R	= hydraulic radius;
C	= cross-sectional average concentration;	Re	= Reynolds number
C'	= deviation of local depth mean concentration from cross-sectional mean;	RMSE	root mean square error;
C ₀	= cross-sectional average concentration at x = 0;	RMSD	root mean square deviation;
\bar{C}	= time-averaged concentration;	RMS	= root mean square;
D	= molecular diffusion coefficient;	S	= channel slope;
D _L	= longitudinal dispersion coefficient (LDC);	S76	= D _L in Smith (1977);
D _T	= transverse dispersion coefficient (TDC);	S-C98 D _L	in Seo and Cheong (1998);
D1	= D _L in equation. (3a);	S _f	= friction slope;
D2	= D _L in equation. (3b);	S _a	= channel longitudinal sinuosity;
D01	= D _L Deng et al. (2001);	T	= time;
DR	= discrepancy ratio;	U	= cross-sectional mean velocity;
Fr	= Froude's number;	u'	= vertical deviations with respect to depth-averaged velocity u;
F75	= D _L in Fischer et al. (1975);	u _*	= shear velocity;
g	= acceleration of gravity;	\bar{u}	= time average velocity;
H	= sectional average flow depth;	x, y	= horizontal Cartesian coordinate;
h	= local depth of flow;	Y2a01 D _L	equation 2a in Yanagi (2001);
I	= non-dimensional triple integral;	z	= vertical coordinate;
I-A91 D _L	in Iwasa and Aya (1991);	β	= channel shape parameter;
K-F02 D _L	in Kashefpour and Falconer (2002);	δ	= channel cross section shape and velocity distribution across the stream;
K-R98 D _L	in Koussis and Rodriguez (1998);	ε	= cross-sectional mixing coefficient;
L	= distance from bend apex to exit measured along meander path;	ε _T	= turbulent diffusion coefficient;
L _m	= meander wave length;	ε _V	= the vertical diffusivity;
L77	= D _L in Liu's (1977);	ε _h	= the horizontal diffusivity;
M	= Measured longitudinal dispersion coefficient;	Φ	= correction factor;
ME	= mean absolute error;	γ	= correction factor;
N	= number of observations;	τ	= shear stress;
n	= Manning's coefficient;	ρ	= fluid density;
NRMSE	normalized root mean square error;	μ	= fluid viscosity

Paper VI

Worldwide oil prize, desalination and population growth correlation study

Bashithalshaaer, R., and Persson K.M. 2009

VATTEN (65): 37-46

WORLDWIDE OIL PRIZE, DESALINATION AND POPULATION GROWTH CORRELATION STUDY

by RAED A.I. BASHITALSHAAER¹ and KENNETH M PERSSON²
Water Resources Engineering-LTH, Lund University; Box 118, SE 221 00 Lund
1 e-mail: Raed.Alshaaer@tvrl.lth.se
2 SWECO VIAK AB, PO Box 286, SE 201 22 Malmö
e-mail: Kenneth_M.persson@tvrl.lth.se; Kenneth.m.persson@sweco.se



Abstract

In this paper, the investment in new desalination capacity, expressed as daily production capacity, was studied as a function of oil production and population increase for a large group of countries for the last 25 years. These countries were selected for their large desalination production and Sweden presented as reference. Oil production correlated well with investments in new desalination capacity. On a yearly basis, the correlation was about 78 %, but taking into account the time needed from investment decision to inauguration of new desalination plants, the correlation increased. The world oil production two years prior inauguration correlated to 88 % with new world desalination capacity during the entire study time.

The total population for the studied countries was compared to the world population. In 1950, about 69 % of world population lived in the chosen countries, decreasing to 63 % in the year 2008 and according to population prognosis continues to decrease to 56 % in the year 2050 with occupied area of about 52 %. The total desalination capacities of these countries are slightly increased from 88 to 92 % in 1996 and 2008 respectively, and decreased to 90 % at 2050.

Increased desalination capacity means increased energy demand. To a large extent, the energy costs are site specific as are the costs of labour and capital, but the reported water price was about 2.5 US \$/m³ desalinated water until the 1980s, decreasing to roughly US \$1.5/m³ in the early 1990s and to about \$0.50/m³ in the late 2003.

Key words – Seawater Desalination and Capacity; Oil Production; Population; Recovery Ratio; Brine Discharge; Salinity

1. Introduction

1.1. General

The main objectives of this study was to find the relationships between desalination plant projects, amount of water resources and population for the oil production and price. Three major questions will be considered for the study countries and globally in this work: Which are the driving forces for the investments in desalination plant projects? What is the percentage of fresh water produced by desalination over renewable water resources? Where is the most growth in population, desalination and oil production?

This paper has been written for evaluation three major parameters (population, oil production and renewable water resources) as driving forces for desalination

projects. The oil productions have good correlation to increasing fresh water from desalination. There have been found good relation between growth in population and oil production countries e.g. Saudi Arabia, United Arab Emirates, Kuwait and Qatar.

Desalination is an important method for producing potable water in the world. Usually a country is considered to risk water shortage if renewable water resources are below 1000 m³/capita/yr (Al-Gobaisi, 1997). Desalination is a quickly growing technology, not the least visual through the large number of regional and international organizations established during the last 30 years (the International Desalination Association (IDA), the Australian Desalination Association, the European Desalination Association (EDS), the Southeast Asian Desalination Association, the American Desalination

Association, and the Middle East Desalination Research Center (MEDRC) (Cooley, et al, 2006)). Desalination has been a freshwater supply opportunity for a long time, especially at remote locations and, especially, on naval ships at sea site. A British patent was granted for such a device in 1852 (Simon, 1998). The island of Curaçao in the Netherlands Antilles has had desalination plants in operation since 1928. A major seawater desalination plant was built in 1938 in what is now Saudi Arabia and an early version of a modern distillation plant was built in Kuwait in the early 1960s (Cooley, et al., 2006).

Desalination is an important source of fresh water in parts of the arid Middle East (e.g. Saudi Arabia, United Arab Emirates, Oman, Qatar and Kuwait etc.), along the shores of the Persian Gulf/Arabian Gulf, Red Sea, Mediterranean Sea, in North Africa, on the Caribbean islands, and other locations where the amount of renewable fresh water is insufficient for the population. Thus, in order to meet the demand where traditional water-supply options or transfers from elsewhere are considered as uneconomical, desalination capacity must increase. The concept of desalination refers to a wide range of processes designed to remove salts from waters of different salinities as collected from different areas see Table 1. All major water sources can be utilized as raw water supply for desalination, except the Dead Sea. Salinity affects the efficiency and the economy of the desalination plants: the more saline raw water sources, the costlier is the production.

1.2. Desalination and energy

The amount of water in the hydrosphere is approximately estimated to be about 1,400 Mkm³, 95.5 % of which is saltwater present in oceans and seas, and the rest 4.5 %, is fresh water (Ruiz et al., 2007). Desalination plants production percentage as function of their raw water sources are shown in Table 2. The difference

Table 1. *Salt concentrations of different world water sources (OTV, 1999; Gleick, 1993; and Magazine, 2005).*

Water source or type	Concentration (g/l, ppt)
Brackish waters	0.5 to 3
North Sea (near estuaries)	21
Gulf of Mexico and coastal waters	23 to 33
Atlantic Ocean	35
Pacific Ocean	38
Persian Gulf/Arabian Gulf	45
Mediterranean Sea	38.6
Red Sea	41
Dead Sea	~300

found in the two references is due to different years of finding this percentage in which 2008–09 is the most recent and accurate values. The installed capacity by technology is as follows: reverse osmosis (RO) 60 %, multi-stage flash evaporation (MSF) 28 %, multi-effect distillation (MED) 9 %, and electrodialysis (ED) 4 % (GWI Desalination data IDA 2008–09).

The specific energy need for desalination of seawater reverse osmosis (SWRO) has decreased with the development of energy reuse systems. At present, 1 cubic meter of desalinated water consumes 3.7 kWh of energy, mainly electricity (Gary, 2006). Although the investment and operational costs of desalination plants depend on where they are located, total production costs decreased from roughly \$2.5/m³ in the late 1970s to \$1.5/m³ in the early 1990s to around \$0.50/m³ 2003 (Pankratz, 2004). The total primary energy supply for desalination by source was in 2002 as follows: Oil 35.8 %, coal 23.0 %, gas 20.9 %, combustible, renewable and waste 10.8 %, nuclear 6.8 %, hydro 2.2 %, geothermal/solar/wind 0.5 % (IEA, 2005). Desalination relies heavily on fossil fuels.

The world average renewable hydrological resources (not considering desalted and reused waters) are about 42,750km³/yr, or 1 % the total volume of superficial waters (fresh or salt). Only six countries host 50 % of the renewable water resources (i.e. Brazil, Canada, Russia, United States, China and India). Five great rivers discharge 27 % of these renewable resources to the sea (Amazon, Ganges-Brahmaputra, Congo, Yellow and Orinoco) (Ruiz et al., 2007 and Valero et al., 2001).

2. Desalination types comparisons

2.1. Desalination and technologies used

There is no single best method for desalination. Feasibility studies should always be executed according to local conditions such as site-specifications, raw water salt con-

Table 2. *Distribution of global desalination capacity by source water.*

Water source	Worldwide installed capacity, %	
	Wangnick/GWI (2005)	GWIDesalination data IDA (2008–09)
Seawater	56	62
Brackish	24	19
River	9	8
Waste water	6	5
Pure	5	5
Brine	<1	

Table 3. Comparison of reverse osmosis (RO) versus thermal multi-stage flash (MSF) in seawater desalination (MEDRC 2002; Lattemann and Höpner).

Properties	Reverse Osmosis (RO)	Multi-Stage Flash (MSF)
Raw water salinity	Up to 65–85 g/L.	About 50 g/L.
Temperature	Approximately ambient seawater temperature.	+5 to 15°C above ambient.
Plume density	Negatively buoyant brine discharge.	Positively, neutrally or negatively buoyant depending on the process of brine mixing.
Chlorine	If chlorine is used to control biofouling, these are typically neutralized before the water enters the membranes to prevent membrane damage.	Approx. 10–25 % of source water feed dosage, if not neutralized.
Cleaning chemicals	Alkaline (pH 11–12) or acidic (pH 2–3) solutions with additives such as: detergents (e.g. dodecylsulfate), oxidants (e.g. sodium perborate), biocides (e.g. formaldehyde).	Acidic (pH 2) solution containing corrosion inhibitors such as benzotriazole derivatives.

centration, economics, the quality of water needed, and local engineering experience and skills (Cooley et al., 2006). There are three types of desalination methods used throughout the world for a wide range of purposes, but mainly for potable water production for domestic and municipal use.

- a. *Membrane Systems*: Reverse osmosis (RO) or Electrodialysis and Electrodialysis Reversal (ED) (Heberer et al., 2001; Sedlak and Pinkston 2001 and NAS, 2004).
- b. *Thermal Processes* (TP): Multi-Stage Flash Distillation (MSF) Multiple-Effect Distillation (MED), and Vapor Compression (VC) (Birkett, 1999 and Wangnick/GWI, 2005).
- c. *Other Desalination Processes*: Different types of water can be desalinated through many other processes including small-scale ion-exchange resins, freezing, and membrane distillation (MD) (Wangnick/GWI, 2005).

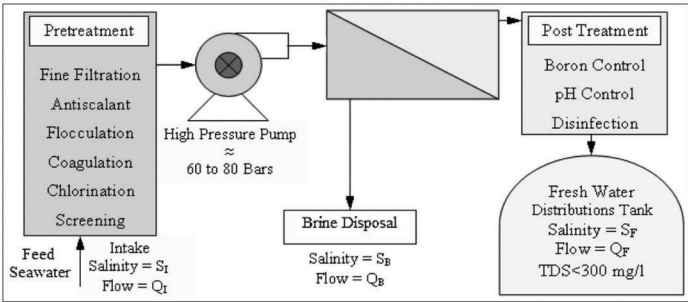
At the beginning of the 1970s, the number of installed reverse osmosis plants grew; these systems have some advantages and some disadvantages compared to thermal systems. Thermal desalination systems produce water

quality of less than 25 parts per million (ppm) as total dissolved solids (TDS) compared to membrane systems of less than 500 ppm, TDS (USBR, 2003). Some of the advantages and disadvantages are presented in Table 3 as a difference between reverse osmosis (RO) and multi-stage flash (MSF).

2.2. Input/Output scheme

There are generally three different types of water flows in a desalination plant: freshwater production Q_F , brine discharge Q_{Brine} , and seawater intake Q_{Intake} , see Figure 1, in which a reverse osmosis system is used for seawater desalination plant. Pre and post treatment processes are also described including some process. S_{Intake} and Q_{Intake} are salinity and volume flux flow of seawater intake, S_{Brine} and Q_{Brine} are salinity and volume flux flow of brine discharge and S_F and Q_F are salinity and volume flux flow of fresh water produced by the desalination plant. From this, $S_{Brine} = S_{Intake}/(1-r)$ and $Q_{Brine} = (1-r)Q_{Intake}$, where r is the recovery ratio, the freshwater yield, typically in the order of 35 to 45% of the intake. Further on, $S_F \approx 0$ and $Q_F = rQ_{Intake}$.

Fig. 1. Reverse osmosis seawater desalination plant typical scheme showing input/output and different stages of treatment.



During the last ten years of desalination development, the recovery ratio r has increased significantly in reverse osmosis plants. For example from Al Shaaer et al., 2007, if seawater intake salinity, S_{Intake} is equal to 41.7 ppt, and the brine directly front of output pipeline is equal to 74 ppt, then as $S_{\text{Brine}} = S_{\text{Intake}}/(1-r)$, the recovery ratio $r = 44\%$.

3. Methodology and data collection

In this study, 36 countries were identified hosting respectively about 88, 92 and 90% of all desalination capacity of the world total capacity at years 1996, 2008 and predicted 2050 see Table 4. Sweden is also included in this study for comparison. The largest desalination

Table 4. Comparison between world and major desalination capacities producers for 1996, 2008 and predicted values 2050 and population in three years.

Country/area	Desalination capacity (Q_F) in 1000 m ³ /day			Population in 10 ⁶		
	Observed		Predicted	Observed		Predicted
	1996	2008	2050	1950	2008	2050
World	20000	47709	192211	2555.9	6677.6	9392.8
Algeria	190.8	1055.9	3044.1	8.89	33.77	44.16
Australia	82.1	587.1	1577.4	8.27	20.60	24.18
Bahrain	283.0	825.2	3022.0	0.115	0.718	0.973
Chile	83.5	260.8	926.7	6.091	16.454	19.387
China	42.0	1092.5	2402.6	562.6	1330.0	1424.2
Egypt	102.1	491.1	1479.6	21.20	81.71	127.56
France	29.1	230.3	603.7	42.52	64.06	69.77
Germany	96.0	356.7	1179.8	68.37	82.37	73.61
India	115.5	771.3	2108.8	369.9	1148.0	1807.9
Indonesia	103.2	242.8	985.2	82.98	237.51	313.02
Iran	423.4	547.8	3138.2	16.36	65.88	81.49
Iraq	324.5	476.6	2519.3	5.163	28.221	56.361
Israel	90.4	630.1	1703.6	1.286	7.112	10.828
Italy	483.7	824.3	3984.7	47.11	58.15	50.39
Japan	637.9	1487.6	6061.8	83.81	127.29	93.67
Kazakhstan	167.4	254.6	1317.3	6.693	15.341	15.100
Korea (South)	266.0	995.8	3283.9	20.85	49.23	45.22
Kuwait	1284.3	2308.7	10822.1	0.145	2.597	6.375
Libya	638.4	940.0	4961.1	0.961	6.17	10.82
Malta	145.0	248.4	1197.3	0.312	0.404	0.396
Mexico	105.1	336.4	1182.9	28.49	110.0	147.9
Netherlands	110.4	251.3	1036.9	10.11	16.65	17.33
Oman	180.6	582.7	2041.7	0.489	3.312	8.359
Qatar	560.8	1026.3	4761.9	0.025	0.929	1.239
Russia	116.1	244.2	1049.9	101.94	140.70	109.19
Saudi Arabia	5006.2	7750.8	39669.3	3.860	28.161	49.707
Singapore	133.7	512.1	1674.0	1.022	4.608	4.635
South Africa	79.5	104.2	592.0	13.596	43.786	33.003
Spain	492.8	3420.7	9258.7	28.063	40.491	35.564
Sweden	1.30	3.812	13.93	7.014	9.045	9.085
Taiwan	101.2	638.3	1771.9	7.981	22.921	20.161
Tunisia	47.4	98.8	426.7	3.517	10.384	12.512
Turkmenistan	43.7	165.8	543.9	1.204	5.180	7.592
UAE	2134.2	6094.7	22532.6	0.072	4.621	8.019
UK	101.4	442.2	1378.0	50.127	60.944	63.977
USA	2799.0	7525.1	28608.4	152.27	303.82	420.08
Sub Total	17602	43825	172862	1763	4181	5224
Percentage, %	88	92	90	69	63	56

Data based on: (U.S. Census Bureau; World Bank 2004; <http://www.worldwater.org/data.html>; Ghabayen et al., 2004; IDA, 2006; IDA, year book 2006–07 and 2007–08; Wiseman, 2006 and Lattemann and T. Höpner, 2008).

capacity is found in Saudi Arabia, with a daily capacity of about 5, 7.75 and 39.7 million cubic meters in 1996, 2008 and predicted 2050 respectively.

Desalination capacity were compared for world and major producing countries, until the beginning of the years 1996 and 2008 and prediction for the year 2050, including population and land area. The prediction for desalination capacity has been obtained by extrapolating the trendline of world desalination data from 1960 to 2008 as the best fit. The trendline was developed by some trials until matching with second degree polynomial and that was used for prediction of year 2050 desalination production globally and each country. Daily oil production and average cost per barrel were used from 1983 to 2008; it was 30.5 dollars per barrel in 1983, the yearly average was 30.6 and in 2008, the oil prize reached a maximum of 134 and an average of 109.6 US dollars per barrel (online from: Energy Information Administration).

From Table 4 it is clear that the population growth in the selected 36 countries will be slower than in the rest of the world. In 1950, about 69% of the world population lived in the selected countries. In 2008, the share had decreased to 63% and in the year 2050, it is estimated to be 56% of world population. With respect to land area, the 36 selected countries represent slightly more than half of the global total land area (52%).

The population used in this study is the data of 1950, 2008 and 2050 prognosis were obtained from U.S. Census Bureau, International: Data Base. The population increase over the 100 year period is about 7 billions people, which is very high relative to desalination and oil production in the whole world. The US Census Bureau growth rate has been used. The population growth rate is calculated using the formula:

$$R(t) = \ln [P(t+1) / P(t)] \text{ where } t = \text{year}; R(t) = \text{growth rate from midyear } t \text{ to midyear } t+1; P(t) = \text{population at midyear } t \text{ and } \ln = \text{natural log (U.S. Census Bureau, 2008)}.$$

Figure 2 is the logarithmic graph and alphabetic order, that shows the world major desalination countries producers to the left side for 1996, 2008 and predicted values for year 2050 and to the right side the amount per capita per year as found to be in 2050. Fresh water produced by seawater desalination is quite close to the world water standard as cubic meters per capita per year. It has been found in year 2050 with the same development the result in Saudi Arabia, United Arab Emirates, Kuwait, Qatar and Bahrain will be 189.3, 666.7, 402.8, 911.7 and 736.5 m³/capita/yr respectively.

4. Results and discussions

The arid Middle East is also the main oil field of the world country producers as they are also the most important desalination producers in the chosen countries. In Table 5, the world desalination capacity is presented with oil production and cumulative oil cost for the years 1983–2008. Oil data available from 1983 until 2008 are compared with the same period of desalination and population in the world and study countries. Capital intensive desalination projects need financing. Freshwater supply is fundamental for the welfare of people, together with wastewater treatment, safe food production and industrial works. Also, water supply needs to follow population growth. Countries with proportionally higher population growth ratios may face larger challenges to tackle water scarcity and increasing oil cost.

The daily oil production and its cost, daily desalination capacity and population increases could be analyzed and compared for the last 25 years. The correlation between daily oil production and its cost and the desalination capacity was clear, see Figure 3. World daily desalination capacity as a function of daily costs for oil correlated to about 78% if the same year of oil production and cost correlated with desalination capacity (Y0) and even better when the desalination capacity was superim-

Fig. 2. Major desalination countries producers and amount per capita per year for 1996, 2008 and prediction for the year 2050.

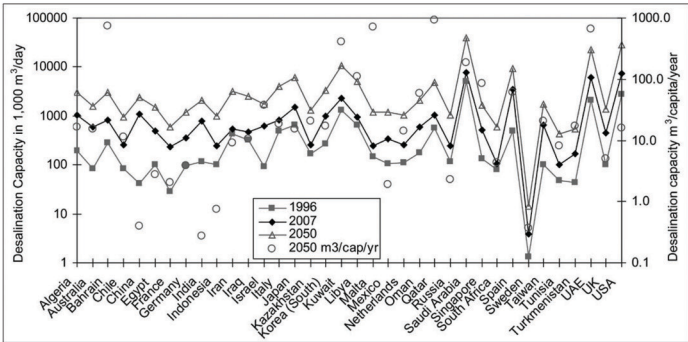


Table 5. World desalination capacity, oil cost and production and yearly population increases from the years 1983 to 2008 (online from: Energy Information Administration)

Year	Population (Millions)	Cumulative Population Increments (Millions)	Yearly oil average cost (US \$/Barrel)	Oil daily production (Million Barrels/day)	Cumulative Oil cost (Billions US \$/day)	Cumulative Desalination capacity (MCM/day)
1983	4690.9	82	30.6	53.3	1.6	1.4
1984	4771.1	162	29.4	54.5	3.2	2.4
1985	4852.6	243	27.9	54.0	4.7	3.5
1986	4936.0	327	15.0	56.2	5.6	4.5
1987	5022.0	413	19.1	56.6	6.7	5.2
1988	5108.5	499	16.0	58.7	7.6	6.5
1989	5194.9	586	19.6	59.8	8.8	7.2
1990	5282.4	673	24.5	60.5	10.3	8.1
1991	5365.7	757	21.5	60.2	11.6	8.7
1992	5448.7	840	20.7	60.1	12.8	9.7
1993	5530.0	921	18.5	60.2	13.9	10.6
1994	5610.1	1001	17.2	61.1	15.0	11.5
1995	5691.0	1082	18.4	62.4	16.1	12.6
1996	5771.4	1162	22.0	63.8	17.5	14.1
1997	5850.8	1242	20.6	65.7	18.9	15.7
1998	5929.7	1321	14.4	67.0	19.8	17.3
1999	6007.5	1398	19.2	65.9	21.1	18.4
2000	6084.9	1476	30.2	68.5	23.2	20.0
2001	6162.3	1553	25.9	68.1	24.9	21.8
2002	6238.8	1630	26.1	67.2	26.7	25.0
2003	6315.2	1706	31.0	69.4	28.8	27.1
2004	6392.4	1783	41.4	72.5	31.8	30.6
2005	6470.3	1861	56.6	73.7	36.0	33.2
2006	6548.7	1940	66.2	73.4	40.9	36.4
2007	6627.5	2018	72.3	73.0	46.1	41.1
2008	6707.0	2098	100	73.7	53.5	46.7

posed 1 year after the year of oil production and cost (Y1: 86 %) and slightly better when superimposed 2 years (Y2: 88 %). In other words, one important driving force for investments in building a new desalination plant projects seems to be incomes from oil. This correlation could help us to make prognosis for new projects related to the fresh

water supply in the oil producing countries, as for example Saudi Arabia and Qatar.

In Figure 4, the increase in world population is correlated with the daily oil production and cost for the last 25 years (data from Table 5). The correlation is equal to 81 % between population and oil cost namely. The annual

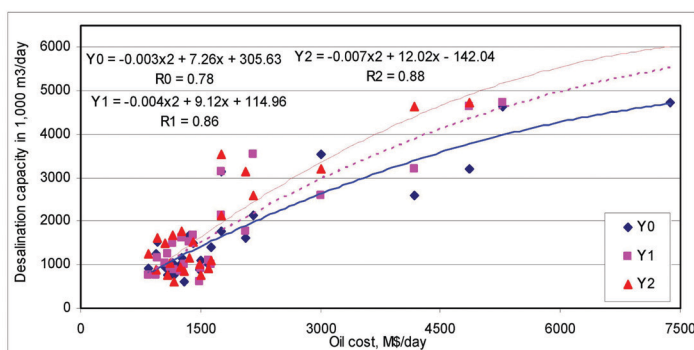


Fig. 3. World daily desalination capacity versus world daily oil costs

Fig. 4. World population versus world daily oil costs

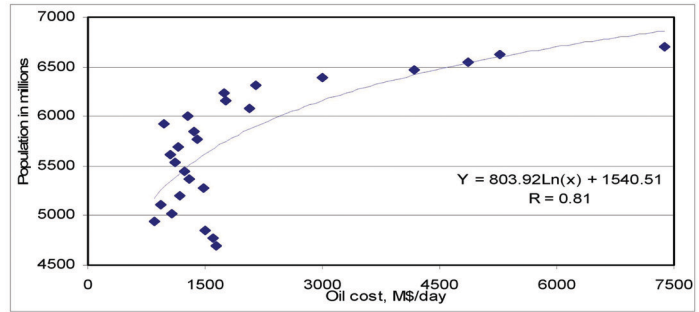
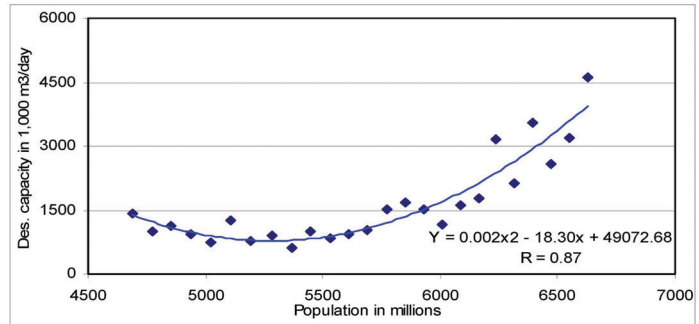


Fig. 5. World daily desalination capacity versus world population



variation in population growth rate is limited. Another important driving force for investments in desalination seems to be the population increase; it is found to correlate with 87 % as shown in Figure 5. As seen in Figure 6 the three main parameters world cumulative daily desalination capacity, cumulative daily oil cost and cumulative population increments in the last 25 years are compared from year 1983 to 2007.

The total annual renewable freshwater supply, population growth rate and the country desalination capacity over country total annual renewable freshwater of the major producer countries are presented in Table 6. The 36 countries account an average of 90 % of the world total

desalination production capacity and about 34.6 % of the world total annual renewable fresh water. These countries are distributed into two groups depending on population growth rate (PGR) in which the first group, countries from 1 to 21, has ($PGR > 1.0$) and the second group, countries from 22 to 36, has ($PGR < 1.0$).

The two groups are shown in Figure 7 as the result of the total country desalination capacity over total renewable freshwater and population growth rate. The year and source of the annual renewable water resources available in this study is taken and recalculated from (Source: <http://www.worldwater.org/data.html>) where the last update was in 2006. The 36 countries account

Fig. 6. World cumulative daily desalination capacity, cumulative oil daily cost and cumulative population increments from year 1983 to 2008

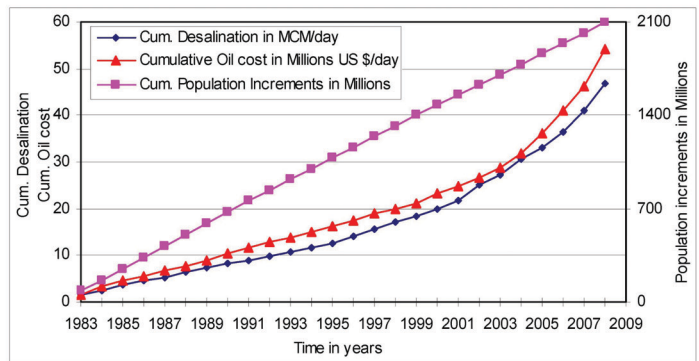


Table 6. Total annual renewable freshwater supply and population growth rate (PGR) in the major desalination producer countries (Update: 2006, Source: <http://www.worldwater.org/data.html>)

Country	Annual renewable water resources (km ³ /yr)	Year	Source	Desalination over renewable water Ratio	100 years PGR 1950–2050
Group 1					
UAE	0.15	1997	f	10.0	4.72
Qatar	0.05	1997	f	5.46	3.90
Kuwait	0.02	1997	f	32.8	3.78
Oman	0.99	1997	f	0.14	2.84
Saudi Arabia	2.40	1997	f	0.97	2.56
Libya	0.60	1997	c,f	0.48	2.42
Iraq	96.4	1997	f	0.002	2.39
Bahrain	0.12	1997	f	1.74	2.14
Israel	1.70	2001	l,m	0.08	2.13
Egypt	86.8	1997	f	0.001	1.79
Mexico	457.2	2000	j	0.0002	1.65
Iran	137.5	1997	f	0.001	1.61
Algeria	14.3	1997	c,f	0.02	1.60
India	1907.8	1999	h	0.0001	1.59
Singapore	0.60	1975	d	0.20	1.51
Indonesia	2838.0	1999	h	0.00002	1.33
Turkmenistan	60.9	1997	m	0.001	1.27
Tunisia	4.6	2003	m	0.006	1.24
China	2829.6	1999	h	0.0001	1.16
Australia	398.0	1995	i	0.0003	1.07
USA	3069.0	1985	n	0.001	1.01
Group 2					
Chile	922.0	2000	j	0.0001	0.93
Taiwan	67.0	2000	r	0.002	0.93
South Africa	50.0	1990	c	0.001	0.89
Kazakhstan	109.6	1997	g	0.001	0.81
Korea (South)	70.0	1999	h	0.003	0.77
Netherlands	89.7	2005	s	0.001	0.54
France	189.0	2005	s	0.0003	0.50
Sweden	179.0	2005	s	0.00001	0.26
UK	160.6	2005	s	0.001	0.24
Malta	0.07	2005	s	1.03	0.24
Spain	111.1	2005	s	0.006	0.24
Japan	430.0	1999	h	0.001	0.11
Germany	188.0	2005	s	0.0004	0.07
Russia	4498.0	1997	c,g	0.00001	0.07
Italy	175.0	2005	s	0.001	0.07

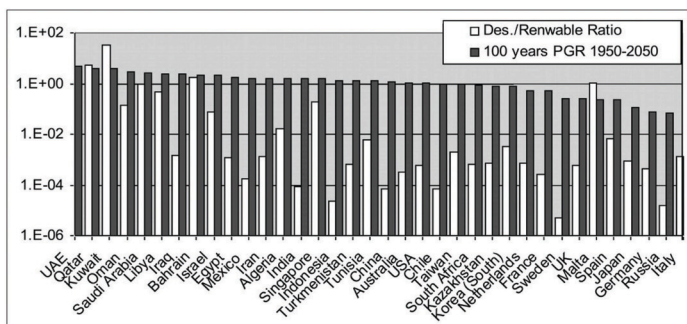


Fig. 7. Results of total country desalination capacity over renewable freshwater supply and population growth rate.

90.7% of the world desalination capacity until mid of year 2008 as found in the calculation. Further on, the countries of the first group have in total 72% of the world desalination capacities (i.e. 79% of the 90.7%), and the countries of the second group account for 18.7% of the total world desalination capacities (or 21% of the 90.7%).

Looking at the shares of renewable freshwater supply is more revealing. In total, the two groups counted for 34.6% of the world total annual renewable fresh water, but this value is distributed so that the countries of the first group has a share of 21.5% of the world total annual renewable fresh water (which make 62% out of 34.6%), while the countries of the second group has a share of 13% of the world total annual renewable fresh water (or 38% out of 34.6%).

Some countries have been found in the first group (Tunisia, Qatar, Kuwait and Bahrain) have to increase their desalination projects to cope the shortage of production and renewable fresh water. This water supply is challenged by the high population growth rate (greater than 1.0) and low amount of renewable fresh water. Some countries in the second group have at present severe problems with fresh water supply due to shortage of renewable water resources (Spain, Italy and South Korea). Investment in desalination seems also to correlate both with high population growths and the obvious lack of renewable water resources.

5. Conclusion

Desalination offers both advantages and disadvantages in terms of energy, environmental impact and population growth needs. The potential benefits of seawater desalination are great since the water supply can be independent of precipitation, but the economic and environmental costs remain high without national and international rules and regulations. In the non-oil countries, desalination is an attractive alternative for freshwater supply if the renewable water resource is very scarce. In oil-producing countries in arid area (e.g. some countries of group one), desalination is at present necessary for water supply and will be even more important with growing population. High revenues from oil export trigger the investment in new desalination plants with a time-lag of 2 years. Oil and desalination comes in pairs. Still, desalination requires high energy input and produces not only freshwater, but also brines with high salt concentrations. These are often discharged directly into the sea. On a local level, continuously discharged brine will result in salinity increases. Such increases in salinity concentration will exacerbate the critical problem of seawater intrusion into coastal groundwater aquifers.

As (Cooley et al., 2006) summarised: Is desalination the ultimate solution to our water scarcity problems? (No!) Is it likely to be a piece of our water production and management scheme? (The answer now is yes)

Acknowledgments

This work was supported by Lund University and partially from the International Desalination Association (IDA) (Channabasappa Memorial Scholarship).

References

- Al-Gobaisi, D.M.A. (1997). Sustainable augmentation of fresh water resources through appropriate energy and desalination technology. IDA World Congress on Desalination and Water Reuse, Madrid, Spain.
- Birkett J. (1999). "Cooley H., Personal communication".
- Cooley H., P.H. Gleick, and G. Wolff. (2006). Desalination, With A Grain Of Salt: A California Perspective.
- Energy Information Administration (online: 2008): http://tonto.eia.doe.gov/dnav/pet/pet_pri_wco_k_w.htm
- Gary C. (2006). Desalination in Australia, IDA News, September/October.
- Ghabayen S., M. McKee and M. Kemblowski. (2004). Characterization of uncertainties in the operation and economics of the proposed seawater desalination plant in the Gaza Strip, Desalination 161, 191–201.
- Gleick P.H. (2006). Pacific Institute. Total Renewable Freshwater Supply, by Country (Update from: <http://www.worldwater.org/data.html>)
- Gleick, P.H. (1993). Water in Crisis: A Guide to the World's Fresh Water Resources. New York: Oxford University Press.
- GWl (2008–2009). Desalination data and IDA desalination year book and CD.
- IDA. (2006). Worldwide Desalting Plant Inventory, No. 19 in MS Excel format, Media Analytics Ltd., Oxford, UK.
- IDA. (2006–2007). International Desalination Association Yearbook.
- International Energy Agency. (2005). Water, a shared responsibility: The United Nations World Water Development Report 2 (WWDR 2), UN-WATER/WWAP/2006/3
- Lattemann S. and Höpner Th., Impact of desalination plants on marine coastal water quality, In: Barth, Abuzinada, Krupp and Böer (Eds.), Marine Pollution in the Gulf Environment, Kluwer Academic Publishers, Netherlands (in review).
- Lattemann S. and T. Höpner. (2008). Environmental impact and impact assessment of seawater desalination, Desalination 220, 1–15
- Magazine. (2005). Water Condition & purification, January. <http://www.lennntech.com/WHO-EU-water-standards.htm>
- MEDRC. (2002). Assessment of the Composition of Desalination Plant Disposal Brines (Project NO. 98-AS-026), Middle East Desalination Research Center (MEDRC), Oman.

- National Academy of Sciences (NAS). (2004). Review of the Desalination and Water Purification Technology Roadmap. Water Science and Technology Board. Washington, D.C.:National Academies Press.
- OTV. (1999). "Desalinating seawater." *Memotechnique*, Planete Technical Section, No. 31 (February):1.
- Pankratz T. (2004). An overview of Seawater Intake Facilities for Seawater Desalination, The Future of Desalination in Texas Vol 2: Biennial Report on Water Desalination, Texas Water Development Board.
- Ruiz-Mateo, M. Antequera and J. Gonzalez. (2007). Discharges to the sea from desalination plants. MEDCOAST-07, 13–17 November, Alexandria, Egypt.
- Raed Bashitialshaaer, Kenneth M. Persson, Magnus Larson, Mustafa Ergil. (2007). Impact of Brine Disposal from EMU Desalination Plant on Seawater Composition, IDA World Congress-Maspalomas, Gran Canaria –Spain October 21–26.
- Sedlak, D.L., and K.E. Pinkston. (2001). Factors Affecting the Concentrations of Pharmaceuticals Released to the Aquatic Environment. Proceedings of the National Groundwater Association, 2nd International Conference on Pharmaceuticals and Endocrine Disrupting Chemicals in Water. Minneapolis, Minnesota and Westerville, Ohio:National Groundwater Association, October 9–11.
- Simon, P. (1998). *Tapped Out: The Coming World Crisis in Water and What We Can Do About It*. New York: Welcome Rain Publishers.
- Sauvet-Goichon B. (2007). Ashkelon desalination plant – A successful challenge, *Desalination* 203, 75–81.
- U.S. Bureau of Reclamation (USBR). (2003). *Desalting Handbook for Planners*. 3rd Edition. Desalination and Water Purification Research and Development Report #72. Denver, Colorado:United States Department of the Interior, Bureau of Reclamation, Water Treatment Engineering and Research Group.
- U.S. Census Bureau International: Data Base; World Bank. (2004). Data updated 6-18-2008. <http://www.census.gov/ipc/www/idb/idbprint.html>
- Wangnick/GWI. (2005). *Worldwide Desalting Plants Inventory*. Oxford, England: Global Water Intelligence, 2005. Data provided to the Pacific Institute.
- Wiseman R. (2006). Editor's corner, *Desal. Water Reuse*, 16 (3) 10–17.
- World wide data base (update online: 2008): <http://www.worldwater.org/data.html>
- Valero A., J. Uche and L. Serra. (2001). Desalination as an Alternative to Spanish National Hydrology Plan. Technical Report, CIRCE and University of Zaragoza.

Paper VII

Improving Water and Electricity Could Ease Border Tensions: A Case Study for Sinai-Gaza

Bashitialshaaer, R., and Persson K.M. 2011

Water policy 2011 (under review)

Improving Water and Electricity Could Ease Border Tensions: A Case Study for Sinai-Gaza

Raed Bashitialshaaer^{*1}, Kenneth M Persson^{*2}

^{*}Department of Water Res. Eng., Lund University-LTH, Box 118; SE-221 00 LUND-Sweden

¹Tel.: +4646222-4367, Fax: 4435, Raed.Alshaaer@tvrl.lth.se; ralshaaer@yahoo.com

²SYDVATTEN AB, Skeppsgatan 19, 211 19 MALMÖ-Sweden; kenneth_M.persson@tvrl.lth.se

Abstract

Desalination can be a cost-effective way to produce fresh water and possibly electricity. The Gaza Strip has had a complex hydro-political situation for many years. Gaza is bordered by the Mediterranean in the west, by Israel in the north and east and by Egypt in the south. Water and electricity consumption in the Gaza Strip is expected to increase in the future due to the increasing population.

In this paper, a solution for Sinai and the Gaza Strip is suggested involving the building of a joint power and desalination plant, located in Egypt close to the border of Gaza. Results of capital and unit costs have been derived from bench-mark studies of 18 different desalination projects mainly in the Middle East countries. The suggested joint Egypt-Palestine project would increase drinking water supply by 500,000 m³/d and the power supply by 500MW, whereof 2/3 is suggested to be used in Gaza and 1/3 in Sinai. The present lack of electricity and water in Gaza could be erased by such a project. But Egypt will probably gain more. More water and electricity will be available for the future development of Sinai; a significant value will be added to the sale of Egyptian natural gas used for water and power production in the project; more employment opportunities can be offered for people living in Sinai; the domestic market for operation and maintenance of desalination plants can be boosted by the suggested project; Egypt may naturally and peacefully increase its cooperation with and presence in Gaza, which should lead to increased security around the border between Egypt and Gaza. This type of project could also get international support and can be a role-model for cooperation and trust-building between neighbours in the Middle East region. This study has also compared with more than five different alternatives.

Keywords: Desalination; Power plant; Palestine-Gaza Strip; Unit costs; Water resources; Environmental impact.

1. Introduction

The Gaza Strip is a small, densely populated area in the Middle East in which groundwater is the main water source. Gaza has several water problems; inefficient water use by the agricultural sector, limited fresh water supply and high water demand, groundwater contamination, seawater intrusion and wastewater disposal. In the Gaza Strip area of Palestine, there is a large gap between water resources and demand. Groundwater is also diminished by pollution, increasing demands, misuse by local people and control by neighbouring countries of Palestinian water resources

(Baalousha, 2006). The citizens of the Gaza Strip have pursued several alternatives to increase water supply; water desalination (house units), use of bottled water, imported water and storm water harvesting (El-Nakhal, 2004). Agriculture accounts for 70% of fresh water use (Al-juaidi, 2009). Water resources in the Gaza Strip have a water balance deficit of about 30% (El-Sheikh et al, 2003). Annual water availability from the Gaza aquifer is 147 decreased to 125 MCM/year, i.e. almost 15% (Aljuaidi et al., 2009).

The lack of progress was due partly to deteriorating security conditions, which have made implementation of development projects problematic, and partly to the inadequacy of existing agreements with Israel which impede Palestinian water sector development (Gray, 2009). The lack of project funding at the present time is the major impediment to development in the Palestine. It also contributes to the generally inadequate allocation and inappropriate location of water resources to the Palestinians (ADC, 2007). At present, maintenance is too difficult for the water sector and pipes and cement are for instance being impounded for Gaza peoples. Despite the pledge of \$4.5 billion dollars of aid money to rebuild Gaza which was made at the conference in Sharm el Sheikh held in March, 2009 (PCHR, 2009). The present average water consumption per capita by the Palestinian population is approximately 55 L/cap/d, or 55% of the WHO design value of 100 L/cap/d (Abu Zahra, 2001).

According to the United Nations Environment Programme, the total inputs and outputs of the Gaza coastal aquifer (in 1998) were estimated at 123 and 154 MCM, respectively (UNEP 2003). The Palestinian Water Authority has studied the water quality of 111 municipal wells in the Gaza Strip. Only 9% of these wells are suitable for human consumption (PWA, 1995). One of the major options for the remedy of water shortages in the Gaza Strip of Palestine and the protection of its coastal aquifer is the utilization of desalination technology (Assaf, 2001). Desalination is already practised in Gaza but on a small scale.

In this study, a bench-mark analysis of seawater desalination was performed for reverse osmosis systems. The basic parameters of cost analysis such as capacity, recovery, membrane life, energy, chemical costs and flux were evaluated based on the effects on capital, operating and total production costs (Akgul et al. 2004). A reverse osmosis desalination project to improve water quality and quantity was previously proposed (El-Nakhal, 2004). According to the PWA plan, desalination seems to be the only viable alternative for water resources (Baalousha, 2006). It has been estimated that

the Gaza Strip will need to develop a seawater desalination capacity of about 120,000 m³/d by 2008 and an additional 30,000 m³/d by 2016 (Ghabayen et al., 2004). Desalination plants in the Gaza Strip area with a capacity of up to 150,000 m³/d have also been suggested, but very little has been implemented until now, partly due to political conditions (Baalousha, 2006). To address this, the new desalination plant is suggested to be located in Egypt but/and also in Gaza to serve two different countries. The suggestion of this project was not possible to cooperate with the Israeli for some reasons such as controlling the whole production and the cost will be more than Egypt.

1.1. Current situation in Gaza

The production capacity of the desalination plants in Gaza varies between 20 and 150 m³/d (Jaber & Ahmed, 2004). These private plants are very small and produce a total of about 2000 m³/d of desalinated water (El-Sheikh, 2004). There are four sources of drinking water, namely municipal water wells (50 MCM/y), agricultural water wells (90 MCM/y), water from an Israeli company “Mekkorot” (5 MCM/y) and brackish water reverse osmosis plants (4 MCM/y) (El-Sheikh, 2003).

Many desalination plants have been discussed and many projects initiated, yet few have been taken into full operation. The municipality located in the middle of Gaza (Dier Albalah) operates a RO plant using brackish groundwater, producing about 1080 m³/d desalinated water with a recovery rate of 75%. There are two RO desalination plants located in Khanyunis City: El-Sharqi, built in 1997, and Al-Saada, built in 1998, with a total production capacity of 2760 m³/d, of which 1200 m³/d comes from El-Sharqi and 1560 m³/d from Al-Saada (El-Sheikh, 2004). In 1998, USAID financed a BWRO plant built by an American company Metcalf and Eddy in Gaza Industrial Zone with production capacity of 1000 m³/d (El-Sheikh, 2003). France and Austria have also financed two seawater RO plants with a capacity of 2400 m³/d and 5000 m³/d respectively (El-Sheikh, 2003).

A small scale desalination plant was built in Gaza but the larger one which was suggested has not yet been built due to the many reasons listed above. Even some of the small plants have been stopped and electricity production is limited in the Gaza Strip. It was reported in UNOCHA (2006) that the electrical capacity in the area remains insufficient most of the time despite the installation of new transformers. This leaves most of the population in Gaza without electricity for up to 18 hours per day and

without water for more than 20 hours per day. Without electricity, the reverse osmosis plants cannot operate either. The current electricity demand in the Gaza Strip, according to the President's Office and the Gaza Power Generating Company (GPGC), is 215 MW but this is expected to increase to 225 MW during the winter months (UNOCHA, 2006).

The current supply available to Gaza, which totals 184 MW, originates from three sources: Gaza Power Generating Company (GPGC) 60 MW (maximum), Israel Electrical Company (IEC) 107 MW and Egypt 17 MW. The Gaza Power Generating Company (GPGC) estimated that the maximum power generated from the power station did not exceed 60 MW while the potential of the original transformers was up to 140 MW (UNOCHA, 2006).

1.2. Water prices

In general, the cost of water and source of energy is important for the production of fresh water in low income and poor countries. The existing agricultural water system in Gaza has a low economic water use efficiency of about \$0.34/m³ compared to a water cost of about \$0.60/m³ for seawater desalination (Issac, 2000; Metcalf & Eddy, 2000; MoA, PWA, and PHG, 2004). Akgul et al. (2008) studied different designs for Mediterranean SWRO membranes. The average unit costs of RO processes have declined from \$5.0/m³ in 1970 to less than \$1.0/m³ at present (Zhou & Tol, 2005).

Large RO-plants have lower specific production costs despite location. The Ashkelon desalination plant, which is also located on the Mediterranean coast, has presented cost figures as low as \$0.52/m³ (Busch & Mickols, 2004). Another example is the Perth desalination plant in Australia, which consumes only 3.7 kWh/m³ energy per cubic meter fresh water (Gary, 2006). In most cases, unit and capital costs of desalination plants depend on where they are located. Pankratz (2004) reported that the production costs decreased from roughly \$2.5/m³ in the late 1970s, \$1.5/m³ in the early 1990s to around \$0.50/m³ by 2003.

El-Sheikh (2003) reported that customers in Gaza are paying an average of 0.25-0.50 \$/m³ for municipal water distribution and they will be able to pay 1.0 \$/m³ of the desalinated water in the distribution network because they already pay \$1.25 for 1m³ desalinated seawater. The energy prices were calculated in the range of 6–9 cent/kWh electricity (Akgul et al., 2008).

Egypt's natural gas sector is expanding rapidly with production of about 1.9 trillion cubic feet (Tcf) and consumption of 1.1 trillion cubic feet in year

2008 ($1000 \text{ ft}^3 = 28.3 \text{ m}^3$). According to the Oil and Gas Journal, Egypt's estimated proven gas reserves stand at 58.5 Tcf, the third highest in Africa, and continue to be an important supplier of natural gas to Europe and the Mediterranean region (U.S. Energy: last update June, 2010).

1.3. Purpose

The purpose of this study is to make a bench-mark analysis of a seawater desalination plant for reverse osmosis with the aim to increase water availability in Gaza and Sinai for a maximum number of people. This proposed project can minimise the cost of water and electricity and improve the other sectors, e.g. agriculture or industry. The purpose is also to stress the importance of joint projects between countries of the Middle East, to reduce tensions, disputes and fighting, and to increase cooperation, mutual trust and security. With examples from Europe, the century long conflict between France and Germany could be settled by economical and political cooperation. In 1950, the Schuman declaration stated that "Europe will not be made all at once, or according to a single plan. It will be built through concrete achievements which first create a de facto solidarity." Through initial cooperation on coal and steel, the countries could gradually work towards a position where they formed the EEC in 1957 and further on to the EU. In 2010, 27 European countries cooperate closely within the EU and more European countries want to join. HRH Prince El Hassan bin Talal of Jordan has in several presentations, speeches and articles argued for the urgent need of a similar development in the Middle East countries. Bridging towards peace and trust between countries must be reached through concrete actions. Yet, peace and trust are both possible if comprehensive processes are adopted in several areas such as security, basic and current; economy with a human content such as health care, fresh water, electricity and education. He has been asking for several years why a plant for solar desalination and electrification of Gaza on the Egyptian side of the Gaza border could not be established. In the opening of WOCMES 2010 in Barcelona, Spain, HRH Prince El Hassan bin Talal said that "The need of stress to promote cultural ties among Middle East nations, noting the importance of developing joint policies to enhance contact at various levels". He affirmed the need to consider the human dimension while drawing developmental plans, calling for closer relations between the Middle East and other parts of the world".

That answers the main question in this paper: Why Egypt? It would be a great opportunity for the Palestinians if Egypt agrees to construct a combined desalination and power plant in the first 5 km from the Gaza border. Cost effective energy that is cheaper than Israeli pricing and possibly less politically sensitive should be of interest to both Egypt and Gaza. A good alternative could be the use of Egyptian natural gas in the power plant supplying electricity not only to the desalination project, but also to Sinai and the Gaza Strip. The suggested project suits very well with the abovementioned need for concrete achievements to tighten the cooperation and relations between neighbours of the Middle East. This project could be a starting point and possibly a role-model for how cooperation can be done for the future.

2. Study Area

2.1. An overview

Gaza has a semi-arid climate with a total area of about 365 km² and a population of 1.55 million with a growth rate of 3.2% (Aljuaidi et al., 2009). The Gaza Strip forms a transitional zone between the semi-humid coastal area in the north and the semi-arid Sinai desert in the south. The Gaza Strip is 40 km long and has an average width of about 9 km. Its area is surrounded by the Negev desert, Israel, Egypt and the Mediterranean Sea (Figure 1). The Gaza Strip area is part of the Palestinian Autonomous areas according to the Oslo agreement that was signed by the USA, Egypt and Israel in 1993. Gaza is divided in five districts known as Gaza, North Gaza, Deir Al-Balah, Khanyounis and Rafah. The locations of the agricultural areas are also shown in (Figure 1). Gaza is located on the western-most part of the shallow coastal aquifer that is exploited for municipal and agricultural water supply. The aquifer in the Gaza Strip is part of the coastal aquifer, which extends from Mt. Carmel in the north to the Sinai desert in the south with a variable width and depth. The total area of the coastal aquifer is about 2000 km² with 400 km² beneath the Gaza Strip (EXACT, 1998).

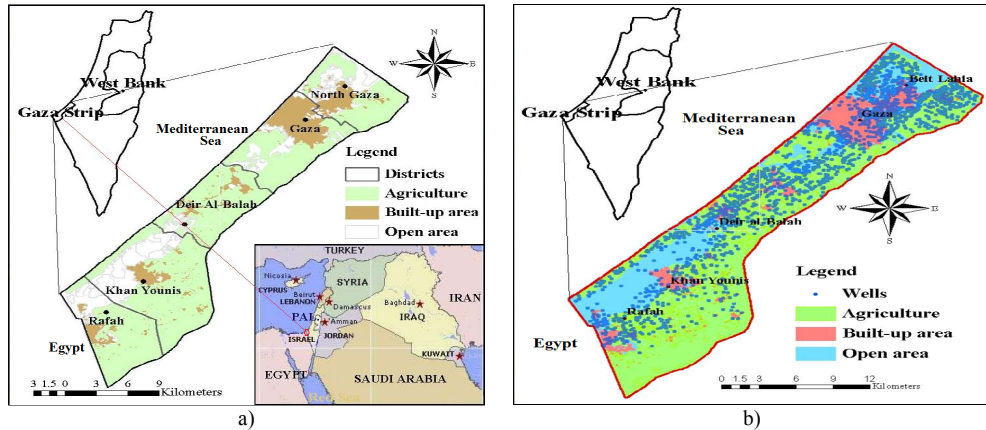


Fig. 1. Gaza strip overall map for a) districts and b) agricultural areas (from: Al-juaidi, 2009)

Annual average rain in the Gaza Strip is between 200 mm (in the south) and 400 mm (in the north), which falls mainly in winter. Groundwater is the main water source in Gaza (El-Nakhal, 2004). The evaporation rate is very high compared with rainfall. The average amount of open water evaporation is about 1,300 mm/year (PBS, 2000). Increased demands for water for domestic and agricultural use dry up most of the agricultural areas. Thus, water scarcity in Gaza is a significant problem and concerns have been highlighted in many studies. Immigration of Palestinian refugees after the 1948 Israeli-Arab war to the Gaza Strip, coupled with the high fertility rate, increased the population of that Palestinian coastal land strip from 50,000 in 1948 to more than 1.5M in the year 2009 (PBS, 2000). Still Gaza faces a high population growth rate and the majority of the population has relatively low incomes (Aljuaidi et al., 2009). Economic development is restricted, among other things by water scarcity and unreliable power supply.

2.2. Water balance in Gaza

It is important to analyse the water balance in the Gaza Strip and to compare water supply with water demand. In 2020, there will be more than 2 M Gazans, double the year 2000 population (PBS, 2000), and the water demand could easily also double from 154 MCM/y, a conservative projection being 216 MCM/y (Metcalf and Eddy, 2000). In Gaza there are no surface water resources except for an occasional water flow in Wadi Gaza during heavy rainfall, which temporarily occurs in 2-3 of the winter months. Another environmental problem is the infiltration of nitrates into

the aquifer from the uncontrolled and excessive use of fertilizers by vegetable growers in their irrigated fields to increase productivity. A further problem is high levels of organic matter in groundwater leakage from sewers and septic tanks where there is no wastewater collection (Assaf, 1997; Shawwa, 2000, and MPIC, 1995). The available groundwater is severely overused due to high rates of population growth and economic development in all areas. Pollution resulting from saline water intrusion, inadequate wastewater treatment, waste disposal and intensive agricultural activities continues to reduce the amount of water available per capita (Ghabayen et al., 2004).

Baalousha (2004) reported that the average annual net sustainable groundwater recharge from precipitation is about 43.3 MCM. Although the total amount of annual inflow to the Gaza aquifer is about 109 MCM as explained in Table 1 to the left, only part of this amount can be considered as a safe yield (about 60 MCM/y). The result reported in this table excerpted from (Baalousha, 2004). Table 1 to the right presents the general water balance in the Gaza strip among five different waters as inputs and outputs (Abu Zahra, 2001). Based on PWA records, the domestic water demand for 2000 was 55 MCM. This domestic demand was predicted to be increase to 182 MCM in 2020 (Metcalf and Eddy, 2000). Also the annual deficit was found about 37 in the year 2000 and predicted to about 107 MCM in 2020 (Metcalf and Eddy, 2000). Water resources should thus be increased by 110-120 MCM/y (330,000 m³/d) to meet this shortage.

Table 1. Water balance in the Gaza Strip in 2000 and 2001

Balance (Metcalf & Eddy, 2000)	Amount MCM	Hydrologic Parameter (Abu Zahra, 2001)	Gaza Strip contribution to water balance	
			Percentage	MCM/y
Inflow:				
Recharge from rainfall	43	Annual rainfall	100	101
Lateral inflow	10	Evapotranspiration	- 52.5	- 53
Irrigation return flow	20	Surface run-off	- 1.98	- 2
Saltwater intrusion	11	Natural recharge	45.5	46
Leakage of sewer system	12	Return flow	8.9	9
Leakage of water system	13	Overall balance		55
Total	109			
Outflow:				
Municipal abstraction	50			
Agricultural abstraction	80			
Natural groundwater discharge	11			
Total	141			

2.3. Water quality in the Gaza Strip

Of the approximately 50 L/capita/d of water delivered to the residents of the Gaza Strip, only about 13 L/capita/d meets WHO quality standards

(PWA, 2000). The problem of groundwater quality especially in Khanyounis city is rather complicated. Both NO_3 and Cl are major pollutants of the aquifer attributed to human use as well as the scarcity of the water resource (Al-Agha, 2005). PWA suggested in year 2000 that the Gaza Strip should develop a seawater desalination plant of about 150,000 m^3/day in order to maintain a fresh water balance in the coastal aquifer and meet water demand for different uses (PWA, 2000).

Maximum nitrate values of 433 mg L^{-1} and mean of 166 mg L^{-1} have been measured, exceeding the WHO standards (45 mg L^{-1}) (World Health Organization, 1996). The corresponding values have also been reported in the case of chloride, where the maximum value is about $1,290 \text{ mg L}^{-1}$, and the mean value is 491 mg L^{-1} compared to the WHO standard of 250 mg L^{-1} (World Health Organization, 1996). According to the PWA, more than 60% of the total amount of groundwater in the Gaza Strip aquifers is of bad quality and not potable according to WHO standards (PWA, 1999). It is believed that fertilizers, in combination with the leached wastewater from septic tanks and non treated wastewater, are responsible for this high level of nitrate.

High fluoride content is also a problem Sansur et al. (1991) concluded that with an increase in salinity in many of the artificial wells in the Gaza Strip, the health effect on the population has become serious and stated that this condition is due to high fluoride content. In the Gaza strip, many people are affected by yellow staining, and discoloration plus mottling (decay) has been observed on the teeth of adult Palestinians in the central and southern Gaza Strip (Assaf, 2001).

3. Methodologies

3.1. Proposal overview

Desalination projects are always related to a number of parameters and factors such as water scarcity, water quality, energy recovery, cost per cubic meter, capital cost, location, land use, operations and maintenances as well as environmental impact. In general, any project has to meet at least the minimum requirements such as:

- Desalination plant allocation systems
- Consumer income and economic acceptance
- Availability of operational materials and chemicals in the area
- Annual cost optimization including workers
- Costs of supply, conveyance and pre and post treatments
- Study different scenarios and comparisons

- Environmental impact analysis
- Economic benefits of water use and net benefits of overall operations.

A Bayesian belief network model based on equations from Poullikhas, (2001) was developed for the Gaza Strip for a seawater RO desalination plant. Poullikhas assumed that the contribution of capital recovery cost varies between 30 and 50% of the cost of produced water, depending on several variables such as plant size, site, process type, etc. Energy is also considered as the major component of the cost which usually lasts up to 30 years for major plants. The O&M cost ranges between 15% and 30%, mainly depending on plant capacity (Bushnak, 1996). More information and details regarding the equations calculation can be found in (Poullikhas, 2001). The model yielded a minimum specific capital cost of 0.224 ± 0.064 US\$/m³ and the minimum operation and maintenance cost was found to be 0.59 ± 0.11 US\$/m³.

The joint project will supply fresh water and electricity to the two areas with one third to the Egyptian part (Sinai) and two thirds to the Palestinian part (Gaza). The advantages are much greater than disadvantages and it is almost no disadvantages for the Egyptian. In this project Egypt will get their amount for free plus selling natural gas, improving water quality and quantity, employers opportunities, materials and tools for repairing and chemicals. All these parts will be supplied from Egypt and considered as advantages. Figure 2 shows the border line between Egypt and Palestine as well as the end point along the Mediterranean Sea coastline. In Figure 2, the triangle on the south-west part of the map encloses possible locations for the proposed project within a 10 km area on and around the Mediterranean coast. It is suggested that the brine from the desalination plant first be mixed with the power plant cooling water and then discharged to the sea to minimise the impact. The closer the plant to the Gaza border, the cheaper it will be to distribute external power, environmental electricity and water to the Gaza Strip.

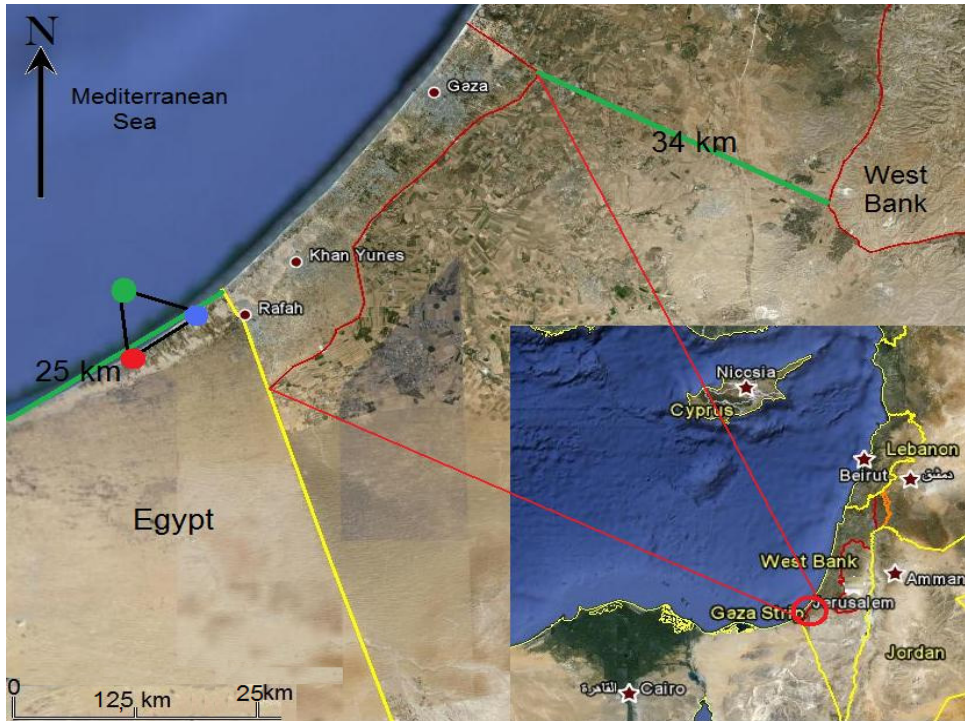


Fig. 2. Proposed desalination and power plant projects in the study area (From: Google Earth 2009)

3.2. Examples of water transport

The transfer water from Sinai to Gaza should not cause any problems. There are many practical examples of water transport from one city to another or from one country to another, see Table 2. Some calculations on transportation costs of water are presented in (Zhou & Tol, 2005). Comparison of these estimates to those of other studies suggests that Kally (1993) may have been overly pessimistic, but most of these studies suggest that the actual costs would have been higher, see Table 2. Kally's estimation is still used because his calculation takes account of not only horizontal distance but also vertical lifting cost. It is important to search for independent sources of energy that might be as cheap as Israeli pricing. A good alternative for energy supply to the power plant could be off-shore gas discovered in the sea close to Gaza (Baalousha, 2006).

Table 2. Cost of water transport to selected projects (from Zhou & Tol, 2005)

City Country	Project Name	Distance Km	Amount MCM	Cost \$/m ³	Reference
Gaza Palestine	Nile to Gaza	200	100	0.214	Zhou & Tol, 2005
Turkish Cyprus	Turkey to Turkish Cyprus	78	75	0.25-0.34 0.26	Gruen, 2000 Kally, 1993
Barcelona Spain	Ebro to Barcelona	900	1000	0.36	Uche et al. 2001
Colorado USA	Colorado river to Phoenix and Tucson	550	1800	0.52 0.05	Kally, 1993 Hahnemann, 2002
Yangtze China	Yangtze to China's north	1150	32	0.74 0.10-0.16	Kally, 1993 Liu & Zheng, 2002
				0.38	Kally, 1993

3.3. Alternatives water supply solution

3.3.1. Water transport

Water transport was one of some alternatives were proposed to supply fresh water to Gaza peoples. As seen in Table 2, Nile to Gaza was suggested as one alternative by Zhou & Tol, (2005), it is comparable with desalinated water. The transport cost per cubic metre is about \$0.214, it is cheaper then desalination but not possible now due to increase in demand by the countries around the river. Water quality from the Nile River will not be good as the desalinated water.

Connecting the West Bank to the Gaza Strip is one possibility, first proposed by Assaf (1985, 1986). It entails connecting the West Bank and the Gaza Strip using a 60-70 km long pipeline of fresh water derived from Lake Tiberia (with Israeli permission) from the West Bank mountain aquifer and/or from the Israeli National Water Carrier. The solution was considered to be highly politically dependent and is now not possible because its level has dropped in recent years due to drought. Further on, water resources are not abundant on the West Bank and increased water consumption in Israel and Jordan.

3.3.2. Artificial recharge

Artificial recharging was previously planned as one possible solution for the Gaza aquifer, advocated in 1985 (Assaf & Assaf 1985) using floodwaters of Wadi Gaza and/or treated wastewater. There are many problems with this supply due to poor water quality in the Wadi of Gaza and lack of wastewater collection systems. Wastewater amount in the Gaza strip is about 13 MCM annually (CAMP, 2000). Approximately 70-80% of the domestic wastewater produced in Gaza is discharged into the

environment without treatment; either directly or through leakage. Also, there are about 18 different pipelines of wastewater discharged into the Mediterranean (UNEP, 2003). Almost all wastewater treatment plants in the Gaza Strip do not function effectively. The flood water amount is approximately 2 MCM/y which not meets the needs of Gaza and decreases of precipitation amount and increasing in the evaporation rate over Gaza are important.

3.3.3. Desalination

A large scale seawater desalination system set up in the Gaza Strip has been suggested previously (Assaf, 2001). A model for a set up like this with a BOO (build, own and operate) contract was demonstrated on the Florida coast in the USA with a fresh water cost of only \$0.6/m³ (Metcalf and Eddy, 2000). Solar plants have been suggested for desalination purposes. Three stages of a co-generation plant with a planned water capacity of 100 MCM/year, a power capacity of 2.5 billion kWh/year and a total panel area of approximately 13 km² have been proposed (Lubna et al., 2008). It was calculated that about 5 km² is required for the collector field to produce 1 TWh/year of electricity (Knies et al., 2005; Trans, 2004). The estimated total cost of this proposal is approximately 1.1–1.3 billion US\$, which is high compared to a joint power and desalination plant. The total land use would be huge and solar panels are expensive.

The desalination plant for the Gaza Strip was designed with a production capacity of 60,000 m³/d in the first phase and 150,000 m³/d in the second phase (El-Sheikh et al., 2003; El-Sheikh, 2004). Ghabayen et al. (2004) planned desalination plant capacity of 140,000 m³/d to produce water quality at maximum 400 ppm TDS, at a recovery rate of 50%. It is obvious that the water supply situation in the Gaza Strip is unsafe. But the localization of a desalination plant here may be jeopardized by insecure political and logistic conditions. Plant localization inside the Gaza Strip is unrealistic for three reasons; political problems, interior problems and energy availability.

In Gaza, there is no guarantee of a power supply to water projects. For example, no safe supply of operational and maintenance materials can be guaranteed. The interior situation in Gaza is characterised by lack of control of available water (chaos due to war) as well as leaks of information and technology. The energy availability and power supply is functioning most of the time despite the political problems. A joint plant catering to both Egyptian and Palestinian needs may decrease the tension. At present it is

not realistic to suggest a joint Israeli-Palestinian desalination or power project. Therefore, as safely as possible and away from any political escalation in the region, the proposal should be planned to supply people with fresh water. To build desalination and a power plant in the same area will currently be the best solution for producing fresh water and electricity to both Gaza and Sinai.

4. Results and Recommendations

4.1. Unit and capital cost results

The reported production unit cost of seawater desalination dropped significantly from 1955 to 2020 and will probably reach less than US 0.5 $\$/\text{m}^3$ in 2020, as shown in Figure 3. Four different technology types were studied and compared for long-term seawater desalination: membrane processes containing reverse osmosis (RO), thermal processes including multistage flash evaporation (MSF), multiple effect evaporation (ME) and vapour compression (VC), see Figure 3. Bashitialshaaer & Persson (2010) extracted data from the International Desalination Association (IDA) yearbook 2006-07, 2007-08, 2008-09 and 2009-10.

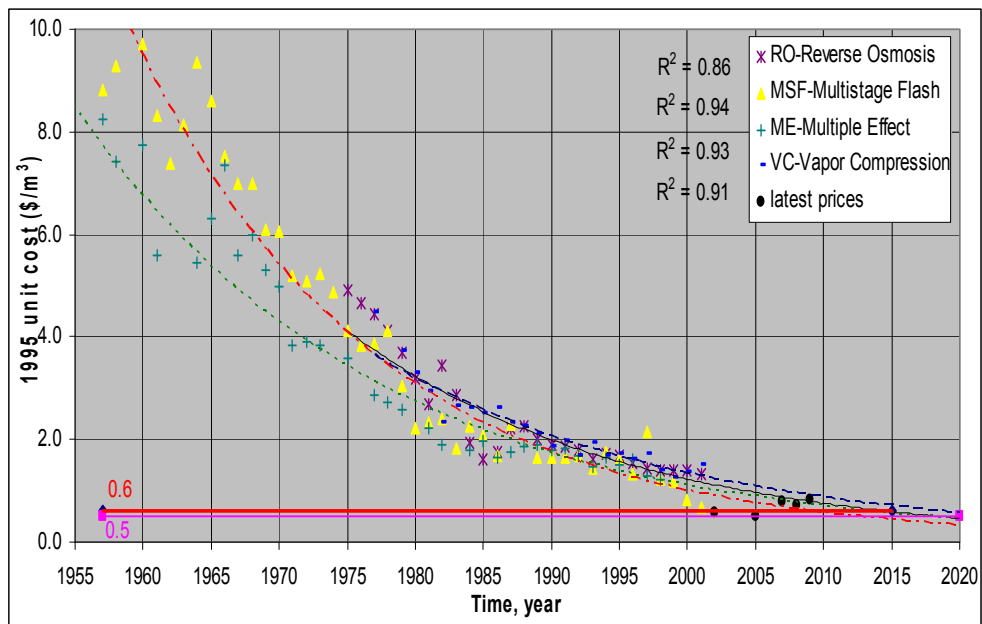


Fig. 3. Unit costs for seawater desalination 1955-2020 for four technologies

The data presented in Table 3 were derived from these yearbooks to help us achieve a better result. These data were collected from 18 different projects mainly in the Middle East countries and some projects with similar intake salt concentration. The desalination plant capital cost for the production of 1 m³ a day was found to be about 1080 \$US (approx. 1 million \$US to produce 1000 m³/d) (Bashitialshaaer & Persson, 2010). The average unit costs presented in Table 3 are well compared with that predicted in Figure 3.

Table 3. Data from 18 different desalination plants including six power plant projects

Project name IDA year book	Date	Total Capacity m ³ /day	In TDS, mg/l	Out	Capital cost \$US/m ³	Energy kWh /m ³	cost \$US /m ³	Within project MW
(2006-2007)								
Ashkelon SWRO, Israel	2005	326144	40679	300	650	3.9	0.53	
Carboneras SWRO, Spain	2002	120000	39000	<500	792	4	0.57	
Fujairah, UAE	2003	454000	40000	<180	843	4.5	NA	500
Shuweihat, UAE	2004	454000	44000	<250	819	3.7	NA	1500
Tuas SingSpring, Singapore	2005	136360	35000	<250	851	4.3	0.47	
(2007-2008)								
Dhekelia, Cyprus	1997	40000	40570	<500	1025	5.3	1.19	
Larnaca, Cyprus	2001	54000	40300	<500	1600	4.52	0.76	
Perth, Australia	2007	143700	36500	30	2400	4.0	1.2	
(2008-2009)								
Hidd (IWPP), Bahrain	07-08	408780	44000	<50	910	NA	0.69	910
Ras Laffan B (IWPP), Qatar	2008	272520	42000	<25	694	NA	0.8	1025
Hamma (SWRO), Algeria	2008	200000	39000	<500	1250	NA	0.82	
Palmachim SWRO, Israel	2007	110000	40233	<300	1000	3.8	0.78	
Skikda SWRO, Algeria	2008	100000	39332	<450	1100	3.6	0.73	
(2009-2010)								
Ghar Lapsi Plant, Malta	85-94	69500	39000		NA	3.2	0.72	
Barcelona-Liobregat, Spain	2009	200000	44800	400	1135	4.2	NA	
Marafiq IWPP-Jubail, KSA	2009	800000	42000	<25	957	1.6	0.83	2745
Alicant 1 & 2, Spain	03-08	130000	40000	400	1185	4	NA	
Rabigh IWSPP, KSA	2007	218000	39600	<10	2249	4.8	NA	360

IDA-International Desalination Association Yearbook; SWRO-SeaWawter Reverse Osmoses; WEB-Water Energiebedrijf; APP-Atomic Power Project; Independent Water Power Project (IWPP); Seawater Reverse Osmosis (SWRO); Integrated water steam & power project (IWSPP); KSA-Kingdom of Saudi Arabia

Also, the mean cost of production for 1 m³ was found to be about 0.79 \$US and the mean energy consumption approximately 4.5 kWh/m³, for a raw water with Mediterranean Sea salt concentration. Building desalination

and power plants in the same location has been practised in Israel, Saudi Arabia and the UAE to supply electricity to the desalination plant directly and the surplus to the power grid. It was found that the average cost of producing 1 Watt from the power plant is equal to about 1 \$US (approx. 1 million \$US to produce 1 MW) (Bashitialshaaer & Persson, 2010).

In Table 4, population change, growth rate and land area for some countries in the Middle East are presented. The population growth rate for the Gaza Strip is very high, with a simultaneous increase in water requirements. The growth rate from mid year of the whole period is the most common way of expressing annual population growth as a rate. The annual population growth rates over 100 years from 1950 and predicted for year 2050 were taken from the U.S. Census Bureau (2008).

Table 4. Population, land area and population growth rate (U.S. Census, 2008)

Country or area	Population			Area	Annual Population growth rate
	1950	2008	2050	Km ²	
Egypt	21,197,691	81,713,517	127,563,256	995,450	1.79
Israel	1,286,131	7,112,359	10,828,462	20,330	2.13
Palestine	1,016,540	4,149,173	9,789,347	6,000	2.26
West bank	771,165	2,611,904	5,580,321	5,640	1.98
Gaza Strip	245,375	1,537,269	4,209,026	360	2.84

The amount of fresh water needed for the Gaza Strip can be calculated from census and population progress data. If we consider a population of about 2 million living in Gaza in 2020 and that the daily fresh water requirement is about 100 litres per capita, the water supply should be 200,000 m³/day. The expected electricity demand is about 350 MW. A combined water production and power plant will have a capital cost of about US \$200 million in addition to the energy cost used for the desalination plant. The people in the Gaza Strip will also increase this amount. The proposal put forward in this study is projected to produce up to 500,000 m³/day of desalinated water and about 500 MW electrical energy. The total amount will be distributed to the Gaza Strip in Palestine and Sinai in Egypt. It will also be possible in the future to transport any excess water from the Gaza Strip to the West Bank. The distance from the last point in the Gaza strip to the closest point on the West Bank is approximately 34 km.

The proposed project should be initiated as soon as possible. The final results and production distribution of the proposed desalination and power

plants are presented in Table 5. The proposal presented in this study is planned to five years but production should be started at the end of the first year and be continued at the same level. It could be distributed as follows: two thirds to Gaza and one third to Egypt from both desalination and power plant projects. Details on how to finance the investment need to be sorted out later, but this type of project is expensive, thus it might be more convenient to carry out the projects step by step. It is possible to get international support from donors such as the World Bank, SIDA and the European Union. If the investment can be financed, then the project schedule time can be made shorter.

As described above, the results in Figure 3 and Table 5 have been derived from bench-mark studies of 18 different desalination projects mainly in the Middle East countries. The calculated mean desalination plant capital cost is about 1080 \$US/m³ a day (approx. 1 million \$US to produce 1000 m³/d and/or 1 \$US to produce 1 l/d).

Table 5. Sample calculation for desalination and power plant proposal

Date	Total Capacity	Within project	Capital Cost, \$US	Gaza Strip	Egypt Sinai
	m ³ /d	kW	million	m ³ /d	m ³ /d
2010	0	0	0	0	0
2011	100000	100000	200	66667	33333
2012	200000	200000	200	133333	66667
2013	300000	300000	200	200000	100000
2014	400000	400000	200	266667	133333
2015	500000	500000	200	333333	166667
Finally	500000	500000	1000	333333	166667

4.2. Impacts and recommendations

Joint-project advantages: Cooperation between the two countries especially water and electricity will could provide secure and trustworthy relationships, in the same manner as has happened between Germany and France.

Environmental effects: In the Gaza Strip, many householders use desalination home units, resulting in a local production of brine that ends up in the sea and increases the salt concentration of the sewage water, making the process of wastewater reuse more difficult and costly (El-Nakhal, 2004). In the absence of stability in the Gaza Strip, there are no regulations for desalinated water, thus there is very little control of the quality of

desalinated water or the brine discharge. A safe supply of desalinated water should decrease the need for home units. With a RO-plant, less brine will be discharged on land in Gaza.

Maintenance impact: The maintenance process needs trained people, and preventing damage to the RO membrane will be costly. In Egypt, it is possible to recruit qualified personnel, and operation and maintenance costs here could be similar or lower compared with world prices.

Groundwater contamination: Brine water is presently disposed off together with domestic wastewater in shallow drainage wells as well as in septic tanks, where it directly infiltrates the aquifers and affects the groundwater (El-Nakhal, 2004). Furthermore, the high pumping rate of groundwater causes seawater intrusion into the Gaza Strip coastal aquifer (Yakirevich, 1998). By supplying alternative drinking water, the need to extract groundwater decreases.

More available water: Currently there is no obvious right to water for the people of Palestine and sanitation in Gaza is inadequate, threatening water quality. With increased safe water supply, it will be possible to promote cooperation among countries sharing water resources and technology in the Middle East and to reduce water stress in the neighbouring countries.

Land impact: The area of the Gaza Strip is small in relation to a large scale safe water supply from an internationally controlled desalination plant. To locate the plant in the Gaza Strip will lead to an expensive desalination project with a high capital cost. Implementation of this project away from the border of Gaza requires a pipeline and pumps with additional energy needs to transport the fresh water to the municipalities.

Energy impact: The cost of energy in desalination plants is about 30% to 50% of the total cost of the water produced. Comparison of the cost components of reverse osmosis for two different energy supplies reveals that energy costs constitute the largest part of the operating costs (70%) (Akgul, 2008). In Gaza almost all the RO plants only operate for 8 hrs a day due to lack of electricity (Baalousha, 2006). The total cost of desalination can be reduced by designing the process as a hybrid (Awerbuch, 1997). In addition, a power plant was established in the Gaza Strip consisting of six turbines, with a total production capacity of 136 MW when fully completed (Baalousha, 2006). This plant is normally out of operation due to damaged parts and lack of appropriate maintenance.

Obviously, to improve safe water and electricity supply in Gaza will immediately help the population of Gaza. Since the cost of water and

electricity will be on par or lower than the present unreliable supply in Gaza, the economy of the project will not be a problem for Gaza either. But interestingly enough, also Egypt will gain substantially from the proposed project. The most important incentives and advantages to Egypt are listed below:

1. This project will increase water quality and quantities and electricity that will be available for the growing population of Sinai,
2. Egyptian natural gas can be used in the project adding value to the gas sales,
3. The plant will need staff. This gives employment opportunities for the people of Sinai,
4. Materials, chemicals and tools for repairing and maintenance of the desalination plant will also be provided from Egypt, which will increase the domestic M&U market
5. Politically, this is an opportunity for Egypt to increase cooperation with and be more present in Gaza; this will lead to increased security around the border between Egypt and Gaza. Already there is an electricity cooperation in operation between Egypt and Gaza governments.

5. Conclusions

Clearly both the desalination and the power plant are vital in the Gaza Strip to supply water and electricity to the people. Desalination as a source of water supply has many advantages and few disadvantages. In the Gaza Strip, sources of energy for desalination and power plant projects are very important in order to create an independent source of electricity, but nothing is secure in this situation. The people of Gaza lack infrastructure and rely on a clean water supply in order for their services to function normally. Although RO is a promising technology, highly professional people are required to operate the desalination plants. Supplies of chemicals required for desalination mean that continuous operation of a plant in Gaza may prove difficult and many existing small units have stopped production for this reason.

Why Egypt? Locating the desalination and power plant in Egypt on the Mediterranean coast is a good solution for both Egyptians and the people of Gaza. From the current experience the cost of water and electricity will be lower than cooperation with the Israeli and the workers are also much lower. This proposal should improve agriculture as well as the

socioeconomic and industry of both areas. More fresh water will be supplied to the peoples and more electricity will be supplied to the industry that may increase the productions. The environmental issue must be studied in great detail before implementing the desalination plant project.

However costs may be reduced by the use of natural gas to produce energy in the same location. The distribution of the production of water and electricity will be supplied as 1/3 for free to Sinai peoples for their land and natural Gaza usage. The rest of the outcome of this project from Gaza peoples will be used for repairing, maintenance and workers costs. One possible solution is to sell all the production from desalination and power plant in order to get back the capital cost in few years and the same time to payback the land rent, gas cost and repairing and maintenance. The only need to start this project is the stepwise capital cost and then the project benefits must cover all expenses.

References

- [1] A. Bushnak, The economy of water desalination, Proc., GULF96, 1996, pp. 2-34.
- [2] Abu Zahra B. A. A. (2001). Water crisis in Palestine, Desalination 136, 93-99.
- [3] ADC-Austrian Development Cooperation (2007). *Water Sector Review*. Jansen and Consulting Team, Ramallah. January 2007.
- [4] Al-Agha M. R. (2005). Hydrogeochemistry and carbonate saturation model of groundwater, Khanyounis Governorate-Gaza Strip, Palestine. Environ Geol 47, 898–906.
- [5] Alice Gray, Water development in the Palestinian Territories since the Oslo Interim Agreement in 1995. Water Policy 11 (2009) 525-536.
- [6] Al-Juaidi A. E. (2009). Water Allocation for Agricultural Use Considering Treated Wastewater, Public Health Risk and Economic Issues. PhD theses, Utah State University.
- [7] Al-Juaidi A. E., Rosenberg D. E. and Kaluarachchi J. J. (2009). Water Management with Wastewater Treatment and Reuse, Desalination, and Conveyance to Counteract Climate Change in the Gaza Strip. AWRA Climate Change Conference Anchorage, Alaska May 4-6.
- [8] Al-Khateeb M. (1993). Palestinian water supplies and demand. A proposal for the development of a regional water master plan, IPCRI, Jerusalem.
- [9] Akgul D., Çfakmakçı M., Kayaalp N., Koyuncu I. (2008). Cost analysis of seawater desalination with reverse osmosis in Turkey. Desalination 220, 123–131.
- [10] Assaf S. A. (2001). Existing and the future planned desalination facilities in the Gaza Strip of Palestine and their socio-economic and environmental impact. Desalination 138, 17-28.
- [11] Assaf S.A. (1997). The pollution of Gaza's underground water resources by nitrates, Conf. on Water and Environment, Technion, Haifa, Israel.

- [12] Assaf K. and Assaf S.A. (1986). Water resources and utilization in the Arab World, Arab Fund, Kuwait Publishers, pp. 93.
- [13] Assaf S.A. and Assaf K. (1985). Food security in the West Bank and Gaza Strip, a comprehensive study for ESCWA/FAO Joint UN Division and AOAD of the Arab League, UN Publication, October.
- [14] Avlonitis S.A. (2002). Operational water cost and productivity improvements for small-size RO desalination plants, *Desalination*, 142, 295-304.
- [15] Awerbuch L. (1997). Dual-purpose power desalination/hybrid systems/energy and economics. IDA Desalination Seminar, Cairo.
- [16] Baalousha H. (2006). Desalination status in the Gaza Strip and its environmental impact. *Desalination* 196, 1–12.
- [17] Baalousha H. (2004). Risk Assessment and Uncertainty Analysis in Groundwater Modelling. Shaker Verlag, Aachen.
- [18] Bashitialshaaer R. and Persson K. (2010). Desalination and Economy Prospects as Water Supply Methods. Water desalination conference in the Arab countries, Riyadh-Saudi Arabia, April 2010.
- [19] Busch, M., and Mickols B. (2004). Economics of desalination—Reducing costs by lowering energy use, *Water Wastewater Int.*, 19(4), 18–20.
- [20] CAMP (2001). Water Quality Baseline Survey- Final Report, Coastal Aquifer Management Program, Palestinian Water Authority, Gaza, pp. 1-54.
- [21] Dima N. W., Maarten A. S., Zaag P. V., Mimi Z., and Gijzen H. J. (2008). Water Footprint of the Palestinians in the West Bank. *Journal of the American Water Resources Association (JAWRA)* 44(2), 449-458.
- [22] El-Nakhal H. A. (2004). Alternatives to tap water: a case study of the Gaza Strip, Palestine. *Environmental Geology* 46, 851–856
- [23] El-Sheikh R. (2004). Regulatory challenges of Palestinian strategies on distribution of desalinated water. *Desalination*, 165, 83–88.
- [24] El-Sheikh R., Ahmed M., Hamdan S. (2003). Strategy of water desalination in the Gaza Strip, *Desalination* 156, 39-42.
- [25] Ettouney, H. M., et al. (2002), Evaluating the economics of desalination, *Chem. Eng. Prog.*, 98, 32– 39.
- [26] EXACT (1998). Executive Action Team, Overview of Middle East water resources. Water Resources of Palestinian, Jordanian, and Israeli Interest.
- [27] Gary C. (2006). Desalination in Australia, IDA News, September/October.
- [28] Ghabayen McKee S., M. and Kemblowski M. (2004). Characterization of uncertainties in the operation and economics of the proposed seawater desalination plant in the Gaza Strip. *Desalination* 161, 191-201.
- [29] GTZ Study, Tahal (1996). Water Planning for Israel Ltd, Middle East regional study on water supply and demand development, Phase II, Options to close the gap -- seawater desalination. Tel Aviv, Israel.
- [30] GTZ Study, Tahal (1995). Water Planning for Israel Ltd., Middle East regional study on water supply and demand development, Phase I, Review of assessment of existing plans. Tel Aviv, Israel.
- [31] Heitmann H.G. (1990). Saline water processing, VCH, New York, Chaps. 12-13.
- [32] HRH Prince El Hassan bin Talal, Opens WOCMES 2010, The World Congress for Middle Eastern Studies (WOCMES 2010) organized by the European Institute of the Mediterranean (IEMed), Barcelona, Spain, 19-24 July, 2010.

- [33] HRH Prince El Hassan bin Talal, Regional Cooperation with International Facilitation. Strategic Foresight Group Conference Water Security in the Middle East, Geneva, Switzerland, 15-16 February, 2010.
- [34] HRH Prince El Hassan bin Talal, "Improving Regional Cooperation on Water: A Key Opportunity for Preventive Diplomacy" The Parliamentarian Network for Conflict Prevention and Human Security, Jordan, Amman, 3-5 November 2009.
- [35] HRH Prince El Hassan bin Talal, The Global Economic Crisis and its impact on Fragile States. Switzerland, Caux, 7/17/2009.
- [36] IDA-International Desalination Association Yearbooks 2006-2007, 2008-2009 and 2009-2010.
- [37] Isaac, J. (2000). Essentials of sustainable water resource management in Israel and Palestine. Arab Studies Quarterly 22(2), 13-32.
- [38] Jaber I. and Ahmed M. (2004). Technical and economic evaluation of brackish groundwater desalination by reverse osmosis (RO) process. Desalination, 165, 209–213.
- [39] Kally, E. (1993). Water and Peace: Water Resources and the Arab-Israeli Peace Process, Greenwood, Oxford, U. K.
- [40] Knies G, Kabariti M, Seifter P, Makhool B, Daibes F. A solar water and power source for Gaza. Paper presented to Forum 2000 in Prague, 9–10 October 2005.
- [41] Lubna K. Hamdan, Maryam Zarei, Russell R. Chianelli, Elizabeth Gardner, Sustainable water and energy in Gaza Strip. Renewable Energy 33 (2008) 1137–1146.
- [42] Metcalf and Eddy Consultants (2000) (Camp Dresser and McKee), Coastal aquifer management program, integrated aquifer management plan (Gaza Strip). USAID Study, Task 3, Executive Summary, Vol. 1, and Appendices B-G. Gaza, Palestine.
- [43] Metcalf and Eddy, Inc. (2000). Integrated aquifer management plan: Final report. Gaza Coastal Aquifer Management Program (CAMP). USAID Contract No. 294-C-00-99-00038-00. 550 p.
- [44] MoA (2007). Ministry of Agriculture, Palestinian Water Authority (PWA), and Palestinian Hydrology Group (PHG). 2004. Technical report and partial results for the 2003 season of agricultural monitoring development support program (Beit Lahia Site).
- [45] MPIC (1995). Ministry of Planning and International Cooperation PA. Govt. of The Netherlands Nitrate pollution study, Gaza environmental profile, Phase II, Environmental Series No. 3, Euroconsult and IWACO Consultants for Water and Environment, Gaza, Palestine, September.
- [46] Pankratz T. (2004). An overview of Seawater Intake Facilities for Seawater Desalination, The Future of Desalination in Texas Vol 2: Biennial Report on Water Desalination, Texas Water Development Board.
- [47] PBS (2000). Palestinian Bureau of Statistics, Ramallah, the West Bank, Palestine.
- [48] PCBS (1997–2004). Palestinian Central Bureau of Statistics, Mid-year projected population in the Palestinian Territory by Governorate. <http://www.pcbs.org/inside/selcts.htm>.
- [49] PCHR-Palestinian Center for Human Rights (2009). *Press Release. 4th May 2009*. Available on PCHR website: [http://www.pcbrgaza.org/tiles/PrcessR/English/2008/Of\)-05-2009_2.html](http://www.pcbrgaza.org/tiles/PrcessR/English/2008/Of)-05-2009_2.html) (last visited 12/05/2009).

- [50] PWA (2000). Palestinian Water Authority, Water desalination study for Gaza Strip.
- [51] PWA (1999). Palestinian Water Authority, Water Resources and Planning Department, Gaza Water Resources.
- [52] PWA (1995). Palestinian Water Authority, Hydrogeological data books of the Gaza Strip, Water Resources Action.
- [53] Poullikkas A. (2001). Optimization algorithm for reverse osmosis desalination economics, *Desalination*, 133, 75-81.
- [54] Sansur R.M., Askar S. and Mashagi H. (1991). Naturally occurring fluorides in underground water and their effect on dental fluorosis among UNWRA schools' children in the Gaza Strip, Center for Environmental and Occupational Health Sciences, Birzeit University, Birzeit, West Bank, Palestine.
- [55] Sbeih M. Y. (1996). Recycling of treated water in Palestine: Urgency, obstacles and experience to date. *Desalination* 106, 165-178.
- [56] Shawwa I. (2000). Desalination, country focus on the Gaza Strip watermark, MEDRC (Middle East Desalination Research Center), Muscat Oman.
- [57] Sommariva C., Hogg H. and Callister K. (2003). Cost reduction and design lifetime increase in thermal desalination plants: thermodynamic and corrosion resistance combined analysis for heat exchange tubes material selection. *Desalination* 158, 17-21.
- [58] Trans-Mediterranean Renewable Energy Cooperation TREC. A renewable energy and development partnership EU-ME-NA for large scale solar thermal power and desalination in the Middle East and in North Africa, 15 April 2004.
- [59] UNEP (2003). Programme United Nations Environmental Program Desk study on the environment in the occupied Palestinian Territories. UNEP, Switzerland, pp 188.
- [60] UNOCHA (2006). United Nations Office for the Coordination of Humanitarian Affairs, OCHA Situation Report Gaza occupied Palestinian territory, Gaza Strip Situation Report 13 December.
- [61] U.S. (2008). Census Bureau International: Data Base; World Bank 2008. <http://www.census.gov/ipc/www/idb/idbprint.html>.
- [62] U.S. Energy Information Administration, Independent Statistics and Analysis (June, 2010): <http://www.eia.doe.gov/cabs/Egypt/NaturalGas.html>
- [63] WHO (1996). World Health Organization, Guidelines for drinking-water quality, 2nd edn: 2, Health criteria and other supporting information, Geneva.
- [64] Wilf M. and Klinko K. (2001). Optimization of seawater RO systems design, *Desalination* 138, 299-306.
- [65] Yakirevich A., Melloul A., Sorek S., Shaath S. and Borisov V. (1998). Simulation of seawater intrusion into the Khan Yunis area of the Gaza Strip coastal aquifer. *Hydrogeology J.*, 6, 549-559.
- [66] Zhou, Y., and Tol R. S. J. (2005). Evaluating the costs of desalination and water transport, *Water Resour. Res.*, 41, W03003, 2005.

Paper VIII

The Dead Sea Future Elevation

Bashitialshaaer, R., and Persson K.M. 2011

Int. J. of Sustainable Water and Environmental Systems, Vol. 2, No. 2 (2011) 67-76

The Dead Sea Future Elevation

Raed Bashitialshaar*, Kenneth M. Persson

Department of Water Resources Engineering, Lund University, PO Box 118, SE-221 00 Lund, Sweden

Abstract

In this paper water and salt mass balances for the Dead Sea were modeled. Precipitation, evaporation, river discharges, ground water flows, input/output from potash companies and salt production, and brine discharge were included in the models. The mixing time in the Dead Sea was modeled using a single-layer (well-mixed) a two-layer (stratified) system. Using the single-layer approach the water level was predicted to change from 411 m below mean sea level (bmsl) (in 1997) to 391 m and 479 m bmsl (in 2097) based on water mass balances including and excluding brine discharge, respectively, and to reach 402 m and 444 m for the two cases based on a salt mass balance. In the two-layer approach the water level after 100 years was predicted to change from 411 m bmsl (1997) to 397 m and 488 m for a water mass balance including and excluding brine discharge, respectively, and to reach 387 m and 425 m for the two cases using a salt mass balance. The water mixing time using the single-layer description increased from 58 to 116 years when excluding brine discharge. Using the two-layer approach the exchange or mixing time increased in both layers, when adding brine discharge to the system, from 1.2 to 1.7 years and 11 to 15.3 years in the upper and lower layers, respectively. Good agreement was found between the models and historical data.

Keywords: Water-Salt balance; Red Sea-Dead Sea Canal (RSDSC); Single-Layer and Two-Layer system; mixing time.

1. Introduction

The Dead Sea is a salt lake in southwestern Asia. It is bounded on the west by Israel and the West Bank and on the east by Jordan, forming part of the Israeli, Jordanian and Palestinian Authority border (Fig. 1). The Dead Sea is fed mainly by the Jordan River, which enters from the north. Several smaller streams also discharge into the Dead Sea, primarily from the east. The Dead Sea has no outlet. Fresh water is transported away by evaporation, which is rapid in the hot desert climate. As a result of large-scale projects by both Israel and Jordan to divert water from the Jordan River for irrigation and other water needs, the level of the Dead Sea has been falling for at least the past 50 years (Gaster, 1997–2006). The level of the Dead Sea was 408.5 m below mean sea level (bmsl) in 1995, being the lowest water surface on earth (Al-Weshah, 2000). At the end of 1997 the water level was 411 m bmsl and the surface area 640 km², (Gavrieli, 1997 & 2000). At the beginning of the last century, the level was about 390 m bmsl and had a surface area of 950 km². In 1966, the Dead Sea covered an area of 940 km² (76% of the lake was in the northern basin), and its total length was 76 km, with an average width of 14 km. The total volume of the water in the Dead Sea was estimated to be 142 km³ (only 0.5% being in the southern basin). The surface area continues to decrease due to the high rate of evaporation and decreasing water inflow. The Dead Sea is located in the northern part of the Great Rift Valley. On the east side of the lake the Moab plateau rises about 1,340 m above sea level, and on the west side the Judea plateau rises to approximately half that height (Asmar, & Ergenzinger, 2002a).

Originally, the Dead Sea consisted of two basins (a northern and a southern basin) divided by the Lisan Peninsula, which extends from the eastern shore out into the lake. The maximum depth in the northern basin was 749 m bmsl, whereas the average depth in the southern basin was only 10 m (Asmar & Ergenzinger, 2002a). The level of the Dead Sea has fallen continuously since the early 1930s, at increasing rates (0.5, 0.7, 0.90, and 0.95 m/y reported in (Steinhorn, & Gat, 1983; Al-Weshah, 2000; JRV, 1996a; Abu-Jaber, 1998), respectively). A summary of estimated rates of evaporation as a function of salinity in the Dead Sea is presented in Table 1, based on a compilation for the period between the late 1950s and 1980 (Levy, 1984b). The salinity (Total dissolved solids, TDS) increased during this period from 225 g/l to 279 g/l. During the past ten years, the level of the Dead Sea has fallen by more than 25 meters, and reached a level of about 416 m bmsl in 2003. Thus, the system is not presently sustainable and various projects aimed at supplying seawater to the Dead Sea have been suggested. The Red Sea-Dead Sea Canal (RSDSC) is being considered as one alternative.

The proposed layout, which may include a desalination plant, is shown in Fig. 1. The inflow of seawater (or reject brine from the desalination plant) into the Dead Sea will have a major impact on its limnology, geochemistry, and biology. The inflow of seawater from the proposed project (RSDSC) (density \approx 1030 kg/m³) to the highly saline Dead Sea (density \approx 1240 kg/m³) can be approximated by the inflow of fresh water to the seawater. The impact of such an inflow can be estimated by comparison with the inflow of fresh water during the rainy winter of 1991/2, when the level of the Dead Sea rose by 2 meters and the surface brine was diluted by up to 30% (Beyth et al., 1993).

*Raed Bashitialshaar, Tel.: +46 46 222 4367

Fax: +46 222 4435; E-mail: Raed.Alshaar@tvrl.lth.se

© 2010 International Association for Sharing Knowledge and Sustainability
DOI:10.5383/swes.02.02.001

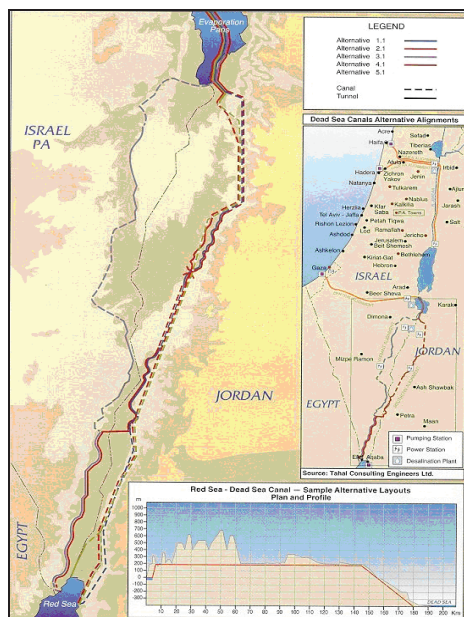


Fig. 1: Red Sea-Dead Sea Canal layout including plan and cross-sectional view (from: JRV 1996a).

Table 1. Estimated evaporation rates as a function of surface salinity in the Dead Sea (Levy, 1984b)

TDS g/l	Level m bmsl	Period	Data source	Evapt. rate (m/y)
225	393	1942/46	Neumann, 1958	1.70-1.75
240	395	1959/60	Neev, 1967	1.47-1.65
256-279	401	1979/80	Anati et al., 1987	1.30-1.54

1.2. The chemistry of the Dead Sea

When the runoff goes into the Dead Sea, the salt content can fall from its usual 35% to 30% or lower (Salt Works, 2001-2006). Under normal conditions, the salinity of the Dead Sea is about nine times greater than the average salinity of the oceans. Depending on the season, the salinity of the uppermost 35 m of the Dead Sea ranges between 30% and 40% and the temperature between 19°C and 37°C. Below a transition zone, the bottom layer of the Dead Sea consistently has a temperature of about 22°C, with complete saturation of halite (or sodium chloride, NaCl). Because the water is saturated, salt precipitates out of solution onto the sea floor.

The Dead Sea is presently also saturated or oversaturated with respect to aragonite (CaCO_3) and anhydrite (CaSO_4) (Gavrieli et al., 1989). Mixing between the calcium-rich Dead Sea brine and a sulfate-rich seawater will result in gypsum precipitation ($\text{CaSO}_4 \cdot 2\text{H}_2\text{O}$) (Gavrieli et al., 2005). The Dead Sea salts are commercially important and their production increases the evaporation of water. Wisniak (2002) presented a description of the properties of the Dead Sea together with a chemical analysis

of the processes utilized to exploit it commercially. Several numerical models have been developed to determine the water balance (Al-Weshah, 2000; Abu-Jaber, 1998). Horizontal variations in temperature and salinity may occur in the Dead Sea (Krumgalz et al., 1995 & 2000), but these are usually neglected in modeling. Due to the particular chemical composition of the water, the accepted definition of "salinity" is not useful for the Dead Sea and it has been replaced by an equivalent salinity (Anati, 1999), referred to as "quasi-salinity". Carnallite ($\text{KMgCl}_3 \cdot \text{H}_2\text{O}$) is next to crystallize out, however, this is only expected to happen when the brine reaches a specific gravity of 1300 kg/m^3 (Steinhorn & Gat, 1983).

Table 2 presents a comparison of elemental analyses of water from the Dead Sea, the Jordan River, and the Mediterranean Sea based on more than 40 years of data. Opinions vary slightly as to which salt content the water of the Dead Sea has. Gavrieli et al., (2005) reported a density and salinity of the Dead Sea of about 1237 kg/m^3 and 342.4 g/l, respectively, whereas Vengosh and Rosenthal (1994) reported the Dead Sea salinity to be about 332.06 g/l. Mixing of the water in the Dead Sea due to low waves and wind is slow compared to that in other water bodies e.g. Seas and Oceans. The Dead Sea may thus be considered a stratified water body, based on 44 available data sets on potential temperature, quasi-salinity, and potential density. These data indicate that the depth of the upper layer of the Dead Sea is about 10% of the maximum depth; defined as the average between June 1998 and December 2007 at the Ein-Gedi 320 station (see Figure 2) (ISRAMAR, 2009).

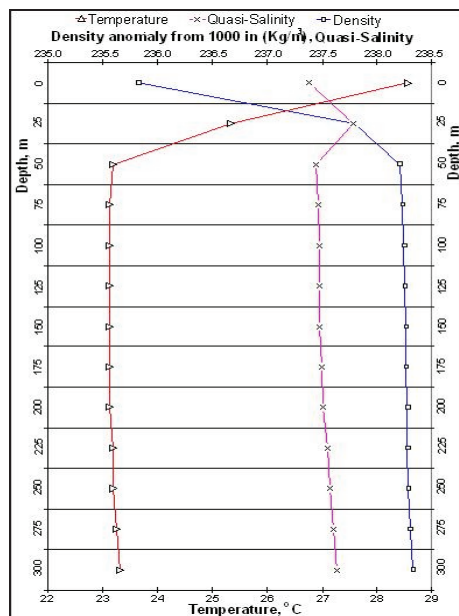


Fig. 2: Potential temperature, quasi-salinity, and potential density of the Dead Sea based on averages from June 1998 to December 2007 at the Ein-Gedi 320 station.

Table 2. Elemental analysis of water from the Dead Sea, the Jordan River, and the Mediterranean Sea concentration are expressed as g/l, (¹¹Gavrieli et al., 2005; ¹⁶Vengosh and Rosenthal, 1994; ^{18,19}Bentor, 1961 and 1969; ²⁰Abu-Khader, 2006; ²¹Katz, 1981; ²²Eckstein, 1970)

Element	Dead Sea					Jordan River		Mediterranean Sea	
	Ref. 19	20	22	16	21	11	19 & 20	23	21
Cl	180.8	208.0	216.0	219.25	224.0	228.6	0.474	23.46	22.90
Mg	34.50	41.96	42.5	42.43	44.0	47.1	0.071	1.558	1.490
Na	33.50	34.94	34.3	39.70	40.1	34.3	0.253	13.34	12.70
Ca	13.00	15.80	17.1	17.18	17.65	18.3	0.080	0.685	0.470
K	6.30	7.56	6.65	7.59	7.65	8.0	0.015	0.466	0.470
Br	4.10	5.92	----	5.27	5.30	5.4	0.004	0.086	0.076

1.3. Results of the previous studies

The decreasing water level in the Dead Sea has been of concern for many years, and the idea of diverting seawater from the Mediterranean Sea or the Red Sea has been discussed several times. Two scenarios for the RSDSC project were studied by Al-Weshah (2000) using a water balance model for the coming 50 years. The first scenario assumes a diversion capacity of 70 m³/s and shows that the Dead Sea will recover its design level of 395 m bmsl in about 40 years. The second scenario assumes a diversion capacity of 60 m³/s and predicts a level of 400.5 m bmsl after about 40 years. The annual net inflow to the Dead Sea from the River Jordan falls from 175 to 60 millions cubic meter (MCM) due to the fact that Jordan is permitted to utilize 20 MCM of the river water directly and to store another 20 MCM in Lake Tiberias during the winter for consumption in the summer months (JRV, 1996a).

Gavrieli and Bein (2006) assuming a diversion capacity of 60 m³/s and a starting elevation in 1995 of about 408.5m bmsl. After 40 years of discharge from a reverse osmosis plant the new elevation was 400.5 m bmsl (Gavrieli & Bein, 2006). In another scenario it was assumed that there was no RSDSC project, and the model showed that the level of the Dead Sea would fall to 444.4 m bmsl. Asmar and Ergenzinger (2002b) modeled a period of 100 years between 1989 and 2088 assuming that the current conditions would prevail. However, the industrial intake increased in the year 2000 by a projected amount of about 25%, leading to a change in water level from 406 to 460m bmsl during the study period in question.

1.4. Objectives of the current study

The extreme decrease in the Dead Sea water level, which is mainly caused by the reduced inflow from the Jordan River, high evaporation, low precipitation, and the intake of water to potash companies around, has resulted in substantial damage to the development of the area around the Dead Sea. The RSDSC project has been considered to be one of the most important elements in a development strategy to provide desalinated drinking water to three countries in the region. The brine discharge from this project is an important alternative to fill the Dead Sea that may significantly raises the level.

The aim of the present study was to investigate methods for understanding the variations of water level and volume of the Dead Sea. However, it is also of interest to predict the impact of the water discharge depending on release point (discharge location for each term) and density values in each term of input and output. Another task is to evaluate the mixing time (i.e. theoretical time for Dead Sea surface water to mix with the entire water body) for the Dead Sea depending on density and salinity of the input and output. It roughly expresses the amount of time that is needed for waters introduced into the Dead Sea to be totally mixed. Two models were developed, namely for a single-layer (well-mixed) system and for a two-layer (stratified) system, to estimate the mixing time when taking changes in the Dead Sea level and surface area into consideration.

2. Overview and background

The principal objective of the RSDSC project was initially to provide desalinated drinking water for the inhabitants of the areas surrounding (Palestinian Authority, Israel and Jordan) (JRV, 1996b). In contrast, the Mediterranean-Dead Sea Canal, first studied in 1973, focused on the generation of electricity and this project was intended to produce about 800 MW during peak hours [26] (Mediterranean-Dead Sea co., 1984). At the end of the 1980s and the beginning of the 1990s the major development goals for the region were re-evaluated. A project was initiated by the Israeli Ministry of Energy and Infrastructure involving hydrostatically driven desalination with reverse osmosis (RO)

membranes to produce fresh water from Red Sea water (Tahal, 1994; Beyth, 2002). The main objectives of the revised project are to provide a sustainable source of fresh water for the region (Palestinian Authority, Israel and Jordan) and to halt the fall in the level of the Dead Sea. The total available hydrostatic head near the Dead Sea end of the proposed canal ranges from 331 to 545 m, depending on the alignment and the pumping head provided at the Red Sea end (Fig. 3) (Al-Weshah, 2000). The capacity of such a conveyance system has been studied for different diversion flow rates ranging from 40 to 70m³/s (JRV, 1996a).

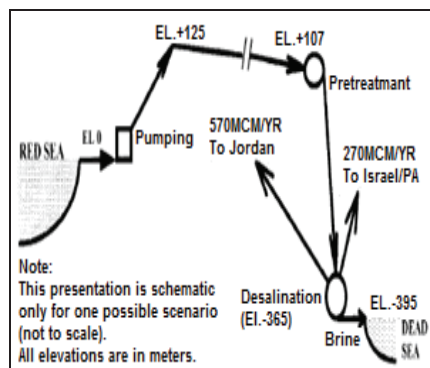


Fig. 3: Schematic layout of the Red Sea-Dead Sea Canal (Al-Weshah, 2000).

The desalination plant is proposed to produce fresh water using the RO method. The estimated annual fresh water production of this plant depends on the capacity of the conveyance system. In one design it could be as high as 850 MCM annually, where the design and economy are limited by the diversion capacity. It is expected that two-thirds of this production will go to Jordan and the rest will go to Israel and Palestinian Authority (JRV, 1996a). The total dissolved solids (TDS) from the desalination plant are expected to be between 200 and 300 mg/l. It is planned to restore the level of the Dead Sea to about 400 m bmsl after approximately 50 years.

Table 3 summarize some properties of the Dead Sea and its output/input, where the river inflow represents the total water received from rivers, springs, and infiltration. Dead Sea level was 390 bmsl, surface area 950 km² and volume of 155 km³ according to the year 1997 and precipitation was found between 70-90 mm and evaporation between 1300-1600mm/y (Gavrieli, & Bein, 2006; Gavrieli, 2000 and 1997).

Table 3. Annual average output/input of the Dead Sea (Gavrieli, & Bein, 2006; Gavrieli, 2000 and 1997)

	Amount (MCM)	Density (kg/m ³)	Salinity (g/l)
Industrial outtake (outtake)	-531	1300	337
Industrial brine (inflow)	+225	1350	500
Brine disposal (inflow) RO	+1100	1045	68
Rivers inflow	+375	1025	20
Evaporation	-928	1000	---
Rainfall	+51.2	1000	---

2.1. Potash and salt works

The salt balance in the Dead Sea is significantly affected by potash and salt exploitation. In the early part of the 20th century, the Dead Sea began to attract interest from chemists who concluded that the lake was a natural deposit for potash and bromine. The Palestinian Authority Potash Company was chartered in 1929 and two more plants were established after 1934; the first plant on the north shore of the Dead Sea at Kalia

and the second in the Sodom area south of the Lashon region. Israel produced 1.77 million tons potash, 206,000 tons elemental bromine, 44,900 tons caustic soda, 25,000 tons magnesium metal, and sodium chloride from the Dead Sea brine in 2001. On the Jordanian side of the Dead Sea, Arab Potash Company (APC), formed in 1956, produces 2.0 million tons of potash annually, as well as sodium chloride and bromine. The power plant on the Israeli side allows the production of magnesium metal (by a subsidiary, Dead Sea Magnesium Ltd.).

2.2. Environmental impact

One of the major aims of the RSDSC project is to compensate for the negative water balance, which strongly affects the Dead Sea water level (see Fig. 4). Figure 4 also presented the main parameters of the Dead Sea to the left at the beginning of the century, level is 390 bmsl, surface area is 950 km² and volume of 155 km³ and to the right the level is 411 bmsl, surface area is 640 km² and volume of 131 km³ is presented at 1997 (Gavrieli, 1997 and 2000). The level recommended in the plan for the Katif alignment was 390 m bmsl (Mediterranean-Dead Sea co., 1984) and only 12 years later for the RSDSC project it was 400 m bmsl (JVA, 1996c). However, the inflow of sea water or concentrated brines could build up an upper layer of lower density, which may create a hypolimnion with unfavorable environmental conditions and high precipitation of gypsum, at the same time causing changes in the biological environment of the epilimnion (Gavrieli, 1997).

The water level has been decreasing over the past 10 years at a rate of about 0.9 m/y, representing an annual water loss of about 600 million cubic meters (MCM). This sharp decrease in water level is due to the withdrawal of fresh water by neighboring countries (over 1000 MCM/y of freshwater), which in the past supplied the Dead Sea. Approximately 200-250 MCM/y of this, corresponding to fall in water level of about 35 cm/y, is attributed to the activities of the Israeli and Jordanian potash and salt works. These industries together pump 400-450 MCM/y from the Dead Sea into evaporation ponds located in the southern basin, where halite and carnallite (KMgCl₃·H₂O) are precipitated. At the end of the process, less than 200 MCM/y of concentrated brines (density = 1.35 kg/l; TDS = 500 g/l) are returned to the Dead Sea (Gavrieli, & Bein, 2006).

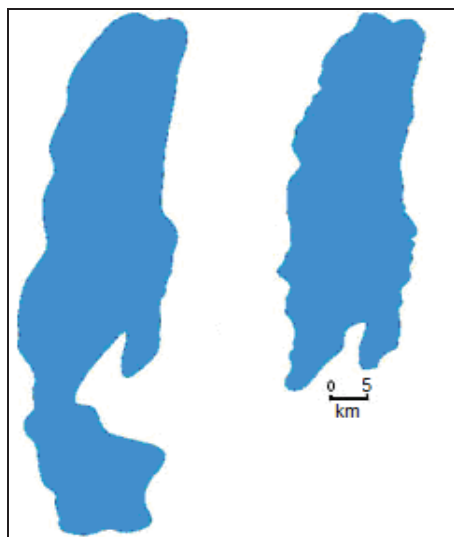


Fig. 4: Level, surface area and volume changes in the Dead Sea at the beginning of the century to the left and at 1997 to the right (Gavrieli, 1997 and 2000)

3. Methodology

3.1. The single-layer system

The system will be described firstly as a single-layer (also called a well-mixed system). The mathematical model used in this study is based on the LOICZ Biogeochemical Modeling Guidelines and has been validated by comparing its performance with other modeling studies of the Dead Sea (Gordon et al., 1996). The model was first employed to describe the dynamic behavior of the Dead Sea using data available in 1997 as initial conditions and simulating the evolution over a 100-year period. Historical data from the period 1976 to 2006 were then used for comparison with simulations obtained with the model. The Dead Sea is not in a steady-state, but was assumed to be close to a steady state during the first year. Water and salt balances may have internal inputs and outputs, but this is only of concern in the two-layer approach. A general mass balance for the Dead Sea system yields:

$$dM/dt = \Sigma \text{Inputs} - \Sigma \text{Outputs} + \Sigma (\text{sinks}) \quad (1)$$

where, dM/dt represents the change in mass of any particular material in the system with respect to time, and Σsinks is the mass of chemical precipitated per unit time. The amount of salt produced has been found in previous study to be approximately 0.1 m annually, and this was included as a sink in the calculations (Lensky et al., 2005).

The various inputs and outputs are illustrated in Figure 5, where the total mass inflow of water from rivers, springs, and infiltration is denoted by Q_{Ri} , and direct precipitation entering the system by Q_P (probably the major source of freshwater in the system). The water used by the Potash Company and other industrial works is denoted Q_{Ind-o} and the brine discharged by these companies Q_{Ind-i} (also called industrial outtake and industrial brine input for the system). The brine discharge from the desalination plant (Q_{RO}), which will come through the RSDSC project is an important factor in this study. Evaporation represents (Q_E) a significant output of fresh water, and is considered to be the most important factor causing the decrease in the Dead Sea level. In principle, the net flow (Q_N), also called the "residual flow" ($Q_N = Q_{Ri} + Q_P + Q_{Ind-i} + Q_{RO} - Q_{Ind-o} - Q_E - \text{sinks}$), can be either to or from the system. It is treated algebraically as an input or an output. The equation describing the water budget of the system can now be rewritten as:

$$(dM/dt)_N = \Sigma(Q_{RO} + Q_P + Q_{Ri} + Q_{Ind-i}) - \Sigma(Q_{Ind-o} + Q_E) - \Sigma \text{sinks} \quad (2)$$

where " $(dM/dt)_N$ " is the same as (Q_N), i.e. the change in the net mass of water with time. This equation describes the water mass budget for the system of interest. It is also possible to write an equation describing the salt mass budget. To obtain the salt budget, an average salinity is assigned to each of the water inputs and outputs. For some of the terms it is sufficiently accurate to assume that the salinity is zero (e.g., precipitation and evaporation (Lensky et al., 2005)). The equation the salt budget is:

$$Q_N S_N = \Sigma(Q_{RO} S_{RO} + Q_P S_P + Q_{Ri} S_{Ri} + Q_{Ind-i} S_{Ind-i}) - \Sigma(Q_{Ind-o} S_{Ind-o} + Q_E S_E) - \Sigma \text{sinks} \quad (3)$$

This equation can be simplified by leaving out the terms in which the salinity is likely to be close to zero:

$$Q_N S_N = \Sigma(Q_{RO} S_{RO} + Q_{Ri} S_{Ri} + Q_{Ind-i} S_{Ind-i}) - \Sigma(Q_{Ind-o} S_{Ind-o}) - \Sigma \text{sinks} \quad (4)$$

where, $S_N = (S_{\text{sys}} - S_{\text{ave}}) / 2$, the average salinity of the whole system (S_N) is the salinity near the boundary between the output

and the input to the system, and it is often adequate to assign this salinity as the average of the adjacent water and the system water. The residual flow (or exchange flow) determines the water mixing time (τ), which is obtained by dividing the system volume (V_{sys}) by the absolute value of the net surface flow, which is estimated from the net flow rate through the receiving water as a result of the water mass balance. Thus, the water mixing time is given by:

$$\tau = V_{\text{sys}} / (|Q_N|) \quad (5)$$

Mixing time in Dead Sea is a calculated quantity expressing the mean time that waters of inputs and outputs (having different composition and salinity) spends to let the system returns to its characteristics. At its simplest this is equals to the result of dividing the Dead Sea volume by the flow in or out (net flow, Q_N) of the system. It roughly expresses the amount of time taken for waters introduced into the Dead Sea to be totally mixed (if possible). This water may be a result of yearly accumulated waters that are added to the Dead Sea, subsequently changing the characteristics of the Dead Sea. It is important that the mixing time of the system is less than one year in order to avoid less dense (e.g. brine water) input from floating in the upper layer, as less dense fluid implies a higher evaporation rate. One example can be mentioned here. When fish is carried into the

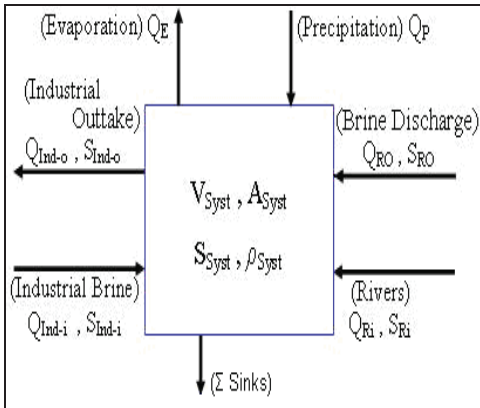


Fig. 5: Schematization of the mass balance for the Dead Sea using a single-layer approach.

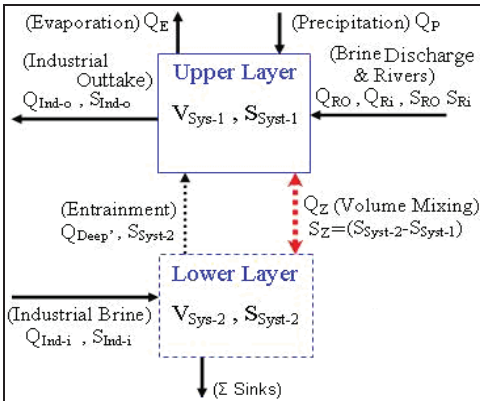


Fig. 6: Schematization of the mass balance for the Dead Sea using a two-layer system, including entrainment flow ($Q_{\text{Deep}'}$), the vertical exchange volume (Q_Z), and the modified exchange time (τ)

Dead Sea by the River Jordan, it dies as soon as the mixing with the saltier waters takes place. This mixing has a specific time. The freshwater doesn't mix immediately with the saltwater and can float for a considerable time on the surface of the Dead Sea. Until the mixing takes place, the freshwater fish and other biota can continue to live in the floating water. Mixing is interesting.

3.2. The two-layer system

The Dead Sea shows relatively strong vertical stratification that can be assumed to resemble a two-layer system (also called a stratified system) (Asmar, & Ergenzinger, 2002a, 2002b & 2003). Such a system is likely to develop in the case of a relatively large fresh water input. Figure 6 illustrates a modified water budget for a two-layer system, which includes entrainment flow ($Q_{\text{Deep}'}$), the vertical exchange volume (Q_Z), and a modified exchange time (τ). The calculations are quite similar to those in the single-layer system, although three further assumptions are needed for the two-layer system:

- The outflow volume associated with freshwater inputs (Q_N) occurs in the surface layer, displacing water in the surface layer of the system ($S_{\text{Sys-1}}$).
- River and industrial flows (Q_{Ri} , $Q_{\text{Ind-i}}$) enter the deep layer, flow upwards into the surface layer, and out again from the surface layer. The combined outflow from the surface layer ($Q_{\text{surf}} + Q_{\text{Ri}}$) has positive sign, whereas both Q_N and Q_{surf} have negative signs.
- The salt balance is maintained through a vertical exchange flow (Q_Z) between the surface and layer and the deep layer (the epilimnion and the hypolimnion).

The calculation of $Q_{\text{Deep}'}$ is possible only if there is a salinity difference between the inflowing deep water and the surface water of the system, $Q_{\text{Sys-1}}$, where $Q_{\text{Sys-1}}$ is about 10% of the total volume of the system. The top layer of the Dead Sea extends approximately 30 m of the total depth of 300 m. Note that this geometry creates a vertical loop circulation, with $Q_{\text{Deep}'}$ flowing upwards within the system (it is also called entrainment flow), carrying water of deep system salinity ($S_{\text{Sys-2}}$) to the surface, which then spread over the surface. To balance the salt, there is an additional term, the vertical mixing term (Q_Z), which exchanges surface and deep water within the system. This vertical mixing term only contributes if there is a vertical salinity difference between the surface and deep water. The salt balance of the surface layer is given by:

$$Q_{\text{RO}}S_{\text{RO}} + Q_{\text{P}}S_{\text{P}} + Q_{\text{E}}S_{\text{E}} + Q_{\text{Ri}}S_{\text{Ri}} + Q_{\text{Ind-o}}S_{\text{Ind-o}} + Q_{\text{Deep}' }S_{\text{Deep}' } - \Sigma \text{ sinks} + Q_Z(S_{\text{Sys-2}} - S_{\text{Sys-1}}) = 0 \quad (6)$$

To find the vertical exchange volume (Q_Z) the salinity terms which are equal to or close to zero must be eliminated. The system inflow is balanced by a vertical flow to the surface layer (Q_Z); and does not enter into the calculations because its magnitude is the same in both vertical directions,

$$Q_Z = (-Q_{\text{Ind-o}}S_{\text{Ind-o}} + Q_{\text{RO}}S_{\text{RO}} + Q_{\text{Ri}}S_{\text{Ri}} - \Sigma \text{ sinks} + Q_{\text{Deep}' }S_{\text{Deep}' }) / (S_{\text{Sys-2}} - S_{\text{Sys-1}}) \quad (7)$$

where $Q_{\text{Deep}'}$ is the flow that enters the deep layer, flows upwards into the surface layer, and out again from the surface layer (circulation):

$$Q_{\text{Deep}' } = Q_N S_1 / S_{\text{Deep}' } \quad (8)$$

where, $S_{\text{Deep}' } = S_{\text{Sys-2}}$. The water mixing times for the two layers are:

$$\tau_1 = V_1 / (Q_{\text{Ind-o}} + |Q_Z|) \quad (9a)$$

$$\tau_2 = V_2 / (|Q_{\text{Deep}' }| + |Q_Z|) \quad (9b)$$

4. Results and Discussion

Data for the Dead Sea were excerpt and collected from varying research to assure the accuracy of the results. This data were collected and calculated considering the changes of meteorological and hydrographical parameters in last 30 years (Gavrieli and Bein, 2006; Gavrieli, 1997 & 2000; Asmar & Ergenzinger, 2002b). This detail of input and output was used for the model validation in the 30 years historical data.

4.1. Single-layer versus two-layer

Two different mathematical models were developed to describe the dynamic behavior of the Dead Sea based on the above-discussed mass balance equations for the single-layer and two-layer systems. The models were employed using data from 1997 and forecasts were made for a 100-year period. The two models

were formulated following the LOICZ Biogeochemical Modeling Guidelines and comparing the results with previous studies of the Dead Sea. Based on the current conditions, the models can be used to predict the future behavior of the Dead Sea for different scenarios, including the proposed RSDSC project. The first model employed encompassed a single-layer for which the water and salt mass balances were derived. Salinity variations and water discharged from the desalination plant were taken into account with and without the proposed project. Significant variations were predicted between the salinities of the output from and input into the system, especially when RSDSC project is considered. Tables 4 and 5 presents a single box model for a well-mixed system used to calculate the water and salt mass balances, giving the residual flow (Q_N) and the mixing time (τ) for: a) salinity variations including RO discharge, and b) salinity variations excluding RO discharge.

Table 4. Results from the single-layer model and two-layer model after one year

		Salinity variation with RO discharge	Salinity variation without RO discharge	Percentage change (%)
Single-layer	Water mass balance:			
	Residual volume, Q_N (MCM/y)	292.2	807.8	63.8
	mixing time, τ (y)	57	110	48.2
	Salt mass balance:			
Two-layer	Residual volume, Q_N (MCM/y)	132	427	69.1
	Residence time, τ (y)	58	116	50.0
	Entrainment volume, Q_{Deep} (MCM/y)	138.3	426	62.8
	Vertical exchange volume, Q_z (MCM/y)	10561.2	7281	31.1
	Exchange time, τ (y)			
	τ_1	1.18	1.68	29.8
	τ_2	11.02	15.3	28

Table 5. Simulations of volume, surface area, level, and cumulative level change in the two models in the Dead Sea with different scenarios, (data based (Gavrieli, 1997 & 2000))

		Water mass balance				Salt mass balance			
		Salinity variation + RO discharge		Salinity variation - RO discharge		Salinity variation + RO discharge		Salinity variation - RO discharge	
Year		Single -layer	Two- layer	Single -layer	Two- layer	Single -layer	Two- layer	Single -layer	Two- layer
1	Vol. (km ³)	131	131	131	131	131	131	131	131
	Area km ²	640	640	640	640	640	640	640	640
	Change (m) (±)	0.0	0.0	0.0	0.0	0.0	0.0	0.0	0.0
	Level (m) bmsl	411	411	411	411	411	411	411	411
30	Vol. (km ³)	139.5	136.96	107.6	105.06	134.8	141.4	118.6	125.14
	Area (km ²)	661.1	654.9	578.0	570.95	649.6	665.79	608.0	625.03
	Change (m) (±)	6.745	4.765	-19.84	-22.09	3.1	8.248	-10.3	-4.788
	Level (m) bmsl	404.3	406.24	431.3	433.41	408.0	402.75	421.3	415.79
60	Vol. (km ³)	148.2	143.13	83.3	78.23	138.8	152.15	105.8	119.08
	Area (km ²)	681.5	669.46	508.5	492.3	659.1	690.61	574.1	609.69
	Change (m) (±)	13.3	9.423	-42.1	-47.24	6.1	16.19	-21.1	-9.694
	Level (m) bmsl	397.7	401.58	453.0	458.56	404.9	394.81	432.1	420.69
90	Vol. (km ³)	157.0	149.29	59.1	51.39	142.7	162.91	93.0	113.02
	Area (km ²)	701.4	683.72	427.8	398.43	668.4	714.58	538.1	593.95
	Change (m) (±)	19.63	13.98	-67.88	-77.26	9.1	23.85	-32.6	-14.73
	Level (m) bmsl	391.4	397.02	479.0	488.58	401.9	387.15	443.6	425.73

Considering the significant differences in the salinities and densities of the input and output and the Dead Sea itself with respect to depth, a two-layer system was judged to provide a better description of the conditions than the single-layer system. The upper layer constitutes in average of about 10% of the total depth, and the rest of the lake constitutes a rather homogeneous lower layer, as shown in Figure 2. The mixing time, (τ), between the two layers, determined by the flow that enters the deep layer (Q_{Deep}) and the vertical exchange volume (Q_z), is an important parameter in characterizing the conditions in the Dead Sea. Table 4 shows a comparison between the results calculation

obtained with the single-layer model and the two-layer model based on previously collected data for 1997 (Gavrieli, 2000). The water and salt mass balances included salinity variations with and without RO discharge. In these calculations, the brine disposal from the desalination plant through the RSDSC was included together with other inputs and outputs (evaporation, rainfall, industrial intake, river inflow and industrial brine). Values of volume, surface area, elevation, and cumulative levels of the Dead Sea for a 100-year period predicted by the single-layer and the two-layer are presented in Figure 7.

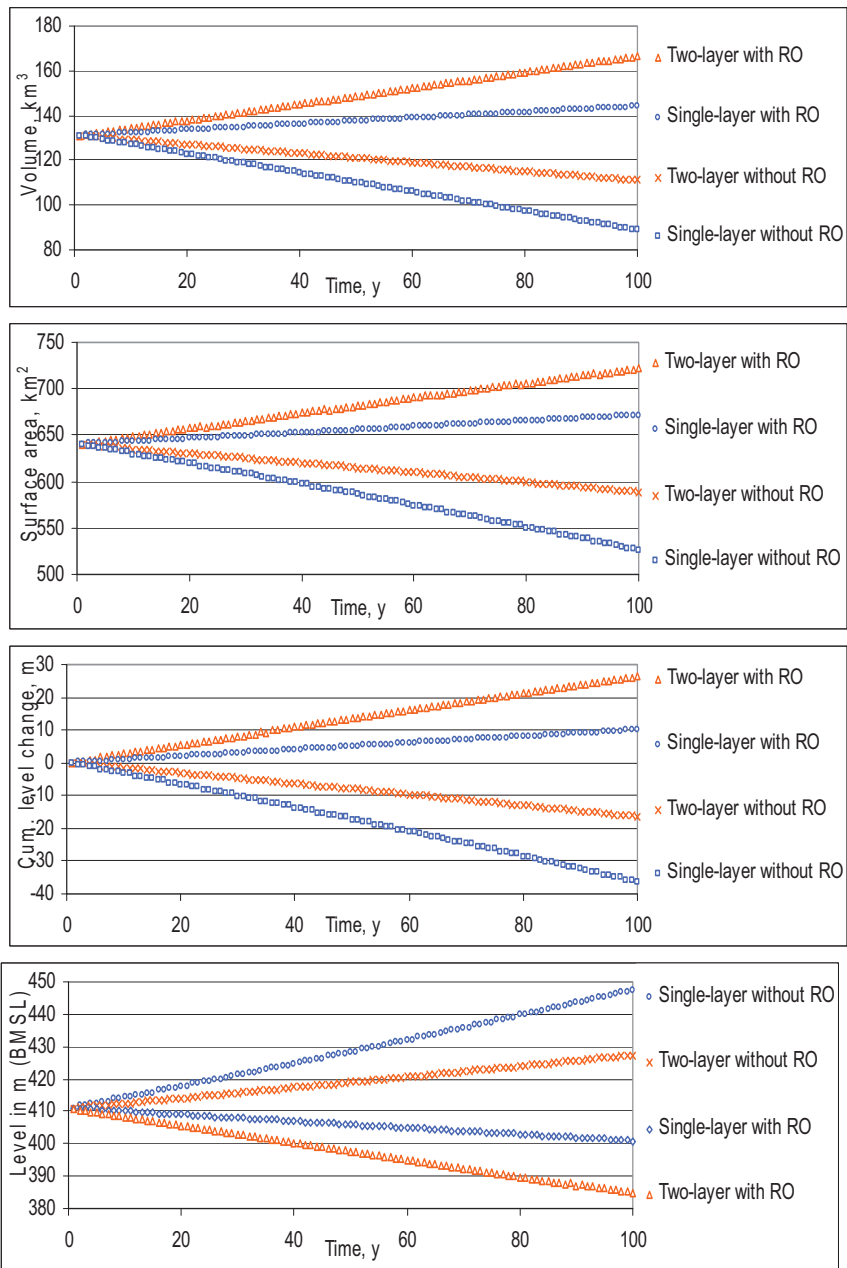


Fig. 7. Predicted Dead Sea volume, surface area, level, and cumulative level change for 100-year period using a single-layer and two-layer model for the salt mass balance considering salinity variations including RO discharge and excluding RO discharge.

4.2. Comparisons between single and two layers

In a single-layer, over a period of 100 years, the elevation was predicted to change from 411 m bmsl (in 1997) to 391.4 m and 479 m bmsl in the cases with and without RO discharge based on a water mass balance, and to reach 401.9 m and 443.6 m bmsl in the two cases based on a salt mass balance. The discharge from the RO-plant affected the level and volume of the Dead Sea significantly. The net residual flow volumes predicted were 292.2 (with RO discharge) and 807.8 MCM/y (without RO discharge), and the mixing time increased by 48.2% when RO discharge was not included in the system. The net residual flow volumes obtained with the salt mass balance were 132 (with RO discharge) and 427 MCM/y (without RO discharge) and the mixing time increased from 58 to 116 years, which is equivalent to about 50% when RO discharge was not included in the system. In the two-layer, after the same period the calculated elevation had changed from 411 m bmsl (in 1997) to 397 m and 488 m bmsl in the two cases (with and without RO discharge, respectively) based on the water mass balance, and to 387 m and 425 m bmsl based on the salt mass balance, respectively. In this model, the exchange times for the upper mixed layer are 1.2 and 1.7 years, including RO discharge and excluding RO discharge, respectively, and 11.0 and 15.3 years for the lower layer with and without RO discharge, respectively. It is found that the exchange time decreased by 29.8% in the upper layer RO discharge was included. When the RO discharge was not included, the exchange time increased by 28% in the lower layer, as can be seen in Table 5. The two-layer model predicted that the amount of (Q_2) needed were about 10.56 and 7.28 ($\times 10^9 \text{ m}^3$) with and without RO discharge, respectively, which represents an increase of 31% that will probably increase the exchange time.

4.3. Historical data comparison

Comparison was also made between historical data and model results using an initial level of 420.6 m bmsl in 2006. Simulation

results covering 30 years, based on water and salt mass balances, using both the single-layer and two-layer model, are presented in Figure 8.

The historical data display significant variations during some years. For example, in 1991 and 1992 there was a large amount of rainfall in the Dead Sea catchment area resulting in a great deal of runoff into the Dead Sea.

The water and salt mass balances using the single-layer model yielded water levels in 1976 of about 398.4 and 398.5 m bmsl, respectively, compared with the 399 m bmsl from historical data. Employing the two-layer model and the water and salt mass balance, a water level of about 401.9 and 400.9 m bmsl, respectively, were predicted for 1976, compared with the observed level 399 m bmsl.

Better agreement was thus obtained when comparing historical data with the single-layer model, with both the water and salt mass balance calculations. Small differences in the results were found with the two-layer model depending on the locations of the output and input and the fact that water with zero or close to zero salinity was excluded, thus omitting the impact of the water with low salinity on the sea level but including all input/output in the water mass balance.

Differences may also be caused by uncertainties in the production of the potash company and the amount of salts extracted from the Dead Sea and poor control of the input and output in the catchment. The annual amount of salt produced was estimated to be approximately 0.1m based on previous study. It was very difficult to find the exact amount of the huge rainfall at the years 1991-92. Beyth et al. (1993), they reported for the same period that the amount of 1.5 billion cubic meters of water was reached the Dead Sea raising it level by about 2 meters.

Therefore, the model results have significant differences in that period because in some the level was added to the Dead Sea was unclear and reported in varying values between 1 to 2 meters. The effected thickness from the additional water formed an upper layer with relatively low salinity was not more than 20 m deep (see Fig. 4 of Beyth et al., 1993).

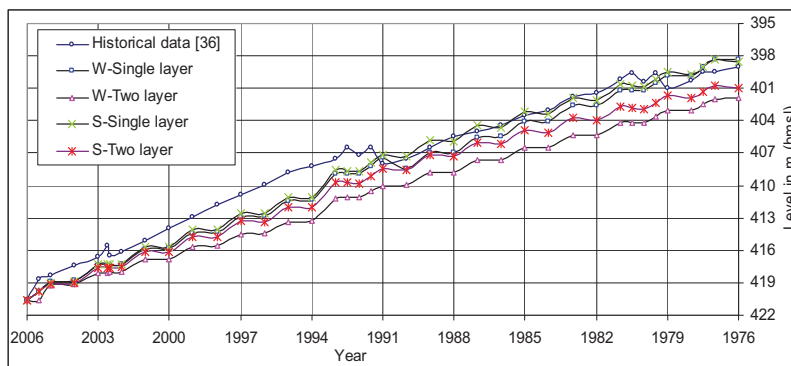


Fig. 8: Level comparison between historical data and the results of calculations based on water and salt balances in the Dead Sea from 2006 back to 1976. W=water mass balance and S=salt mass balance, (²⁶Beyth, 2007).

5. Conclusions

Two models, namely a single-layer model and a two-layer model, were used to predict the behavior of the Dead Sea over periods of various lengths. It was shown that the results depend strongly on differences in the salinity of the input and output water, and the possible disposal of brine from a planned RO desalination plant, which is a part of the Red Sea-Dead Sea Canal project.

This study included simulations of the conditions in the Dead Sea with the models over a period of 100 years, assuming that the current conditions continue or that brine discharge from the RO desalination plant is added to the system.

Mixing times for part of the system with the whole system were significantly different: the two-layer model predicted much lower values than the single-layer model when the RSDSC project was included. Based the results of the two models, the

two-layer description seems to give better results than the single-layer system because the two-layer is describing the condition of the Dead Sea. Compared to previous studies, the single-layer and two-layer models proved to be robust alternatives to the traditional water and salt balance techniques, enabling successful calculations of the water exchange through a relatively simple description of a complex and dynamic system such as the Dead Sea.

The single-layer model predicted 1.4% and 2% higher water levels than the two-layer model using the water mass balance, with and without RO discharge, respectively, while the two-layer model yielded 3.7% and 4% higher values than the single-layer system using the salt mass balance, with and without RO discharge, respectively. Uncertainties in the amount of salt extracted and the production of other chemicals by industrial works that counted as outtake from the Dead Sea that could be one reason for the discrepancies.

References

- [1] Abu-Jaber, N. S. (1998). A new look at the chemical and hydrological evolution of the Dead Sea. *Geochimica et Cosmochimica Acta* 62 (9): 1471–9.
- [2] Abu-Khader M. M. (2006). Viable engineering options to enhance the NaCl quality from the Dead Sea in Jordan. *Journal of Cleaner Production* 14: 80–86.
- [3] Al-Weshah, R.A. (2000). The water balance of the Dead Sea: an integrated approach. *Hydrological Processes* 14 (1): 145–54.
- [4] Anati, D.A. (1999). The salinity of hypersaline brines: concepts and misconceptions. *International Journal of Salt Research* 8: 1–16.
- [5] Asmar, B.N. and Ergenzinger, P. (2003). Effect of the Dead Sea–Red Sea canal modelling on the prediction of the Dead Sea conditions. *Hydrological Processes* 17 (8): 1607–21.
- [6] Asmar, B.N. and Ergenzinger, P. (2002a). Dynamic simulation of the Dead Sea. *Advances in Water Resources* 25: 263–277.
- [7] Asmar, B.N. and Ergenzinger, P. (2002b). Prediction of the Dead Sea dynamic behaviour with the Dead Sea–Red Sea canal. *Advances in Water Resources* 25 (7): 783–91.
- [8] Bentor, Y.K. (1969). On the evolution of subsurface brines in Israel. *Chem. Geol.*, 4: 83–110.
- [9] Bentor, Y.K. (1961). Some geochemical aspects of the Dead Sea and the question of its age. *Geochim. Cosmochim. Acta*, 25: 239–260.
- [10] Beyth, M. (2007). The Red Sea and the Mediterranean-Dead Sea canals project and Israeli Hydrological Service.
- [11] Beyth, M. (2002). The Red Sea and the Mediterranean Dead Sea canals project.
- [12] Beyth, M., Gavrieli, I., Anati D. and Katz, O. (1993). Effects of the December 1991–May 1992 floods on the Dead Sea vertical structure. *Israel J. Earth Sci.* 42: 45–47.
- [13] Eckstein, Y. (1970). Physicochemical limnology and geology of a meromictic pond on the red sea shore. *Geological Survey of Israel, Limnology and Oceanography*, Vol. 15, No. 3. pp. 363–372.
- [14] Gaster, T.H. (1997–2006). The Dead Sea Scriptures in English translation with introduction and notes, Doubleday Anchor Books, (Online Encyclopedia 2006).
- [15] Gavrieli, I. and Bein, A. (2006). Formulating A Regional Policy for the Future of the Dead Sea - The "Peace Conduit" Alternative, Geological Survey of Israel.
- [16] Gavrieli, I., Amos B. and Aharon, O. (2005). The Expected Impact of the Peace Conduit Project (The Red Sea-Dead Sea Pipeline) On the Dead Sea, Mitigation and Adaptation Strategies for Global Change 10: 3–22.
- [17] Gavrieli, I. (2000). Expected effects of the infloat of seawater on the Dead Sea; GSI Current Research 12: 7–11.
- [18] Gavrieli, I. (1997). Halite deposition from the Dead Sea: 1960–1993: In book "The Dead Sea: the lake and its setting", edited by Tina M. Niemi, Zvi Ben-Avraham, Joel R. Gat. Oxford University Press, Oxford, pp. 161–170.
- [19] Gavrieli, I., Starinsky A. and Bein, A. (1989). The solubility of halite as a function of temperature in the highly saline Dead Sea brine system. *Limnol. & Oceanogr.* 34: 1224–1234.
- [20] Gordon, Jr. D. C., Boudreau, P. R., Mann, K.H., Ong, J.-E., Silvert, W.L., Smith, S.V., Wattayakorn, G., Wulff F. and Yanagi, T. (1996). LOICZ Biogeochemical Modeling Guidelines. LOICZ Reports & Studies No 5: 1–96.
- [21] ISRAMAR (2009). Israel Oceanographic and Limnology Research, Israel Marine Data Center: <http://isramar.ocean.org.il/> (last update October, 2009).
- [22] JRV (1996a). (Jordan Rift Valley). The JRV Integrated Development Study: Water Resources. The Harza JRV Group.
- [23] JRV (1996b). The Harza Group, Red Sea-Dead Sea Canal Project, Draft Prefeasibility Report, Main Report. Jordan Rift Valley Steering Committee of the Trilateral Economic Committee.
- [24] JVA (1996c). (The Jordan Valley Authority). Tourism development project of the East Coast of the Dead Sea. Feasibility Study Report. Amman, Jordan.
- [25] Katz, A., Starinsky, A. and Taitel-Goldman, N. (1981). Solubilities of gypsum and halite in the Dead Sea and in its mixtures with seawater *Limnol. Oceanogr.*, 26(4): 709–716.
- [26] Krumgalz, B.S., Hecht, A., Starinsky A. and Katz, A. (2000). Thermodynamic constraints on Dead Sea evaporation: Can the Dead Sea dry up? *Chemical Geology* 165: 1–11.
- [27] Krumgalz, B.S., Pogorelsky R and Pitzer, K.S. (1995). Ion interaction approach to calculations of volumetric properties of aqueous multiple solute electrolyte solutions. *Journal of Solution Chemistry* 24: 1025–38.
- [28] Lensky, N. G., Dvorkin, Y. and Lyakhovsky, V. (2005). Water, salt, and energy balances of the Dead Sea Water Resources Research, VOL. 41.
- [29] Levy, Y. (1984b). Evaporation from the Dead Sea. *Mediterranean-Dead Sea projects*, Earth Sci. Res. Admin., Summ. Res. Surveys 5: 201–210.
- [30] Mediterranean-Dead Sea co. (1984). *Mediterranean-Dead Sea Project Planning and Prefeasibility*, (in Hebrew) pp. 114.
- [31] Salt Works (2001–2006). <http://www.saltworks.us/shop/product.asp?idProduct=8>
- [32] Steinhorn, I. and Gat, J.R. (1983). The Dead Sea. *Scientific American* 249: 84–91.
- [33] Tahal (1994). *Mediterranean-Dead Sea Hydroelectric Project: Updating of works for reevaluation of alternatives*. Summary Report (in Hebrew): Prepared for the Ministry of Energy and Infrastructure: 2 vols. 1-106p., 2-64p.
- [34] Vengosh, A., and Rosenthal, E. (1994). Saline groundwater in Israel: it's bearing on the water crisis in the country. *J. Hydrol* 156: 389–430.
- [35] Wisniak, J. (2002). The Dead Sea a live pool of chemicals. *Indian Journal of Chemical Technology* 9 (1): 79–87.

Paper IX

Impact on Seawater Composition from Brine Disposal at EMU Desalination Plant

Bashitialshaaer, R., Persson, K.M., Larson, M., and Ergil, M. 2007

Proceedings 11th IDA World Congress-Maspalomas, Gran Canaria –Spain, October 21-26,
2007.

Impact of Brine Disposal from EMU Desalination Plant on Seawater Composition

Authors: Raed A.I. Bashitialshaaer, Kenneth M. Persson, Magnus Larson, Mustafa Ergil

Presenter: Raed A.I. Bashitialshaaer
PhD researcher-Lund University, Sweden

Abstract

This study deals with the desalination plant at the Eastern Mediterranean University (Cyprus) and its environmental impact. The reverse osmosis plant produces normally 42m³/hr potable water from 120m³/hr feed. The feed concentration reaches up to 36,000ppm TDS, while an approximate amount of 73.8m³/hr is led out from a pipe of 10inches diameter with a concentration of about 56,000ppm and the permeate 400ppm of potable water. A maximum brine discharge concentration of about 74,180ppm TDS was recorded close to the outlet. During brine disposal an increase in salinity in the coastal zone is observed. To overcome the potential impact of brine disposal and facilitate an optimal operation in the coastal and marine environment, the basis for a solution strategy was developed.

Due to the high salt concentration in the brine disposal to return the sea, impacts on the environment can result from the brine discharge, which contains some chemicals used in the desalination process that may affect the coastal areas and the marine ecosystem negatively. Many plants use biocides such as chlorine to clean pipes or to pre-treat the water. These chemicals should be removed before the brine is released to the ocean, which is not always the case.

A part of this study started 10 days after the plant had been fully stopped, in other words the plant had zero discharge to the sea during the analysis period when repairs took place. Based on measurements during this period, comparisons could be made between full-capacity brine discharge and non-working plant. The pipeline of the brine discharge into the sea was located in shallow water, and the measurement depth in front of the pipe outlet was 30 cm and the average depth in the investigated region was about 2.5m. Corresponding data were taken during operation of the reverse osmosis plant as well. Finally, a simple two-dimensional mathematical model of the discharge and an evaluation of the effect of the brine disposal on the marine chemistry was developed.

I. INTRODUCTION

1.1 General

With population growth and the recent several year long droughts contributing, concerns about water scarcity have emerged causing several communities and researchers to propose construction of desalination plants. Because virtually all seawater desalination plants will be located in the coastal zone, the construction and operation of the facilities generally will have to adopt to strict environmental protection rules for costal zones and other legislative issues related to desalination discharge. The legal demand on desalination plants vary however between countries. More knowledge of how brine discharge affects recipients is needed.

As a case study, the effects of brine disposal from a desalination plant of the Eastern Mediterranean University (EMU) were investigated in detail and a comparison was made with some other desalination plants. During brine disposal the increase in salinity within the coastal water was significant. To overcome this potential impact of the brine disposal on the coastal and marine environment during operation, the basis a solution strategy was developed. A part of this study started 10 days after the plant had been fully stopped, in another words, the plant had (zero) discharge to the sea during the analysis period because of repair. Therefore, it was a good opportunity to determine the time for the coastal area where the brine was discharged to reach the normal conditions of the seawater.

II. DESALINATION AND BRINE DISPOSAL IMPACTS

2.1 Desalination Plants

Desalination, the process of removing salt, other minerals, or chemical compounds from impure water, has provided a limited source of potable water especially in the Middle East countries (e.g. Libya, United Arab Emirates, Oman, Saudi Arabia, and Cyprus). The water from the sea, ocean, and Gulf resources is used for the desalination plant input to provide potable water to coastal and island communities whose ground and/or surface water supplies have been reduced or eliminated. Water shortages may be the result of events such as droughts, contamination, salt water intrusion, or limited water sources, even after water conservation methods have been implemented. Thus, desalination has received increasing attention in drought years when water supplies become greatly threatened or diminished. The conventional desalination methods are mainly based on physical separation processes that use seawater having a brine concentration of 4,000–35,000 ppm [1].

2.2 Desalination Plants Worldwide

Until April 2004, the total desalination capacity of RO-plants was close to 3,500,000 MGD (16×10^9 m³/d), which is half of the entire desalination capacity worldwide. Membrane desalination is the fastest growing technology, and it is expected to become the prevalent desalination technology for the 21st century. Table 1 provides summary information on the global production of desalinated water by plant capacity and desalting process [2].

Unit Capacity (m ³ /day)	Capacity MCM/d	Capacity MGD	Number of plants	Capacity RO %
100-500	22.57	4,965	12,433	39.1
500-4,000	21.36	4,699	6,436	37.9
4,000-60,000	14.48	3,186	1,311	25.7
Total	58.41	12,850	20,180	35.3

Table 1: Summary of worldwide desalination plant capacity [2]

2.3 Waste Discharges from Desalination Plants

The major parameters of water discharged from the desalination plants mainly depend on the desalination technology used; the quality of the intake water; the quality of water produced; and the pretreatment processes, cleaning and washing of some parts, and RO membrane storage. In general, discharges from desalination plants may have the following types of potentially adverse constituents and qualities [3]:

- High salt concentrations discharged to the coast;
- Turbidity levels above those of receiving waters;
- Different type of chemicals from pretreatment processes of the input;
- Chemicals used to preserve the RO membranes.

Salt concentrations may be reduced by mixing brines with other discharges, such as wastewater; yet, this mixing may also cause sewage contaminants and other particulates to aggregate in particles of different sizes than they would otherwise. This effect influences rates of sedimentation, and is highly important for determining the well-being of benthic organisms that may be buried or burdened by an increase in deposition of unstable and/or finely suspended materials. If the particles are smaller and stay in suspension, they could interfere with transference of light in the ocean, which would diminish the productivity of kelp beds and phytoplankton. In addition, redistribution of trace metals and nutritionist (e.g., iron, ammonia, and phosphates) could change the phytoplankton community to one that is unappetizing to fish and may also be toxic (for example, by increasing the possibility or prolonging the occurrence of a "red tide" condition) [4].

2.4 Brine Discharge and Hydraulic Effects

The desalination process creates brine with salinities higher than naturally found in coastal waters of Cyprus and in greater volumes than the freshwater produced. Disposal of brine into coastal waters is an economical option for the desalination projects if legally allowed. After discharge, dense brine water flows below the less-dense ambient water to form a stratified cap over the bottom sediment. Typically, it is not the quantity of salt discharged that causes a problem; it is the mixing rate and the brine's fate prior to complete mixing that determines impacts. If natural forces of plume flow, wind mixing and tidal currents are slow to mix the brine with the overlying water, biogeochemical processes in the sediment may deplete the available dissolved oxygen near the bottom, causing hypoxic (low oxygen) conditions that harm aquatic life [5,6].

The following potential coastal zone impacts should be considered in evaluating proposals for the desalination plants:

- Impacts to the marine environment from continuous discharges of hazardous chemicals from brine disposal;
- Impacts to commercial fishing and navigation during construction of intakes and outfalls and during operation;
- Interference with public access and recreation from pipelines, wells or other structures;
- Noise from pumps during operation;
- Impacts on the desalination process from pollution near the intake pipes;
- Use of landfill disposal space for solid waste disposal.

2.5 Environmental Acceptance

To develop an environmentally acceptable project, the developer needs to address the latest issues of desalination plant technology while taking into consideration the sustainable development principles. In such cases, the national and public authorities should be encouraged to consider sustainable development in the early stages of the planning process (e.g., site selection, plant capacity, and brine discharge).

2.6 Chemical Analysis of Brines from Reverse Osmosis Plants

Brines are not just concentrated seawater. All desalination plants use chlorine or other biocides, which are hazardous to the coastline environment and this is known as pre-treatment processes. Moreover, in case if the plant is shut down for any reason some chemicals (usually sodium bisulfite) will be used to protect membrane. These chemicals should be treated before discharge to the sea, to reduce any potential effects. Due to these chemicals, some fish like Larval fish that feed on the phytoplankton could be forced beyond nearshore waters, where they may not survive. The concentration of major ions in the brine appears logically to be proportional to those measured in the input. The study of chemical analysis for the brine, input, potable water, and water from evaporation ponds (or bores) were determined from both United Arab Emirates and Sultanate of Oman [7]. Table 2 provides feed-water and brine disposal for the chemical characteristics data to selected small-scale desalination plants in Oman and UAE. These data were obtained from a single sampling of water and brine from various (RO) desalination plants during field visits.

Chemical Parameter	Name of the plant							
	Qidfa I		Qidfa II		Jabal al-Dhana		Omani plant Esherjah	
	Feed	Brine	Feed	Brine	Feed	Brine	Feed	Brine
Calcium (ppm)	464	617	533	730	636	760	490	841
Magnesium (ppm)	1640	2150	1620	2240	2140	2660	1,100	1,900
Sodium (ppm)	11,900	15,100	12,200	15,800	14,200	17,700	8,630	14,800
Chloride (ppm)	23149	30,540	23,484	32,004	27,098	34,839	15,868	24,062
Sulfate (ppm)	2787	3931	3181	4500	3121	4602	4,104	6,139
E.C (µS/cm)	55,700	73,300	56,130	78,000	65,900	81,100	41,900	61,100
TDS (ppm)	40,592	53,177	41,661	56,158	47,940	61,587	48,510	--
Potassium (ppm)	574.0	767.0	581.0	805.0	661.0	950.0	631	--

Table 2: Chemical characteristics of feed-water and brine disposal of Oman and UAE plants [7]

III BRINE DISCHARGE STUDIES

3.1 Studies of Salinity Changes in Recipients

Some researchers have studied and reported the effect of brine discharge from desalination plants. Perez and Quesada [8] provided a study of the brine discharge of the Gran Canaria desalination plant. Their samples were taken in front of the brine discharge outfalls, at the bottom, intermediate and surface level, about 20m from the outfalls. As seen from the data, the initial dilution of the brine over the first few meters was high and it continued almost uniformly through the whole column of the water.

The brine concentration decreased from a salinity of 75.1 (discharge salinity in psu) to a salinity of 38.4 at the seabed and 37.0 on the surface. At a location about hundred meters away, the salinity of the sampled water was very near to the normal values for the seawater of the area, that is, in summer it is around 37 practical salinity units (psu). The theoretical studies indicated that the brine tends to gather at the bottom, once it stops being affected by the effects of the discharged jet and it reaches a balance with the surrounding environment according to the density conditions [8].

Another example was obtained from Javea desalination plant which is located at the Mediterranean coast in Spain [9]. Highest salinities were located inside the Channel of the Fontana and in the proximities of the outlet. The salinities of the superficial water ranged between 37.3 and 43.5 psu, at the bottom between 37.4 and 42.3 psu, and in the interstitial water between 37.4 and 39.9 psu. These tendencies required in the samplings carried out during the 2004. In summer similar influence areas were obtained while in winter the dilution was very high and a certain increment of salinity was only observed in the internal part of the channel [9].

Surface salinity could be homogenous around the brine discharge pipe with no clear trend at any position. The dilution close to the discharge took place rapidly, but an increased salinity could be found far from the outlet. It was possible to observe an increase higher than 0.5psu above an average salinity in the area up to 4km from the discharge. These results and conclusions were found after three surveys of the Alicante desalination plant during February, April, and August 2004 [10].

IV THE EMU PLANT

4.1 Study Area

The Mediterranean Sea covers an area of 2.5 million square kilometers (km²), excluding the Black Sea, and has an average depth of about 1500 m. As a sea it is rather unique in that it is almost completely surrounded by land: Europe to the north, Africa to the south, and Asia Minor to the east. During winter time, a combination of cold air temperature and mixing of the surface water due to storms destroys the thermo-cline [11]. The EMU's plant is located at the coast of Cyprus. It is one example of a Mediterranean Sea Island where seawater is used for desalination due to lack of sufficient groundwater supply within the country.

The Eastern Mediterranean University is the oldest and the largest university in Cyprus with over 13,500 students, including dormitories with a capacity of 4,500 students and more than 2,000 staff. The University is located in a campus stretching over an area of 2,000,000m², near the city of Famagusta. Within the campus area, 154,000m² of green areas exist with over 60,000 trees.

For a considerably period of time, the University had been supplied with insufficient amounts of water from the Famagusta Municipality. The municipal water carries a level of salt (TDS) that is too high both for indoor uses and for irrigation purposes. This insufficient amount of water was supplemented by water obtained from wells belonging to the University and/or water purchased from external sources.

However, these sources of water were usually unreliable due to frequent droughts in the Island, as well as generally having poor quality. At present, daily water needs for the University is determined to be $2,000\text{m}^3$ and $1,200\text{m}^3$ of this amount is currently supplied from the Municipality, while the rest is obtained from a desalination plant belonging to the University, which operates through the principle of reverse osmosis (RO). The desalination plant was built in 1998 and has a capacity of $1000\text{ m}^3/\text{day}$ (location shown in Figure 1). At present the University plans to increase the capacity of this plant to meet the increase in the number of student to a total amount of $3,000\text{m}^3/\text{day}$ [12].

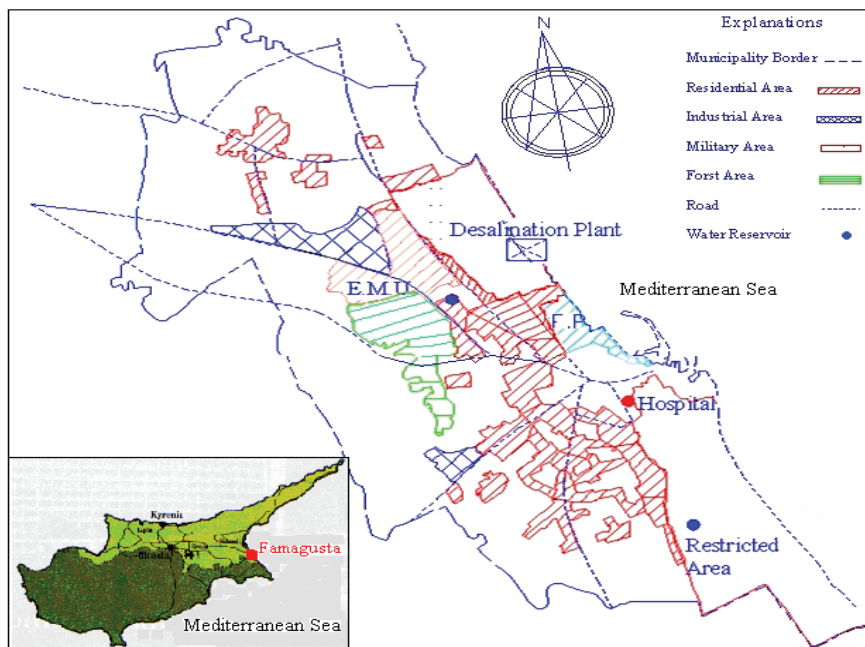


Figure 1: Desalination plant location in Famagusta city, North Cyprus

4.2 In and Output of EMU Desalination Plant

The RO-system utilized in the EMU desalination plant is fed with $115.83\text{m}^3/\text{hr}$ seawater obtained from three parallel pipes 30m from the coastline at an average depth of 15m. The seawater contains 36,000-40,000ppm as TDS. To save membrane life, around 36.3% of the feed water is obtained as permitted output (permeate) and the remaining amount is considered to be waste discharge (brine disposal). In this way, 42 m^3 of seawater per hour is released as a high quality output (EMU desalination plant produces water quality of less than 400ppm (TDS), which can be used for drinking water), while an approximate amount of $73.8\text{m}^3/\text{hr}$ is led out of the system as a brine with salt concentration of about 56,000ppm TDS [12].

V. METHODOLOGY AND SAMPLING

In this study some chemical and other factors have been analyzed as a function of the brine disposal from the desalination plant. Some of the analytical results from the beginning of the study period are presented in Table 3 (Ca, Mg, Cl, SO₄, Na, pH, K, Electrical Conductivity, Alkalinity, and TDS).

The sampling locations were assigned with respect to an x and y axis; x is the location of each point towards seawater and perpendicular to the coastline and y is the location assigned parallel to the coastline. The sampled parameters are important for fish life and coastline environmental impact. The laboratory analysis of this study was carried out by the State Laboratory of North Cyprus.

Samples were collected in the vicinity of the brine discharge outlet. One sampling point was located directly in front of the outlet (pipe outlet system) with the purpose of determining the initial concentration of the brine and the discharge at the surface of shallow seawater.

The other positions from where the samples were collected were determined by fixing steel bars with exact dimensions using measurements in y and x coordinates and extending a rope for each to ensure that during each sampling day having the same points in the field would be used in the aimed area as shown in Figure 2.

The following is a description of the sampling points and how they are denoted:

- Two reference points were selected taking into consideration the ecological status and the bathing areas 65m away from the pipe outlet to the right and left to compare the results of the analysis (denoted as S_{R65m} and S_{L65m}).

PhD THESIS FIRST EXPERIMENT 02-03-2005



Picture 1: Taking samples and recording on them

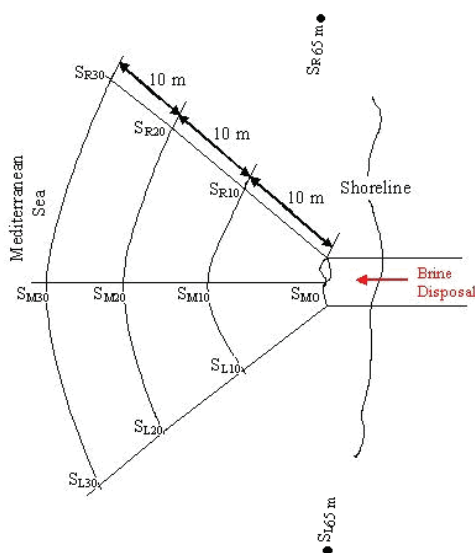
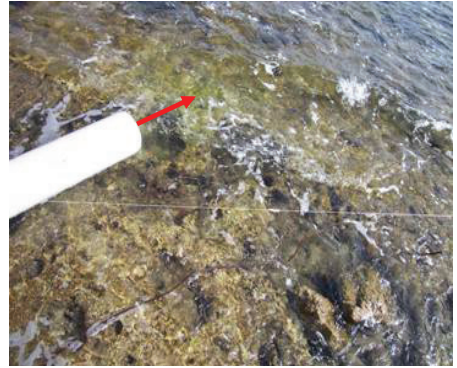


Figure 2: Outlet from desalination plant and sampling positions

- Samples were collected in the open sea separated with a distance of 10m between each point, with a sampling period of 15 days; the samples were collected following three radial lines starting from the discharge point with a separation from midline of about 45° each.
- Samples taken on the left hand side were denoted (S_{L10} , S_{L20} and S_{L30}), on the right hand side (S_{R10} , S_{R20} , and S_{R30}) and along the middle points (S_{M0} , S_{M10} , S_{M20} , and S_{M30}).



Picture 2: Brine disposal pipeline towards the sea

Table 3 presents both the overall average of zero-capacity discharge versus full-capacity discharge to compare some of the chemical variation with respect to time. As seen in (Picture 1), samples were collected and recorded twice a month trying to find calm weather each time. During most of the sampling the weather was good but during one sampling event it was windy with marked wave action along the coastline that may have affected some of the data. The pipeline of the brine discharge towards the sea and the depth conditions are shown in (Picture 2). The depth close to the pipe outlet was about 30cm and the average depth in the investigated shore area was 2.5m.

Sample name	Coordinates		Concentrations, ppm						El. Cond. $\mu\text{S/cm}$
	X (m)	Y (m)	TDS	Ca	Mg	Cl	Na	SO_4	EC
M_{0m}	0	0	38,360	480	1,458	22,720	11,800	862	52,800
M_{10}	0	10	38,020	520	1,397	23,075	11,800	211	46,500
M_{20}	0	20	38,350	500	1,390	22,720	11,800	740	45,400
M_{30}	0	30	38,610	500	1,519	23,075	11,800	672	48,600
R_{10}	7,07	7,07	38,570	480	1,480	22,543	11,800	1,102	43,000
R_{20}	14,14	14,14	38,480	480	1,495	22,898	11,800	767	48,700
R_{30}	21,21	21,21	38,600	460	1,519	22,720	11,800	1,056	46,500
R_{65}	65	0	40,200	440	1,568	22,010	11,800	3,217	51,000
L_{10}	-7,07	7,07	40,790	520	1,384	22,543	12,600	2,098	47,800
L_{20}	-14,14	14,14	39,060	480	1,593	22,72	11,800	1,080	51,900
L_{30}	-21,21	21,21	38,620	520	1,507	23,075	11,800	671	43,800
L_{65}	-65	0	38,560	500	1,519	23,075	11,800	647	49,500

Table 3: Sampling results at the beginning of the study, 2nd March 2005

	Full Capacity Brine Discharge						Zero Capacity Brine Discharge					
	TDS ppt	EC mS/cm	Ca ppt	Mg ppt	Cl ppt	Na ppt	TDS ppt	EC mS/cm	Ca ppt	Mg ppt	Cl ppt	Na ppt
M_{0m}	74.18	83.4	0.84	2.438	34.26	22.40	41.72	50.46	0.51	1.613	23.90	12.73
M₁₀	58.77	62.5	0.64	1.678	24.85	18.00	41.06	47.03	0.52	1.568	23.64	12.57
M₂₀	51.82	60.9	0.58	1.495	23.96	16.00	40.69	50.35	0.51	1.561	23.02	12.37
M₃₀	52.58	60.5	0.62	1.580	23.25	16.00	41.72	47.47	0.53	1.615	24.02	12.73
R₁₀	56.41	61.4	0.58	1.605	23.96	17.40	42.37	50.54	0.51	1.591	24.32	13.00
R₂₀	52.08	60.9	0.50	1.776	25.92	16.00	41.08	49.53	0.51	1.591	23.34	12.50
R₃₀	53.46	61.0	0.54	1.617	23.43	16.40	41.54	48.79	0.51	1.587	23.55	12.67
R₆₅	50.90	60.3	0.46	1.568	24.14	16.00	41.87	52.17	0.49	1.574	23.61	12.77
L₁₀	52.26	59.8	0.62	1.470	22.72	15.60	41.90	47.80	0.51	1.542	23.70	12.87
L₂₀	51.58	60.2	0.60	1.470	22.54	15.80	42.53	52.08	0.52	1.599	23.84	13.00
L₃₀	49.65	60.4	0.54	1.752	22.72	14.80	41.43	50.41	0.51	1.511	23.52	12.77
L₆₅	49.93	60.1	0.48	1.580	22.37	15.20	42.42	50.27	0.52	1.615	24.08	12.97
R₁₀₀	50.90	60.3	0.46	1.568	24.14	16.00						
L₁₀₀	52.29	59.9	0.44	1.654	21.48	15.80						

Table 4: The average of zero-capacity discharge (2nd March 2005-18th May 2005) versus full-capacity discharge at October, 19 2006

VI. MATHEMATICAL MODELING

6.1 Theoretical Formulation

A mathematical model was developed of the brine discharge and its spreading in the nearshore based on simple jet theory. It was assumed that the conditions were uniform through the water column and that the discharge behaved like a plane jet that expanded primarily due to entrainment of ambient water at the sides. Some distance away from the discharge point the assumption of vertical uniformity will clearly be violated and the brine will spread as a gravity current along the bottom, but observations in the study area indicated that the conditions did not vary significantly through the water column. Friction along the bottom was also neglected in the model discussed here.

Three equations govern the evolution of the jet, that is, conservation of water flow, momentum flux, and flux of the constituent of interest, expressed as, respectively (compare with [13]),

$$\frac{d}{dx}(\sqrt{\pi}u_mhb) = 2\alpha hu_m \quad (1)$$

$$\frac{d}{dx}\left(\sqrt{\frac{\pi}{2}}\rho u_m^2hb\right) = 0 \quad (2)$$

$$\frac{d}{dx}\left(\frac{\sqrt{1+\lambda^2}}{\lambda}\sqrt{\pi}(c_m - c_a)u_mhb\right) = 0 \quad (3)$$

where u is the velocity, b the width, c the concentration, h the water depth, x a coordinate pointing offshore, ρ a representative density, α an entrainment coefficient, λ an empirical coefficient relating the spread of concentration and velocity in the jet ($\lambda=1.2$), and subscripts m and a denote conditions at the centerline and in the ambient, respectively. In the derivation of equations 1-3, self-similar profiles were assumed for the velocity and concentration following a Gaussian distribution yielding $u(x, y) = u_m(x) \exp\left(-(y/b(x))^2\right)$ and $c(x, y) - c_a = (c_m(x) - c_a) \exp\left(-(y/b_T(x))^2\right)$, where y is an alongshore coordinate and b_T the width of the concentration profile. The equations will not be valid until some distance downstream the discharge point where the initial top-hat distributions have been transformed to Gaussians shapes. It was assumed in the present study that the first sampling point was sufficiently far from the pipe exit to fulfill the conditions for self-similarity.

Solving Eqs. 1 and 2 yields the evolution of the centerline velocity,

$$u_m = \left(\frac{1}{u_o^2} + 2\sqrt{2}\alpha \frac{\rho}{M_o} \int_0^x h(x) dx \right)^{-1/2} \quad (4)$$

where u_o is the velocity and M_o the momentum flux (conserved during jet evolution) at $x=0$. The solution is valid for an arbitrary variation in the bottom elevation assuming constant conditions alongshore. The centerline concentration of a constituent is given by,

$$c_m - c_a = (c_{mo} - c_a) \left(1 + 2\sqrt{2}\alpha \frac{\rho u_o^2}{M_o} \int_0^x h(x) dx \right)^{-1/2} \quad (5)$$

where c_{mo} is the centerline concentration at $x=0$.

6.2 Comparison with Field Measurements

The measurements along the centerline of the brine discharge were compared with the theoretical solution given by Eq. 5. A plane-sloping bottom profile according to $h(x) = h_o + mx$ was assumed, where h_o is the water depth at the first measurement point (M_o) and m the bottom slope ($h_o=0.3$ m and $m=0.073$; $\int_0^x h(x) dx = h_o x + mx^2 / 2$). The entrainment coefficient was set to $\alpha=0.054$ following [13], the flow at the pipe exit was $Q=73.8$ m³/hr=0.0205 m³/s, and the diameter $D=0.254$ m. The momentum flux was estimated from $M_o = \rho U^2 \pi D^2 / 4$, where $U = 4Q / \pi D^2$.

Only one parameter was difficult to specify in the solution, namely u_o , which is the velocity at $x=0$ corresponding to the centerline velocity at point M_o . The exit velocity at the pipe is assumed to follow a top-hat distribution and the centerline velocity for a Gaussian distribution that would produce the same flow rate and momentum flux is $u_{mp} = \sqrt{2}U$. However, because point M_o is located some distance downstream the pipe exit and the transition of the profile from a top-hat to a Gaussian is complex and might not have taken place completely, a calibration coefficient was introduced to modify the value of the velocity at $x=0$ according to $u_o = C_v u_{mp}$. A value of $C_v = 0.5$ was applied in all calculations.

The measured concentration in point M₀ was used as input value in Eq. 5 and the ambient concentration was set as the average between points R₆₅ and L₆₅.

Figure 3 displays the results of a comparison between calculated and measured concentrations for the studied constituents. In general good agreement is obtained between the simple model and the measurements, although over- or under-prediction is observed depending on the particular constituent studied.

This is a study of the first desalination plant that was built in Northern Cyprus belonging to the Eastern Mediterranean University for distilling seawater. Due to new development their must be improved control of this facilities in order to know the effects of the discharge and to minimize any type of environmental impact. The plant is not big nor is the discharge, compared with typical municipal desalination plants. Still the recipient has an increased salinity for 10-20 m from the discharge pipe outlet. Possibly could this be minimized by using more outlets and/or longer pipelines towards the sea. Changing the direction of the brine discharge could also minimize the impact on the coastline.

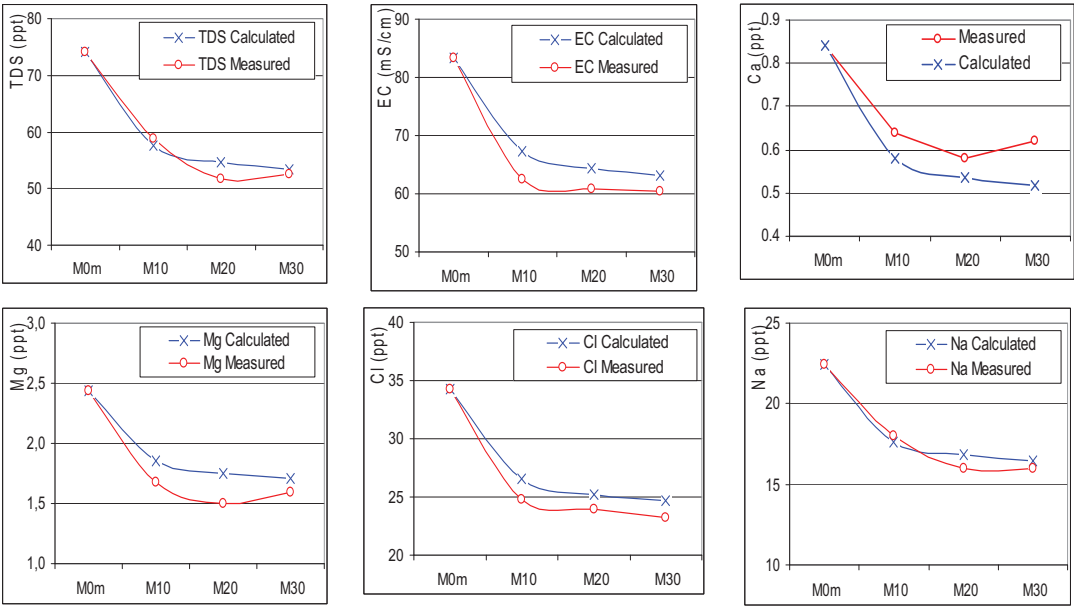


Figure 3: Comparison between calculated and measured spatial evolution of the concentration along the centerline of a brine discharge for different constituents

VII. RESULTS AND RECOMMENDATIONS

Since the starting up of the desalination plant and the brine discharge to the coastline, no study was carried out concerning the dispersion and dilution of the discharged water, but most of the analyses were performed during no-discharge conditions. Therefore, these data were suitable to analyze the brine disposal as well to be able to define the environmental impact that may be present in the area. As mentioned above, the analysis was carried for the period between the 2nd of March 2005 and the 18th May 2005 at the time the plant had been stopped for repair (zero-brine discharge). Subsequently, another sampling test was carried out when the plant was working full capacity (full-capacity brine discharge) in order to compare between both analyses.

In order of getting a real representation of the salinities variations in the space an interpretation of the data campaign was made using the kriging technique. Some of the samples varied significantly due to the influence of the seasonal effect in the hydrodynamic conditions and climatic changes (e.g. wind speed, wave force, rainfall, and evaporation).

In these campaigns, the samples have been taken from twelve different stations homogeneously distributed surrounding the brine discharge and each of the sampling point was positioned with a rigid steel bar (accuracy of $\pm 0.5\text{m}$ around the point). The samples were analyzed in the State Laboratory of Northern Cyprus (Governmental) with an accuracy of ($\pm 5\%$). As seen in (Figure 4) the concentrations at the most distant sampling points of Total Dissolved Solid, Calcium, Magnesium, Sodium and Electrical Conductivity indicate that the normal seawater characteristics are reached. The (TDS) average of reject brine area with no-discharge period show a low degree of variability ranging from (38,000-43,000 ppm).

In general, higher concentrations are recorded closer to the outlet, whereas they are quite uniformly distributed in the rest of the study area. Thus, it was observed that the total concentration of the effluent takes place over a short distance which could be explained by the initial dilution of the brine discharge before and after the desalination plant using the seawater for intake and return. When working and non-working periods are compared, it has been observed that the Total Dissolved Solid (TDS) and Electrical Conductivity (EC) both significantly differ during the two periods as shown in (Figure 4a and b). In the case of Calcium (Ca) and Magnesium (Mg) only the point close to the outlet displays higher concentrations and the rest is quite similar (Figure 4c and d). For the Chloride (Cl) and Sodium (Na) the same behaviour as in the two cases above was observed at the outlet (Figure 4e and f).

Considering the improvement in desalination technology, attention must be given to evaluate desalination from environmental, technical, and economical perspective. The two-dimensional spatial distribution of various chemicals for both, a) full-capacity brine discharge and b) an average results for zero-capacity brine discharge are presented in (Figures 5a and b). It may be observed how some of the chemicals mix after being discharged from the outfall (Figure 5a) with higher concentrations around the outlet pipe and minimum values about 30m away. In (Figure 5b) uniformly distributed concentrations occur all over the period for most of the tested chemicals, which means the stable conditions could be possible for small scale plant after three months. Also this indicates that when the desalination plant have (zero) brine disposal for a period of three months or more, there could be a good chance for refreshing the seawater at the area where the brine was discharged.

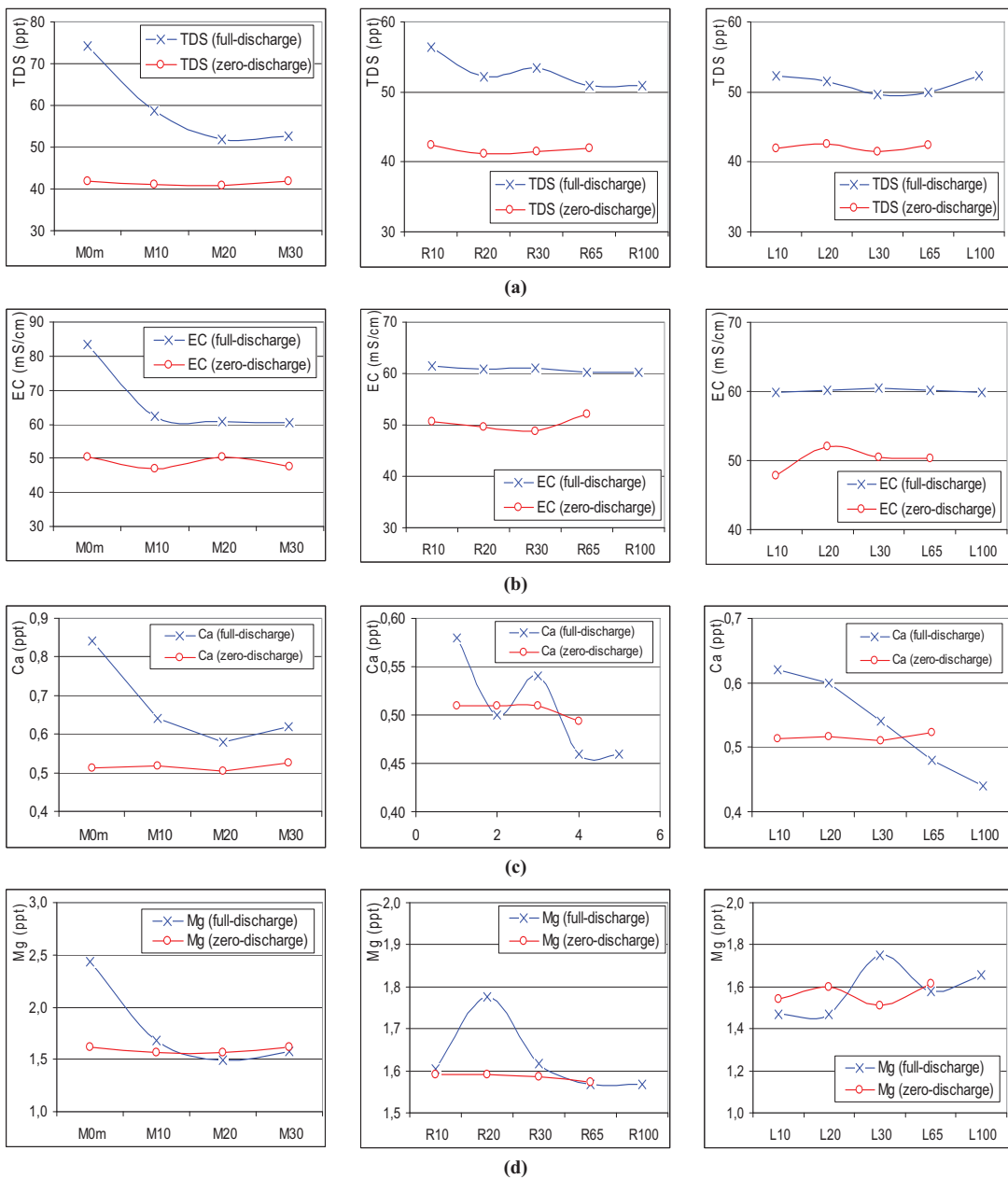


Figure 4: Comparison between full-capacity brine discharge and the average of zero brine discharge between 2nd March 2005-18th May 2005 with respect to location

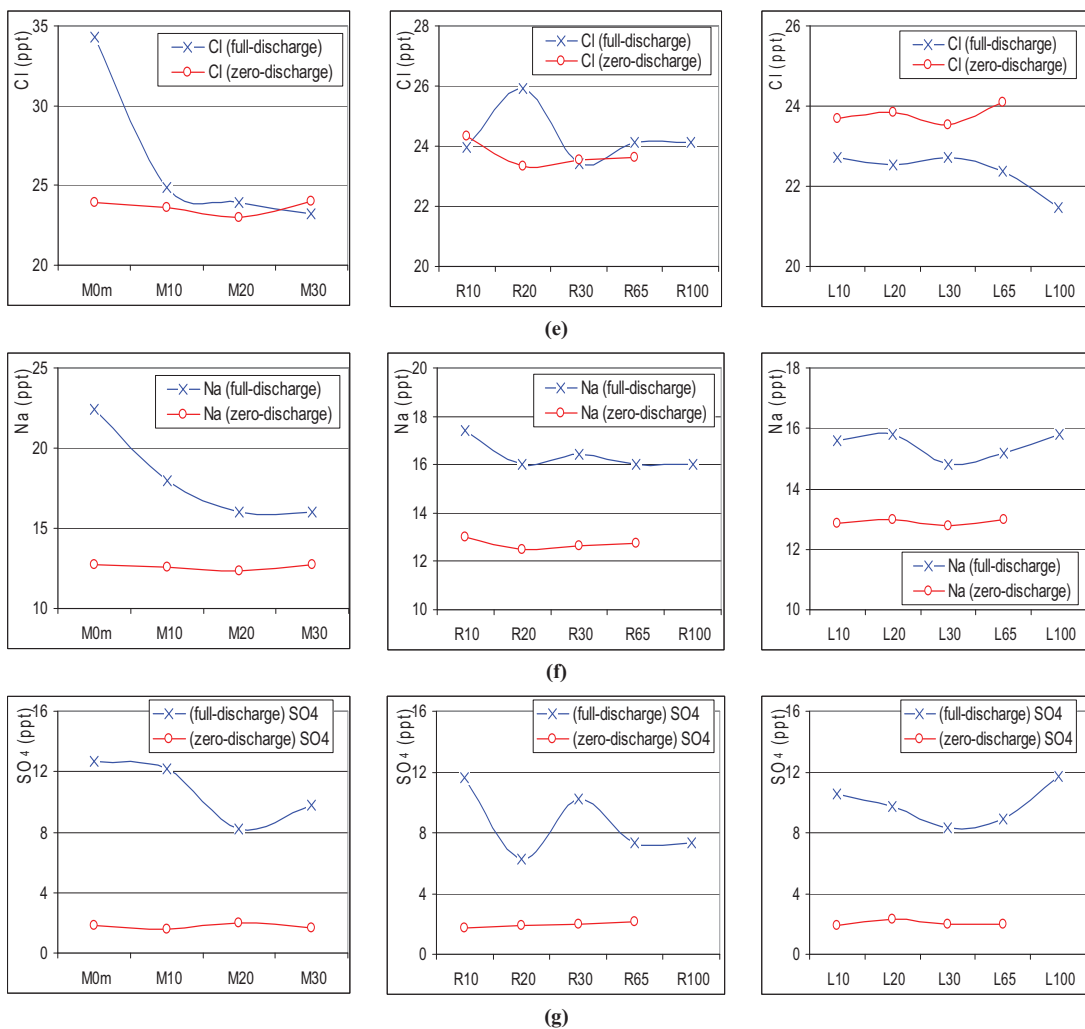


Figure 4(cont'd): Comparison between full-capacity brine discharge and the average of zero brine discharge between 2nd March 2005-18th May 2005 with respect to location

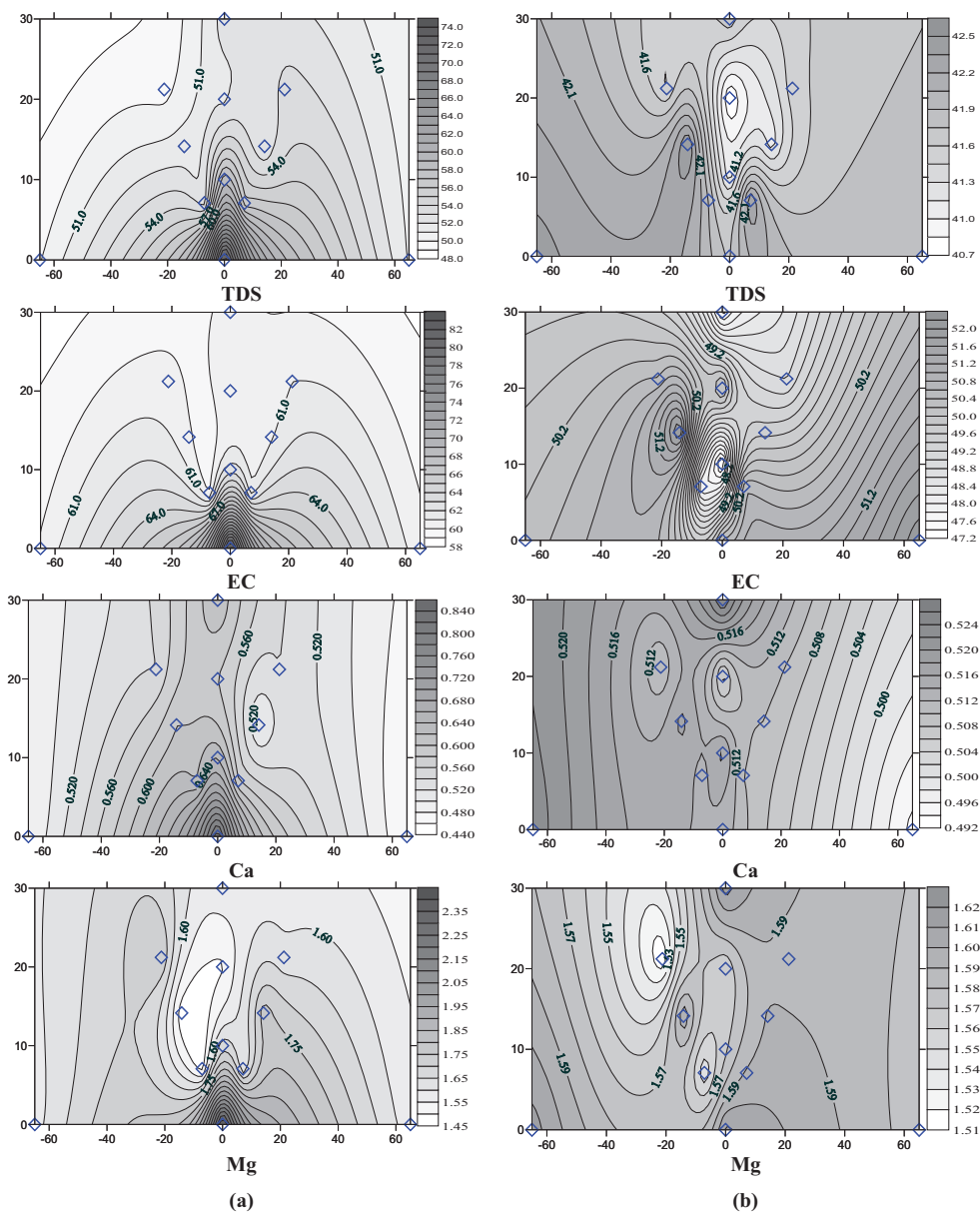


Figure 5: Two-dimensional spatial distribution of various chemicals: a) results for full-capacity brine discharge and b) an average results for zero-capacity brine discharge in between 2nd March 2005-18th May 2005

VIII. CONCLUSION

This is a study of the first desalination plant that was built in Northern Cyprus belonging to the Eastern Mediterranean University for distilling seawater. Due to new development their must be improved control of this facilities in order to know the behaviour of the discharge and to minimize any type of environmental impact. For that reason a sampling system should be established on site to measure during the operation of the desalination plant to observe the impacts on the coastline.

In this work it has been shown how the possible environmental impacts associated with the discharge of brine from a desalination plant can be minimized by means of planning more outlets or longer pipelines towards the sea. Changing the direction of the brine discharge could also minimize the impact on the coastline.

The general observations from this study is that preventing or reduce the coastal impact during the operational time of any plant (small or larger scale), due to the effect of brine discharge, can be considered necessary for future projects in the Mediterranean area or else where.

Coastal desalination plants discharge the brine waste containing high salt concentration directly into the sea. As shown above in (Figure 2) continuously discharging brine wastes directly to the coastline will result in salinity increases. Unfortunately, such increases in salinity will intensify, instead of improving, the critical problem of seawater intrusion into coastal groundwater aquifers.

Finally, in this case the impact of brine disposal operations on coastal and marine environments can be avoided by having more than one outfall (a series of outfalls) to the sea and this idea can be applied to the input as well idea to save membrane life.

IX. ACKNOWLEDGMENTS

This work was partially supported by the International Desalination Association (Channabasappa Memorial Scholarship).

X. REFERENCES

- [1] El-Yakubu J.B. and Ibrahim A. A., 2001, "Chemical conversions of salt concentrates from desalination plants", *Desalination* 139 (2001) 287–295.
- [2] Val Frenkel, Kennedy/Jenks Consultants, 2004, "Desalination Methods, Technology, and Economics", *Desalination Conference Santa Barbara, California April 16, 2004*
- [3] Pers. Comm. and Dr. Phillip McGillivray, NOAA, 1991.
- [4] Susan M.H. and Oggins Cy R., 1993, "Seawater Desalination in California" *California Coastal Commission, report, 1993.*
- [5] Ritter, C. and Montagna P.A., 1999. "Seasonal hypoxia and models of benthic response in a Texas bay". *Estuaries* 22:7-20.
- [6] Morehead S., Simanek C., and Montagna P.A., 2002, "GIS database of hypoxia (low oxygen) conditions in Corpus Christi Bay", *Final Report to Coastal Coordination Council, Coastal Management Program Grant no. 01-214, UTMSI Tech. Report No. 2002-001. 2 Volumes.*

- [7] Ahmed M., Shayyab W.H., Hoey D., and Al-Handaly J., 2001, "Brine disposal from reverse osmosis desalination plants in Oman and the United Arab Emirates", *Desalination* 133 (2001) 135-147.
- [8] Perez Talavera J.L. and Quesada Ruiz J. J., 2001, "Identification of the mixing processes in brine discharges carried out in Barranco del Toro Beach", south of Gran Canaria, *Desalination* 139 (2001) 277–286.
- [9] Manuel Fariñas et al., 2005, "Javea Desalination Plant: Environmental Study on the Brine Discharge" International Desalination Association World Congress: SP05-121.
- [10] Fernandez-Torquemada Y., Sanchez-Lizaso J.L., and Gonzalez-Correa J.M., 2005, "Preliminary results of the monitoring of the brine discharge produced by the SWRO desalination plant of Alicante (SE Spain)", *Desalination* 182 (2005) 395–402.
- [11] Schembri P.J., Department of Biology, "Marine Ecology of the Mediterranean", University of Malta.
- [12] Mukaddes O., 2004, "A comparative Study for MSF & MEE Desalination Systems using Alternative Energy Sources", July 2004.
- [13] Fischer, H.B., List, J.E., Koh, R.C.Y., Imberger, J., and Brooks, N. 1979. "Mixing in inland and coastal waters," Academic Press, New York, NY.
- [14] Ibrahim A.A., PhD Dissertation, KFUPM, Dhahran, Saudi Arabia, 1993.
- [15] Mickley M., Hamilton R., Gallegos L. and Truesdall J., 1993, "Membrane Concentration Disposal", AWWA Research Foundation, Denver, 1993.
- [16] Morton A.J., Callister I.K., and Wade N.M., 1996, "Environmental impacts of seawater distillation and reverse osmosis processes" *Desalination*, 108 (1996):1-10pp
- [17] World Health Organization, *Guidelines for Drinking Water Quality*, Vol. 3, Quality Control, After the First Impression 1985, Geneva, 1988.
- [18] <http://www.resources.ca.gov/ocean/97Agenda/Chap5Desal.html>.
- [19] <http://www.cham.co.uk/website/new/cfdintro.htm>.
- [20] Ben R. Hodges, 2005-2006, "Fate in Desalination Brine in Texas Coastal Bays and Estuaries" (2005-2006)
- [21] http://www.ce.utexas.edu/prof/hodges/project_pages/project_desalination_brine.htm.